AD NUMBER

AD475660

NEW LIMITATION CHANGE

TO

Approved for public release, distribution unlimited

FROM

Distribution authorized to U.S. Gov't. agencies and their contractors; Foreign Gov't. Info.; May 1965. Other requests shall be referred to Advisory Group for Aerospace research and Development, Neutilly-Sur-Seine [France].
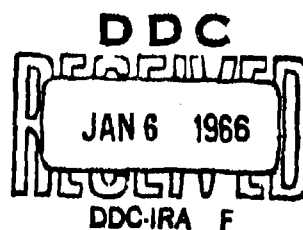
AUTHORITY

AGARD ltr, 30 Jun 1970

AGARDograph

THE THEORY OF HIGH SPEED GUNS

MAY 1965

DISCLAIMER NOTICE
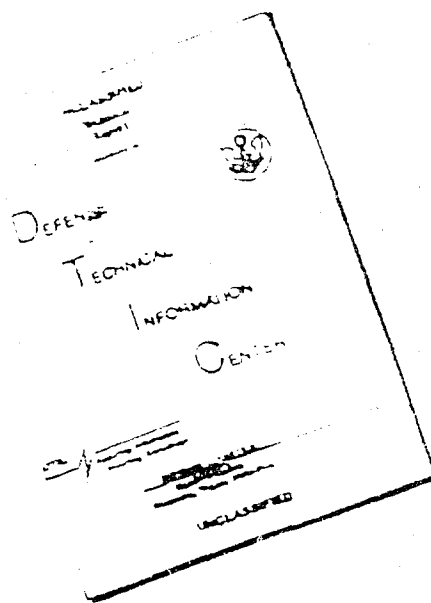
THIS DOCUMENT IS BEST QUALITY AVAILABLE. THE COPY FURNISHED TO DTIC CONTAINED A SIGNIFICANT NUMBER OF PAGES WHICH DO NOT REPRODUCE LEGIBLY.

AGARDograph-91

NORTH ATLANTIC TREATY ORGANIZATION

ADVISORY GROUP FOR AEROSPACE RESEARCH AND DEVELOPMENT

(ORGANISATION DU TRAITE DE L' ATLANTIQUE NORD)

THE THEORY OF HIGH SPEED GUNS

by

Arnold E. Seigel,

United States Naval Ordnance Laboratory
White Oak, Silver Spring, Maryland

May 1965

This is one of a series of publications by the NATO-AGARD Fluid Dynamics Panel.
Professor Wilbur C. Nelson of The University of Michigan is the editor.

SUMMARY

This monograph summarizes the gas dynamics of high-speed guns, utilizing a gas of low molecular weight at high temperature. Theory and test results are presented. The reader is assumed to be an advanced student in engineering. The fundamental ideas and equations are fully developed.

SOMMAIRE

La monographie suivante s'occupe en resumé de la dynamique des gaz des canons à grande vitesse en employant un gaz de poids moléculaire bas à haute température. On rend compte de la théorie et des résultats d'expériences. Il est admis que le liseur sera au courant au sujet du génie civil avancé. Les principes et les formules sont largement exposés.

623.428-823.1:533.6.078

CONTENTS

NOTATION

A, A_1, A_1	cross-sectional area of barrel
A, A_c	cross-sectional area of chamber
a	sound speed
a_{00}	sound speed of the gas at x_{00}
b	covolume
D, D_1	diameter of barrel
D_0	diameter of chamber
f	covolume in semi-empirical entropic equation (66-1)
E	internal energy of a system in general
F	frictional force per unit mass at wall on gas layer due to boundary layer
G	mass of propellant gas in a PP Gun, or mass of gas in barrel of constant base pressure gun
$\bar{G}$	mass of gas in back chamber of a two-stage gun
H	Lagrangian coordinate defined as $\int \rho \, dx$
h	enthalpy
L	barrel length
m	molecular weight
M	projectile mass
$\bar{M}$	mass of piston in pump tube of two-stage gun
n	number of moles, or exponent in empirically fitted isentropic equation
PP Gun	preburned propellant gun
PPIG Gun	preburned propellant gun with an ideal gas propellant
p	pressure
$\bar{p}$	spacial average pressure
q	heat transfer per unit mass to gas layer

$\bar{R}$	universal gas constant
R	gas constant for a mole of a particular gas (equals $\bar{R}/m$)
s	entropy
t	time coordinate
T	temperature
U	internal energy of a system independent of motion, gravity, capillarity, electricity, and magnetism
u	velocity
u_0	velocity of a projectile propelled by a constant pressure (p_0)
u_p	projectile velocity
Δu_p	increase of projectile velocity due to chambrage
$\Delta u_{p\,\infty}$	increase of projectile velocity due to infinite chambrage
$u_{p\,1st}$	velocity of projectile when first wave reflected from breech reaches it
u_{esc}	escape velocity
u_{p_f}	projectile velocity with boundary layer and friction effects
$u_{p_{f=0}}$	projectile velocity without boundary layer and friction effects
u_{p_1}	projectile velocity when there is gas in front of the projectile
$u_{p_{1=0}}$	projectile velocity when there is no gas in front of the projectile
V	projectile velocity at muzzle
v	specific volume
x	distance coordinate
x_p	position of projectile
x_0	length of chamber in PP gun
x_{00}	the x coordinate of characteristic line at $t = 0$ in the gas in a constant base pressure gun
α	value of acceleration of gas and projectile in the constant base pressure gun equal to $p_0 A_1/M$

α	fraction of additional gas particles, used in thermal equation: $p = \rho(1 + \bar{\alpha})RT$
$\tilde{\alpha}$	constant in van der Waals equation of state which accounts for the attractive forces between molecules
β	parameter which is exponent of semi-empirical entropic equation of state (Equation (66-1))
γ	ratio of specific heats
ϵ	defined as $(u_p + \sigma_p - \sigma_0)/\sigma_0$ (see Equation (24-3)), used in p-u relation for chambered $x_0 = \infty$, PPIG Gun
κ	parameter which occurs in semi-empirical equation (Equation (66-1))
ξ	the x coordinate on a characteristic line in the gas of a constant base pressure gun
ρ	density
σ	Riemann Function defined from $d\sigma \equiv (dp/a\rho)_s$
τ	the t coordinate on a characteristic line in the gas of a constant base pressure gun

Subscripts

c	denotes position in chamber at entrance to transition section
f	denotes gas directly in front of projectile
g	denotes gas directly behind shock in barrel
i	denotes position in barrel at exit of transition section
p	refers to gas directly behind the projectile or to the projectile
0	refers to initial state of gas in chamber of PP gun, or to conditions behind projectile in a constant base pressure gun
00	refers to position on characteristic at $t = 0$ in gas of constant base pressure gun
1	denotes initial state of gas in barrel in front of projectile or state of gas in front of shock
2	denotes state of gas behind shock

★   denotes sonic conditions

★★   denotes time when gas becomes sonic at the $x = 0$ position in a constant base pressure gun

Other Symbols

$\dfrac{D}{Dt}$ denotes time rate of change of a quantity when traveling with the velocity of a disturbance $(u \pm a)$; thus

$$\frac{D}{Dt} \equiv \frac{\partial}{\partial t} + (u \pm a)\frac{\partial}{\partial x}$$

$\dfrac{d}{dt}$ denotes time rate of change of a quantity when traveling with the velocity of a gas particle (u); thus

$$\frac{d}{dt} = \frac{\partial}{\partial t} + u\frac{\partial}{\partial x}$$

Bars over quantities denote nondimensional quantities; defined in text.

Ideal gas – a gas described by the equations $pv = RT$ and $pv^{\gamma} = $ constant.

PART I. INTRODUCTORY REMARKS

Section 1

Purpose of Monograph

In the year 1945, after 700 years of shooting guns, the maximum velocity of projectiles was 10,000 ft/sec. However, within the past 20 years projectile velocities obtained from guns have risen spectacularly to a value of 37,060 ft/sec.* This surprisingly large gain in velocity during a relatively short period of time was the result of a vigorous effort pursued to make possible the study of hypervelocity phenomena in the laboratory. The increase in projectile velocity was a reflection of the increase in our knowledge of the interior ballistics process; the increase in knowledge still continues, and, coupled with our advancing technology, gives promise of effecting in the next 20 years equally large projectile velocity increases. Projectile velocities of 60,000 ft/sec by 1985 seem not only possible but probable.

What is the extent of our knowledge of interior ballistics which made possible the startlingly large gain in projectile velocity? This monograph will address itself to answering this query. It will summarize our understanding of the gas dynamics of high-speed guns, those firing projectiles above 10,000 ft/sec. As is now well known, in order to achieve high speeds, a gun must use a hot "light gas" as a propellant, that is, a gas of low molecular weight at high temperature. This require-ment for a hot light gas propellant becomes obvious from the interior ballistics theory as unfolded below. ,

The reader is assumed not to be an expert in the field of interior ballistics, but is assumed to be a graduate student in engineering. Consequently, the fundamental ideas and equations are rather fully presented; thus, included in some detail in the main text and appendices are explanations of the method of characteristics. Included also are methods for calculating gun performance which have now become unnecessary because of the use of electronic computing machines; nevertheless, these methods aid in the understanding of the interior ballistics. It is hoped that the more knowledge-able reader will adjust to the inclusion of much elementary material and to the repetitious style used for clarity.

Section 2

The Basic Requirements for a High-Speed Gun

The basic factors determining the speed of a projectile propelled from a gun may be simply obtained by applying Newton's force equation to the projectile. Schematically, the projectile, during its travel in the gun barrel, may be represented as in the sketch on the following page.

---

* NASA, Ames Research Center (April 1965).
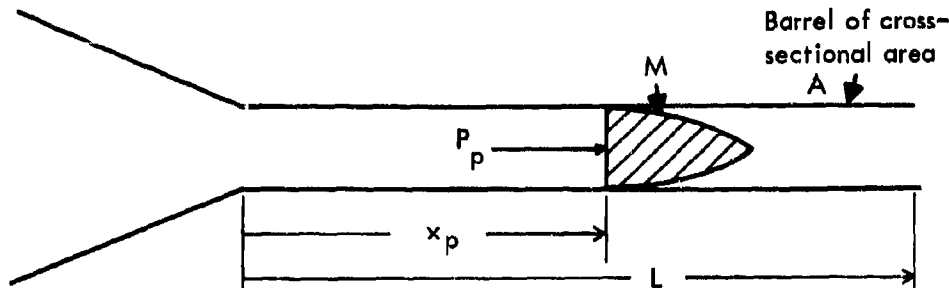
The projectile mass is denoted by M , the length of barrel by L , and the cross-sectional area of the barrel by A . The propellant pressure at the back end of the projectile is denoted by the letter p_p . At any instant of time Newton's Law applied to the projectile yields*

$$M \frac{du_p}{dt} = Mu_p \frac{du_p}{dx_p} = p_p A \tag{2-1}$$

where u_p is the instantaneous projectile velocity and x_p is the corresponding distance traveled by the projectile.

If Equation (2-1) is integrated, it becomes

$$MV^2/2 = A \int_0^L p_p dx_p \tag{2-2}$$

where V is the muzzle velocity of the projectile. With $\bar{p}$, the spatial average propelling pressure, defined as

$$\bar{p} = \frac{1}{L} \int_0^L p_p dx_p \tag{2-3}$$

the projectile velocity becomes

$$V = \sqrt{2\bar{p} AL/M} . \tag{2-4}$$

This result, Equation (2-4), indicates essentially the factors upon which the projectile velocity depends. To increase the projectile velocity, one must increase the value of the quantities under the square root sign. Thus, the one step in achieving a higher projectile velocity is to change the sizes of the projectile and barrel so as to increase the value of AL/M ; this requires, for a given cross-sectional area A of the barrel, that M be made smaller and L larger. (Note that if a gun is made larger by geometrically scaling it, AL/M remains the same.) However, practicality limits these changes, for M may be made only so small for a given barrel diameter and L may be made only so large (as frictional and gas dynamic effects lower $\bar{p}$ substantially if the barrel is too long – see below).

---

* For purposes of this discussion, the air pressure in front of the projectile and the frictional force acting on the projectile have been assumed negligible.

Unfortunately, after having made AL/M as large as practical, it is found with a conventional propellant gun that the projectile velocity is still much below that desired.

From the above considerations one is led to the conclusion that after AL/M is made as large as practical, *the only method of achieving high velocity is to increase the average propelling pressure $\bar{p}$* .

The reason for the difficulty in obtaining a high average pressure in the case of a gun *using a conventional powder propellant* is illustrated by the following sketch.
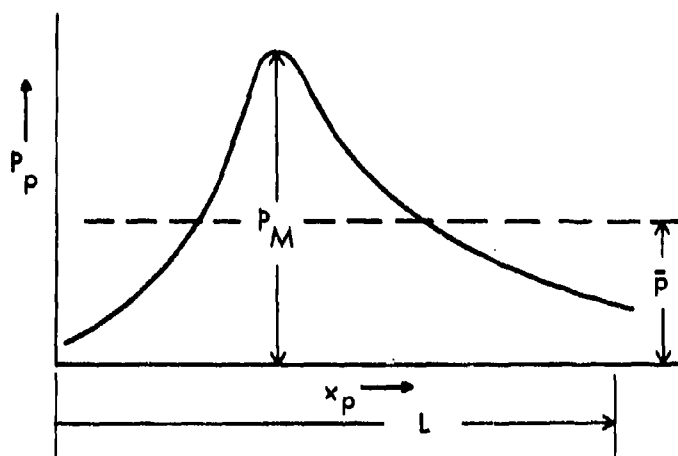
Here the pressure behind the projectile in the conventional gun is plotted as a function of its travel. The rise in pressure from zero to the peak pressure p_M results from the burning of the propellant; as will be shown below, the rapid pressure decrease thereafter results mainly from the propellant inertia as the propellant gas accelerates to push the projectile. It is evident from the sketch that the average pressure $\bar{p}$ is considerably below the peak pressure p_M for the conventional propellant.

Of course, increasing the amount of propellant in the chamber would increase p_M and thus $\bar{p}$, but the strength of the gun limits the value of p_M . By using the maximum amount of conventional gunpowder which may be contained even by specially strengthened guns, velocities of about 12,000 ft/sec have been reached with low mass projectiles. This velocity is about the maximum achievable with the conventional propellant gun system.

As indicated in the preceding paragraph, there is obviously a practical limit to the strength of the parts of a gun. The main parts of a gun system are (a) the projectile, (b) the barrel, and (c) the gun chamber or chambers. The values of stresses experienced by each of these components is dependent on the pressure pulse to which it is subjected. (The rate of pressure application, as well as the value of the peak pressure, determines the stresses experienced.) In practice, the chambers and barrels of guns may be designed to withstand static pressures up to about

130,000 lb/in^2 without being permanently deformed; a rugged projectile, similarly, may be designed to withstand 130,000 lb/in^2, whereas a fragile projectile may only withstand, perhaps, 250,000 lb/in^2.[*] Parts which are expendable may be designed to deform but not rupture at transient pressures as high as 1,000,000 lb/in^2.

This discussion points to the main requirement in achieving a high projectile velocity after having made AL/M as large as possible: the requirement of obtaining a high average pressure $\bar{p}$ behind a projectile, *while at the same time* limiting the pressure rise in all parts of the gun system so as not to cause unacceptable damage to the parts.

Section 3

The Velocity Attainable by Use of a Constant Base Pressure Propellant

For a gun of given geometry propelling a given projectile, the quantities A, L, and M are fixed. For this gun system there is a maximum allowable pressure p_0 which the projectile can sustain. Under idealized circumstances one could hope that the pressure of the propellant propelling the projectile would be constant and equal to p_0 during the entire projectile travel. (Thus, $\bar{p} = p_0 =$ a constant.) This situation is shown in the following sketch.

---
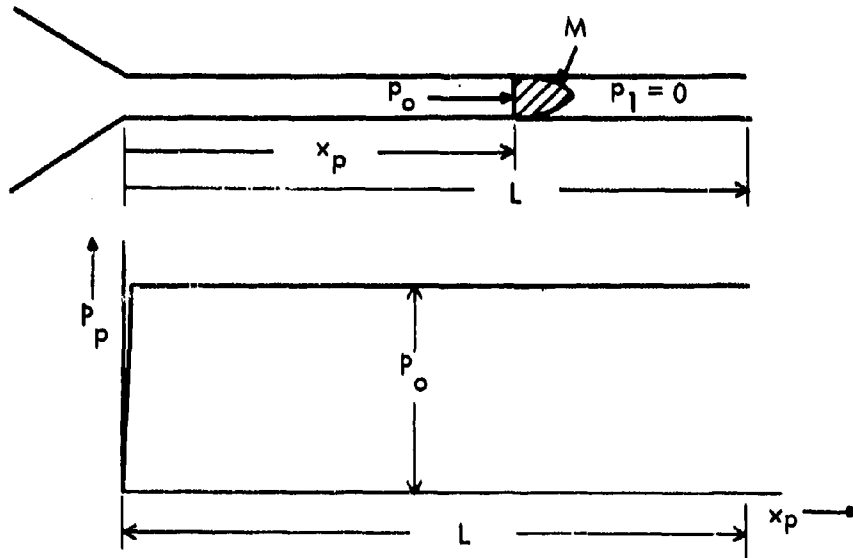
[*] Instead of the stress capability of the projectile, one may discuss the acceleration capability. The latter description may be more pertinent if the projectile carries "g" limited payloads.

Such an imagined propellant, whose propelling pressure would be maintained at a constant value, is known as a "constant base pressure propellant" or "constant pressure propellant". In this case the projectile velocity attained would be the *maximum attainable velocity for the given gun system*. This velocity, denoted as u_0, is easily calculated by applying Newton's Law to the projectile. Thus[*]

$$M \frac{du_p}{dt} = Mu_p \frac{du_p}{dx_p} = p_p A = p_0 A \qquad (3\text{-}1)$$

which, when integrated along the barrel length, yields

$$u_0 = \frac{2p_0 A L}{M} \; . \qquad (3\text{-}2)$$

The first calculation one should make for a given gun when attempting to assess its possibilities of attaining high velocity is the calculation of u_0; for u_0 is the highest velocity attainable.

If, for example, a sphere is chosen as the projectile, u_0 becomes

$$u_0 = \sqrt{\frac{2p_0 A L}{M}} = \sqrt{\frac{2p_0 (\pi D^2/4) L}{(\pi D^3/6) \rho_p}} = \sqrt{\frac{3p_0}{\rho_p} \left(\frac{L}{D}\right)} \qquad (3\text{-}3)$$

where ρ_p is the density of the projectile. Thus, for a very light projectile such as a nylon sphere ($\rho_p = 1.2$ g/cm^3) in a gun with a long barrel (L/D = 300), with $p_0 = 100,000$ lb/in^2 (a relatively high pressure), Equation (3-3) yields $u_0 = 75,000$ ft/sec.

For the same gun with $p_0 = 30,000$ lb/in^2, u_0 is calculated to be 42,000 ft/sec.

It becomes obvious that, even in the idealized case of a constant propelling pressure, one needs for high velocity extremely long guns, high pressures, and low projectile masses; these needs are even more pronounced in the actual case where the average propelling pressure is much below the peak pressure. Thus, the quest for a high velocity gun becomes a quest for a propellant which will maintain the propelling pressure at a high value.

---

[*] Here, for the purpose of obtaining the maximum attainable velocity, the friction on the projectile and air pressure in front of it are assumed negligible.

PART II. THE PREBURNED PROPELLANT (PP) GUN - GENERAL

Section 4

Description of the Preburned Propellant Gun

In this section will be considered the gun system in which the propellant has been completely reacted before the projectile is allowed to move. This gun system is termed a "Preburned Propellant" Gun and designated as a PP Gun. The gun is visualized as consisting of a chamber of diameter D_0 joined by means of a transition section to a barrel of diameter D_1. The projectile is positioned initially so that its back end is at the beginning of the barrel section. Immediately before the projectile begins to move, the reacted propellant produces in the chamber a gas at an initial and peak pressure p_0 and sound speed a_0, temperature T_0, etc. (See the following sketch.)
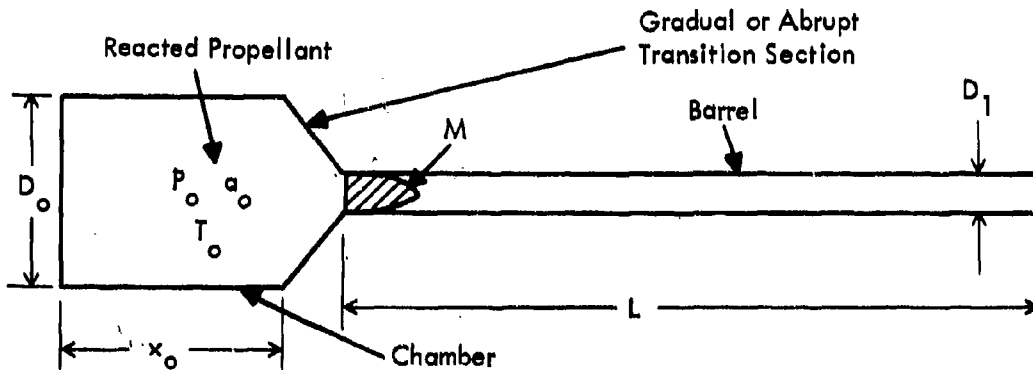
When the chamber diameter is greater than the barrel diameter ($D_0/D_1 > 1$) the gun is described as a "chambered" gun, or a gun with "chambrage". When the chamber diameter is equal to that at the barrel, the gun is described as "having no chambrage", or as a "constant diameter gun".

In practice a preburned propellant gun may employ a diaphragm to separate the propellant in the chamber from the projectile; this diaphragm is ruptured when the propellant has completed its reaction. Another possibility is the use of a "shear disc" around the projectile itself which shears when the reaction has been completed. One type of a preburned propellant gun is that which uses as a propellant a non-reacting gas (such as compressed helium).

In a preburned propellant gun the projectile is restricted from movement until the pressure has reached a peak value; it will be shown below that, after the projectile is released, the pressure behind the projectile decreases as the projectile increases in velocity and moves along the barrel. (See the following sketch.)
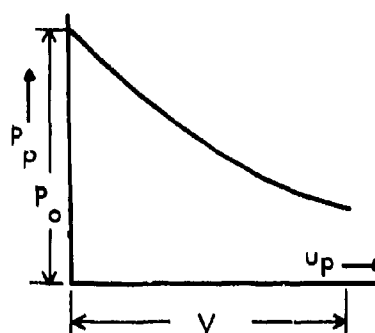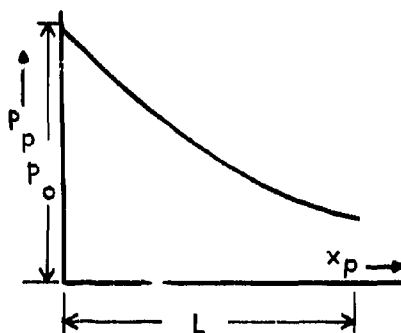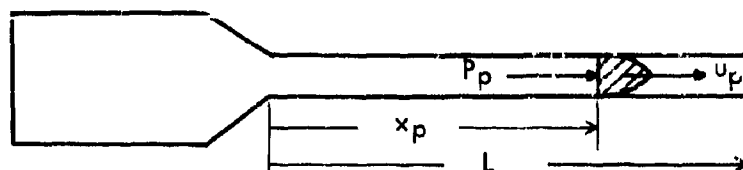
The attainment of high velocity in this case requires that the pressure decrease be minimized; for maximum velocity one would wish for the constant pressure propellant previously mentioned which would maintain its pressure at the peak value p_0 behind the projectile during the projectile's entire travel.

If the pressure behind the projectile were maintained at the initial peak value p_0, the velocity in this idealized case is as calculated in Equation (3-2),

$$u_0 = \sqrt{2p_0 AL/M} \ .$$

In practice a velocity equal to the velocity u_0 for the preburned propellant gun is unattainable; this is a consequence of the fact that in such a gun, as will be shown below, the pressure behind the projectile inevitably *must* drop as the projectile velocity increases; unfortunately, the greater the projectile velocity, the greater will be the drop.

Section 5

A Qualitative Description of the Pressure Disturbances
Occurring During Firing of a Preburned Propellant Gun

When the projectile in a gun begins to move, it momentarily leaves a slightly evacuated or a lower pressure space behind it. The layer* of gas that was initially behind the projectile quickly moves (an infinitessimal amount) toward the projectile

---

* The gas is imagined to be composed of thin layers or discs of gas which are perpendicular to the axis of the gun.

into this evacuated space. Because there is now more space available to this first
gas layer, its pressure drops. The layer of gas immediately behind the first layer of
gas then, likewise, finds itself next to a slightly evacuated space (as a result of
the first layer's motion) and so it likewise moves into the evacuated space. Similarly,
each successive layer in turn moves into the space in front of it which has been just
previously evacuated. This progression of successive movement is a disturbance in the
gas which proceeds at the speed of sound. Since this disturbance is characterized by
the fact that it decreases the pressure and density of the gas through which it passes,
it is termed a rarefaction disturbance. (Other names for the disturbance are impulse,
wave, wavelet, or pulse; the adjective "acoustic" or "sound" is often put in front of
these terms.)
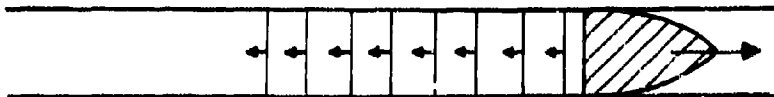
It is seen that the pressure drop accompanying the disturbance results from the fact
that the projectile has accelerated and in turn each layer of gas has been accelerated.
The quantitative value for this pressure drop from the accelerating projectile motion
is given below. Qualitatively, the more quickly each layer of gas moves into its
neighbor's evacuated space, the less is the pressure drop and the better able is the
gas to push on the propellant. Thus, a good propellant gas would be one of low
"inertia" in this process of successive movement. †

During the entire movement of the projectile in the barrel, the projectile continues
to produce these rarefactions which travel toward the breech at the local velocity
of sound of the propellant gas. Consequently, the pressure of each layer of the gas
behind the projectile drops continuously as the projectile accelerates toward the
muzzle; in particular, the pressure of the gas layer directly behind the projectile
drops the most, since all of the rarefactions first travel through this gas layer.

In a gun with no chambrage, i.e., a constant cross-sectional area gun, each layer
of gas similarly moves into the space vacated by its front neighbor until the layer
of gas next to the breech begins to move forward. The breech layer then begins to
move into the space vacated by its neighbor, but there is no neighbor behind it to
fill up the space it is vacating; therefore, it is retarded in its motion and by so
doing leaves the space ahead into which it is moving somewhat evacuated. The neighbor
in front of the breech layer feels this slightly evacuated space behind it and so it
is retarded in its forward motion; this retardation of each neighbor in turn proceeds
toward the projectile, resulting in a progression of a rarefaction disturbance which
travels from the breech end toward the projectile end.

---

† It is shown below that the quantitative expression for the gas inertia is "$a\rho$"; for an ideal
gas $a\rho$ is inversely proportional to the initial sound speed for a given initial pressure
Equation (11-3).

This disturbance, which originates at the breech end, is termed a "reflected" rarefaction and is a result of the fact that there is a breech end. All of the rarefactions produced by the projectile reflect from the breech in this manner; they travel toward the projectile, transmitting the information to the gas and the projectile that there is a limited quantity of gas to fill the evacuated spaces. These reflected rarefactions lower the pressure of the gas through which they travel further than if there had been no breech. In particular, when these reflected rarefactions reach the back end of the projectile, they lower the pressure behind the projectile; consequently, the projectile velocity is not as large as it would have been if these reflected rarefactions had not reached the projectile.

A more complex phenomenon occurs in a gun with chambrage. In such a gun, as a rarefaction traveling in the barrel toward the breech reaches the increasing area section, the evacuated space is filled by gas flowing from a larger volume layer; consequently, the pressure in the space is raised to higher value than if the gas had moved from the constant diameter smaller bore layer. In turn, each layer of gas in the transition section leaps into the space evacuated by the layer in front of it and each tends to raise the pressure a little more than if they had been gas layers of the same diameter as the bore. In effect, therefore, the rarefaction impulses which are produced from the back of the moving projectile when they come to the change of area of the transition section are partially reflected as *compression* disturbances; these compression impulses travel toward the projectile. Upon reaching the projectile they raise the pressure behind the projectile, and therefore the projectile velocity, to a value above that of a gun with no chambrage. Thus, the rarefactions produced by the projectile in a chambered gun upon reaching the change of area section are partially reflected as *compression* impulses and partially transmitted as rarefactions. The transmitted rarefactions continue their travel toward the breech still as rarefactions; at the breech they are reflected again as rarefactions and, at the transition section of area decrease, a portion is reflected as a rarefaction and the remaining portion continues its travel toward the projectile as a rarefaction. This sequence of events continues as the projectile moves along the barrel.

In summary, changes in pressure of the gas behind the projectile occurring in a preburned propellant gun are these: (1) There is a drop in pressure from accelerating projectile motion which is present during the entire projectile travel. (2) There is a drop in pressure caused by rarefactions reflecting from the breech which are present in the latter stages of the projectile motion when these reflections reach the projectile. (3) There is a rise in pressure from the compressions reflected from the change in area section which is present during the entire projectile motion.

Rarefactions reflected from breech

Rarefactions from accelerating projectile motion

Compressions reflected from transition section
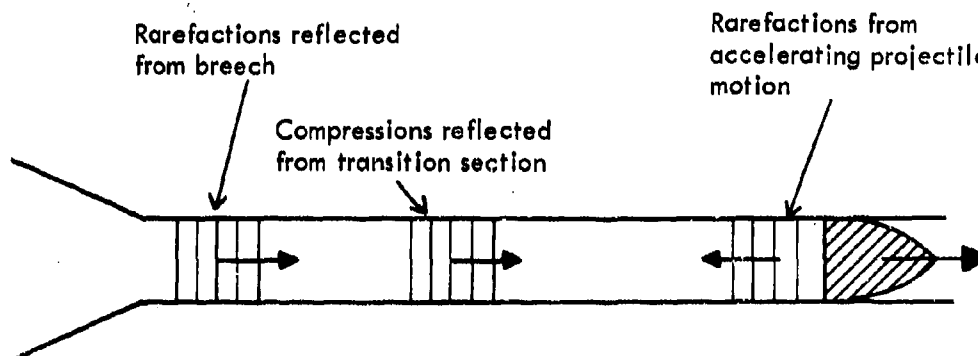
Section 6

The Derivation of the Equations for
Disturbances Traveling in the Gas*

It is apparent from the discussion in Section 5 that changes in the gas are brought about by the acoustic disturbances which travel in both directions in the propellant gas. Although only infinitesimal changes result from the passage of each disturbance, *finite changes* result from the passage of a multitude of these disturbances. Let the changes wrought by a single infinitesimal disturbance traveling with velocity D into a differential layer of gas in a constant diameter tube be examined. Let this layer before the passage of the disturbance have a pressure p , a density ρ , and gas velocity u ; after the disturbance passes the layer, these quantities are increased by differential amounts as shown in the following sketch.
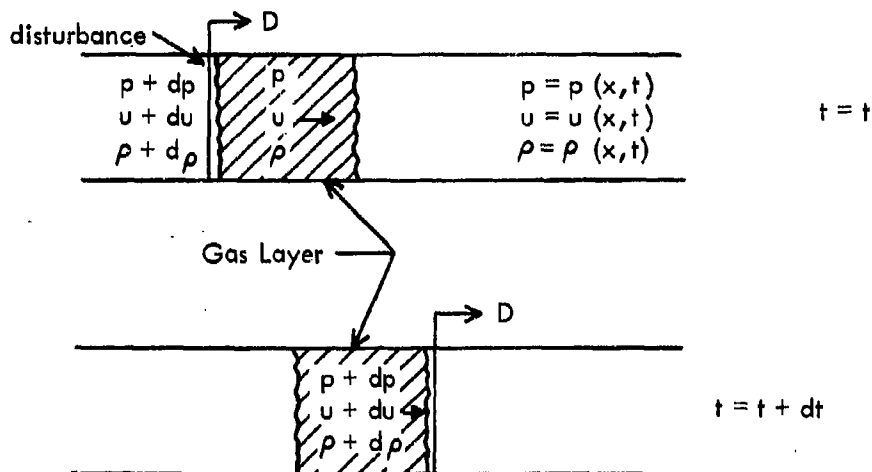
As indicated in the sketch, the layer of gas to be examined is traversed by the disturbance in time dt . Thus, it is initially (D-u)dt long, and after passage of the disturbance it is (D-u-du)dt long, as may be discerned from the next sketch.

---
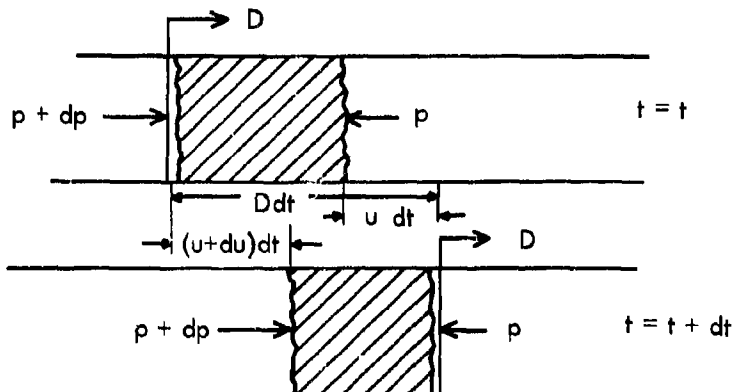
* See Appendix B for an alternate derivation.

The mass of gas is therefore expressible in terms of the gas layer's length before or after traversal by the disturbance wave; hence

$$A(D - u)\rho\, dt = A(D - u - du)dt\,(\rho + d\rho) \tag{6-1}$$

where A is the cross-sectional area of the tube.

During the entire time of passage of the disturbance wave a pressure of value $p + dp$ acts on the left end of the layer, while a pressure of value p acts in the opposite direction on the right end of the layer. Thus, the net pressure acting on the layer is dp. The acceleration of the layer is the velocity change du experienced by it divided by the elapsed time dt. Thus, Newton's Law applied to the layer is

$$\underbrace{Adp}_{\text{net force}} = \underbrace{A\rho(D - u)dt}_{\text{mass}}\ \underbrace{\frac{du}{dt}}_{\text{acceleration}} . \tag{6-2}$$

If du is eliminated from Equations (6-1) and (6-2), one obtains

$$(D - u)^2 = \frac{dp}{d\rho} . \tag{6-3}$$

The assumption is here made that the infinitesimal changes which occur during the passage of the disturbance are isentropic (that is, reversible and adiabatic); thus, the right hand side of Equation (6-3) is the square of the sound speed of the gas, a^2.

Equation (6-3) becomes

$$D - u = a$$

or

$$D = u + a . \tag{6-4}$$

This disturbance is thus found to travel with the speed of sound relative to the gas. Equations (6-2) and (6-4) may be combined to give

$$dp = a\rho du . \tag{6-5}$$

This is the fundamental expression for the pressure change across a "u + a" disturbance wave.

In a similar manner a disturbance traveling upstream could be analyzed. Such a disturbance is shown in the following sketch.

12
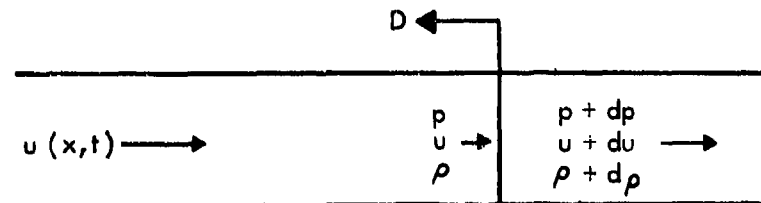
In this case it will be found that

$$dp = -a\rho du \qquad (6\text{-}6)$$

across a "u – a" disturbance.

By examining the above equations one may determine the significant propellant gas property which governs the magnitude of the pressure change due to the passage of a disturbance in a constant diameter tube. Equations (6-5) and (6-6) may be rewritten as

$$\left.\begin{array}{l} dp = (a\rho dt)\,(du/dt) \\[2mm] dp = -(a\rho dt)\,(du/dt) \end{array}\right\} \qquad (6\text{-}7)$$

for the pressure change across a downstream and upstream disturbance wave, respectively. The quantity "aρ", the gas acoustic impedance or acoustic inertia, is the mass per unit time traversed by a disturbance wave; it is thus properly identified as the inertia of the propellant gas.

For small aρ, the pressure change will be small to effect a given velocity change; for large aρ, the pressure change must be large to effect a given velocity change. Thus, *the acoustic inertia aρ of the gas is seen to be the fundamental gas property which determines the magnitude of pressure changes required to produce given velocity changes.* It will be discussed further in Section 9.

For convenience, Equations (6-5) and (6-6) are usually rewritten in terms of changes which occur when traveling with or along the disturbance rather than those which occur when traveling across the disturbance. Hence, since the change *across* a "u + a" disturbance equals the change *along* a "u – a" disturbance, and vice versa, Equations (6-5) and (6-6) become

$$dp + a\rho du = 0 \qquad (6\text{-}8)$$

along a "u + a" disturbance path,

$$dp - a\rho du = 0 \qquad (6\text{-}9)$$

along a "u – a" disturbance path.

These equations are known as the characteristic equations; they permit a numerical solution to the interior ballistics problem in the case of a gas flowing isentropically in a constant diameter tube. This solution is possible because the infinitesimal changes described in Equations (6-8) and (6-9) result in the finite changes which occur in the gas.

Section 7

Summary of Equations Applicable to an Isentropic
Gas Expansion in a Constant Cross-Sectional Area Tube

The meaning of the equations in Section 6, which apply to a gas which expands in a constant cross-sectional area tube is discussed in Appendix C; the equations are derived in a more rigorous fashion in Appendix B. It is assumed there that the gas expansion is one-dimensional. Further, it is assumed that the flow is adiabatic and reversible (isentropic), that is, that friction and heat-transfer effects within the gas are negligible. (The irreversible effects are discussed in Part VIII.) These assumptions have been shown to be a good approximation[1, 2] and permit a relatively simple solution to the interior ballistics problem.

In Appendix B the one-dimensional momentum and continuity equations applied to a layer of gas isentropically expanding in a constant diameter tube are transformed into the characteristic equations. These equations are there written in terms of the "Riemann Function" σ, defined as

$$d\sigma = (dp/a\rho)_s \cdot \qquad (7\text{-}1)$$

They are

$$du + d\sigma = 0 \qquad (7\text{-}2)$$

along the path of a characteristic line of slope $dx/dt = u + a$ and

$$du - d\sigma = 0 \qquad (7\text{-}3)$$

along the path of a characteristic line of slope $dx/dt = u - a$. The $u + a$ and $u - a$ characteristic lines are thus the paths of disturbances. These equations are the same as derived in the previous section. For consciseness they may be written as (see Appendices A and C):

$$\frac{D}{Dt}(u \pm \sigma) = 0 .$$

Equations (7-2) and (7-3) may be integrated to yield

$$u + \sigma \text{ is constant} \qquad (7\text{-}4)$$

along the path of a disturbance traveling with speed $u + a = dx/dt$ and

$$u - \sigma \text{ is constant} \qquad (7\text{-}5)$$

along the path of a disturbance traveling with speed $u - a = dx/dt$.

The two sets of characteristic lines (disturbances) may be drawn in the xt-plane. As explained in Appendix C, the $u \pm a$ characteristic lines have a slope equal to $u \pm a$ in this plane. Along each $u \pm a$ characteristic line the quantity $u \pm \sigma$ remains constant.
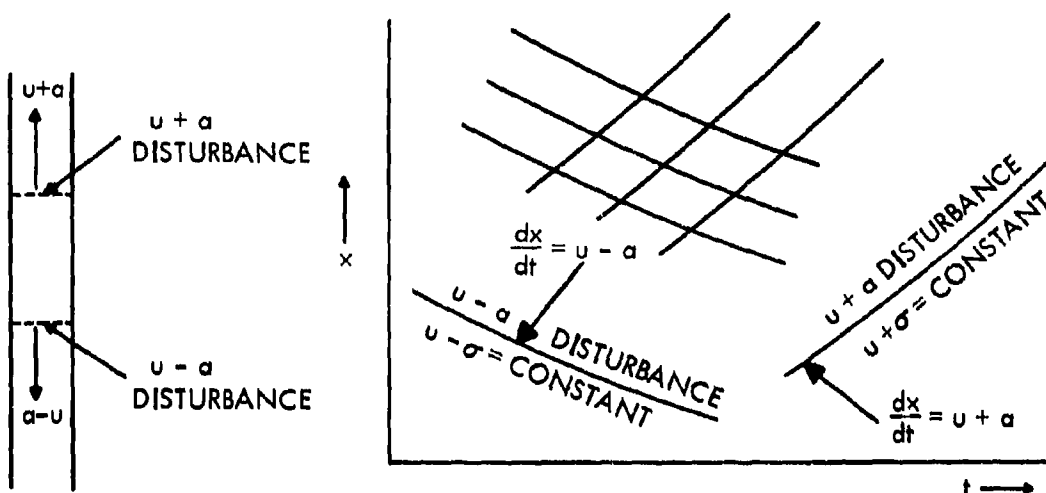
The characteristic Equations (7-4) and (7-5) may be applied to the gas expansion in any constant diameter tube (e.g., in the gun barrel or in the gun chamber) as demonstrated in the sections below. In particular, these equations, together with the gas equation of state, may be directly applied to a constant diameter gun.

In general, the solution of these equations is effected numerically by progressively solving for conditions at the intersections of the $u + a$ with $u - a$ characteristics (see Appendix C and Appendix E). In special cases a numerical solution is unnecessary and the characteristic equations may be solved analytically.

Section 8

The Characteristic Equations for the Effectively
Infinite Length Chamber, $D_0/D_1 = 1$, PP Gun

A preburned propellant gun having a constant diameter chamber joined to a barrel of the same diameter is considered. Before the projectile has begun to move the gun appears as in the following sketch.
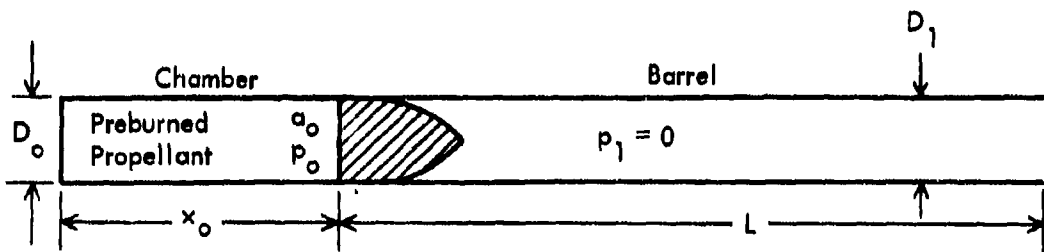
The fact that the chamber and barrel diameter are equal is specified by the Equation $D_0/D_1 = 1$. Equations (7-3) and (7-4) may be applied to such a gun.

When the projectile motion begins, a rarefaction disturbance is sent back with the speed of sound (a_0) into the gas behind it. The path of this disturbance is shown as the line A-B-C in the following sketch.[*]
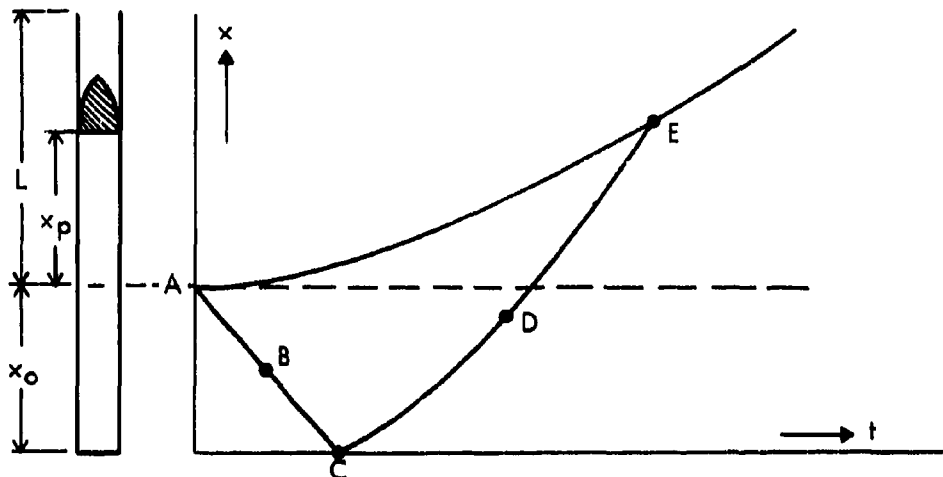
This disturbance reaches the back end at C and reflects. The reflected disturbance is shown as C-D-E in the sketch. As explained in Appendix D, the region A-C-E-A is known as a "simple wave" region. Because no reflected disturbance reaches this region, the *entire* region is described by the equation

$$du + d\sigma = 0$$

or equivalently

$$du + dp/a\rho = 0 \ . \tag{8-1}$$

This becomes upon integration

$$u + \int dp/a\rho = 0 \tag{8-2}$$

or in terms of σ,

$$u + \sigma = \sigma_0 \tag{8-3}$$

where u is taken to be equal to zero at $p = p_0$ and $\sigma = \sigma_0$.

A gun whose chamber length x_0 is sufficiently long so that the first reflected wave C-D-E does not reach the projectile before it reaches the end of the barrel is termed as "infinite chamber length gun" or an "effectively infinite chamber length gun",

---

[*] Usually in an x-t plot, as in the sketch, the projectile path is drawn as a single line which actually represents the path of the *back end* of the projectile.

and is designated by the notation "$x_0 = \infty$". The behavior of the projectile in such a gun is unaffected by the presence of the back or breech end; the projectile performance is the same as it would be in a gun whose chamber length were truly infinite. Thus, the gas behind the projectile in an infinite chamber length gun is characterized by Equations (8-1), (8-2), and (8-3).

Section 9

Role of the Acoustic Inertia in the
$D_0/D_1 = 1$, $x_0 = \infty$, PP Gun

In Section 6 it was noted that, for the expansion of a gas in a tube, the acoustic impedance $a\rho$ plays the role of the inertia of the gas. For the $x_0 = \infty$, $D_0/D_1 = 1$, PP Gun the acoustic impedance may be directly related to the pressure drop behind the projectile.

Thus, Equation (8-1) describes any part of the gas behind the projectile in an $x_0 = \infty$, $D_0/D_1 = 1$, gun; it may be rewritten as

$$dp = -a\rho du .$$ (9-1)

(This is in contrast to the situation in a PP gun which has $D_0/D_1 = 1$ and x_0 not equal to ∞, for then Equation (9-1) only applies to "u + a" disturbances.) From Equation (9-1) it is apparent that, when the velocity increases behind the projectile, the pressure decreases. Moreover, Equation (9-1) indicates that the drop in pressure for a given velocity increase is directly proportional to $a\rho$. Thus, in this unsteady expansion process the measure of the propelling gas inertia is $a\rho$; *the drop in the pressure of the propelling gas (and, in particular, of the gas directly behind the projectile) is a direct result of the gas inertia* $a\rho$ *(and an inevitable result unless* $a\rho$ *can be made zero).*

Equation (9-1) may be integrated to yield for the $D_0/D_1 = 1$, $x_0 = \infty$, PP gun the velocity of the gas at any point in the flow

$$u = \int_{p}^{p_0} \frac{dp}{a\rho} .$$ (9-2)

It is seen that the velocity of the gas expanding from rest at initial pressure p_0 in a $D_0/D_1 = 1$, $x_0 = \infty$, PP gun depends only on the acoustic impedance as a function of pressure for the isentrope.
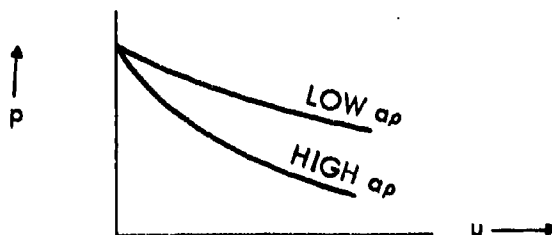
For a $D_0/D_1 = 1$, $x_0 = \infty$, *PP gun the relationship between* $a\rho$ *and* p *determines the entire propellant performance.*

Section 10

The Equation for the Projectile

By application of Newton's Law to the projectile one obtains

$$M \frac{du_p}{dt} = p_p A_1 \tag{10-1}$$

where p_p is the pressure directly behind the projectile and u_p is the velocity of the projectile. The barrel is here assumed evacuated and the frictional forces on the projectile are assumed negligible.

Section 11

The Equations for an Ideal Propellant Gas in a PP Gun With $D_0/D_1 = 1$. $x_0 = \infty$

The words "PPIG Gun" designating "Preburned Propellant Ideal Gas Gun" refer to a PP Gun with an ideal gas propellant.

An ideal (or perfect) gas is here defined by the following thermal and isentropic equations. (See Appendix J)

$$p = \rho RT \tag{11-1}$$

$$p = \rho^\gamma p_0 / \rho_0^{\ \gamma} \tag{11-2}$$

where the subscript "0" indicates the initial rest state from which the gas expands. The acoustic impedance becomes, for the isentrope

$$a\rho = p_0 \sqrt{\frac{\gamma}{RT_0}} \left(\frac{p}{p_0}\right)^{\frac{\gamma+1}{2\gamma}} = \frac{\gamma p_0}{a_0} \left(\frac{p}{p_0}\right)^{\frac{\gamma+1}{2\gamma}} \quad . \tag{11-3}$$

The sound velocity may be expressed for the ideal gas as

$$a^2 = \frac{\gamma p}{\rho} = \frac{\gamma \bar{R} T}{m} = \gamma RT \tag{11-4}$$

and the Riemann function is calculated to be

$$\sigma = \frac{2}{\gamma - 1} a \tag{11-5}$$

where σ is taken to be zero at $a = 0$.

The gun is shown in the following sketch just before the projectile is released.
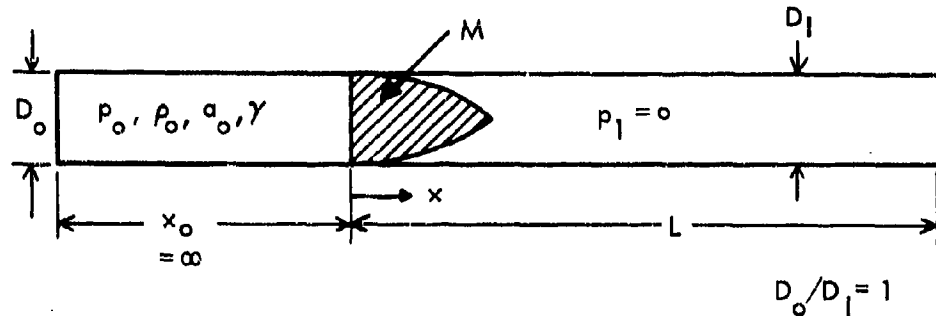
From Equations (8-2) and (11-3) the pressure may be related to the velocity for the expansion of the ideal gas in a constant diameter gun

$$\frac{p}{p_0} = \left(1 - \frac{u}{\frac{2}{\gamma-1} a_0}\right)^{\frac{2\gamma}{\gamma-1}} . \qquad (11-6)$$

In the limit of $\gamma = 1$, this equation assumes the form

$$\frac{p}{p_0} = e^{-u/a_0} \qquad (11-7)$$

Equation (11-6) is the pressure-velocity (p-u) relationship for an ideal gas expanding in a $D_0/D_1 = 1$, $x_0 = \infty$, PP Gun. It is an important equation in that it provides an insight into the factors determining the value of the propelling pressure. It applies to each part of the expanding gas; in particular, it applies to the gas behind the projectile.

Immediately apparent from Equation (11-6) is the fact that the magnitude of the dimensionless pressure p/p_0 primarily depends on the magnitude of the dimensionless velocity u/a_0 . For low speed guns, in which $u/a_0 \ll 1$, p/p_0 is nearly one, and the pressure drop is negligible. For high speed guns, the drop is seen to be devastating.

The effect of γ on the pressure drop is evident from the plot of Equation (11-6) for varying γ . This plot is shown in Figure 1 and in the upper sketch on the following page. It is noted from the plot that *the lower the γ the less is the pressure drop*, but the pressure drop is still present even when γ is equal to one.

As indicated before, of greater influence on the pressure drop is the gas initial sound speed a_0 . This is apparent if a plot of p versus u is made from Equation (11-6) for various initial sound speeds. Such a plot is shown in the lower sketch on the following page.
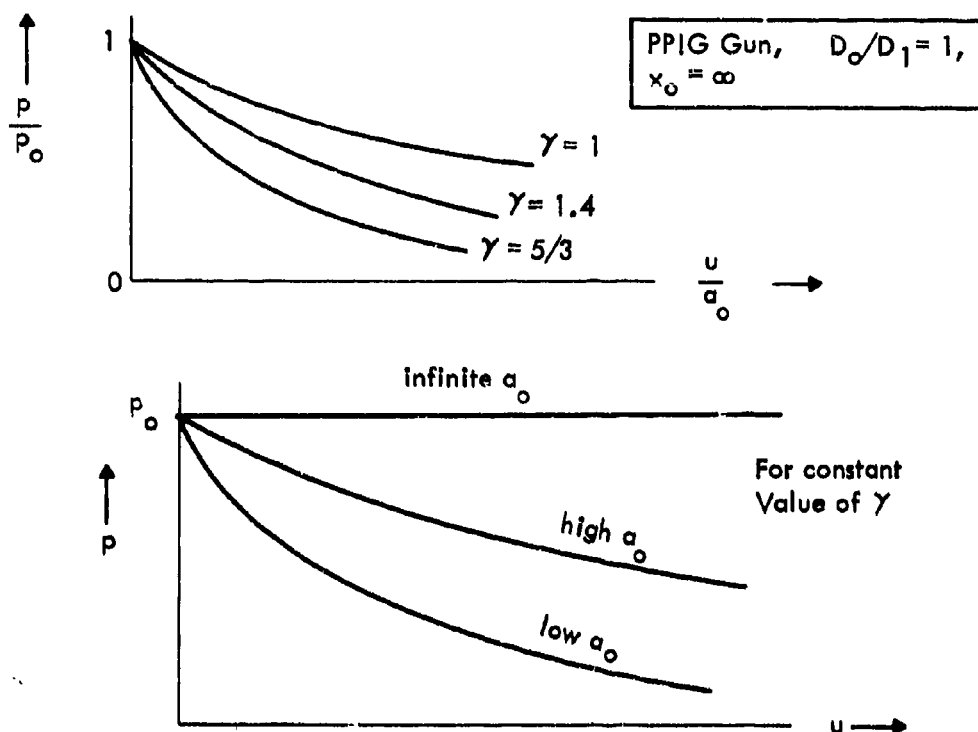
The higher the initial sound speed, the lower is the pressure drop. (This conclusion could have been arrived at by noting from Equation (11-3) that the acoustic impedance (which determines the pressure drop) of the ideal gas is inversely proportional to the initial sound speed.) Thus, for an ideal gas expanding in a $D_0/D_1 = 1$, $x_0 = \infty$, PP Gun, a gas with a high initial sound speed is required to minimize the pressure drop. If the initial sound speed is infinite, there is no drop in the pressure of the gas as its velocity increases.

It is seen from Equation (11-6) that the pressure drops to a value of zero when the gas velocity reaches a value of $2a_0/(\gamma-1)$*. This velocity is termed the "escape velocity".

$$u \text{ esc} = \frac{2}{(\gamma - 1)} a_0 \qquad (11-8)$$

for a $D_0/D_1 = 1$, $x_0 = \infty$, ideal gas expansion in a PP Gun. A gas, upon expanding to this velocity, can push no more since its pressure has dropped to zero. The escape velocity is one measure of the merit of a propellant gas; however, from Equation (11-6), which may be rewritten as

---

* For the limiting case of a $\gamma = 1$ gas, this quantity the "escape velocity", is infinite, as may be seen from Equation (11-7) or (11-8).

$$\frac{p}{p_0} = \left(1 - \frac{u}{u_{esc}}\right)^{\frac{2\gamma}{\gamma-1}} \tag{11-9}$$

it is seen that p/p_0 depends on γ as well as u_{esc}.

More insight into the relative roles of the propellant gas initial sound speed and specific heat ratio is provided by plotting p/p_0 from Equation (11-6) as a function of $a_0/\gamma u$. This plot is shown in Figure 2 and in the following sketch.
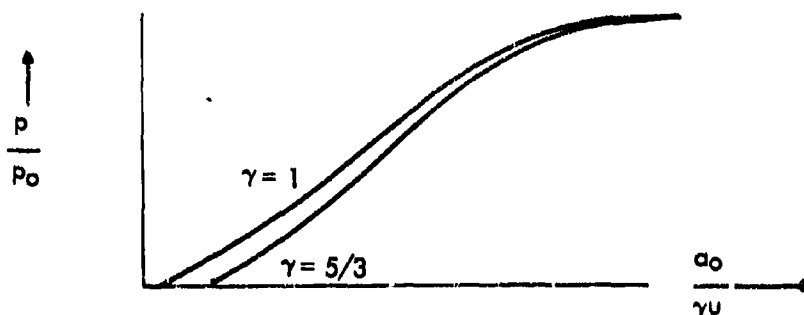
This plot is nearly a single curve for all γ values* with the equation

$$\frac{p}{p_0} = e^{-\gamma u/a_0} \tag{11-10}$$

approximating all the γ curves. Hence, *the pressure drop occurring at a given velocity may be thought of as depending essentially on the parameter a_0/γ*; the greater this parameter, the less is the pressure drop for a $D_0/D_1 = 1$, $x_0 = \infty$, PPIG Gun.

Since an increase in the gas initial sound speed is more effective and is more easily effected than a decrease in the specific heat ratio, a propellant gas with a high a_0 has been sought. For the ideal gas the sound speed is proportional to the square root of the temperature divided by the molecular weight. Thus, by the above considerations of the preburned propellant $D_0/D_1 = 1$, $x_0 = \infty$, gun *one is led to use as a propellant gas a low molecular weight gas*, such as hydrogen or helium at *elevated temperatures*.

---

* That this plot should be nearly a single curve results from the fact that a series expansion of Equation (11-6) reveals a dependence of p/p_0 only on $\gamma u/a_0$ for low values of $\gamma u/a_0$ and from the fact that, at high values of $\gamma u/a_0$, p/p_0 becomes zero at values of $a_0/\gamma u$ which are nearly the same. Also note that, for an ideal gas

$$\frac{\gamma u}{a_0} = \int_{p/p_0}^{1} \left(\frac{p}{p_0}\right)^{\frac{\gamma+1}{2\gamma}} d\left(\frac{p}{p_0}\right)$$

the integral of which is only weakly dependent on γ.

Section 12

The Equations for the Motion of the Projectile
Propelled in a $D_0/D_1 = 1$, $x_0 = \infty$, PPIG Gun

The behavior of a projectile propelled by an ideal gas in a $D_0/D_1 = 1$, $x_0 = \infty$, PP Gun may be obtained by inserting the expression for the gas pressure (Equation (11-6)) into Newton's Law for the projectile (Equation (10-1)). If this is done, and the integration performed, an analytic expression is obtained for the distance traveled by the projectile as a function of the projectile velocity.

$$\frac{p_0 A_1 x_p}{Ma_0^2} = \frac{2}{\gamma+1} \left\{ \frac{\dfrac{2}{\gamma-1} - \dfrac{\gamma+1}{\gamma-1}\left[1 - \dfrac{u_p(\gamma-1)}{2a_0}\right]}{\left[1 - \dfrac{u_p(\gamma-1)}{2a_0}\right]^{(\gamma+1)/(\gamma-1)}} + 1 \right\}$$

(12-1)

or

$$\frac{p_0 A_1 x_p}{Ma_0^2} = e^{u_p/a}\left(\frac{u_p}{a} - 1\right) + 1$$

(12-2)

for a $\gamma = 1$ gas. (See References 3, 4 and 5.)

Equation (12-2) is plotted for different values of γ in Figure 3 and in the following sketch.
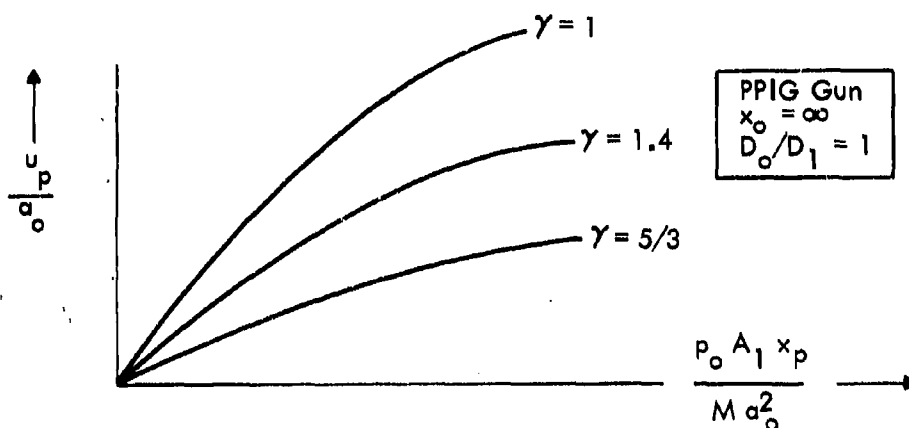
The ordinate in this figure is a dimensionless projectile velocity, u_p/a_0; the abscissa is the dimensionless distance traveled by the projectile, $p_0 A_1 x_p/Ma_0^2$.

It is noted from the Equation (12-1) that, as $p_0 A_1 x_p/Ma_0^2$ becomes infinite, $u_p(\gamma-1)/2a_0$ approaches one, i.e., the projectile velocity approaches the escape velocity. However, in practice *the projectile velocity is rarely, if ever, more*

than one half the escape speed*. This is a consequence of the fact that at the high
projectile speeds the propellant pressure p becomes so low (see Equation (11-6))
that gas and projectile frictional resistance and sometimes the gas pressure in front
of the projectile, neglected here, equal the propelling gas pressure force. The
effects of friction and gas pressure in front of the projectile are discussed in
Section 40.

A most useful presentation of Equation (12-1) may be obtained by plotting the
dimensionless projectile velocity u_p/u_0 versus dimensionless initial sound speed
$a_0/\gamma u_0$. The quantity u_0, defined as $\sqrt{(2p_0 A x_p/M)}$, is the projectile velocity
attainable if the projectile is propelled by a constant pressure p_0. This plot
is shown in Figure 4 and in the following sketch.
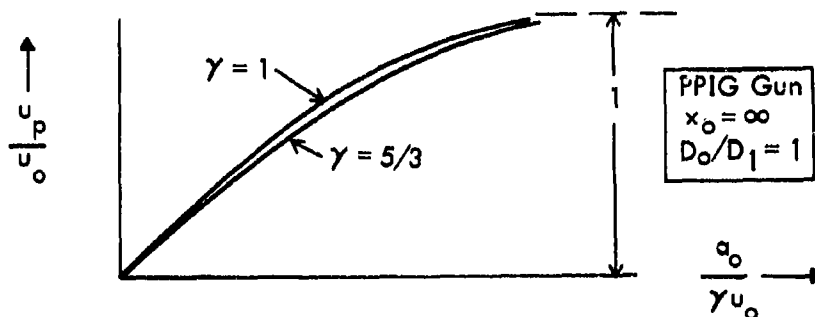
It is seen that this plot is nearly a single curve for all γ values[†].

The ordinate u_p/u_0 may be thought of as an efficiency of the propellant gas in
its ability to maintain the pressure behind the projectile at a value equal to p_0.
(Note: $u_p/u_0 = \bar{p}/p_0$.) It is seen that this efficiency is high for high dimensionless
sound speed and low for low dimensionless sound speed. Thus, *the propelling pressure
is only maintained at a high level by an ideal propellant gas when the initial sound
speed is high.*

Figure 4 illustrates the basic facts about a $D_0/D_1 = 1$, $x_0 = \infty$, PPIG Gun. *The
projectile velocity* for a gun of given geometry (of given AL/M) and initial propellant
pressure p_0 *is a function of essentially* a_0/γ *only.* A relatively high velocity
requires a relatively high a_0/γ. Moreover, a high efficiency (u_p/u_0) requires a
high value of $a_0/\gamma u_0$ or a low value of $\gamma u_p/a_0$ (as seen by the inclined lines of
constant $\gamma u_p/a_0$ in Figure 4). Since the projectile velocity mainly depends on
a_0/γ, the effect of a decrease in γ is seen to be the same as the effect of an
increase in initial sound speed a_0. Both change the ratio a_0/γ by the same amount.
By the same token a decrease in γ may be compensated for by that decrease in a_0
which would maintain the ratio a_0/γ the same.

---

* The velocity of the driver gas in a shocktube in which the initial driven gas pressure is made
as low as possible will approach more closely the escape speed.

† That this plot is nearly a single curve for all γ values follows from the fact that p_p/p_0
is approximately a function only of $a_0/\gamma u_p$ (see Equation (11-10)).

Since the value of γ for ideal gases may be altered relatively little (from $\gamma = 5/3$ to $\gamma = 1$), and not as desired, the ratio a_0/γ is practically increased only by increasing the sound speed a_0 ; in this way high projectile velocity is obtained in an $x_0 = \infty$, $D_0/D_1 = 1$, PPIG Gun.

Section 13

The Finite Chamber Length, $D_0/D_1 = 1$, PP Gun

If the length of the chamber is not effectively infinite, disturbances originating at the projectile reflect from the back end of the chamber, and subsequently reach the projectile (see Appendix D). Before these disturbances reach the projectile the motion of the entire gas is described by the simple wave relation, $u + \sigma = \sigma_0$. However, after reflections reach the projectile, the gas expansion is no longer a simple wave expansion, and the sum of $u + \sigma$ may be shown to be less than σ_0. Then, the equations which must be used are the characteristic equations (7-4) and (7-5) rewritten below.

$$u + \sigma = \text{a constant} \tag{13-1}$$

for lines of

$$dx/dt = u + a$$

$$u - \sigma = \text{a constant} \tag{13-2}$$

for lines of

$$dx/dt = u - a .$$

The gas equation of state relations are, for the isentrope,

$$p = p(\rho) \tag{13-3}$$

$$a = a(\rho) \quad \text{for a given entropy} \tag{13-4}$$

$$\sigma = \sigma(\rho) \tag{13-5}$$

and Newton's Law for the projectile is

$$M \frac{du_p}{dt} = p_p A , \tag{13-6}$$

The solution of these equations in the finite chamber length, constant diameter, gun case requires a numerical step-by-step procedure which can be done by hand computing, as outlined in Appendix E.

Obtaining the chamber length x_0 necessary to be effectively infinite requires a calculation of the path of the first reflected impulses. For a PP Gun of constant diameter *with an ideal propellant gas*, Heybey[3] has obtained an analytic expression for x_0 as a function of the velocity of the projectile ($u_{p_{1st}}$) at which the
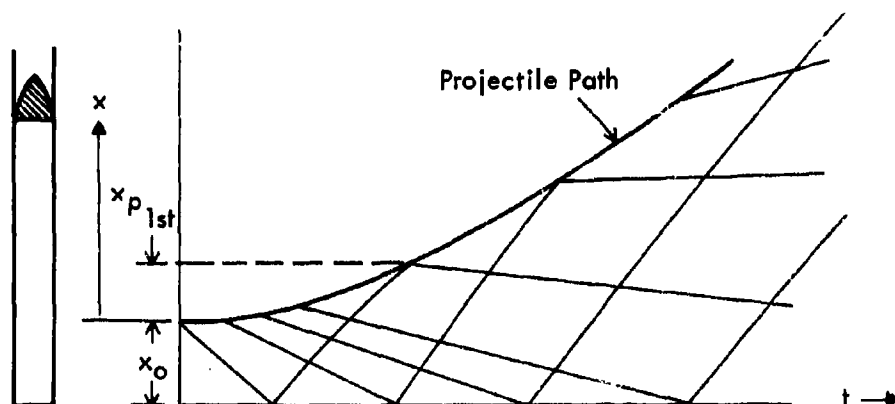
first reflected impulse reaches the projectile. This may be transformed to yield

$$\frac{p_0 A_1 x_0}{M a_0^2} = \frac{2}{\gamma + 1} \left\{ \frac{1}{\left[1 - \frac{u_{p_{1st}}(\gamma - 1)}{2 a_0} \right]^{(\gamma + 1)/2(\gamma - 1)}} - 1 \right\}$$ (13-7)

which for $\gamma = 1$ becomes

$$\frac{p_0 A_1 x_0}{M a_0^2} = e^{u_{p_{1st}}/2 a_0} - 1$$ (13-8)
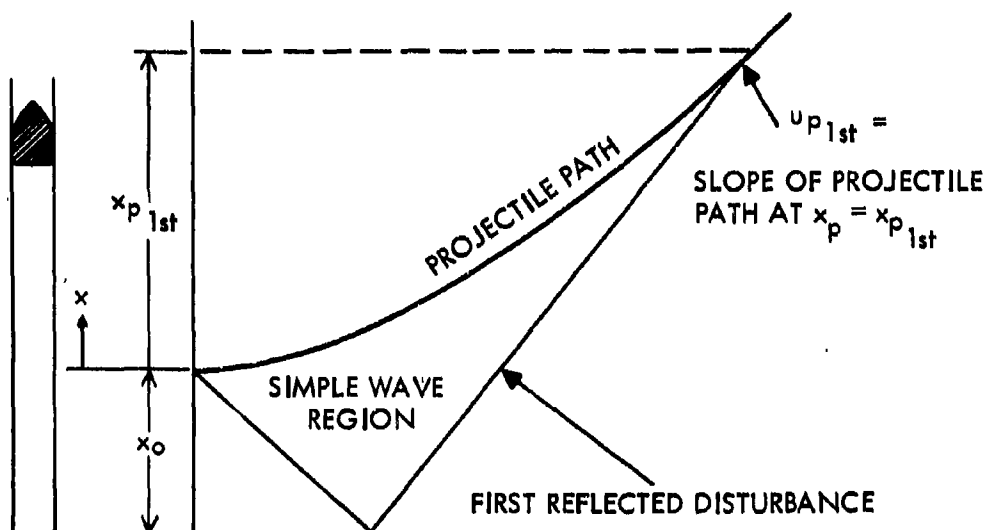
From Equation (13-8), and from the projectile u_p versus x_p relation of Equation (12-1), x_0 may be plotted as a function of the distance traveled by the projectile, $x_{p_{1st}}$, when the first reflected wave reaches it. This is done in Figure 5 and in

the following sketch, from which it is noted that $x_{p_{1st}}/x_0$ is proportional to x_0. From the figure

$$\frac{x_{p_{1st}}}{x_0} \simeq 2.5 \frac{p_0 A_1 x_0}{Ma_0^2}$$

(13-9)
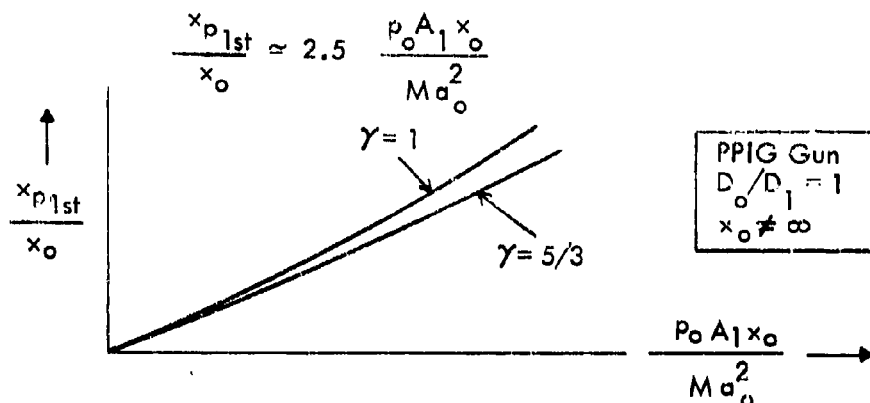
The disturbances reflected from the back of the chamber "transmit" the information that there is a finite quantity of gas in the chamber. The effect of these reflected disturbances is to decrease the pressure behind the projectile below that which it would be without reflections; this is illustrated in the following sketch, which is a plot of the pressure behind the projectile as a function of projectile velocity.
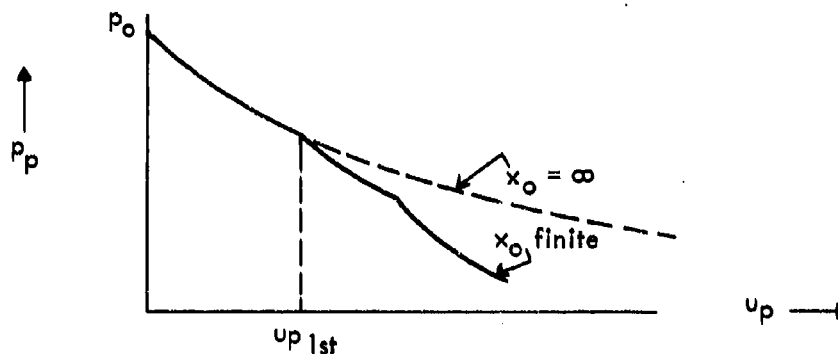
This plot can be redone in terms of dimensionless pressure p_p/p_0 versus dimensionless velocity u_p/a_0. This is shown in the sketch on the following page. Each dimensionless chamber length $p_0 Ax_0/Ma_0^2$ would have a different p_p/p_0 versus u_p/a_0 curve after the first reflection has reached the projectile. It is noted from these sketches that each time the reflection from the back end of the first reflection reaches the projectile, the pressure-velocity plot has a discontinuity of slope. However, a velocity-travel plot of the projectile is found not to have an obvious discontinuity of slope.

$$\frac{p_0 A x_0}{M a_0^2} = \text{infinite}$$

$$\frac{p_0 A x_0}{M a_0^2} = \text{finite}$$

$\dfrac{p_p}{p_0}$

$\dfrac{u_{p\,1st}}{a_0}$

$\dfrac{u_p}{a_0} \longrightarrow$

$x_0 = \infty$

$x_0 = \text{finite}$

$u_{p\,1st}$

u_p

x_{p1st}

$x_p \longrightarrow$
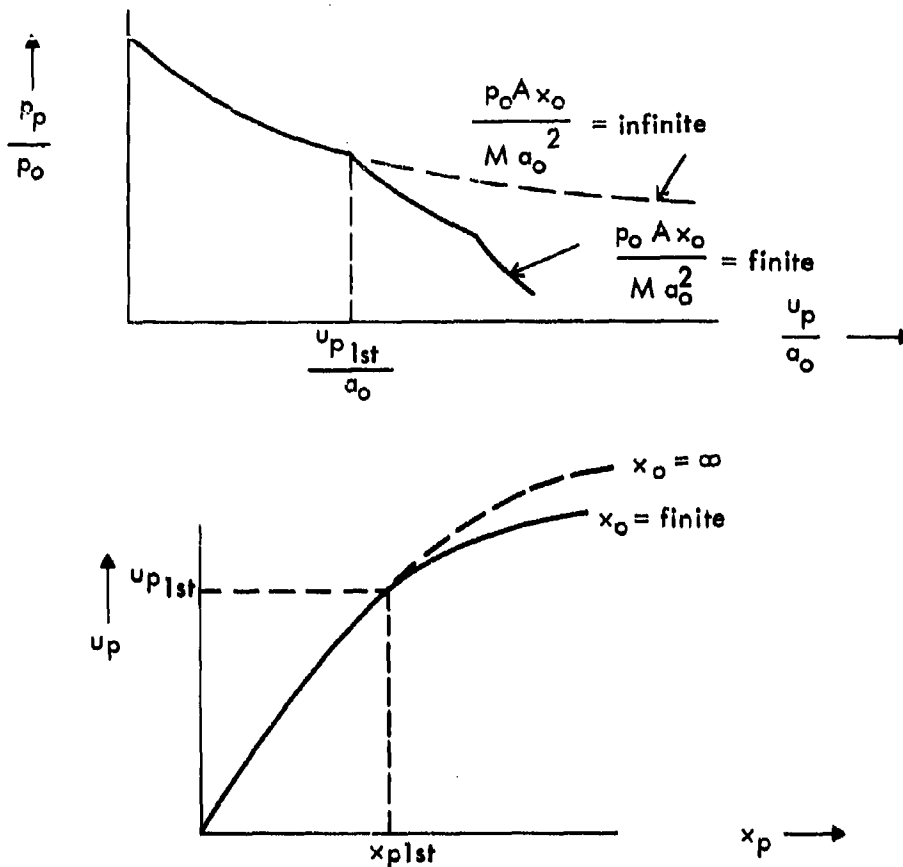
In the case of an effectively infinite length chamber the performance of the projectile may be expressed in terms of dimensionless projectile velocity (u_p/a_0) versus dimensionless travel distance $(p_0 A x_p/Ma_0^2)$. In the finite length chamber preburned propellant gun, a numerical solution may be calculated for each dimensionless chamber length $(\bar{x}_0 = p_0 A x_0/Ma_0^2)$. Thus, a dimensionless velocity versus travel plot for various dimensionless chamber lengths may be obtained. Such a plot is shown in Figure 6 for a $\gamma = 1.4$ gas. The points where the finite x_0 curves depart from the $x_0 = \infty$ curve may be calculated from equation (12-7) or obtained from Figures 3 and 5.

Classically, the dimensionless parameter G/M where G is the mass of the gas in the chamber, has been shown to be an important interior ballistics parameter (see Appendix F). The dimensionless chamber length $\bar{x}_0$ may be transformed into the dimensionless mass ratio G/M by the relation

$$\bar{x}_0 = \frac{p_0 A_1 x_0}{Ma_0^2} = \frac{G}{\gamma M} \tag{13-10}$$

PPIG Gun
$D_0/D_1 = 1$
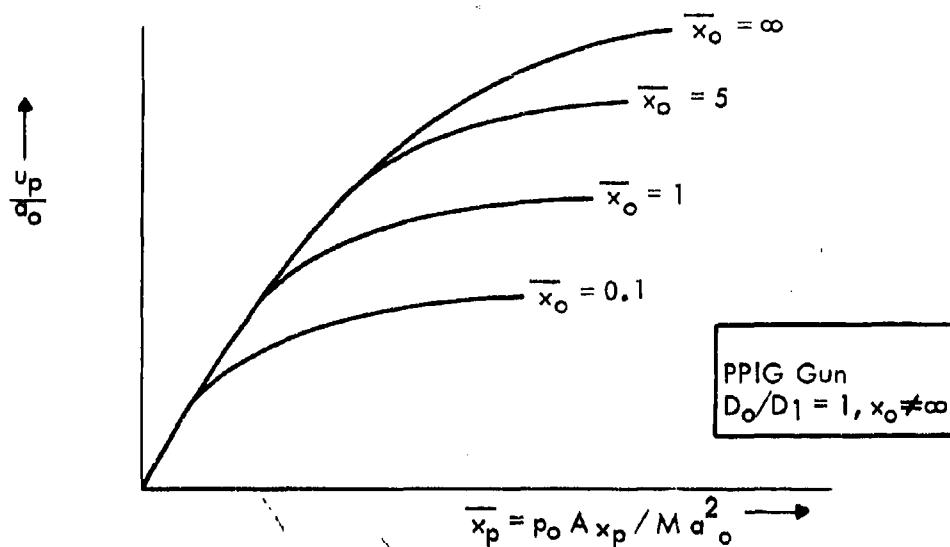
where the ideal gas relation $\gamma p_0 / \rho_0 = a_0^2$ has been used. The performance curves for a finite chamber length gun now take the form shown in the following sketch.
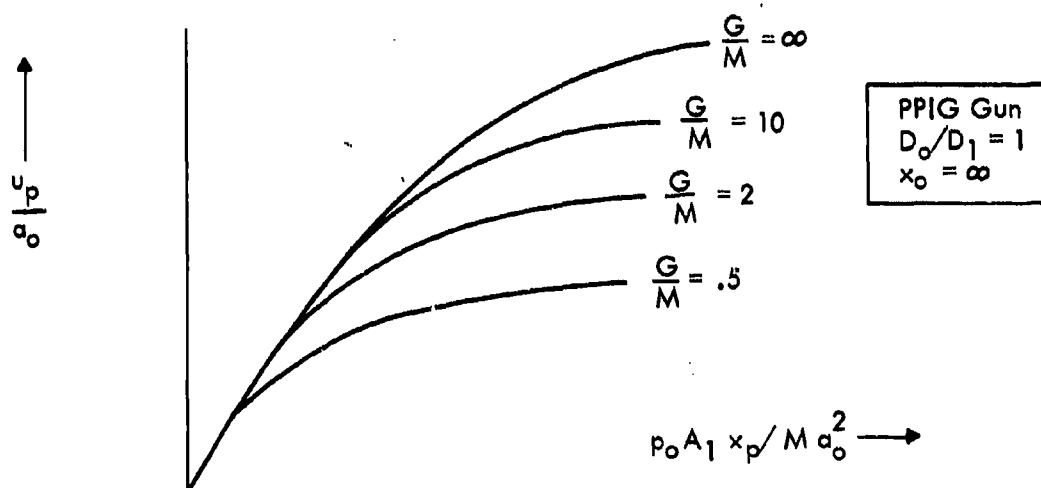
A plot such as this is given in Figure 7 for the $\gamma = 1.4$ gas. Other plots for different γ values are given in the $D_0/D_1 = 1$ plots of Figures 20 and 21. Hence, the behavior of a projectile propelled by an ideal gas in a preburned propellant gun with constant diameter and finite chamber length is fully specified by the plots in these figures*.

---

* These plots are the results of numerical calculation using the characteristic equations above and are further described in Part V.

PART IV. THE CHAMBERED PREBURNED PROPELLANT GUN

Section 14

Qualitative Discussion of the $D_0/D_1 > 1$, PP Gun

The chambered gun consists of a chamber joined to a smaller diameter barrel, as shown in the following sketch.
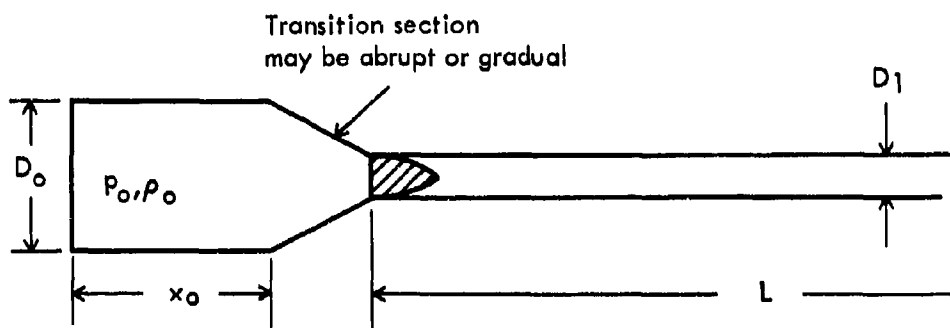
In conventional ballistics calculations chambrage is treated by assuming that the actual chamber can be replaced by an equal volume imagined chamber of cross-sectional area equal to the bore cross-sectional area (see Special Solution discussion in Appendix F); thus the performance of a gun is considered only a function of the gas to projectile mass, G/M, and is not dependent upon the geometry of the chamber. That this is not a valid procedure is evident from the discussion that follows.

It seems reasonable that the greater the chambrage of a gun the greater is the proportion of the rarefaction (which had previously come from the projectile) that is reflected at the transition section as a compression. One may consider that for an infinite D_0/D_1 gun no part of the reflected rarefaction produced from the projectile will be transmitted through the transition section as a rarefaction; all of it would be reflect as a compression moving toward the projectile.

The length of the chamber, x_0, determines the time taken for rarefactions to reflect from the breech; the smaller x_0 is, the more quickly the reflections reach the projectile and tend to lower the projectile velocity. Also, the smaller the x_0, the more quickly the rarefactions travel back and forth in the chamber and lower the pressure in the chamber.

Hence, one concludes that increasing either the chamber length x_0 or the chamber diameter D_0 will increase the projectile velocity. However, increasing D_0 provides the opportunity of increasing the projectile velocity to a greater value than by increasing x_0; this is seen from the following example: With infinite x_0 and finite D_0 equal to diameter of the bore, the projectile receives neither reflected rarefactions nor compressions. However, with infinite D_0 and finite x_0 the projectile receives

only compression impulses and as a result the projectile velocity is greater than in the finite D_0 infinite x_0 case.

It will be shown in Section 28 that the numerical results for chambered gun performance with an ideal propellant gas indicates the following:

(a) For PPIG guns with equal G/M, the larger the chambrage, the larger will be the projectile velocity in the initial stages of motion (before a number of reflections have occurred between breech and projectile).

(b) For PPIG guns with equal G/M, in the latter stages of motion (after a number of reflections have occurred), the projectile velocities will be approximately the same for all guns, no matter the value of the chambrage.

(c) In agreement with (a) for an infinite value of G/M (in which case no reflections come from the breech), the greater the chambrage, the greater will be the projectile velocity for PPIG guns.

Section 15

The Gas Dynamics Equations for a Chambered PP Gun

In order to determine analytically the behavior of the expanding propellant gas in a chambered gun, the assumption is again here made for convenience that the flow is isentropic (see Section 40 for the non-isentropic case).

The previously derived one-dimensional characteristic equations are applicable to the constant diameter chamber and are applicable to the constant diameter barrel.

$$\frac{D(u \pm \sigma)}{Dt} = 0 \qquad (15\text{-}1)$$
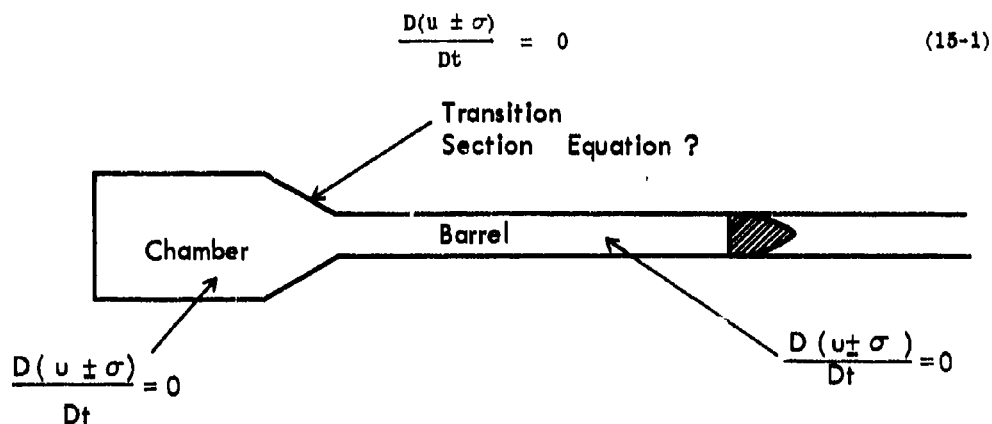
The gas flow in the transition section, which joins the chamber to the bore, is actually a two-dimensional unsteady flow. However, it is not feasible to solve the two-dimensional unsteady equations. There are two possible approximate methods of treating the flow through the transition section. The first method is to assume that the change in area from the chamber to the barrel occurs gradually so that the flow

may be assumed to be one-dimensional. Then, the one-dimensional characteristic method can be applied to this change in area section. The characteristic equations become, for the change in area section,

$$\frac{D(u \pm \sigma)}{Dt} = \frac{\partial}{\partial t}(u \pm \sigma) + (u \pm a)\frac{\partial}{\partial x}(u \pm \sigma) = \mp \frac{au}{A}\frac{dA}{dx} \qquad (15\text{-}2)$$

where u is the gas velocity, a is the sound speed, σ is the Riemann function, and A is the cross-sectional area of the gas layer at position x in time t. (For the derivation and application of these equations see, for example, Reference 5, 6, 7 or 8.) These equations require a tedious numerical procedure to solve, and are generally not suitable for hand computation. It is to be noted, however, that the quantity $u \pm \sigma$, in contrast to the constant diameter case, does not remain constant for disturbances in the transition section.

The second approach, and one chosen to be employed here as being more convenient and a good approximation to the actual situation, is to assume the following: *At any given time the rate of change of mass and energy within the transition section is negligible relative to the differences between the exit and entrance fluxes of these quantities;* thus, the changes due to variations of time are assumed negligible relative to those due to the variations in position within the control volume. This assumption is made clear by taking as a control volume the transition section as shown in the following sketch.
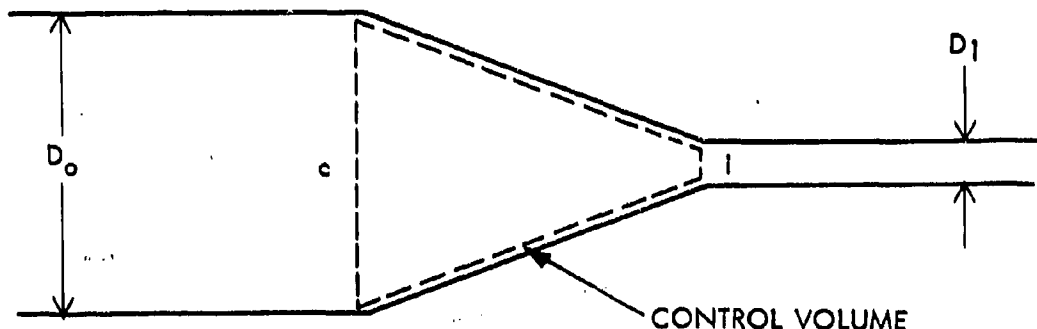
Then the applicable equations[8] of continuity and energy are, respectively*

$$\left(\frac{\partial m}{\partial t}\right)_{Con\ Vol} = (\rho uA)_c - (\rho uA)_i \qquad (15\text{-}3)$$

and

$$\left(\frac{\partial E}{\partial t}\right)_{Con\ Vol} = \left[\left(h + \frac{u^2}{2}\right)(\rho uA)\right]_c - \left[\left(h + \frac{u^2}{2}\right)(\rho uA)\right]_i \qquad (15\text{-}4)$$

---

* Although it is not assumed that the flow within the transition section is necessarily one-dimensional, it is assumed that the flow at the entrance and exit planes of the transition section is one-dimensional.

where m and E are the mass and internal energy in the transition section. By our assumption above, the two unsteady terms on the left hand sides of Equations (15-3) and (15-4) are negligible.

It is to be observed that, if the transition is rather sudden, the control volume is small; hence, the unsteady terms on the left of these equations being proportional to the magnitude of the control volume, are necessarily small; thus, in the case of a sudden transition, the assumption above is automatically valid.

With this assumption the equations which are applicable to relate the conditions at the entrance of a transition section to those at the exit of the transition section are the quasi-steady equations of continuity and energy. Thus, *at each instant of time*, the applicable equations are

$$h_c + \frac{u_c^2}{2} = h_1 + \frac{u_1^2}{2} = \text{function of time} \tag{15-5}$$

$$\rho_c u_c A_c = \rho_1 u_1 A_1 = \text{function of time} \tag{15-6}$$

Since the flow has been assumed isentropic, the thermodynamic relation between enthalpy and pressure is

$$dh = (dp/\rho)_s \tag{15-7}$$

and

$$h_1 - h_c = \int_{p_c}^{p_1} dp/\rho . \tag{15-8}$$

Equation (15-5) becomes

$$\frac{u_1^2 - u_c^2}{2} = \int_{p_1}^{p_c} dp/\rho . \tag{15-9}$$

It is shown in Reference 9 and may be shown from Equations (15-3) and (15-4) that the use of the quasi-steady flow equations to describe the gas flow between the chamber and barrel of the gun yields a larger projectile velocity than would be yielded by the use of the actually applicable unsteady equations. However, experimental results from a chambered preburned propellant gun by Seigel and Dawson[10] have demonstrated that the difference was sufficiently small as to be unmeasurable. These experiments were made with a gun using room temperature air at about 3,000 lb/in^2 as a propellant. The gun had a 0.50 in diameter barrel which could be joined to various chambers of varying diameter up to 2.5 in. The chambers were joined to the barrel by means of a 30° half-angle taper*. The projectiles were one-gram plastic projectiles which were sheared by the compressed air in the chamber. A schematic of the gun system is shown in Figure 8(a). The measured projectile velocities were compared to the theoretically predicted velocities based on the use of the quasi-steady equations above. (These theoretically predicted velocities will be discussed below.) The comparison is shown in Figure 8(b). It is observed from the figure that *the quasi-steady flow approximation in the transition section yields good agreement with experiment*.

---

* The experimental results, based on one test with a 90° half-angle taper, seem not to depend on the magnitude of the angle of taper.

The following sketch shows the characteristics diagram for a chambered PP Gun
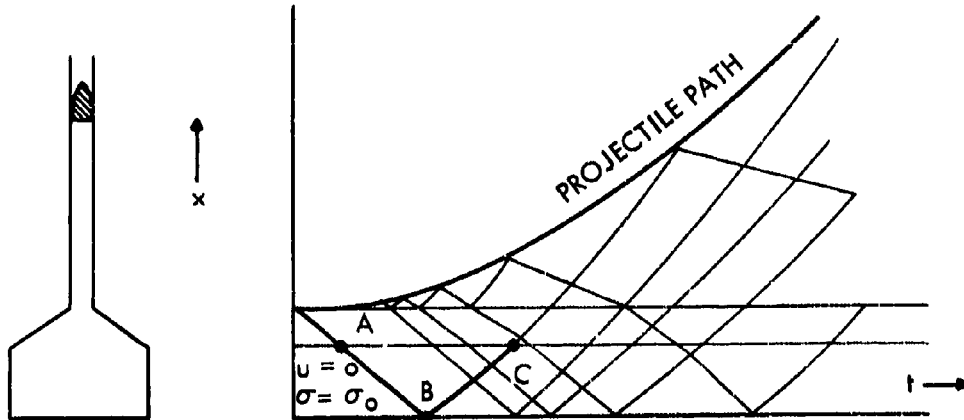
Characteristics may be drawn in the transition section by fairing them from the known conditions at the inlet to the known conditions at the exit. The simple wave region in the chamber for which $u + \sigma = \sigma_0$ is denoted by the letters A-B-C .

With Equations (15-1), (15-6) and (15-8) and the isentropic equation of state of the gas, it is possible to calculate quantitatively the behavior of the projectile in a preburned propellant chambered gun.

Section 16

Demonstration of the Advantage of Chambrage
for the PP Gun with $x_0 = \infty$

The preburned propellant guns to be compared are a constant diameter gun and a chambered gun, both having infinite length chambers. It has been shown that, for the $x_0 = \infty$ constant diameter PP gun, the sum $u + \sigma$ is always equal to a constant value, σ_0 . However, it will be shown below that for a chambered PP gun with $x_0 = \infty$, the sum of $u + \sigma$ behind the projectile is greater than σ_0 ; consequently, the projectile velocity is greater for a chambered gun than for a constant diameter gun.

Let us examine a chambered PP gun with $x_0 = \infty$. Since the chamber is infinitely long, there exists a simple wave region in the chamber. Hence, $u + \sigma = \sigma_0$ in the chamber, and, in particular, at the entrance to the transition section position "o",

$$u_0 + \sigma_0 = \sigma_0 . \tag{16-1}$$

Within the transition section at any time the quasi-steady flow equation applies, which becomes in the differential form

$$u du = -dp/\rho . \tag{16-2}$$
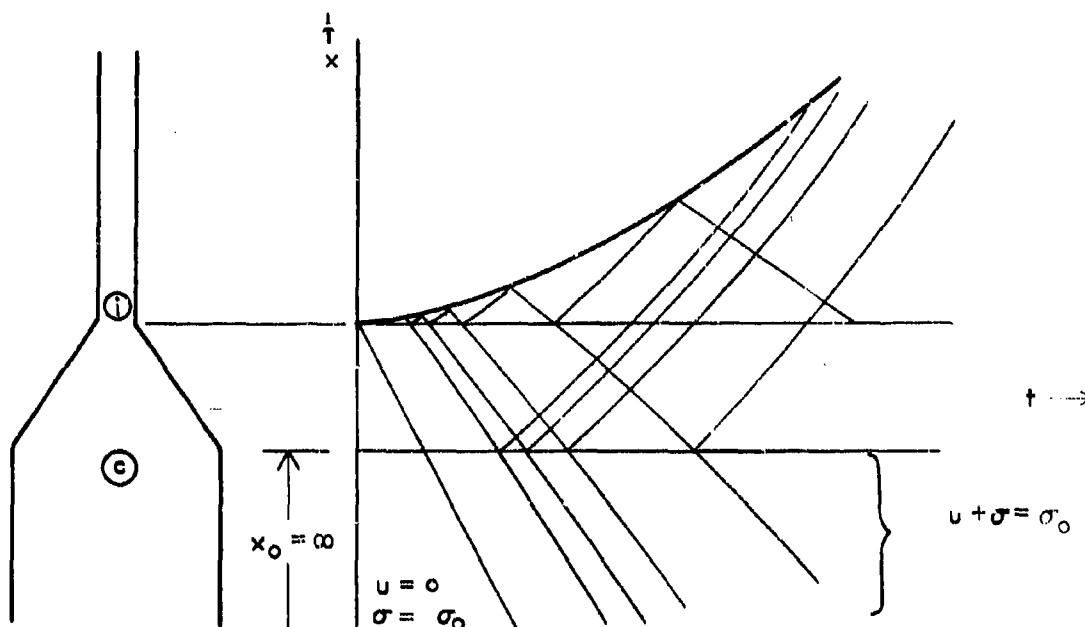
The differential change in $u + \sigma$ in the transition section is, from the definition of σ and from Equation (16-2),

$$d(u + \sigma) = du + d\sigma = du + \frac{dp}{a\rho}$$

$$= du\left(1 - \frac{u}{a}\right) = du(1 - M) \qquad (16\text{-}3)$$

where M is the Mach number in the transition section.

Equation (16-3) demonstrates that $u + \sigma$ *increases in the transition section*, since the flow there is always subsonic. Hence, at the entrance to the barrel, and consequently at the projectile*,

$$u_p + \sigma_p > \sigma_0 \qquad (16\text{-}4)$$

Since σ is a monotonic function of pressure, the greater the quantity $u + \sigma$ behind the projectile, the greater will be the projectile velocity. It is thus concluded that *the projectile velocity in a chambered* $x_0 = \infty$, *PP gun will be greater than that in a* $D_0/D_1 = 1$, $x_0 = \infty$, *gun.*

---

* The same result may be arrived at by examining the characteristic equations (15-2) which apply in an area change.
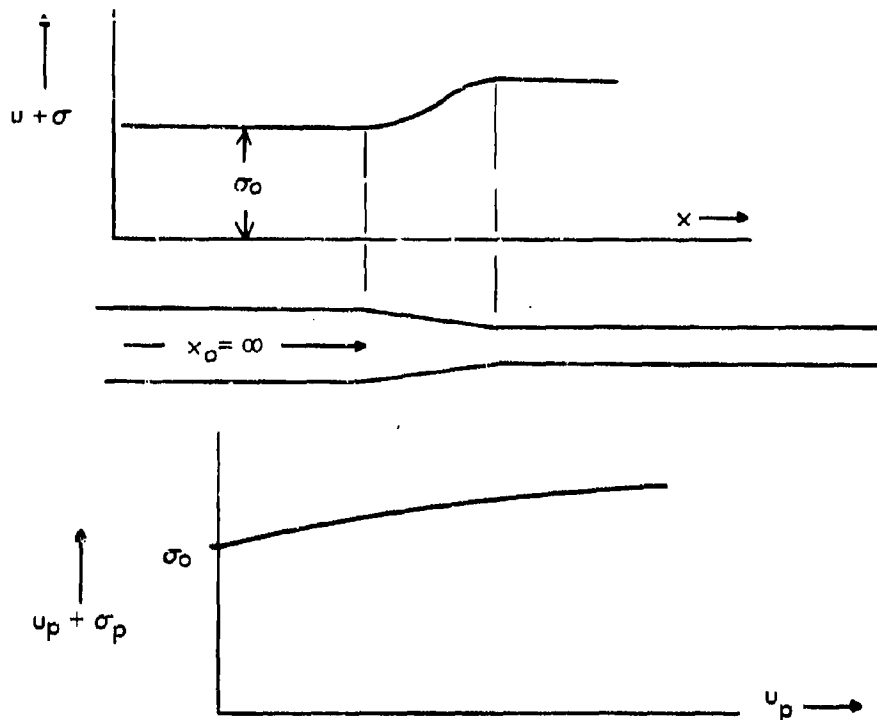
This result *is true regardless of the equation of state of the gas.*

It is noted that the velocity increase in the transition section is

$$udu = -\frac{dp}{\rho} \quad . \tag{16-5}$$

This is in contrast to the expression for the velocity increase in the constant diameter, $x_0 = \infty$, chamber flow which is

$$du = -\frac{dp}{a\rho} \quad . \tag{16-6}$$

It is thus seen that although a low "$a\rho$" as a function of p is desirable for the expansion in the constant diameter, $x_0 = \infty$, chamber, a low "ρ" as a function of p is desirable for the expansion in the transition section of such a gun. In the case of an ideal gas, both $a\rho$ and ρ are inversely proportional to the initial sound speed. Thus, the higher the initial sound speed, the greater will be the projectile velocity in a chambered or unchambered gun. However, in the case of a gun in which the propellant behavior is non-ideal, the performance is not specified by the initial sound speed, as will be shown in Section 63.

Section 17

The Special Case of the PP Gun with Infinite Chambrage

If the diameter of the chamber is infinitely large relative to that of the barrel, the quasi-steady equation of continuity yields

$$u_c = \frac{\rho_i}{\rho_c} \frac{A_i}{A_c} \doteq 0 \ . \tag{17-1}$$

Therefore, the gas remains virtually at rest at the entrance to the transition section and its pressure, density, etc., do not change from their initial values. Thus,

$$p_c = p_0 \tag{17-2}$$

$$\rho_c = \rho_0 \ . \tag{17-3}$$

Equation (15-9) for the barrel entry velocity becomes

$$\frac{u_i^2}{2} = \int_{p_i}^{p_c} \frac{dp}{\rho} \ . \tag{17-4}$$

The unsteady constant cross-sectional area characteristic equations apply in the barrel, so that, in particular,

$$u_p + \sigma_p = u_i + \sigma_i \ . \tag{17-5}$$

Equations (17-4) and (17-5), with Newton's equation for the projectile and the equation of state of the gas, are sufficient to determine the behavior in this gun. The characteristics diagram appears as sketched.
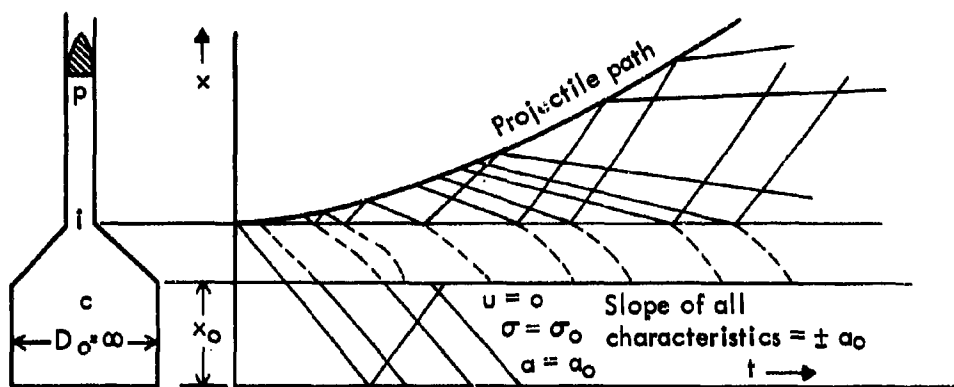
In the chamber the gas remains substantially at rest in its initial state, and all the characteristic lines there have a slope of $\pm a_0$. Numerical computation need only be done for the barrel section, and this fact simplifies such computation for

the $\bar{D}_0/\bar{D}_1 = \omega$, PP Gun. The length of the chamber x_0 for this case has absolutely no influence, because by assuming infinite chambrage an infinite quantity of propellant gas is assumed to be in the chamber.

Numerical results for this infinite chambrage case are given below.

Section 18

The General Equations for the Chambered
PP Gun with Effectively Infinite Length Chamber

As in the situation of a gun with no chambrage, a gun with chambrage may have an "effectively infinite length chamber" ($x_0 = \infty$); in that case the chamber length x_0 is sufficiently long that rarefactions from the back end of the chamber do not reach the projectile during its travel in the barrel.
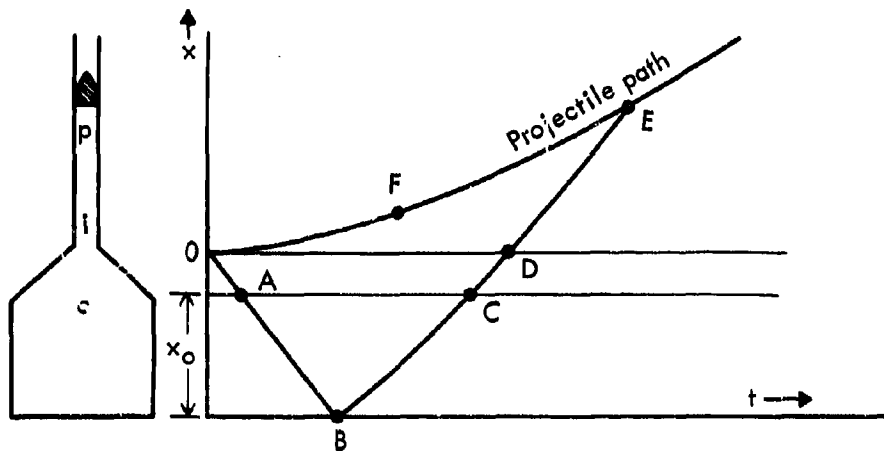
Thus, in the sketch, O-F-E represents the projectile path; the first disturbance O-A-B , upon reflection from the back end, reaches the projectile at E . The region in the chamber (A-B-C in the x-t diagram) where reflections have not reached is therefore a simple wave region, entirely describable by the equation

$$u + \sigma = \sigma_0 \quad . \tag{18-1}$$

In particular, this equation may be applied at the entrance to the transition section, so that

$$u_0 + \sigma_0 = \sigma_0 \quad . \tag{18-2}$$

The conditions at (c) may be related to those at (i) by the quasi-steady Equations (15-6) and (15-9).

$$(\rho u A)_0 = (\rho u A)_1 \tag{18-3}$$

$$\frac{u_0^2}{2} + h_0 = \frac{u_1^2}{2} + h_1 \quad . \tag{18-4}$$

The characteristic equations apply to the barrel section, viz.,

$$\frac{D(u \pm \sigma)}{Dt} = 0 \quad . \tag{18-5}$$

With the assumption that the projectile is unopposed by frictional forces or gas pressure in front, the projectile motion is described by the equation

$$M \frac{du_p}{dt} = A_1 p_p \quad . \tag{18-6}$$

The equation of state of the isentropic expansion of the gas may be expressed as

$$\left. \begin{array}{rcl} p &=& p(\sigma) \\[2mm] \rho &=& \rho(\sigma) \\[2mm] h &=& h(\sigma) \\[2mm] a &=& a(\sigma) \end{array} \right\} \text{ for the isentropic} \quad . \tag{18-7}$$

The complete behavior of gas and projectile in an $x_0 = \infty$, PP gun may be obtained from Equations (18-1) through (18-7).

Section 19

The Conditions at the Barrel Entrance in a PP Chambered Gun with $x_0 = \infty$

Let the $u - a$ disturbances coming from a projectile in a PP chambered gun with $x_0 = \infty$ be examined. As the projectile velocity increases, the velocity u of the gas behind the projectile increases, and the sound speed a decreases. Thus, the quantity $u - a$, the disturbance speed, increases. This is evident in an x-t diagram (as sketched) by the increase in slope of the $u - a$ lines.
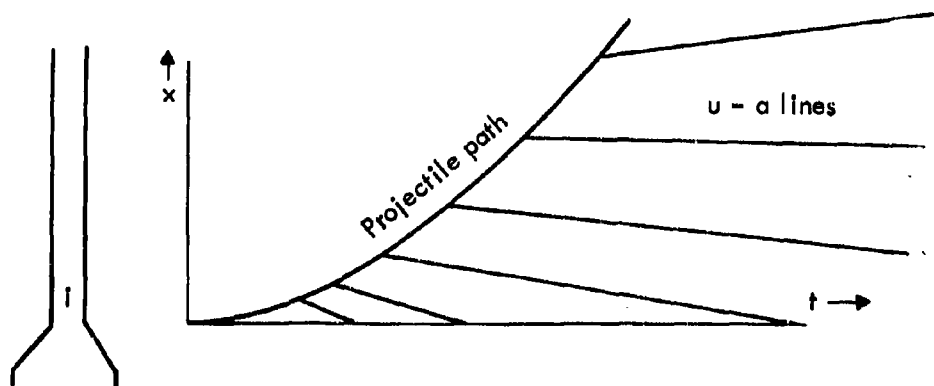
As time elapses, the slope of the $u - a$ disturbance lines at the barrel entrance approaches zero, i.e., the flow approaches the sonic (Mach one) condition. As seen in the sketch, the slope $u - a$ changes more and more slowly as time goes on and the flow approaches sonic; thus steady flow is approached with increasing time.
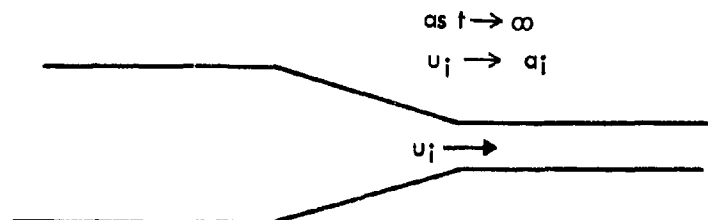
Moreover, it is obvious from the x-t characteristics diagram that the slope of the $u - a$ disturbance coming from the projectile cannot be greater than zero at the barrel entrance; if the slope of the $u - a$ disturbance line would be greater than zero it would not reach the barrel entrance but would travel away from it.

The fact that at large times the flow becomes steady and sonic in the barrel entrance of an $x_0 = \infty$, PP Gun is often used to approximate the flow at earlier times (see Section 25).

Section 20

Equations for the $x_0 = \infty$, Chambered PP Gun with an Ideal Gas Propellant

For the case of an ideal propellant gas the sound speed, enthalpy, pressure, and density are simply related to the Riemann function (see Appendix I).

$$a = (\gamma - 1)\sigma/2 \tag{20-1}$$

$$h = a^2/(\gamma - 1) = (\gamma - 1)\sigma^2/4 \tag{20-2}$$

$$p = p_0(\sigma/\sigma_0)^{2\gamma/(\gamma-1)} \tag{20-3}$$

$$\rho = \rho_0(\sigma/\sigma_0)^{2/(\gamma-1)} \ . \tag{20-4}$$

With the above relations, the general equations in Section 18 for the $x_0 = \infty$, chambered PP Gun may then be expressed in terms of the two independent variables, u and σ, as follows:

(a) the simple wave characteristic equation relating the conditions of the gas at any point in the chamber with the rest conditions at the breech

$$u + \sigma = \sigma_0 \tag{20-5}$$

(b) the above equation applied to the conditions of the gas at the entrance to the transition section

$$u_c + \sigma_c = \sigma_0 \qquad (20\text{-}6)$$

(c) the quasi-steady continuity and momentum equations relating conditions at the entrance to those at the exit of the transition section

$$(\sigma_1/\sigma_0)^{2(\gamma-1)} = A_0 u_0/A_1 u_1 = A_0 u_1/A_1 u_1 \qquad (20\text{-}7)$$

$$u_0^2/2 + (\gamma - 1)\sigma_c^2/4 = u_1^2/2 + (\gamma - 1)\sigma_1^2/4 \qquad (20\text{-}8)$$

(d) the characteristic equations in the barrel

$$\frac{D}{Dt}(u \pm \sigma) = 0 \qquad (20\text{-}9)$$

(e) and Newton's equation for the projectile acceleration

$$M\frac{du_p}{dt} = p_0 A_1 (\sigma_p/\sigma_0)^{2\gamma/(\gamma-1)} \quad . \qquad (20\text{-}10)$$

From Equations (20-5) through (20-10), the entire behavior of the gas and projectile can be computed for a PPIG chambered gun with an effectively infinite length chamber. The actual numerical technique for so doing is outlined in Reference 11. Discussion of the results of numerical computations of these equations is given in Section 28.

Section 21

Obtaining the Maximum Projectile Velocity (Escape Velocity) for the Chambered PPIG Gun with an $x_0 = \infty$ Chamber

By the use of the equations presented in Section 18, the maximum projectile velocity (which is the same as the escape velocity) can be obtained as a function of the ratio of chamber diameter to barrel diameter. In an $x_0 = \infty$ PP Gun, the maximum projectile velocity is attained by an unopposed projectile in the limit of infinite travel in the barrel, for then the propelling pressure becomes zero. Although this velocity is an idealized limit, it is instructive to see the effect of chambrage on this limit.

As the projectile velocity increases in the chambered gun with infinite chamber length and infinite barrel length, steady state conditions in the transition section are approached, and the velocity at the exit of the transition section approaches the local sonic velocity*. When the projectile has reached its maximum velocity (the escape velocity), the propelling pressure behind the projectile will have dropped to

---

* As pointed out in Section 19, the maximum velocity with which gas can issue from the chamber into the barrel of a PP chambered gun with $x_0 = \infty$ is the local velocity of sound.

zero; at this time steady state conditions will exist in the transition section, and the gas will be flowing into the barrel at sonic speed.
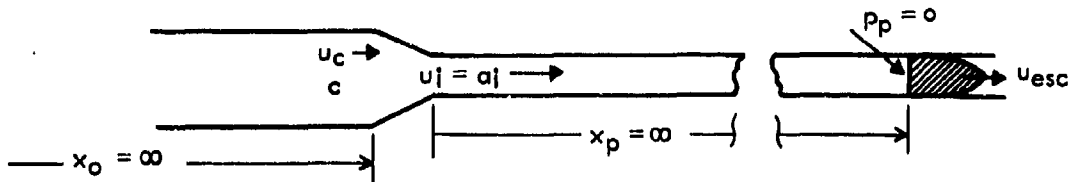
Thus, the steady flow Equations (18-3) and (18-4) will *exactly* apply, and, in addition, the velocity at the transition section can be equated to the sonic velocity without approximation. Therefore, for the case of the ideal gas propellant, the equations which apply at this time are the following:

Continuity:
$$(\sigma_1/\sigma_c)^{2/(\gamma-1)} = A_0 u_0/A_1 u_1 \qquad (21\text{-}1)$$

Energy:
$$u_c^2 + (\gamma - 1)\sigma_c^2/2 = u_1^2 + (\gamma - 1)\sigma_1^2/2 \qquad (21\text{-}2)$$

Sonic condition:
$$u_1 = a_1 = (\gamma - 1)\sigma_1/2 \quad . \qquad (21\text{-}3)$$

All of the quantities in these equations are for the time when the projectile velocity is a maximum.

As the chamber is effectively infinite in length, Equation (20-6) can be applied to the gas in the chamber at the entrance to the transition section at this time.

$$u_c + \sigma_c = \sigma_0 \quad . \qquad (21\text{-}4)$$

To determine the escape velocity, the impulses traveling downstream from the transition section toward the projectile may be examined. For each of these impulses the quantity $u + \sigma$ is a constant (by Equation (20-9)), a different constant for each impulse, equal to $u_1 + \sigma_1$, since they travel from the exit of the transition section. When the projectile is traveling at escape speed, the pressure of the gas directly behind it is zero, and hence the Riemann Function σ_p of this gas, by Equation (20-3), is zero. Therefore, at this time

$$u_{esc} = (u + \sigma)_{projectile} = u_p + \sigma_p = u_1 + \sigma_1 \qquad (21\text{-}5)$$

where u_{esc} is the projectile escape velocity. From Equation (21-3), the escape velocity becomes

$$u_{esc} = \frac{\gamma + 1}{\gamma - 1} a_1 = \frac{\gamma + 1}{2} \sigma_1 \quad . \qquad (21\text{-}6)$$

From Equations (21-1) through (21-6), the relation between the escape velocity and the ratio of chamber to barrel cross-sectional area (or chamber to barrel diameter) can be obtained for the infinite chamber length gun.

$$\frac{A_0}{A_1} = \frac{D_0^2}{D_1^2} = \left[\frac{\bar{\bar{u}}_{esc}}{1 + \sqrt{\left(\frac{\gamma-1}{2}\right)\left(\bar{\bar{u}}_{esc}^2 - 1\right)}}\right]^{\frac{2}{\gamma-1}} \left[\frac{\bar{\bar{u}}_{esc}}{1 - \frac{2}{\gamma-1}\sqrt{\left(\frac{\gamma-1}{2}\right)\left(\bar{\bar{u}}_{esc}^2 - 1\right)}}\right] \qquad (21\text{-}7)$$

where $\bar{\bar{u}}_{esc}$ is defined as

$$\bar{\bar{u}}_{esc} \equiv \frac{\gamma-1}{2}\frac{u_{esc}}{a_0} \qquad . \qquad (21\text{-}8)$$

For a propellant gas of $\gamma - 1.4$, the projectile escape velocity is plotted in
Figure 9(a) as a function of D_0/D_1 as calculated from Equation (21-7). It is evident
from Equation (21-7) that, as expected, the escape velocity for an infinite chamber
length, constant diameter gun $(D_0/D_1 = 1)$ is $2a_0/(\gamma-1)$ or, dimensionlessly, $\bar{\bar{u}}_{esc} = 1$.
Further, it is seen that, as D_0/D_1 approaches an infinite value, $\bar{\bar{u}}_{esc}$ approaches
the value of $(\gamma + 1)/2$, that is, u_{esc} becomes

$$u_{esc} = \sqrt{\frac{\gamma+1}{2}}\frac{2a_0}{\gamma-1} \qquad . \qquad (21\text{-}9)$$

It is noted that the increase in escape speed between chambrage and infinite
chambrage is

$$\Delta u_{esc(\infty)} = u_{esc(D_0/D_1=\infty)} - u_{esc(D_0/D_1=1)} = \left(\sqrt{\frac{\gamma+1}{2}} - 1\right)\frac{2a_0}{\gamma-1} \qquad (21\text{-}10)$$

which in the limit of $\gamma = 1$, becomes equal to $0.5\ a_0$. Calculation yields the
fact that *the increase in escape speed is approximately equal to half the initial
sound speed for all gases with* γ *between 5/3 and 1.* This is seen in the table.

γ →	1	1.2	1.4	1.6	5/3
$\Delta u_{esc(\infty)}$ →	$0.50\ a_0$	$0.49\ a_0$	$0.48\ a_0$	$0.47\ a_0$	$0.46\ a_0$

A plot of Δu_{esc} is plotted in Figure 9(b) versus $(D_1/D_0)^2$, the reciprocal of the
area ratio. This plot is found to be almost a single straight line for all γ values
and is easily committed to memory.

The increase of escape speed may be made dimensionless by dividing it by the
increase of escape speed for infinite chambrage. The resultant dimensionless quantity
is then the percentage increase in escape speed.
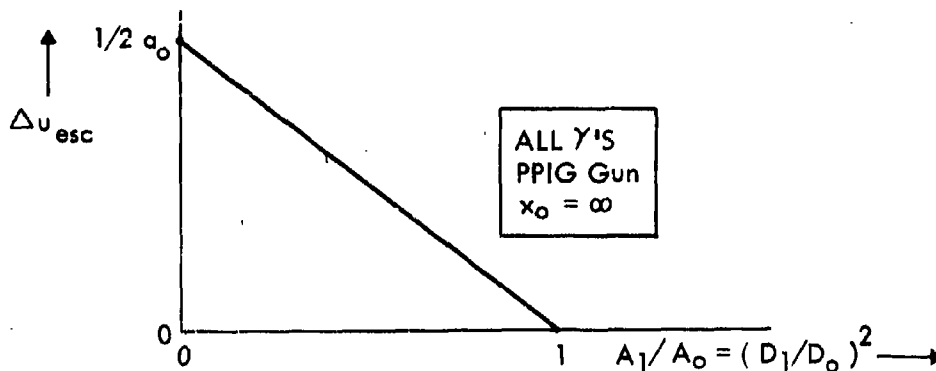
Percentage increase in

$$u_{esc} = \frac{\Delta u_{esc}}{\Delta u_{esc\,(\infty)}} = \frac{u_{esc} - \dfrac{2a_0}{\gamma - 1}}{\left[\left(\dfrac{\gamma+1}{2}\right)^{\frac{1}{2}} - 1\right]\dfrac{2a_0}{(\gamma-1)}} \quad . \tag{21-11}$$

A plot of percentage increase in u_{esc} versus $(D_1/D_0)^2$ for different γ's is presented in Figure 10. It is seen that nearly a single curve for all γ values represents this percentage; it is practically independent of γ .

Section 22

Discussion of the Projectile Velocity Increase
in an $x_0 = \infty$, PPIG Gun Due to Infinite Chambrage

The result of calculations, as outlined in Reference 9, for the case of a $\gamma = 1.4$ ideal propellant gas in a gun with infinite chambrage is shown in Figure 11; here, projectile velocity is plotted as a function of projectile travel. On this same figure is given the result for an $x_0 = \infty$, PPIG Gun of diameter ratio one (calculated from the analytic expression of Equation (12-1)).

From this figure it may be seen that the velocity increase due to chambrage (Δu_p) increases with increasing travel and very soon approaches a value equal to one half the initial sound speed; at infinite travel the difference is exactly the difference in escape speeds, that is,

$$\Delta u_p = \Delta u_{esc\,(\infty)} = \left[\sqrt{\frac{\gamma+1}{2}} - 1\right]\frac{2a_0}{\gamma - 1} \simeq 0.5\, a_0 \tag{22-1}$$

for $x_p = \infty$.

A plot is sketched of Δu_p versus u_p/a_0 for the $D_0/D_1 = 1$ gun (all values at each point on the curve taken for the same $p_0 AL/Ma_0^2$).

Δu_p

$\left(u_{p_{D_o/D_1 = \infty}} - u_{p_{D_o/D_1=1}} \right)$

$\gamma = 1.4$
PPIG GUN
$x_o = \infty$

$\dfrac{2 a_o}{\gamma - 1} \left(\sqrt{\dfrac{\gamma+1}{2}} - 1 \right) \approx .5 a_o$

$(u_p/a_o) \xrightarrow{\quad} D_o/D_1 = 1$
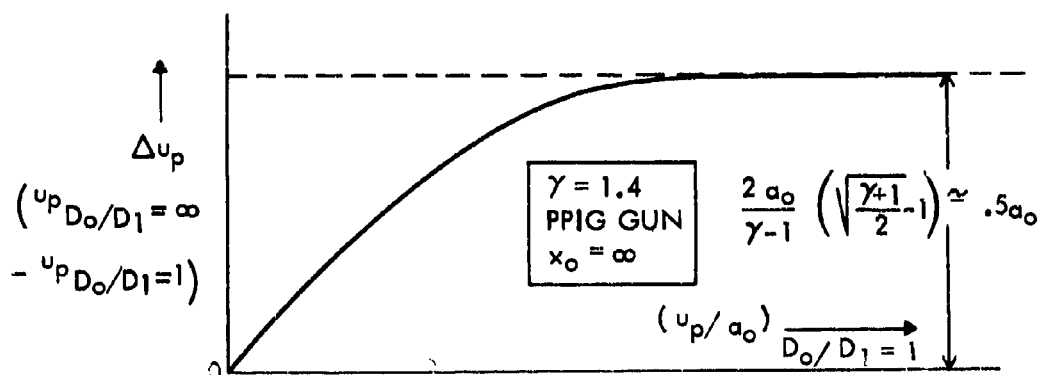
The velocity difference curves obtained from calculations done for other values of γ appear similar to this curve for the $\gamma = 1.4$ propellant gas.

It had been previously noted that the performance of the $x_o = \infty$, constant diameter PPIG Gun depends essentially on the parameter a_o/γ (e.g., see Figure 4). Therefore, it is reasoned that the various Δu_p curves for different γ values may be brought into near coincidence if plotted against $\gamma u_p/a_o$ rather than u_p/a_o. This turns out to be the case, as seen from Figure 12. It is noted from this Figure that the behavior of Δu_p for all the γ curves may be approximated as being linear at low values of $\gamma u_p/a_o$ and equal to 0.5 a_o at values of $\gamma u_p/a_o$ above about 3. By using this approximation Δu_p versus $\gamma u_p/a_o$ appears as shown in Figure 13 and in the following sketch*.

Δu_p
increase in u_p due to infinite chambrage

$1/2\ a_o$

All γ's
PPIG GUN
$x_o = \infty$

$(\gamma u_p/a_o) \xrightarrow{\quad} D_o/D_1 = 1$

3
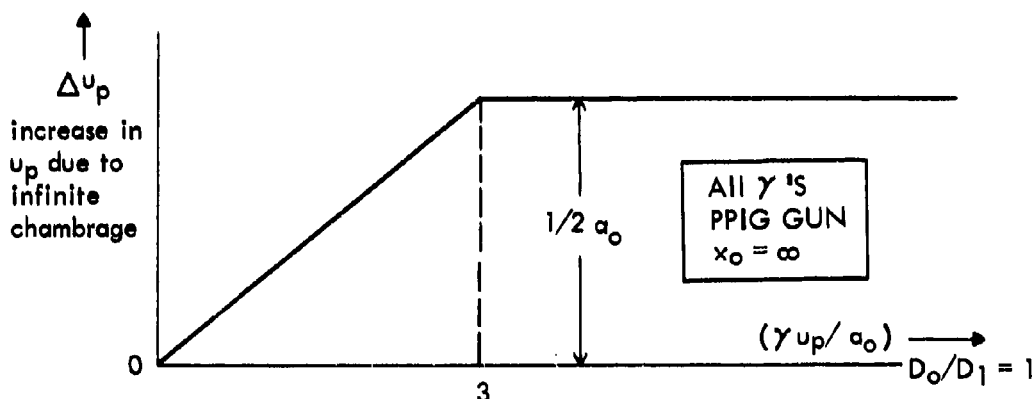
It is seen that the *effect of infinitely chambering an* $x_o = \infty$ PPIG Gun *is to increase the projectile velocity by about* $a_o/2$ *at the most*.

---

* Charters (p.50, Reference 86) discusses a similar approximation.

Section 23

The Projectile Velocity Increase for an $x_0 = \infty$,
PPIG Gun With Any Value of Chambrage

From Figure 9 (or Equation (21-7)) the diameter ratio of the PPIG Gun which will yield an increase in escape velocity midway between that of the $D_0/D_1 = 1$ gun and the $D_0/D_1 = \infty$ gun may be obtained. This diameter ratio is found to be approximately equal to 1.5 for any γ propellant gas. The calculation of projectile behavior for a $D_0/D_1 = 1.5$ gun with a $\gamma = 1.4$ propellant yields the result shown in Figure 14; also shown in this figure are the results for a $D_0/D_1 = 1$ gun and a $D_0/D_1 = \infty$ gun.

It is apparent from the curves of Figure 14 that the velocity of the $D_0/D_1 = 1.5$ gun is approximately half way between the $D_0/D_1 = 1$ and $D_0/D_1 = \infty$ guns for all values of projectile travel. Thus, the $D_0/D_1 = 1.5$ gun which yields an increase of the escape velocity of 50% is seen to yield approximately an increase of projectile velocity (Δu_p) of 50% for all velocities. It is thus postulated that the curve of Figure 9 (or Figure 10), therefore, which applies to the percentage escape velocity increase, may be applied to the percentage velocity increase of an $x_0 = \infty$, PPIG chambered gun at any projectile velocity. Calculation confirms this postulate. Figure 10 is thus replotted in Figure 15 with the ordinate now labeled as the percentage velocity increase due to any value of chambrage versus the gun diameter ratio squared.

This curve may be approximated by the straight line,

$$\Delta u_p = \Delta u_{p\infty} [1 - (D_1/D_0)^2] \quad . \tag{23-1}$$

With this equation the plot of Figure 13 may be transformed to yield the velocity increase due to any value of chambrage at any velocity; this is seen in the sketch on the following page.
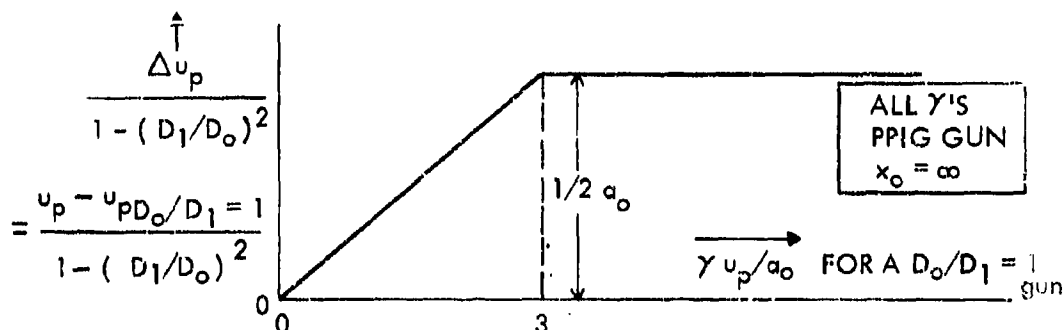
To calculate the velocity of an effectively infinite length chambered gun, one need only calculate the velocity of a gun without chambrage and add to this the value of Δu_p . Hence, any performance curve for an $x_0 = \infty$, PPIG Gun with no chambrage becomes one for a gun with chambrage if for the projectile velocity u_p is substituted $u_p - \Delta u_p$*.

In this manner the plot of Figure 4 has been replotted in Figure 16 to apply to the case of a PPIG chambered gun with an effectively infinite length chamber.

Section 24

The Pressure-Velocity Relation for the Gas in an $x_0 = \infty$, PPIG Chambered Gun

The pressure-velocity relation for the gas directly behind the projectile in a PPIG chambered, $x_0 = \infty$, gun may be obtained by reasoning similar to the above. With the $p\text{-}\sigma$ relation for the ideal gas, Equation (20-3), the pressure behind the projectile may be expressed in terms of the $u + \sigma$ behind the projectile.

$$\frac{p_p}{p_0} = \left(\frac{u_p + \sigma_p}{\sigma_0} - \frac{u_p}{\sigma_0} \right)^{2\gamma/(\gamma-1)} \tag{24-1}$$

which may be rewritten as

$$\frac{p_p}{p_0} = \left(1 + \epsilon - \frac{u_p}{\sigma_0} \right)^{2\gamma/(\gamma-1)} \tag{24-2}$$

where ϵ is defined as

$$\epsilon = \frac{u_p + \sigma_p - \sigma_0}{\sigma_0} \quad . \tag{24-3}$$

---
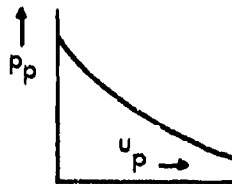
* This approximation will yield projectile velocities correct to within a few percent.

46

For a $\gamma = 1$ gas, Equation (24-1) becomes

$$\frac{p_p}{p_0} = e^{(r - u/a)} \qquad (24-4)$$

where r is defined as

$$r \equiv \frac{u_p + \sigma_p - \sigma_0}{a} . \qquad (24-5)$$

The sum $u_p + \sigma_p$ is equal to σ_0 at the start of projectile motion in an $x_0 = \infty$, PPIG chambered gun; this sum approaches the escape speed at large values of projectile travel at which time the gas velocity at the throat approaches sonic velocity. A plot of $u_p + \sigma_p$ obtained from calculated results indicates a behavior which may be approximated as sketched and as shown in Figure 17.
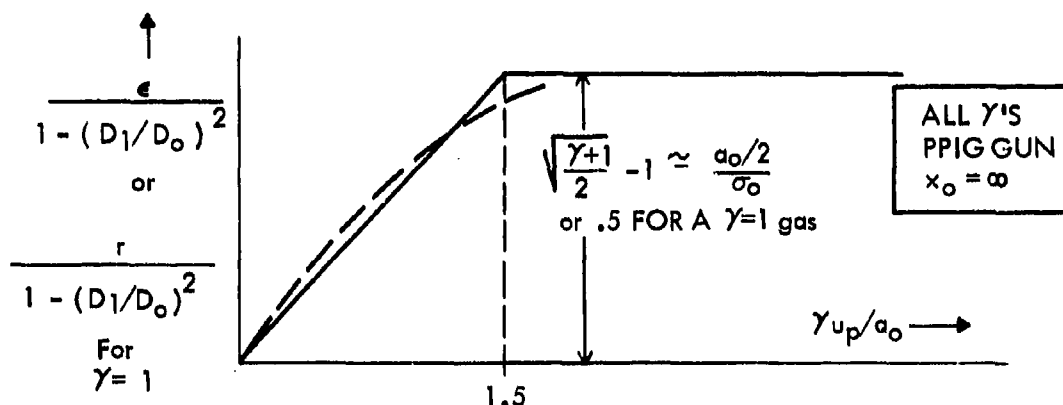
Thus, $p_p/p_0 = (1 + \epsilon - u_p/\sigma_0)^{2\gamma/(\gamma-1)}$ becomes

$$p_p/p_0 = \left\{ 1 + \left[\sqrt{\frac{\gamma+1}{2}} - 1 \right] \left[1 - (D_1/D_0)^2 \right] \frac{\gamma u_p}{1.5\, a_0} - \frac{(\gamma-1)u_p}{2a_0} \right\}^{2\gamma/(\gamma-1)} \qquad (24-6)$$

for $\gamma u_p/a_0 \leqslant 1.5$, and

$$p_p/p_0 = \left\{ 1 + \left[\sqrt{\frac{\gamma+1}{2}} - 1 \right] \left[1 - \left(\frac{D_1}{D_0} \right)^2 \right] - \frac{(\gamma-1)u_p}{2a_0} \right\}^{2\gamma/(\gamma-1)} \qquad (24-7)$$

for $\gamma u_p/a_0 \geqslant 1.5$.

It is seen from the sketch that the approximation is made that the gas flow becomes sonic at the barrel entrance at a time which corresponds to a projectile velocity of $1.5\, a_0/\gamma$.

If desired, the expression for projectile propelling pressure, Equation (24-2), with ϵ from Equations (24-6) and (24-7) may be inserted into Newton's equation to calculate projectile velocity as a function of travel. However, the velocity-travel relation for the $x_0 = \infty$ chambered PPIG Gun is more easily obtained as outlined in Section 23.

Section 25

The Barrel Entry Sonic Approximation to Calculate the Projectile Behavior in an $x_0 = \infty$, PPIG Chambered Gun

In an $x_0 = \infty$, PPIG chambered gun, the flow into the barrel approaches sonic flow with increasing time. However, for convenience in calculating the projectile velocity-travel history, the approximation is sometimes made that the flow is *always* sonic at the barrel entry. Thus, the equation for pressure

$$\frac{p_p}{p_0} = \left[1 + \epsilon - \frac{u_p(\gamma - 1)}{2a_0} \right]^{2\gamma/(\gamma - 1)}$$

becomes

$$\frac{p_p}{p_0} = \left[1 + \left(\sqrt{\frac{\gamma + 1}{2}} - 1 \right)(1 - A_1/A_0) - \frac{u_p(\gamma - 1)}{2a_0} \right]^{2\gamma/(\gamma - 1)} \tag{25-1}$$

or, for the $\gamma = 1$ propellant gas, it becomes

$$\frac{p_p}{p_0} = e^{\left[\frac{1}{2}\left(1 - \frac{A_1}{A_0} \right) - \frac{u_p}{a} \right]} . \tag{25-2}$$

It is to be noted that, when Equation (25-1) is used in Newton's equation to obtain the projectile velocity-travel relation, the result is precisely that obtained for the $D_0/D_1 = 1$ case (Equation (12-1)) except that for p_0 in Equation (12-1) one substitutes

$$p_0 \left[1 + \left(\sqrt{\frac{\gamma + 1}{2}} - 1 \right)\left(1 - \frac{A_1}{A_0} \right) \right]^{\frac{2\gamma}{\gamma - 1}}$$

and for a_0 in Equation (12-1) one substitutes

$$a_0 \left[1 + \left(\sqrt{\frac{\gamma + 1}{2}} - 1 \right)\left(1 - \frac{A_1}{A_0} \right) \right]$$

$$\left. \right\} \tag{25-3}$$

The plot of Equation (12-1) in Figure 3 or Figure 4 may be applied to a chambered gun by using the substitutions of Equation (25-3).

48

The sonic assumption above gives a relatively good approximation for the projectile behavior in an $x_0 = \infty$, PPIG chambered gun. However, more accurate results are easily obtained, as outlined in Section 23.

Section 26

The Calculation of the First Reflected Disturbance
in a PPIG Chambered Gun

The analysis above has been for a chambered PP Gun having a chamber length which is *effectively* infinite ($x_0 = \infty$). Obtaining the magnitude of the chamber length necessary to be effectively infinite in a PPIG Gun requires a step-by-step numerical calculation of the path of the first reflected disturbance. The cases of $D_0/D_1 = 1$, 1.5, and ∞ are here first considered. The $D_0/D_1 = 1$ case has been discussed in Section 13 (see Equation (13-7)) and the results are shown in Figure 5.

For simplicity in calculating the path of the first reflected impulse in the case of the chambered guns, the length of the transition section between the chamber and barrel is taken to be zero.
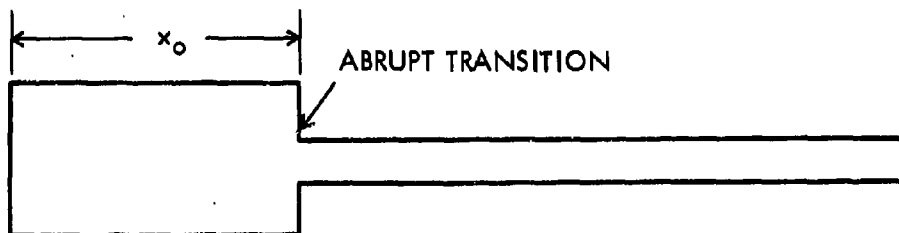
Examination of Equations (17-1), (17-2), and (17-3) demonstrates that, for the infinite chambrage gun ($D_0/D_1 = \infty$), the velocity of the gas in the chamber section is zero and the pressure, sound velocity, and other gas conditions in the chamber remain constant at their initial values. Thus, the disturbances in the chamber section travel at the initial sound velocity; the time required for the first impulse to travel from the transition point to the breech and back (point P in the following sketch) is equal to $2x_0/a_0$.
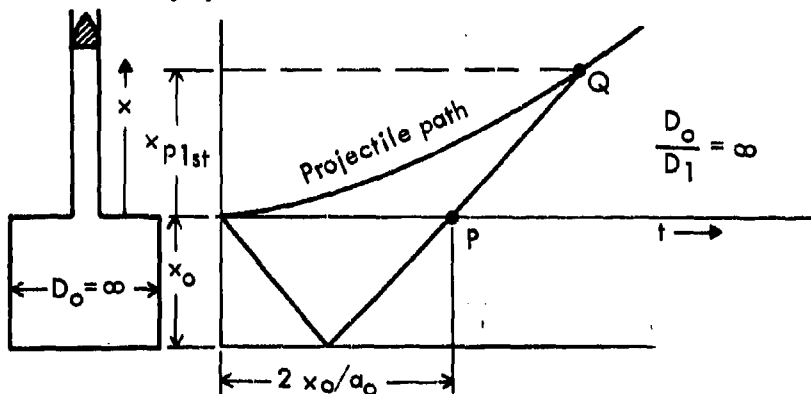
Each value of time along the x = 0 line (beginning of the barrel) obtained from numerical results of the infinite chambrage calculations previously referred to can be taken to correspond to the time at P . Then the velocity $u_{p_{1st}}$ and position $x_{p_{1st}}$ of the projectile when the first disturbance reaches it at Q can be obtained from the infinite chambrage calculation by following the downstream impulse from P . In this manner paths of the first reflected impulses for $D_0/D_1 = \infty$ are obtained. The resultant $D_0/D_1 = \infty$ plots are shown in Figures 18 and 19.

For the $D_0/D_1 = 1.5$ case, the characteristics equations can be applied in the chamber section (where $u + \sigma = \sigma_0$) to obtain the path of the first reflected impulse. From the points R and S obtained in the previously referred to $D_0/D_1 = 1.5$ calculation on the x = 0 line (see following sketch), point T can be calculated; from T and U the point V can be calculated, etc.

$D_0/D_1 = 1.5$
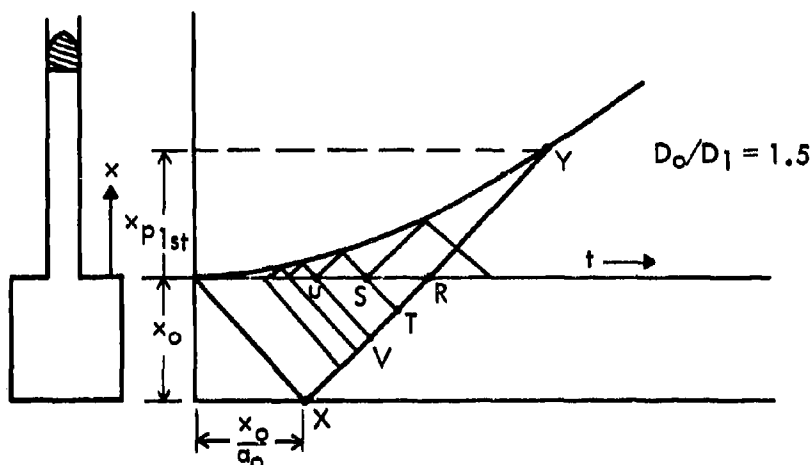
Point X, which specifies x_0 , is the intersection of the downstream characteristic R-T-V... and the first upstream impulse (of slope $-2/(\gamma-1)$). Since point Y on the projectile path has been calculated previously, the first reflected impulse path is completely known. In this manner the chamber length to be effectively infinite was calculated for the diameter ratio equal 1.5 case.

The results of the three diameter ratios calculations are shown in Figures 18 and 19 and illustrate that the $D_0/D_1 = 1.5$ case falls again approximately midway between the $D_0/D_1 = 1$ and $D_0/D_1 = \infty$ cases; therefore, chamber lengths necessary to be effectively infinite for diameter ratios other than 1, 1.5, or infinity may be calculated by interpolating the results of Figures 18 and 19 as shown in the sketch on the following page (inverse area ratio interpolation).

50
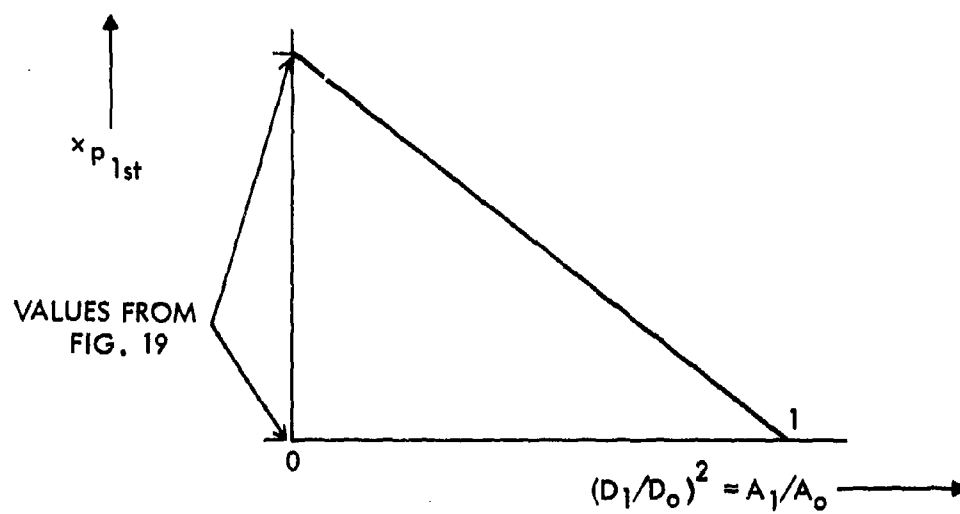
PART V. COMPLETE NUMERICAL RESULTS FOR THE PROJECTILE BEHAVIOR IN A PPIG CHAMBERED GUN

Section 27

Calculations by Means of Electronic Computing Machines

The method of characteristics as outlined above may be numerically applied to calculate the performance of a PP Gun system. However, in the cases where the chamber is not effectively infinite in length, hand calculation becomes extremely lengthy and tedious. Further, the accuracy of the calculated results depends on the spacing of the numerical points. The greater the spacing, the greater the error; hand calculation, particularly, does not allow small spacing and thus calculating by means of electronic computing machines offers great advantages relative to hand calculation. Not only is much time saved, but accuracy may be substantially increased.

At the present time there are two methods generally used by computing machines to calculate the behavior of the projectile in a gun. The first is the method of characteristics[55, 56] already discussed. The second method is a Lagrangian scheme in which the gas is broken into small layers to each of which is applied Newton's Law. The pressures acting are assumed to vary negligibly over a small time interval during which the calculation is made to determine the movement of the sides of each layer. The movement of the sides of each layer determines the new volume for each layer and therefore the new pressure for each layer.

$$M_2 \frac{\delta u_2}{\delta t} = (p_1 - p_3)A$$

$$u_2' = u_2 + \frac{(p_1 - p_3)A(\delta t)}{M_2}$$

$$\delta x_{2(C.G.)} = u_2 \delta t + \frac{(p_1 - p_3)}{M_2} \frac{A(\delta t)^2}{2}$$

The process is then repeated determining the motion of the layers of gas under the influence of the newly calculated pressures. The method also has incorporated into it an ability to take into account shocks. This scheme is based on the method devised by von Newmann and Richtmyer[12, 13]. The application of this method to two-stage gun calculations is described in References 14 and 33. It is interesting to note that the method is also applicable to the flow of solids and liquids as well as gases; moreover, it can be extended to apply to unsteady two-dimensional problems.

Section 28

Numerical Results for the PPIG Chambered Gun

Calculations have been obtained by the use of both of the computing schemes outlined above. The results may be expressed in terms of dimensionless plots similar to those

of Figures 6 or 7, that is, $\bar{u}_p$ vs $\bar{x}_p$, or they may be in terms of other dimensionless variables. Thus, a plot of dimensionless projectile velocity versus projectile travel for a given geometry (i.e., for a given D_0/D_1 and given G/M*) has been found convenient. The results of computations made for the US Naval Ordnance Laboratory at the Naval Weapons Laboratory on electronic computing machines are given for an ideal gas propellant in a prebu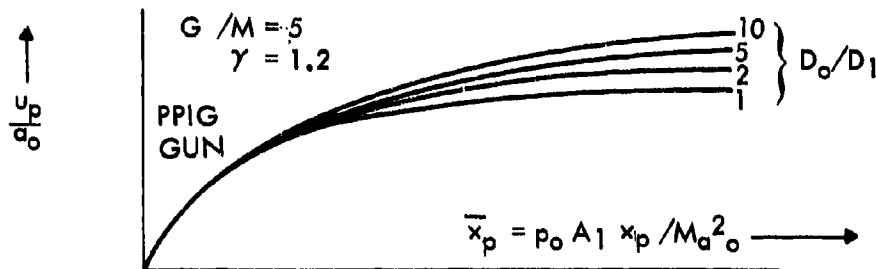rned propellant gun in a series of figures (Figure 20 and Figure 21). The plots in Figure 20 present curves of u_p/a_0 vs $\bar{x}_p$ for varying values of G/M and a given D_0/D_1 and γ as shown in the following sketch.

$$\frac{u_p}{a_0}$$

$$D_0/D_1 = 2.5$$
$$\gamma = 1.4$$
PPIG GUN

$$\frac{G}{M} = \infty$$
5
1
$$\frac{1}{4}$$

$$\bar{x}_p = p_0 A_1 \, x_p / M a_0^2 \longrightarrow$$
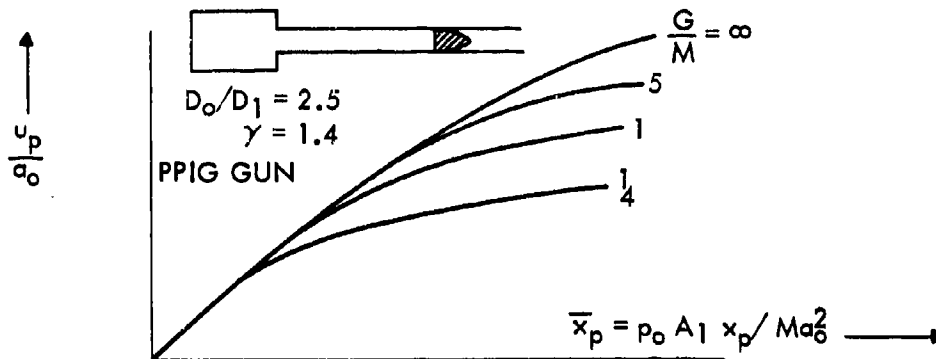
The curve marked G/M = ∞ is the infinite chamber length case.

These curves are replotted in Figure 21 as u_p/a_0 vs $p_0 A_{xp}/Ma_0^2$ for varying values of D_0/D_1 and a given G/M and γ.

$$\frac{u_p}{a_0}$$

G /M = 5
$$\gamma = 1.2$$
PPIG GUN

10
5
2
1
$$\Big\} \; D_0/D_1$$

$$\bar{x}_p = p_0 A_1 \, x_p / M a_0^2 \longrightarrow$$

These plots in Figures 20 and 21 thus present the entire performance of a projectile in an ideal gas preburned propellant gun with chambrage.

It is noted from the plots of Figure 21 that for finite values of G/M the projectile velocity curves for every D_0/D_1 become coincident at large values of projectile travel.

---

* As pointed out previously, G/M is a measure of the dimensionless chamber length, x_0, as seen from the expression G/M = $\gamma \bar{x}_0 A_0/A_1$ = $(\gamma p_0 A_1 x_0/Ma_0^2)(A_0/A_1)$.
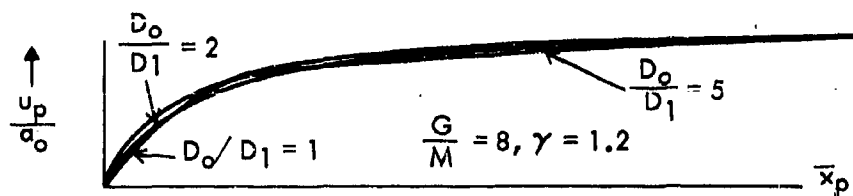
Thus, the projectile velocity at large travel is essentially a function of G/M alone, and not the chamber geometry.

(In Appendix F the Pidduck-Kent Special Solution to the PP Gun problem is discussed. This solution has long been thought to approach the accurate solution to the PP Gun performance in the limit of large travel. This seems to be true, as seen from a comparison of the Special Solution to the results computed by the electronic computing machine in Figure 21. It is noted that the value of velocity for a given projectile travel, as obtained from the Special Solution, oscillates about the value computed by the electronic computing machine and approaches the computed value at large values of projectile travel. *The Special Solution yields an amazingly good approximation to the performance of a PPIG gun.*)

54
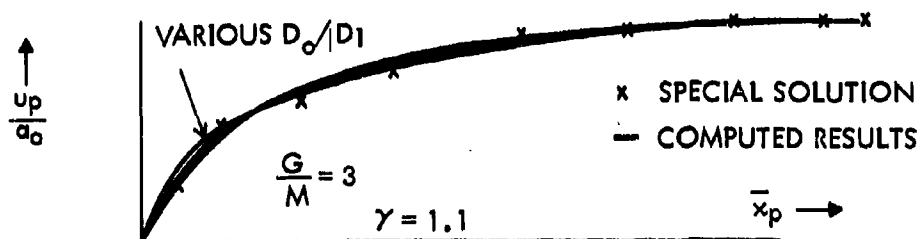
PART VI. THE INFLUENCE OF GAS IN THE BARREL
IN FRONT OF THE PROJECTILE

Section 29

The Compression Phenomenon and the Applicable Equations

If there is gas in the barrel in front of the projectile, the forward motion of the projectile will be resisted by this gas. The one-dimensional gas dynamic equations may be used to determine the retarding effect of this gas in front.

Because the projectile compresses the gas in front of it as it moves, compression impulses are sent forward from the projectile front end, each compression traveling faster than the one preceding it*. Hence, the compressions converge and a shock forms at some point S ahead of the piston; this shock increases in strength as the projectile velocity increases.
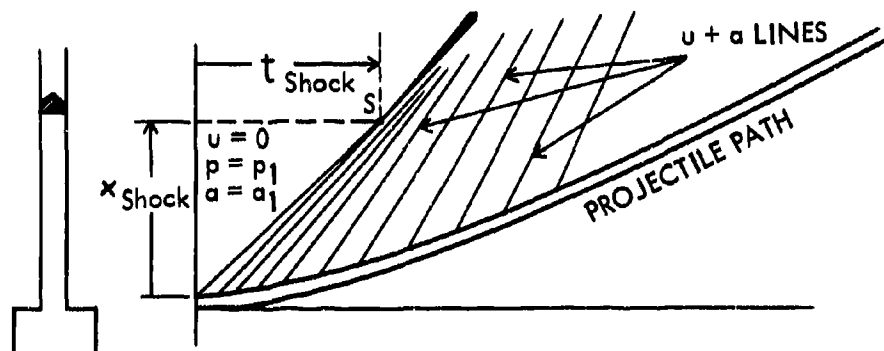
The coordinates at which the shockwaves begin relative to the projectile initial position may be obtained analytically by the method described in Reference 15 or 16 (also see Reference 58) as

$$t_{shock} = 2a_1/[(\gamma_1 + 1)(du_p/dt)in]$$ (29-1)

$$x_{shock} = a_1 t_{shock}$$ (29-2)

where the subscript "1" refers to the initial state of the gas in front of the projectile and $(du_p/dt)in$ is the initial projectile acceleration. In practice for high-speed guns, x_{shock} and t_{shock} are calculated to be relatively very small. The shock forms almost immediately in front of the projectile. An x-t diagram is shown in the sketch on the following page.

---

* This is true because, as the projectile increases its velocity, it pushes the gas ahead of it at an increasing velocity, and at the same time it heats it more. As a result both the local gas velocity u and the local sound speed a are increased, causing the velocity at which the compressions are sent forward from the projectile front end, u + a , to increase.
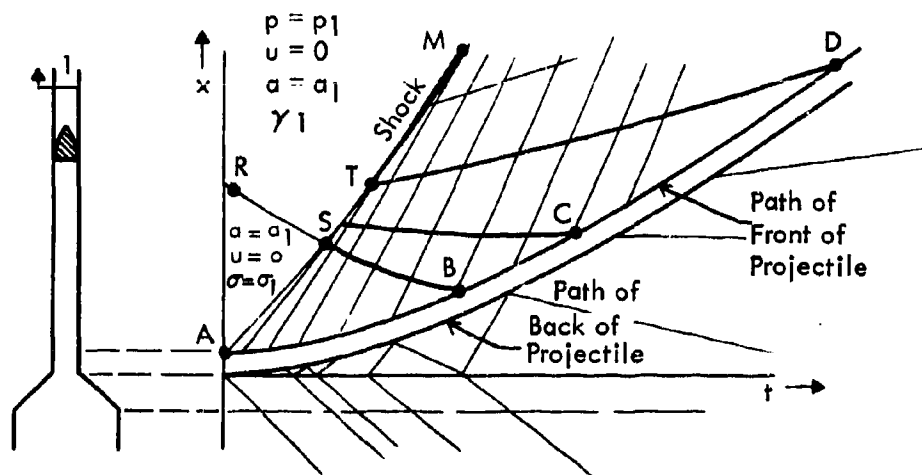
In the sketch the line A-B-C-D represents the projectile path. The line A-S
represents the first compression disturbance (which moves with velocity a_1). The
shock path is indicated by the line S-T-M .

To determine the projectile behavior requires the use of

1. the unsteady one-dimensional characteristics equations applied to the propellant
   gas in the region in back of the projectile,

2. the unsteady one-dimensional characteristics equations applied to the gas in
   front in the region A-D-M-A in front of the projectile,

3. the shock equations applied across the shock,

4. Newton's equation applied to the projectile.

$$M \frac{du_p}{dt} = A(p_p - p_f) \tag{29-3}$$

Thus, a calculation involves continuous iteration and is much better suited to an
electronic computer than a human powered computer. (Some details of the procedure for
this calculation may be obtained from Reference 5.)

Until the projectile experiences a disturbance coming from the shock (at B in the sketch) the pressure in front of the projectile is related to the projectile velocity analytically. Thus, the region A-S-B is a simple wave region* for which

$$u - \sigma = -\sigma_1 \quad . \tag{29-4}$$

If the gas in front is considered an ideal gas then Equation (29.4) may be transformed to an expression for the pressure in front of the projectile up to point B.

$$p_f = p_1[1 + (\gamma_1 - 1)u_p/2a_1]^{2\gamma_1/(\gamma_1-1)} \quad . \tag{29-5}$$

After point B , the pressure must be obtained by the iterative procedure referred to above.

Section 30

An Approximation for the Pressure of the Gas in Front of the Projectile

The projectile acceleration in guns very quickly approaches low values; therefore, the disturbances traveling back and forth between the projectile and shock substantially equalize the conditions in the gas so that approximately the pressure and velocity behind the shock at g directly behind the shock are equal to those at f directly in front of the projectile.
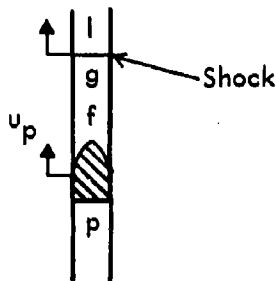
The shock equations yield the following relation for the pressure and velocity behind the shock:

$$p_g/p_1 = 1 + \left(\frac{u_g}{a_1}\right)^2 \frac{\gamma(\gamma+1)}{4} + \gamma\frac{u_g}{a_1}\sqrt{1 + \left(\frac{\gamma+1}{4}\right)^2\left(\frac{u_g}{a_1}\right)^2} \tag{30-1}$$

---

* A simple wave region, as mentioned previously, occurs next to a region of constant state (i.e., constant velocity, pressure, etc.). In this instance the gas in the region R-A-S is in a constant state at its original undisturbed rest condition. The irreversible shock S-T-M , however, makes it impossible to employ the characteristic equations across the shock; the region B-S-M-D-B is thus not a simple wave region.

(Appendix G summarizes the equations for a shock moving into a gas at rest.) Since, as mentioned,

$$p_f \simeq p_g$$

$$u_f \simeq u_g$$

(30-2)

Equation (30-1) becomes

$$\frac{p_f}{p_1} = 1 + \left(\frac{u_p}{a_1}\right)^2 \frac{\gamma_1(\gamma_1+1)}{4} + \frac{\gamma_1 u_p}{a_1} \sqrt{1 + \left(\frac{\gamma_1+1}{4}\right)^2 \left(\frac{u_p}{a_1}\right)^2}$$

(30-3)

where u_p is the projectile velocity; this equation approximates the pressure in front of the projectile during the latter part of its motion in the barrel. For large values of u_p/a_1 Equation (30-3) becomes

$$\frac{p_f}{p_1} \simeq 1 + \frac{\gamma_1(\gamma_1+1)}{2}\left(\frac{u_p}{a_1}\right)^2 \simeq \frac{\gamma_1(\gamma_1+1)}{2}\left(\frac{u_p}{a_1}\right)^2 \quad .$$

(30-4)

In practice, for high speed guns x_{shock} and t_{shock} are calculated to be relatively extremely small; the shock forms almost immediately in front of the projectile at the start of motion. The process of equalizing the pressure and velocity between the shock and the projectile occurs rapidly; thus, Equation (30-3) is a good approximation for use to obtain the pressure in front of the projectile. With this approximation Newton's equation becomes

$$M \frac{du_p}{dt} = A[p_p - p_f(u_p)] \quad .$$

(30-5)

The pressure behind the projectile p_p, as discussed in previous sections, depends on the geometry of the chamber. For an $x_0 = \infty$, $D_0/D_1 = 1$, PPIG

$$p_p = p_0 \left[1 - \frac{(\gamma-1)u_p}{2a_0}\right]^{2\gamma/(\gamma-1)}$$

(30-6)

and Newton's equation may then be integrated numerically to yield the projectile velocity-travel history. For an $x_0 = \infty$, $D_0/D_1 > 1$, gun Equation (24-2) may be used. Without too much error the sonic approximation in the barrel entrance (Equation (24-8)) could be applied, i.e.,

$$\frac{p_p}{p_0} = \left\{1 + \left[\sqrt{\frac{\gamma+1}{2}} - 1\right]\left[1 - \frac{A_1}{A_0}\right] - \frac{(\gamma-1)u_p}{2a_0}\right\}^{\frac{2\gamma}{\gamma-1}}$$

(30-7)

and again Equation (29-9) may be numerically integrated. Reference 17 has done this integration for the case $D_0/D_1 = \infty$.

In the case $x_0 = \infty$, a step-by-step numerical solution of the characteristic equations is required to obtain p_p as a function of u_p.

Section 31

A Convenient Approximation to Obtain the Projectile
Behavior With Pressure in Front of the Projectile

To avoid the tediousness of the numerical integration which is generally necessary, a convenient approximation for the effect of the counterpressure in front of the projectile has been developed by Seigel[18]. It is hypothesized that the percentage velocity reduction due to the counterpressure will have approximately the same functional relationship without regard to the particular gun. To obtain this functional relationship the most simply calculated gun system is chosen, a constant base pressure gun in which the propelling pressure is maintained constant at a value of p_0. (See the following sketch.)

The pressure in the front is approximated from Equation (30-4) as

$$p_f = p_1 \left[1 + \frac{\gamma_1(\gamma_1 + 1)}{2} \left(\frac{u_p}{a_1} \right)^2 \right] . \tag{31-1}$$

Newton's law applied to the projectile becomes

$$\frac{M}{A} \frac{u_p du_p}{dx_p} = p_0 - p_1 \left[1 + \frac{\gamma_1(\gamma_1 + 1)}{2} \left(\frac{u_p}{a_1} \right)^2 \right] . \tag{31-2}$$

This equation may be easily integrated to give the velocity u_{p_1} for the case of counterpressure.

$$u_{p_1}^2 = \frac{2a_1^2(p_0 - p_1)}{\gamma_1(\gamma_1 + 1)p_1} \left[1 - e^{-\frac{\gamma_1(\gamma_1 + 1)p_1 A_1 x_p}{M a_1^2}} \right] . \tag{31-3}$$

Dividing u_{p_1} by the velocity of the projectile with no gas in front $u_{p_1} = 0$, where

$$u_{p_1 = 0} = \sqrt{\frac{2p_0 A_1 x_p}{M a_0^2}}$$

one obtains

$$\frac{u_{p_1}}{u_{p_1 = 0}} = \sqrt{\left[1 - \frac{p_1}{p_0} \right] \left[\frac{1 - e^{-y}}{y} \right]} \simeq \sqrt{\frac{1 - e^{-y}}{y}} \tag{31-4}$$
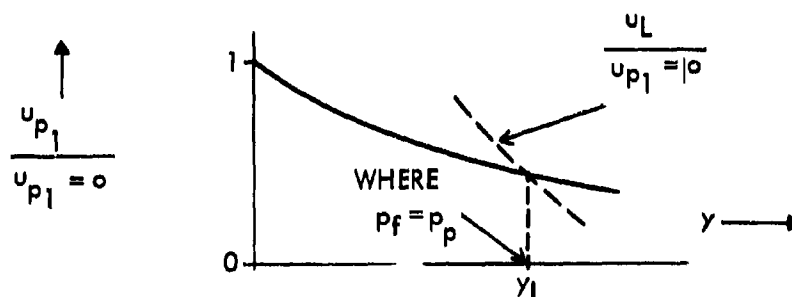
where

$$y = \frac{(\gamma_1 + 1)(\gamma_1) p_1 A_1 x_p}{M a_1^2} . \tag{31-5}$$

This equation then, derived for a constant driving pressure, by our hypothesis should be true for any gun no matter the variation of the driving pressure; it states that the percentage change in projectile velocity due to a counterpressure is essentially only a function of the parameter y .

This equation is plotted in Figure 22. It is applicable until the increasing pressure in the front becomes equal to the decreasing pressure in the back (as will be the case for large values of the abscissa y). At that time $p_p = p_f$ and the velocity of the projectile denoted by u_L no longer increases.
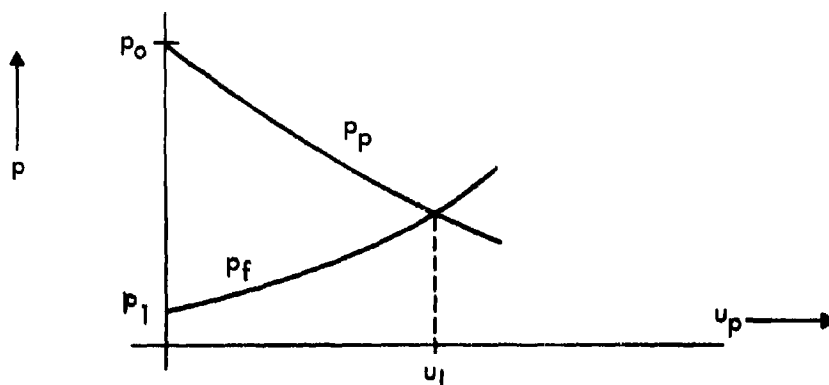
(For an $x_0 = \infty$ gun the velocity u_L is seen to be the same as the contact surface velocity in a shocktube having initially p_0 on one side of the diaphragm and p_1 on the other. The method of calculating u_L for the $x_0 = \infty$ is outlined in Reference 18.) If u_L turns out to be greater than the value of u_p , as obtained from Figure 22, then Figure 22 may be used. If u_L is less, u_{p_1} is then taken to be equal to u_L , and the value of y at which the projectile attains the velocity u_L is obtained by superimposing a calculated plot of $u_L/u_{p_1} = 0$ on Figure 22 as shown in the following sketch.

The intercept then indicates the value of y where $p_f = p_p$ and where the projectile has achieved its constant, limiting velocity.

The effect of the gas pressure in front of the projectile, as obtained from Figure 22, has been compared to the results of numerical integration for an $x_0 = \infty$, $D_0/D_1 = 1$, gun by the author and has been found to agree very well. It is suspected that the figure will apply to chambered guns of finite chamber lengths as well.

# PART VII. THE RELATION OF A PREBURNED PROPELLANT GUN
TO A SHOCKTUBE

Section 32

### The Equivalence of a PP Gun With Zero Mass
Projectile to a Shocktube

A preburned propellant gun in which the barrel initially contains a gas (such as air) is very similar to a shocktube. As shown below, the gun becomes identically the shocktube in the limiting case when the projectile mass approaches zero.

During the course of teaching unsteady flow in the classroom, the author has observed that the logical process of learning for the student involves a discussion of first the gun and then the shocktube. After the student understands the gas dynamics of the PP gun with gas initially in the barrel, the following sequence of reasoning introduces him to the shocktube.

A PP gun with gas in front of the projectile is visualized before the projectile has moved, as in the following sketch.
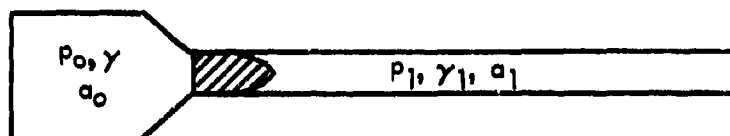
As the projectile increases in velocity, the pressure of the propellant gas directly behind it decreases and the pressure directly in front of the projectile increases.
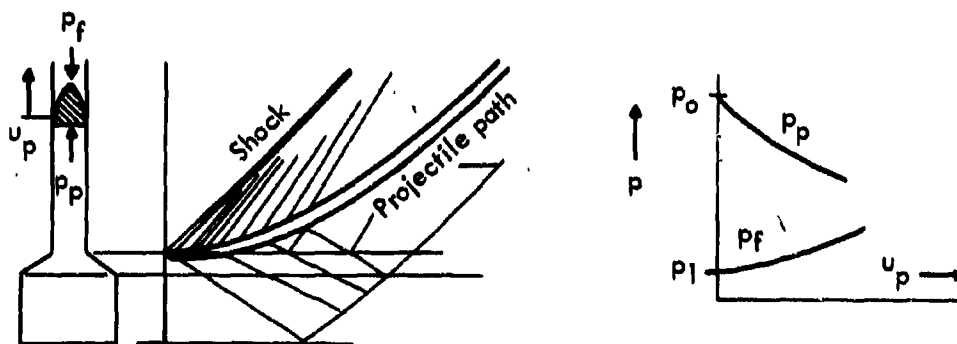

The variation of these pressures with projectile velocity, for example, in the case of a $D_0/D_1 = 1$, $x_0 = \infty$, PPIG/gun, is obtained from Equation (30-6) and Equation (30-3).

$$p_p = p_0 \left[1 - \frac{u_p(\gamma - 1)}{2a_0} \right]^{2\gamma/(\gamma - 1)} \tag{32-1}$$

$$p_f \simeq p_1 \left\{ 1 + \frac{\gamma_1(\gamma_1 + 1)}{4}\left(\frac{u_p}{a_1}\right)^2 + \frac{\gamma_1 u_p}{a_1}\sqrt{1 + \left[\frac{(\gamma_1 + 1)u_p}{4a_1}\right]^2} \right\} . \tag{32-2}$$

In the case of longer and longer barrel lengths, the value of the pressure behind the projectile approaches that of the pressure in front of the projectile, and the projectile then reaches practically a constant velocity, designated as u_L'.
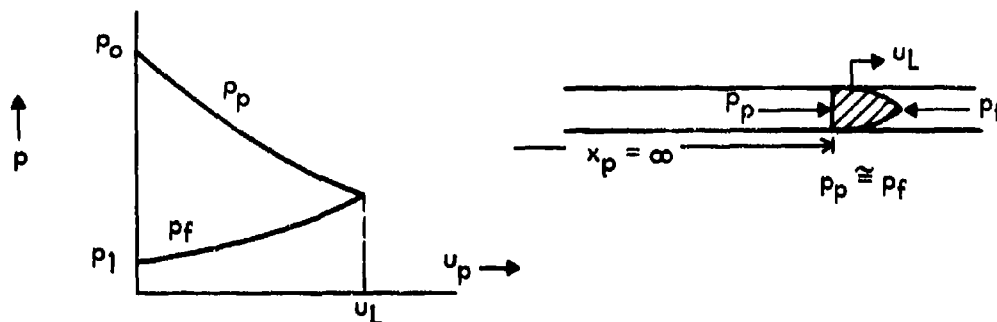
For example, in the above example a $D_0/D_1 = 1$, $x_0 = \infty$, gun this velocity may be calculated by equating p_p to p_f in the equations.

The rapidity with which the velocity u_L is approached by the projectile is evident from an examination of Newton's equation for the projectile.

$$du_p/dt = A_1(p_p - p_f)/M . \tag{32-3}$$

For a gun of given D_0/D_1 and $x_0 = \infty$, both p_p and p_f, and hence their difference Δp, are essentially functions only of the projectile velocity*.

---
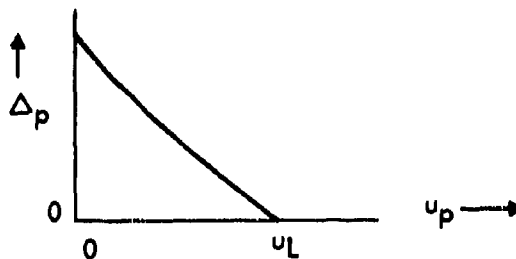
* This is true regardless of the length of x_0 if the projectile mass approaches zero, in which case reflections do not reach the projectile until after the projectile is moving at velocity u_L.

Thus,

$$\frac{du_p}{dt} = A_1[p_p(u_p) - p_f(u_p)]/M = A_t\Delta p(u_p)/M . \tag{32-4}$$

From this equation it is seen that at a given projectile velocity the projectile acceleration is inversely proportional to the projectile mass M. Thus, the smaller the mass, the more quickly the projectile accelerates to the velocity u_L.
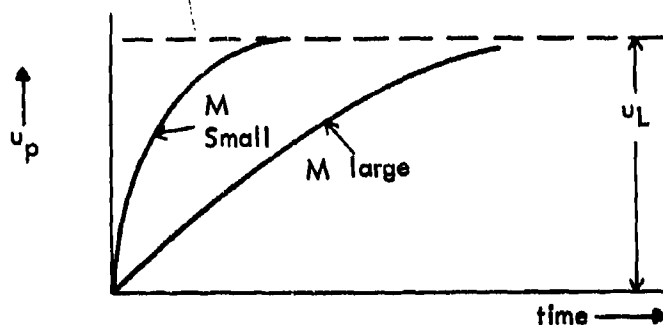

Making M smaller may be seen in the following sketch to alter the characteristics diagram by causing corresponding events to happen more quickly.
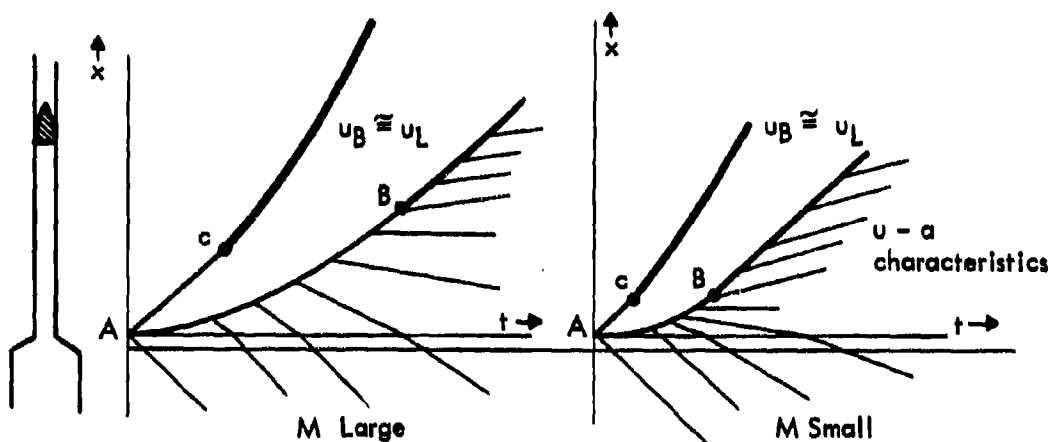
The characteristics diagram for small M appears like that for large M except that time has been contracted (as if one views the large M diagram from far away). The contraction causes the u-a characteristics in the small M case to tend to come from a single point.

Examining Newton's equation again one concludes that *at any finite* Δp other than zero the projectile acceleration is infinite in the limit of zero M.
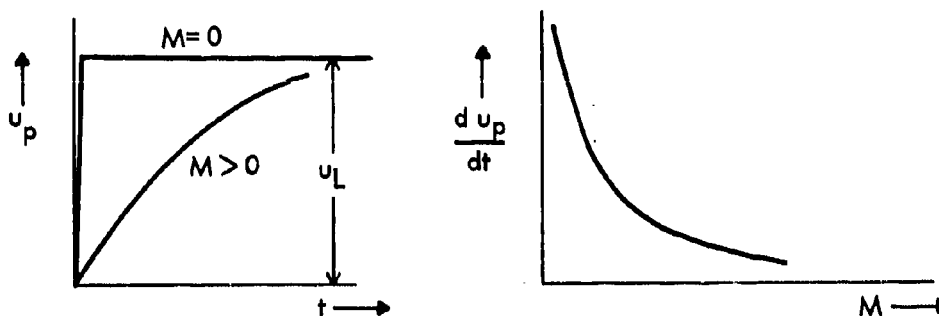
But Δp remains greater than zero until the projectile velocity becomes equal to u_L .
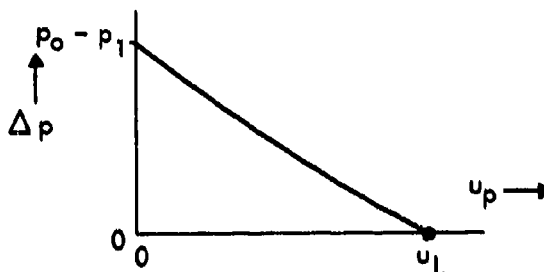
Hence, the acceleration of an $M = 0$ projectile is infinite for an instant.
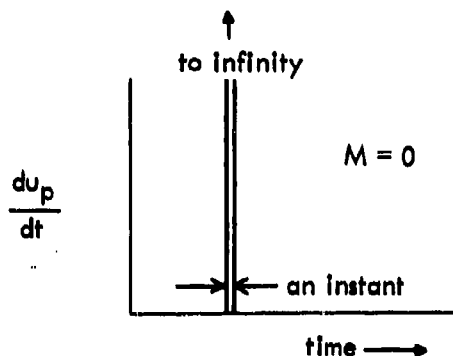
As a result, *a massless projectile attains the velocity* u_L *instantaneously.* When u_L is attained, Δp becomes zero. There is then no further change in projectile velocity.

The time that is required for a shock to form in front of a projectile is obtained from Equations (29-1) and (29-2) as

$$t_{shock} = \frac{2}{\gamma_1 + 1} \frac{a_1}{(du_p/dt)_{initial}} \ . \tag{32-5}$$

In this case of a massless projectile it has been demonstrated that the initial acceleration is, for one instant, infinite. Thus, by Equation (32-5) the shock forms instantaneously immediately in front of the massless projectile; the strength of this shock corresponds in strength to the projectile velocity (gas velocity) u_L . The events which took place at different times t_A , t_B , and t_C in the x-t sketches shown above take place instantaneously in the massless projectile case. In the x-t plane the shock and projectile paths are thus straight lines emanating from the origin. In this situation the gun is a shocktube, the projectile becomes a demarcation, known as a "contact surface" or "interface" between the propellant gas and the gas initially in the barrel (the driven gas). The propellant gas is known as the "driver gas".
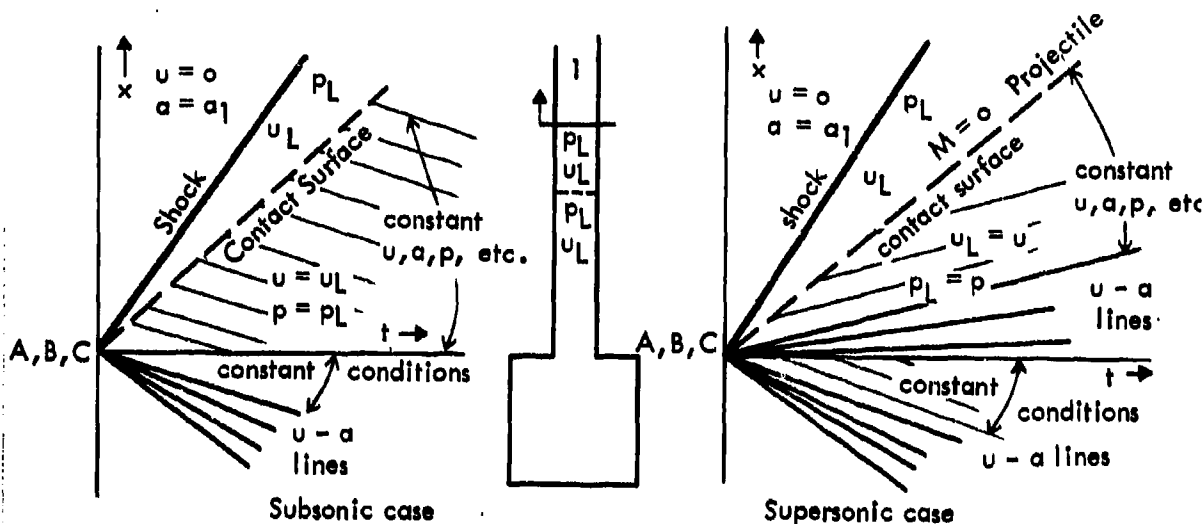
The $u - a$ rarefactions all originate at the origin and are termed "centered rarefactions".

Subsonic case   Supersonic case

As seen from the captions under the characteristics diagrams, the propellant behavior in the shocktube may be described as being "subsonic" or "supersonic", depending on the gas flow immediately behind the projectile. (The slope of a "$u - a$" line is obviously negative for subsonic flow and is positive for supersonic flow.) Whether the gun be chambered or not, in the limit of zero mass of projectile the gun becomes a shocktube of the same geometry.

Section 33

The Performance of a Shocktube in the Strong Shock Case

To determine the performance of the shocktube one need only equate the pressure behind the massless projectile to the pressure in front and calculate u_L , the interface velocity.

If the driven gas is initially at a very low pressure, it will not offer too much resistance to the massless projectile or interface. In that case the interface would

achieve a velocity u_L slightly less than the escape velocity u_{esc}. Approximating the interface as u_{esc}, the pressure in front of the interface, which is that behind the shock, may be calculated from the shock Equation (32-2).

$$\frac{p_2}{p_1} = \frac{\gamma_1(\gamma_1 + 1)}{2} \left(\frac{u_{esc}}{a_1}\right)^2 \quad . \tag{33-1}$$

From the shock relations it may be shown that (see Appendix G)

$$\frac{\rho_2}{\rho_1} \to \frac{\gamma_1 + 1}{\gamma_1 - 1} \quad . \tag{33-2}$$

for strong shocks, and so

$$\frac{p_2/\rho_2}{p_1/\rho_1} = \frac{T_2}{T_1} = \frac{a_2^2}{a_1^2} = \frac{\gamma_1(\gamma_1 - 1)}{2} \left(\frac{u_{esc}}{a_1}\right)^2$$

or

$$a_2^2 = \gamma_1(\gamma_1 - 1)u_{esc}^2/2 \tag{33-3}$$

or

$$\frac{u_{esc}}{a_2} = \sqrt{\frac{2}{\gamma_1(\gamma_1 - 1)}} \tag{33-4}$$

$$= \text{Mach number of gas in front of contact surface.}$$

Thus, the Mach number behind the shock for the strong shock, low p_1, case is at most $\sqrt{2/[\gamma_1(\gamma_1 - 1)]}$.

Section 34

The Significant Difference Between a Gun and Shocktube

Since the shocktube is a gun in the limit of projectile mass going to zero, the qualitative conclusions reached as to performance of guns apply to shocktubes; the chambrage effects and real gas effects are the same, the criteria for good performance are the same. However, there is a significant difference between the gun and shocktube; namely, in the shocktube the equalization of the pressure between the front and back of the interface *occurs instantaneously*; in the gun the equalization of pressures between the front and back of the projectile *requires an infinite time*. This difference manifests itself as a difference in the pressure-velocity relation for the expanding gas when chambrage exists.

In an $x_0 = \infty$, PP Gun with no chambrage the pressure-velocity relationship behind the projectile is governed by the condition that all disturbances reaching the projectile originate from the propellant gas at its initial rest state. Thus,

$$u + \sigma = \sigma_0 \qquad (34\text{-}1)$$

or

$$du + dp/a\rho = 0 \qquad (34\text{-}2)$$

applies to the gas behind the projectile regardless of the fact that the projectile is or is not accelerating. The same equation applies to the gas behind the interface of a shocktube, and hence the shocktube gas would be described by the same p-u relation as for the propellant gas in the $D_0/D_1 = 1$ gun.
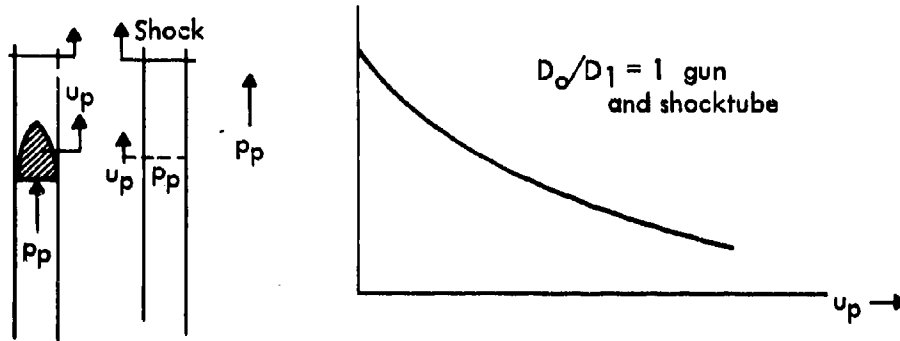
For the chambered gun, disturbances reaching the gas behind the projectile come from the exit of the transition section. At this point conditions are continuously changing with time because the projectile continuously accelerates and continuously sends back disturbances to the transition section, which is thus always lagging behind in its adjustment to the accelerating projectile.
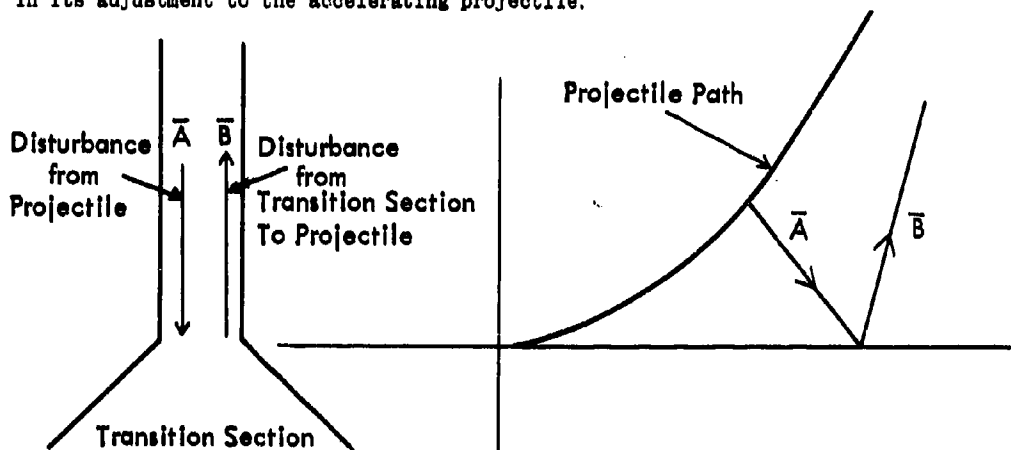
Conditions behind the projectile in the gun are thus determined by tho *two* characteristics equations* applied in the barrel.

---

* It is to be noted that, in both the gun and shocktube cases, the quasi-steady equation udu + dp/aρ = 0 applies. However, for the shocktube, conditions within the transition section are actually steady; for the gun the equation is an approximation for the actual unsteady flow.

$$du + dp/a\rho = 0 \qquad\qquad (34\text{-}3)$$

$$du - dp/a\rho = 0 \quad . \qquad\qquad (34\text{-}4)$$

In the chambered shocktube, the gas at the exit of the transition section is at a constant state. Only the disturbance coming from the transition section exit to the projectile is required to determine the p-u of the gas behind the interface; only the *one* differential equation for the downstream disturbance

$$du + dp/a\rho = 0 \qquad\qquad (34\text{-}5)$$

is required.

This difference between gun and shocktube may be seen by applying these equations to the situation in the following sketch.
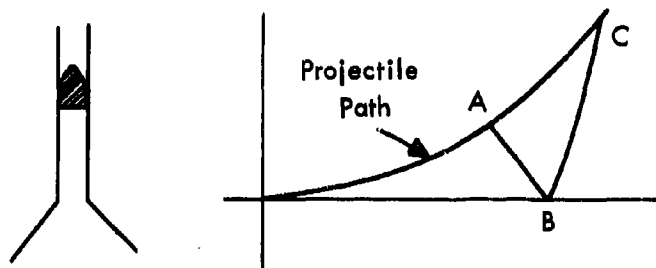
The following equations apply:

$$u_A - \sigma_A = u_B - \sigma_B \qquad\qquad (34\text{-}6)$$

$$u_C + \sigma_C = u_B + \sigma_B \quad . \qquad\qquad (34\text{-}7)$$

It is seen that the conditions at B which determine those at the projectile C depend on those at the projectile at some previous time A . In the case of the shocktube, conditions at A and C are identical.

Thus the $u + \sigma$ at the projectile in a chambered gun lags that at the interface of a shocktube; this situation results in the p-u curve of the shocktube as being above that of the gun as shown in the following sketches.
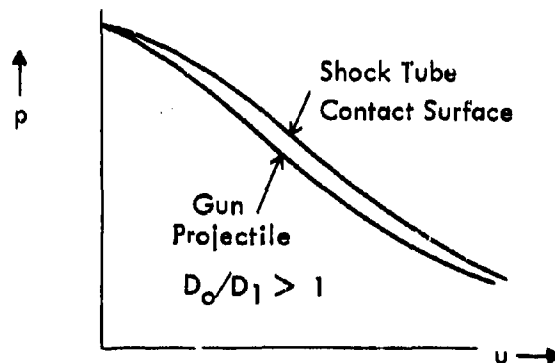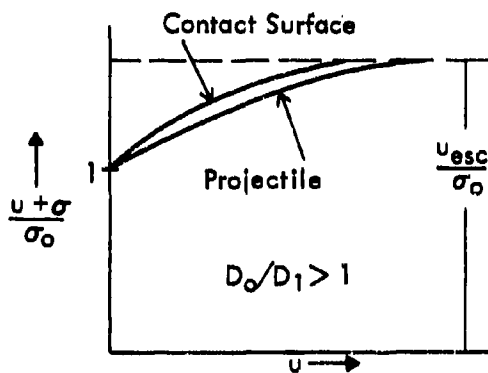
The significant parameter which governs how quickly the conditions in the gun become almost constant is the dimensionless ratio $p_1 a_0^2 / p_0 a_1^2$; this conclusion is obtained from the expression for dimensionless projectile acceleration:

$$M(du_p/dt) = (p_p - p_f)A ,$$

or

$$\bar{u} = u/\sigma_0$$

with

$$\bar{t} = p_0 A t/M\sigma_0$$

$$\frac{d\bar{u}_p}{d\bar{t}} \simeq (1 + \epsilon - \bar{u}_p)^{\frac{2\gamma}{\gamma-1}} - \frac{p_1}{p_0}\left\{\frac{\gamma_1(\gamma_1+1)}{(\gamma_1-1)^2}\left(\frac{a_0}{a_1}\right)^2 \bar{u}_p^2\right\} . \qquad (34\text{-}8)$$

The larger the ratio $p_1 a_0^2 / p_0 a_1^2$, the more quickly conditions in the gun become constant and the more alike will be the p-u curves of gun and shocktube. (Of course, the difference between the shocktube and gun p-u curves also disappears as the chambrage becomes less.)
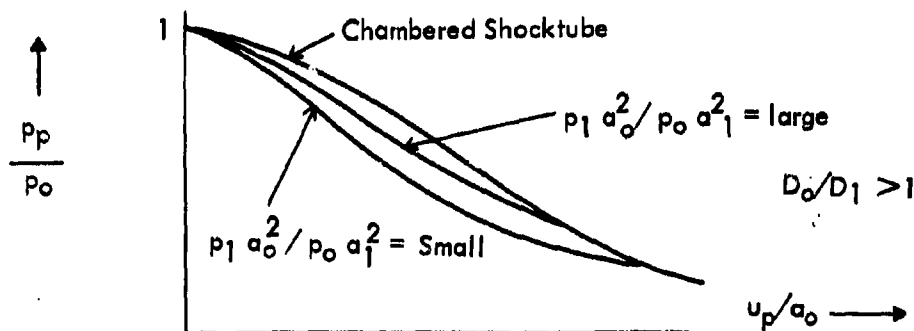
The maximum difference between chambered shocktube and gun occurs when the pressure in front of the diaphragm is zero. Pressure-velocity curves for this case are shown in Figures 42 (for an ideal gas) and 43 (for an Abel gas with $b/(v_0-b)$ equal to 8.09). It is to be noted that at large u_p (when conditions become constant in the gun) the gun curve approaches that of the shocktube.

PART VIII. THE APPLICABILITY OF THE ISENTROPIC THEORY TO GUNS

Section 35

Is the Gun Process Isentropic?

An isentropic process (i.e., a reversible adiabatic process) is one in which the effects of friction and heat transfer are absent. Isentropicity requires that the process be infinitesimally slow, that the gradients be infinitesimally small. Since the expansion process in a gun is a rapid one (of a few milliseconds duration) one could well question the assumption that in a gun the expansion is isentropic. There definitely exist gradients of temperature, velocity, and pressure throughout the quickly expanding propellant gas.

Every real process, of course, is irreversible, for the occurrence of a finite process is the consequence of the existence of finite gradients. However, it is realized that the irreversibilities associated with the process of rapid expansion are inherently smaller than those associated with the process of rapid compression or of retardation of expansion. This is true because in an expansion process the gradients within the gas tend to decrease, whereas in the compression process they increase, resulting in turbulence and shock. Thus, in the case of a gas which is allowed to expand rapidly from one equilibrium state to another, although the entire process is foredoomed to be irreversible, most of the irreversibility occurs during the slowing down part of the process.

Thus, the question is not if the expansion process in a gun is isentropic, but to what extent is it non-isentropic? This query to the present has not been completely answered; the answer requires both analytical and experimental considerations.

Section 36

Experimental Results for Guns with Heated Propellants

A multitude of data has been obtained in the laboratory and in the field on the performance of guns using heated propellants. Almost every laboratory has successfully and in its own individual manner fitted its own experimental results to its own theory. Thus, for example, good agreement between theory and experiment has been reported by AEDC[81, 82], General Motors[94], Ames Research Center[27, 83], Carde[37], BRL[33], NRL[103], NOL[14], and so on (see, for example, Figure 28). However, in almost all cases comparisons between these gun experiments and theory lack the desired accuracy to assess the validity of the assumption of isentropicity. The reasons for this lack are the following:

(a) The initial conditions are usually not those of a preburned propellant gun and sometimes are very poorly known.

(b) The amount of data obtained during a firing is inadequate; in most cases only projectile velocity and chamber pressure are measured.

(c) Usually the data measured lack accuracy.

(d) Usually the propellant gas thermodynamic data are not accurately known.

(e) In the case of two-stage guns the complexity relative to a single-stage gun makes the above deficiencies even more serious.

In sum total, these data indicate that the isentropic theory gives good agreement with the experimental results at lower velocities; at the higher velocities (12,000 ft/sec to 36,000 ft/sec) the theory yields velocities which seem to be significantly higher than the experimental velocities.

Section 37

Experiments with a Compressed Gas Laboratory Gun - Description of the ERMA

It has only been relatively recently that precise experiments have been performed with guns in the laboratory. This has been accomplished by using a compressed room temperature gas as a propellant in a carefully controlled manner. An experimental PP Gun for basic research (designated ERMA for the initial letters of the descriptive title "expansion rate measuring apparatus") was conceived and used first at the van der Waals Laboratory in Amsterdam[1, 4, 5, 19, 20]. A copy of this instrument was later installed at the Institute of Molecular Physics at the University of Maryland[21, 22].

ERMA is a constant diameter steel gun of 12.00 ± 0.001 mm diameter. The assembled ERMA is shown in the following sketch; the projectile holder is shown in Figure 23.
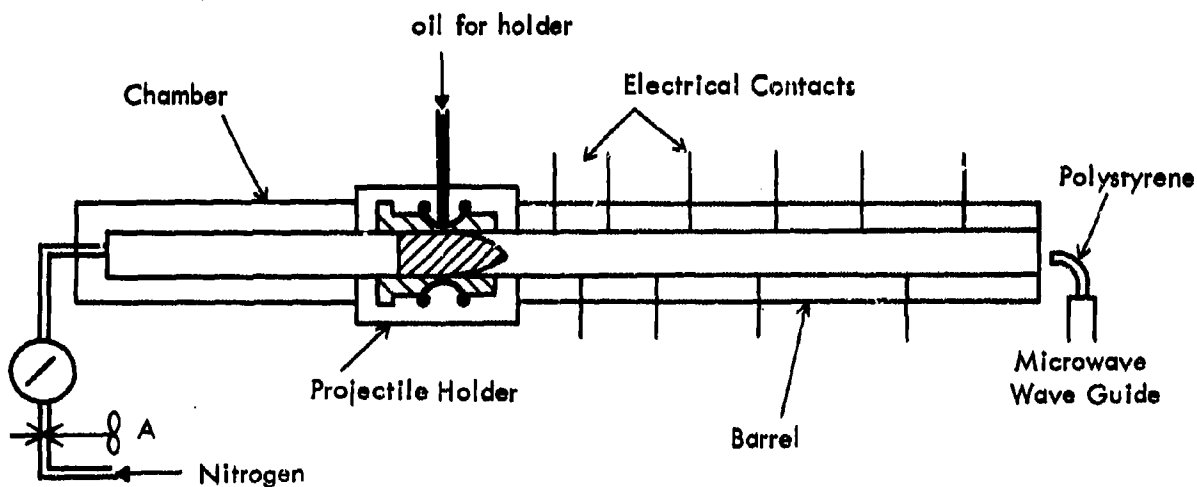
The propellant gas (usually nitrogen) is slowly bled into the chamber from a reservoir by a control valve A. The projectile holder, by means of externally applied oil pressure, restrains the projectile from movement until the pressure is at the desired

level in the chamber. The barrel is approximately 50 cm long. In the barrel are ten small electrical contacts spaced at progressively greater intervals from the initial projectile position. Each contact serves to measure projectile displacement-time by completing an electrical circuit when the projectile passes the contact. In front of the muzzle is a replaceable polystyrene extension of a wave guide which transmits the signal for a microwave interferometer system to and from the projectile as it moves; the microwave signal thus also provides the displacement-time history of the projectile as it moves in the barrel.

To initiate the movement of the projectile the oil pressure to the projectile holder is lowered, releasing the projectile. The data measured during the movement of the projectile along the barrel is thus a series of travel-time (x-t) points. There are ten points obtained from the electrical contacts and 150 x-t points obtained from the microwave interferometer. (The two methods of measurement are in excellent agreement[21].) As the projectile leaves the barrel, it shatters the polystyrene wave guide extension which may be replaced for the next firing. The projectile itself is caught undamaged in a column of cotton waste and re-used. Projectile muzzle velocities varied from 250 to 350 metres per second.

The propellant used in ERMA was compressed gas (usually nitrogen) up to pressures of 3,000 atmospheres at room temperature. The pressure and temperature of the compressed gas in the chamber were precisely known ($\pm$ 1 atm and $\pm$ 0.05°C, respectively) when the projectile was released. The projectile mass and diameter are also accurately measured. The position of the projectile, as measured from the 150 microwave data points, is accurate to $\pm$ 0.001 cm for a given time. An accurate knowledge of the isentropic data for the propellant gas was obtained from actual p-v-t measurements; these data permitted a calculation of the projectile behavior which could be compared to the experimentally measured x-t points. Although most of the experiments were performed using a chamber of effectively infinite length, some experiments were done with a short length chamber.

Section 38

The ERMA Experimental Results

A typical result from one of the ERMA experiments appeared as in the sketch on the following page.

More than 200 experiments were performed, and the experimentally obtained projectile travel was compared to the travel as predicted from the insentropic theory.

The important result obtained from these experiments for projectile velocities of the order of the initial sound speeds was the following: The experimental projectile behavior was close to that predicted by the isentropic theory; specifically, the projectile velocity was from the travel-time measurements determined to be about two percent lower than isentropic theory would predict.

Thus, for the first time a quantitative determination of the discrepancy between the isentropic theory and experimental gun performance was made. (After correcting for the two percent velocity discrepancy by use of a four percent opposing pressure,

the predicted behavior for a firing with a short chamber in which reflections occurred was in excellent agreement with experiment (see Fig. 24 and Ref. 23). Moreover, the travel-time data obtained from the ERMA experiment with argon as a propellant has been used in an inverse manner to calculate previously unknown isentropic gas data[22].
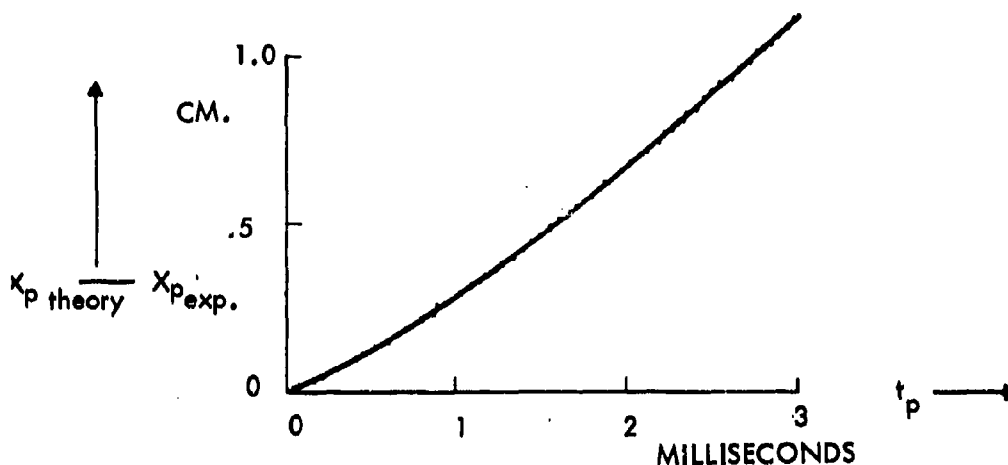
The discrepancy of two percent in velocity, it must be emphasized, occurred for the case where the projectile speed was of the order of the initial gas sound speed. (As indicated below, it is believed that the discrepancy would increase with increasing projectile speed.) Moreover, in the ERMA case, heat transfer occurs from the barrel walls to the gas, rather than in the opposite direction as it does for the usual heated propellant gun. Thus, heat transfer in ERMA tends to increase the projectile velocity.

The causes of the discrepancy between isentropic theory and experiment have as yet been completely resolved. The analysis of the ERMA experiment indicated that the discrepancy was a result of the gas-wall boundary-layer friction and heat transfer and projectile-barrel friction. For the ERMA experiments the discrepancy could be approximately accounted for by assuming counterpressure to be acting on the projectile equal to four percent of the propelling pressure.

Section 39

Analytical Considerations of the Effects of Non-isentropicity

It is not necessary to examine the small gas layers microscopically to determine whether they may be considered as isentropically changing their state or not. It is only necessary to examine microscopically the gradients existing within the gas. From the phenomenological laws governing the irreversible phenomena caused by such gradients, it is possible to calculate the effects of the irreversibilities; the significance of these irreversible effects may be assessed by comparing them to the other changes occurring during the process.

(a) *The temperature gradients between energy modes*

The possibility exists that during the expansion of a propellant gas the energy modes are not in equilibrium. However, calculation indicates that for the types of gas propellants and for the densities and for the expansion times involved in guns, the various energy modes (vibrational electronic, rotational, dissociation, etc.) remain substantially in equilibrium with the translational mode. There are thus no significant time lag effects*.

(b) *The viscous effect between gas layers*

The force equation applied to a layer of gas with the viscous friction term included is

$$\frac{\partial u}{\partial t} + u\frac{\partial u}{\partial x} = -\frac{1}{\rho}\frac{\partial p}{\partial x} + \frac{1}{\rho}\frac{4}{3}\frac{\partial}{\partial x}\left(\mu\frac{\partial u}{\partial x}\right) . \tag{39-1}$$

For the preburned propellant gun the magnitude of each of the various terms of Equation (39-1) may be calculated (with the assumption of an isentropic process). It is found from computation that the viscous gradient term is negligible relative to the other terms in the equations. For an actual experimental gun (the ERMA gun referred to in Section 37) the following values were calculated:

$$\frac{4}{3}\mu\frac{\partial^2 u}{\partial x^2} = 0.05 \times 10^{-6} \ kg/cm^3$$

$$\frac{\partial p}{\partial x} = 10 \ kg/cm^3 .$$

Thus, it is seen that the effect of the gas viscosity within the gas is not important. (This is true even if turbulence existed within the gas.)

(c) *The heat-transfer effect between gas layers*

The effect of heat transferred from one part of the gas to another by conduction can be calculated. The temperature change per unit time at a point within the gas by conduction is

$$\frac{\partial T}{\partial t} = \frac{k}{\rho c_v}\frac{\partial^2 T}{\partial x^2} \tag{39-2}$$

where the conductivity k is assumed constant, and c_v is employed rather than c_p, since the isentropic process is more nearly one of constant volume. This temperature change due to conduction has been calculated for guns and has been found to be negligible. For example, in the case of an actual experimental gun (the ERMA gun referred to in Section 37)

---

* There are some exceptions, such as the expansion of room temperature carbon dioxide behind a light projectile.

$$\frac{k}{\rho c_v} \frac{\partial^2 T}{\partial x^2} = 2 \times 10^{-3} \ {}^{\circ}C/sec \ .$$

For the 3×10^{-3} seconds of the expansion the temperature change was $6 \times 10^{-6} \ {}^{\circ}C$, a negligible amount. (This conclusion would remain true even if turbulence existed.)

(d) *The effect of friction and convective heat transfer between the walls and the gas*

Because the propellant gas is in motion relative to the walls of the barrel and chamber, a boundary layer is formed; this boundary layer is a manifestation of the friction existing between the moving gas and stationary walls; similarly, because of the temperature difference between the walls and gas, a thermal boundary layer is present (see following sketch).
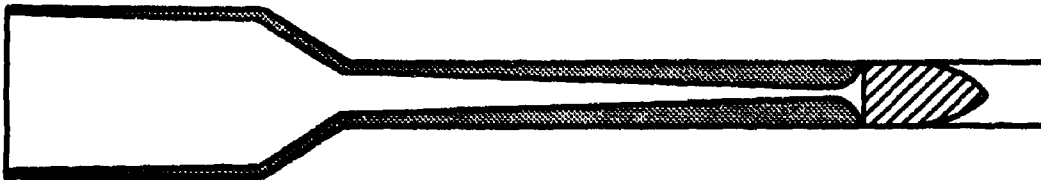
Although the boundary layer behavior in shocktubes has been analyzed rather successfully for the gas behind the shock, this is not the case for the driver gas region in the shocktube. Both for the shocktube and the gun, the driver gas boundary layer is completely unsteady; analysis has therefore not been successful. The transition Reynolds numbers defined by local flow properties and the time a particle has been in motion appears to be in the region of a million. A review of the boundary layer work done in shocktubes is given by Glass[24].

Williams[25] analyzed the driver gas region of a shocktube on the basis of an "equivalent steady pipe flow". He assumed the flow to be fully developed turbulent flow immediately because of the large Reynolds numbers attained by the driver gas almost immediately. A similar analysis has been applied to the propellant gas of a gun[26]. With the assumption of a fully developed turbulent flow the effects of the boundary layer are obtained in a one-dimensional analysis by assuming the friction force to be acting at the wall.
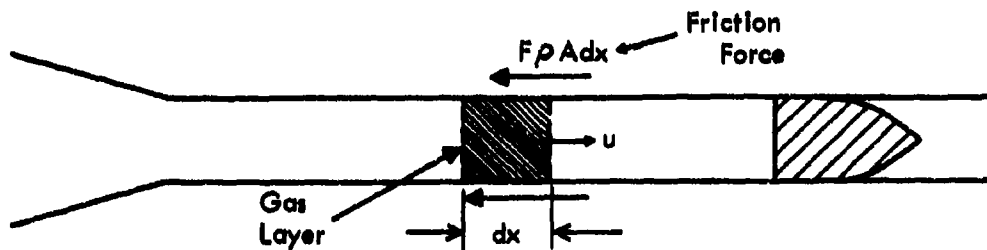
The steady flow turbulent skin friction coefficient is used; thus, the friction force per unit mass is

$$F = \frac{4}{\rho D_1} \frac{1}{2} c_f \rho u^2$$ (39-3)

where the skin friction coefficient c_f is taken as for turbulent steady flow

$$c_f = 0.049(Re_{D,u})^{-\frac{1}{5}} .$$

To obtain the heat loss from the gas, Reynolds analogy is assumed to hold. Thus

$$\frac{1}{2} c_f = \left(\frac{\tilde{h}}{c_p \rho u}\right)(Pr)^{-\frac{2}{3}}$$ (39-4)

where $\tilde{h}$ is the heat-transfer coefficient, Pr is the Prandtl number and c_p is the specific heat; the rate of heat transfer per unit mass is

$$-\dot{q} = \frac{4}{\rho D_1} \tilde{h}(T_{recov} - T_{wall})$$ (39-5)

The entropy change due to the friction and heat transfer is, by Equation (H-9) of Appendix H,

$$T \frac{ds}{dt} = Fu + \dot{q} .$$ (39-6)

The entropy change equation may be used with the characteristics equations of Appendix H to obtain the behavior of the gas and projectile. In Reference 26, however, the entropy change was used to calculate the behavior by use of the von Neumann-Richtmyer method on an electronic computing machine.

The results of this analysis yield calculated projectile velocities that are below those obtained for the frictionless, isentropic case. Figure 25, taken from Reference 26, gives some comparative results. It is thought that this analysis approximates the effects of heat transfer and friction in guns; it is hoped that future analyses will improve the approximations. As indicated above, gun experimental results have not separated the effects of boundary layer induced heat transfer and friction from that of barrel erosion and projectile friction. Swift[64] reports some experimental and analytical results on convective heat losses in guns.

As indicated above, boundary layer losses increase with increasing velocity (see Equation (39-3)); these losses reduce the propelling pressure behind the projectile.

76

When the propelling force drops to a value equal to the bore friction, no further acceleration will occur. Experience with existing light gas guns indicates that this point occurs probably between 200 and 400 calibers. However, by effecting a constant base pressure, as discussed in Part X, the number of calibers would be increased.

(e) *Heat loss by Radiation*

The heat loss by radiation from the propellant gas in guns is generally negligible. This conclusion may be reached by calculating the radiation heat loss with the assumption that the gas radiates like a black body. Such an assumption will yield the maximum radiative heat loss*.

With the assumption of a black body, the radiated energy Q becomes

$$Q = KT^4(\Delta t)A_s \qquad (39\text{-}7)$$

where K is the Stefan-Boltzmann constant, Δt is the time interval during which radiation occurs, and A_s is the surface area of the radiating gas; the temperature of the wall has been assumed negligible in this expression. The radiated energy transferred from the propellant gas may be set equal to the energy change of the gas. Thus,

$$Q = nc_v\Delta T \qquad (39\text{-}8)$$

where n is the number of moles, c_v the average specific heat, and ΔT is the average temperature drop of the propellant gas. From Equations (36-7) and (36-8) the temperature change of the propellant gas becomes

$$\Delta T = \frac{KT^4(\Delta t)A_s}{nc_v} \qquad (39\text{-}9)$$

Inserting numerical values appropriate to high-speed guns into Equation (36-9) results in a calculated temperature drop ΔT which is negligible. For example, let us consider the case of a two-stage gun when the pump tube piston has compressed the hydrogen propellant to the peak values of temperature and pressure indicated below:

$$p = 300,000 \text{ lb/in}^2$$

$$T = 6000^\circ K$$

$$v = 5500 \text{ cm}^3$$

---
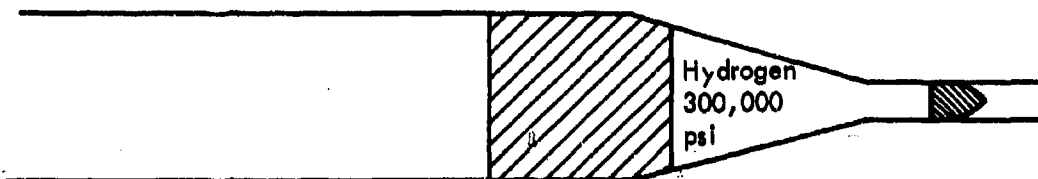
* An exact calculation is almost impossible to make because, in general, the values of emissivity for propellant gases are unknown.

$$A_s = 1500 \text{ cm}^2$$

$$n = 250 \text{ moles}$$

$$c_v = 8 \text{ cal/mole}^{\circ}\text{K} .$$

With K equal to 1.36×10^{-12} cal/cm^2 sec($^{\circ}$K)^4 the temperature drop for a period of two milliseconds (Δt) is

$$\Delta T \simeq 3^{\circ}\text{K} .$$

This is a negligible drop in propellant gas temperature.

Experimental and theoretical results obtained for the reservoirs of hot shot wind tunnels at AEDC[59] confirm the above conclusions; the radiative heat losses are negligible during the time of interest for the conditions of temperature and density existing in a PP gun or in a two-stage gun.

(f) Projectile-barrel friction

The discussion will be restricted to smoothbore guns. The effect of projectile-barrel friction is evident from experience with light gas guns. This experience indicates that when the barrel is greater than 200 to 400 calibers in length, the projectile may actually decrease in velocity. There is hardly any experimental data on the magnitude of the bore friction itself.

Some information may be obtained from the results of the ERMA experiments. These experiments were in general, done with well-machined cylindrical projectiles (12.148 ± 0.0005 mm) in a well-machined barrel (12.166 ± 0.001 mm). The experiments indicate that, by changing projectile materials and projectile lubricants, the discrepancy between isentropic theory and experiment may be somewhat changed. Definite evidence of projectile friction was noted either by loss of weight of bronze projectiles or by gradual increase of barrel diameter with hardened steel projectiles. The accuracy with which steel projectile diameters were made seemed to have no effect on the discrepancy. (One group of projectile diameters was machined to ± 0.0002 mm; the other, to ± 0.0015 mm.)

The closeness of fit between projectile and barrel made no difference in the discrepancy. (Projectile diameters varied between 12.146 and 12.159 mm in a barrel of diameter 12.166 mm)

It was, however, found that the discrepancy between isentropic theory and experiment could be significantly reduced by decreasing the rubbing area of the projectile. This was done by machining a projectile of uniform diameter to form a projectile with a waist in the center and two rings of contact. This decrease in rubbing area of about 50 percent resulted in a decrease in velocity discrepancy from 2.4% to 1.6% (see sketch on the following page). One could extrapolate this result to zero rubbing area and conclude that with projectile friction absent the velocity loss would be 0.8% or about 1%. One could thus ascribe half of the 2% velocity discrepancy in the ERMA case to projectile-barrel friction, the other half to boundary layer. At the present state of ignorance on the role of bore friction,
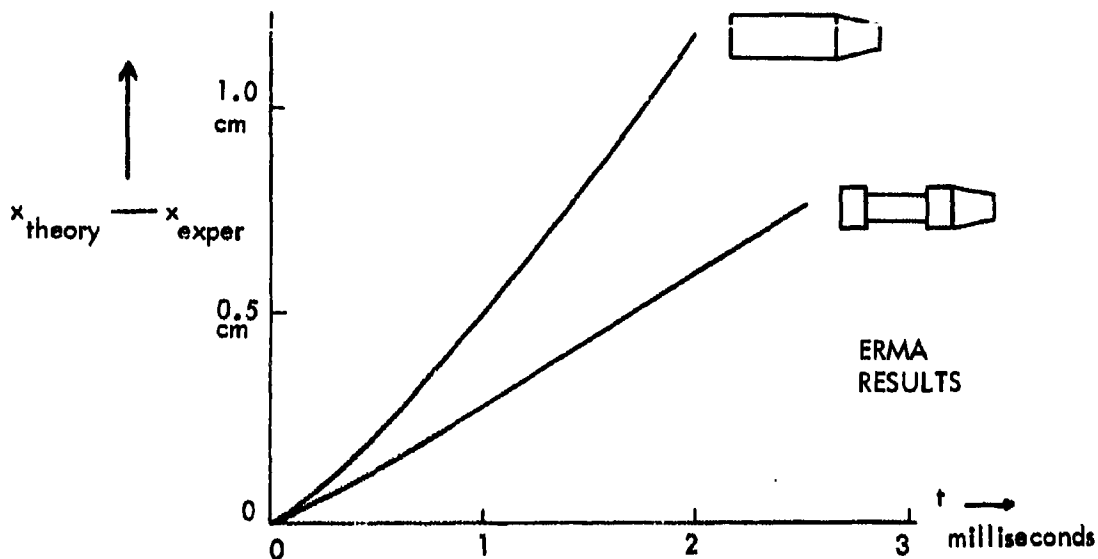
it is probably as good as any method of accounting for it by assuming a counter frictional pressure proportional to the propelling pressure.
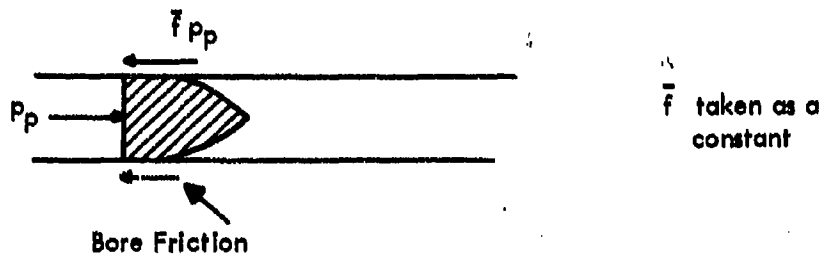
For very smooth bores a value of 2% (which results in a 1% velocity decrement) is recommended for this percentage. One certainly is left with an unsatisfactory feeling about the ability to calculate projectile friction for a given gun. What is required are more ERMA-type experiments combined with more sophisticated boundary layer analyses.

Section 40

Conclusions as to Methods of Accounting for Boundary Layer and Projectile Friction

The relatively careful study done in the ERMA experiments indicates that the isentropic theory predicts a projectile velocity which is about 2% higher than achieved experimentally. In this study the propellant was initially at room temperature; the steel projectile was carefully machined; the projectile velocity was of the order of the gas initial sound speed.

However, as described above, experimental results for guns using high temperature light gases firing projectiles between 12,000 ft/sec and 30,000 ft/sec indicate a larger discrepancy between the experimental results and the isentropic theory. This discrepancy seems to increase with increasing projectile velocity. *One universal difficulty in calculation is that the initial conditions for the experiment are not well known; in most cases the isentropic equation for the expanding propellant gas is also not well known.*

Experimental and theoretical results indicate that the discrepancy is a result of boundary layer effects and projectile friction. However, at the present time, the validity of the methods being employed to account for these effects has not been satisfactorily demonstrated. It is for this reason that an approach based on dimensionless analyses is suggested in Reference 18. If one analyzes the effects of the irreversibilities on projectile velocity, it is concluded that the ratio of projectile velocity with frictional effects (boundary layer and projectile friction) u_{pf} to that without frictional effects $u_{pf=0}$ is mainly a function of

$$\frac{u_{pf}}{u_{pf=0}} = \phi \left(\frac{\gamma u_p}{a_0} , \frac{L}{D} \right)$$

with other dimensionless parameters such as Reynolds number, etc., being considered not essentially important. (The effect of γ, it is noted, is accounted for by incorporating it into the quantity u_p/a_0, the parameter found to be significant in Section 12 for determining theoretical PP Gun velocities.)

Based on the experimental results with high velocity guns at the US Naval Ordnance Laboratory, a curve of $u_{pf}/u_{pf=0}$ has been plotted versus $\gamma u_p/a_0$ and is shown in Figure 26 and in the following sketch.
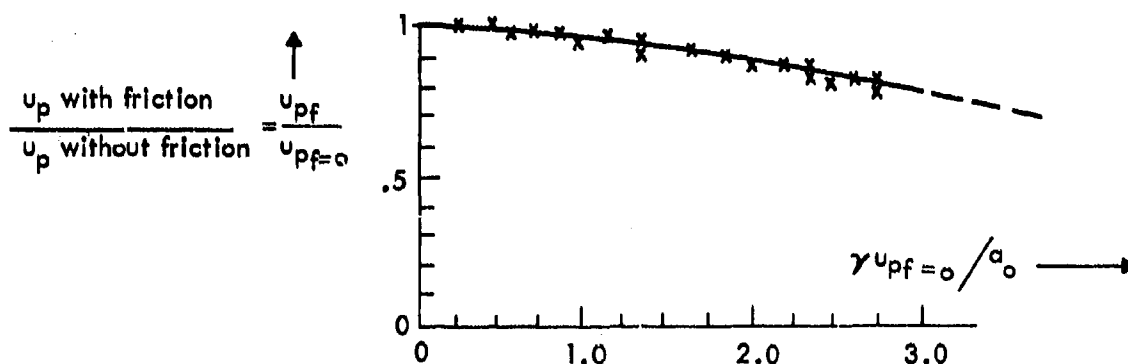
These experimental results were obtained from single stage H_2-O_2-He propellant guns and two-stage hydrogen guns; sizes of these guns varied from 0.22 in bore diameter to 4 in bore diameter; actual velocities, from 10,000 to 23,000 ft/sec. Tentatively, it is proposed that this plot be employed to take account of the frictional and heat-transfer effects until more careful theoretical-experimental studies better define these effects. It is to be noted in Figure 26 that below $\gamma u_p/a_0$ of 1½ the friction effects appear to be not important. Above this value of $\gamma u_p/a_0$ these effects become more and more significant. The plot of Figure 26 demonstrates again the desirability of a high sound speed which is seen to cause the frictional effects to be small relative to the inertia effects in a high-speed gun.

IX. METHODS OF HEATING THE PROPELLANT

Section 41

Use of the Heat of a Chemical Reaction

It has been previously demonstrated that the basic property of a propellant required for high projectile velocity is a low acoustic inertia; in the case of an ideal gas (a reasonable approximation in most cases) this is equivalent to a high initial temperature and low molecular weight (or a high initial sound speed). In practice, the need for a low molecular weight propellant is satisfied by using helium or hydrogen. There are a number of ways to increase the propellant gas temperature. One method of heating the propellant gas is to use the heat produced by a chemical reaction. Often used is the reaction of hydrogen and oxygen. Thus, the propellant becomes a steam-heated hydrogen or helium propellant.

The conditions after heat addition of the steam-heated hydrogen or helium propellant may be calculated as accurately as desired. (Such calculations have been done by Benoit[107].) A commonly used reaction is the following:

$$8 \text{ He} + 3 \text{ H}_2 + \text{O}_2 \rightarrow 8 \text{ He} + \text{H}_2 + 2 \text{ H}_2\text{O} + \text{heat} \quad .$$

The resultant propellant mixture has a molecular weight of 6.5, a temperature around 2700°K and a sound speed of 7000 ft/sec. The resultant pressure is about seven times the initial loading pressure. The average value of γ to be used during expansion is about 1.45. As seen from these values, the sound speed is low relative to the value for a pure hydrogen or helium propellant at a temperature of 2700°K.

Moreover, the possibility of detonation occurring is present when using H_2 and O_2 to heat the hydrogen or helium propellant. Experience at the US Naval Ordnance Laboratory indicates that detonation may be prevented in chambers of diameter less than about 4 in if the gases are well mixed, the ignition is accomplished simultaneously at many points, and the reaction is allowed to go to completion before the diaphragm is ruptured. However, for chambers above 6 in in diameter at initial pressures of the room temperature mixture above 6000 lb/in² detonations will almost always occur.

Because of the possibility of detonation and the relatively low sound speed attained, hydrogen-oxygen to heat chemically the propellant is not widely used. Other disadvantages are the amount and pressure capability of the gas handling equipment required and the necessity to provide ignition. One advantage is that the chamber to be used may be relatively small. The use of other chemicals (e.g., compounds of aluminium and oxygen) to heat has not been very successful. The maximum velocities attained in H_2, O_2, He guns are around 13,000 ft/sec. Reference 61 describes the performance of such a gun. See also References 87 and 90.

Section 42

Use of Electrical Arc Heating

Heating hydrogen by means of an arc discharge has been done in a number of laboratories. For example, see Reference 62. At high imputs of electrical energy,

the experimental projectile velocities are less than theoretically predicted. It is speculated that the hydrogen gas propellant is contaminated by metallic electrode particles, thus increasing the molecular weight of the hydrogen propellant (see Reference 79). The maximum velocities attained in arc heated guns are around 18,000 ft/sec. At the present time such guns are not attractive for producing high velocity.

Section 43

Shock Heating

Heating hydrogen, helium, or steam-heated helium by means of a shockwave has been attempted (see for example, References 27, 28, and 117 for experimental and analytical results). The shockwave is generated by a propellant in a chamber attached to the back of the gun (see following sketch).
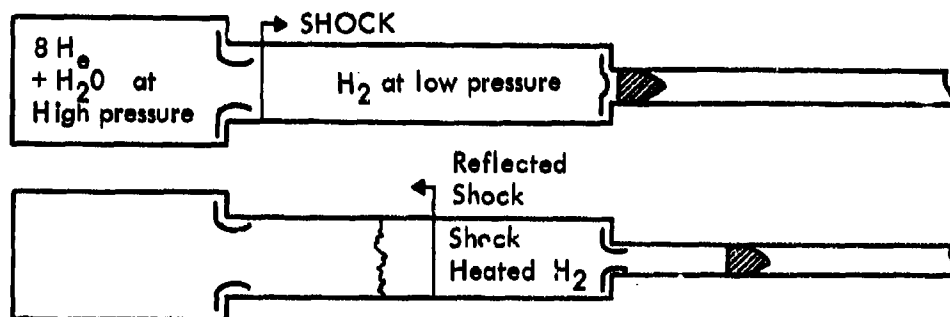
Results at the US Naval Ordnance Laboratory with such a gun indicated that the projectile velocities were 25 to 35% below those theoretically predicted. It was concluded that the shock was not well formed, and that a light piston separating the H_2 from the H_2O and He would be desirable.

Such a gun using a light piston to separate a driver from the shock-heated helium was used[28] at Ames Research Center, NASA. This gun is shown in the following sketch.
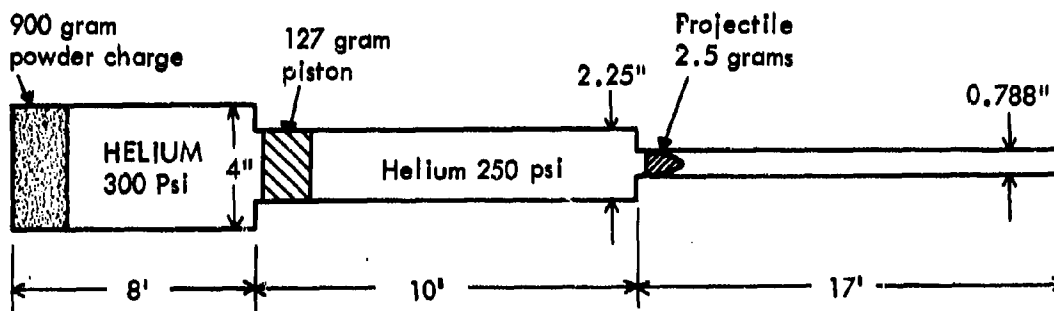
The muzzle velocity obtained by the 2.5 gram projectile with the initial
conditions illustrated above was 22,670 ft/sec. This type of gun is relatively
simple to operate and need not be expensive.

Since the propellant gas is shock-heated, a smaller compression ratio is required
by the shock-heated gun than by a gun using a heavy piston to isentropically compress
the propellant gas. Consequently, the shock-heated propellant gun may be smaller
in length than a gun using isentropic compression. However, the shock-heated gun
will, because of the low inertia of the light piston, not maintain the propellant gas
pressure for as long a time as for the heavy piston isentropic compression gun.
Moreover, the light piston is not an efficient heater of the propellant gas, as
pointed out by Lemke[78] and Baker[115]; increasing the piston velocity does not produce
a significantly higher peak temperature, because the higher piston velocity requires
a higher initial pressure to limit the peak pressure. Experimental results confirm
the fact that the light piston shock-heated gun produces lower projectile velocities
than the heavy piston isentropic compression gun. The two stage piston gun is
discussed below.

Section 44

The Two-Stage Gun - General Description

The first successful light gas gun was developed by the New Mexico School of Mines
around 1948 (see References 29, 88, and 89). Hydrogen was used to propel light
spheres at velocities up to 14,000 ft/sec. The hydrogen was compressed and heated
by a single stroke piston driven by a gunpowder propellant. The barrels used were
0.25 in and 0.38 in diameter.
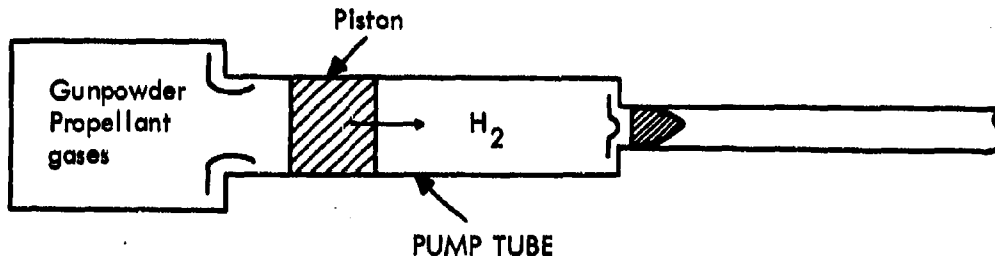
It was thought that the compression ratio required by such a piston compressed
hydrogen gun would make the chamber impractically large for guns with barrels above
the 20 mm size. Thus, for a number of years guns using other methods of heating the
propellant were used.

Experience through the years, however has demonstrated that to date the only
successful method of attaining projectile velocities above 20,000 ft/sec is to use
the original concept of the New Mexico School of Mines gun, the concept of heating a
light gas by means of piston compression. Today's so-called "two-stage" guns use
this concept.

The sequence of events occurring in a two-stage gun is illustr⸱⸱⸱   ⸱⸱⸱⸱ 27.
Initially, the pressure p_0 of the back chamber gas is high relative   ⸱⸱⸱ pressure
p_1 of the pump tube (front chamber) gas (hydrogen or helium). In operation the high
pressure gas in the chamber ruptures the diaphragm "A" and then pushes the piston of
mass M into the gas in the pump tube, heating it and compressing it; this heating
and compression is effected, generally, by shockwaves* which travel back and forth in
the hydrogen (or helium) between the piston and projectile. When the pressure in the
pump tube reaches a sufficiently high value, the diaphragm "B" separating the pump
tube from the barrel ruptures, and the projectile is propelled along the barrel by the
gas in the pump tube. The shocks which exist in the hydrogen (or helium) may travel to
and be reflected from the projectile.

It is possible by this method to obtain much higher sound speeds in the compressed
gas in the pump tube than could be achieved in the propellant gas in a single chamber
by heating it chemically or electrically. Thus, the gas in the pump tube reaches a
higher value of sound speed than the value of sound speed a_0 in the chamber. Of
course, all the energy imparted to the gas in the pump tube comes from the gas in the
back chamber; the piston provides an efficient means to transfer this energy; its
inertia makes it possible to compress the gas in front to very high internal energies
at the expense of the internal energy of the gas in the back of the piston.

The two-stage gun not only affords a method of heating the propellant gas, *but also
of maintaining the pressure at a constant value directly behind the projectile.* To
so maintain the pressure constant behind the projectile requires that the pressure in
the pump tube increase with time at a specified rate. Thus, the proper movement of
the piston in the two-stage gun may effect this rate.
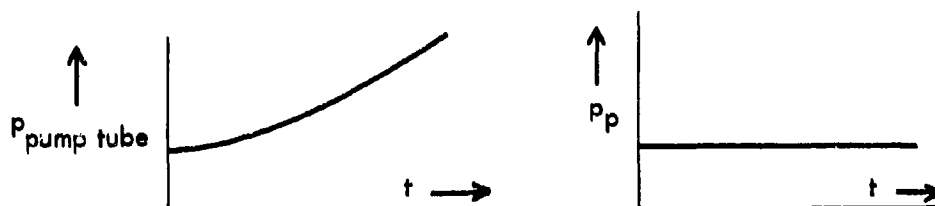
The application of the two-stage gun to maintain the propelling pressure constant was
suggested by Curtis[36] and independently by Wilenius[97] and Winkler[35]; it is discussed
in Part X, "The Constant Base Pressure Gun".

---

* The strength of the shocks depends on the magnitude of the piston speed; light pistons,
traveling at high speeds, produce strong shocks; heavy pistons, traveling at low speeds,
produce weak shocks. (The magnitude of the piston speed is taken relative to the sound
speed of the gas in front of the piston.)

Section 45

The Two-Stage Gun – Approximate Calculation Method

To calculate by hand the events which occur in such a gun is a tedious, impractical task. The occurrence of shocks complicates the calculation considerably. The methods outlined previously in this monograph may be applied to the calculation as indicated in the following sketches.*

$$\frac{D(u \pm \sigma)}{Dt} = 0$$
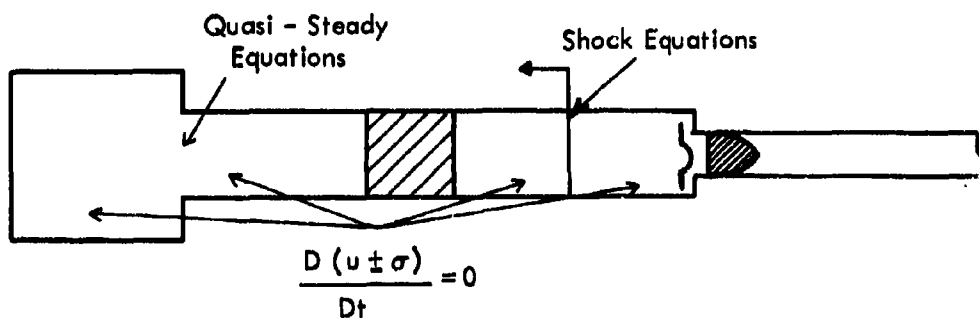
BEFORE PROJECTILE RELEASE


$$\frac{D(u \pm \sigma)}{Dt} = 0$$
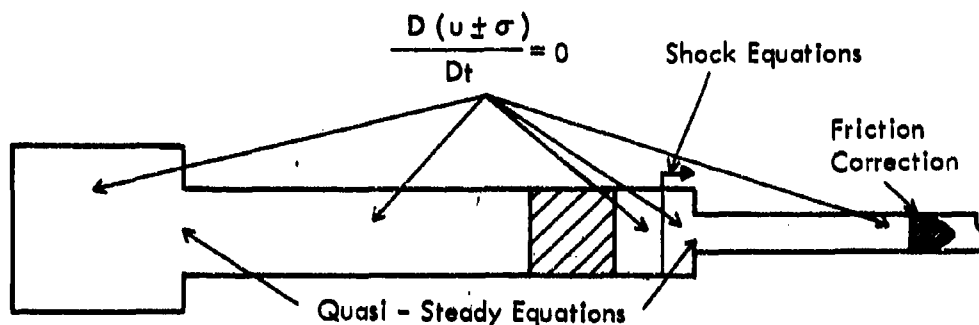
AFTER PROJECTILE RELEASE

To simplify the calculation for hand computation, the following approximate method of analysis has been advantageously used for either a light piston (shock compression) or a heavy piston (isentropic compression) gun†.

---

* It is assumed that the back chamber contains a preburned propellant. If, however, powder propellant is used, conventional ballistic methods (see, for example Reference 30) may be employed to calculate the pressure behind the piston. For a more exact analysis of a gun with a burning propellant, see Carriere[3].

† One should note References 17 and 78 through 83, where approximate analyses are presented for a two-stage gun system. Also see Reference 117 for the shock-heated case.

(a) The initial phase of the motion of the piston may be calculated by applying the results for the preburned propellant gun performance (e.g., Figure 21) to the piston and accounting for the propellant gas in front (Fig. 22).
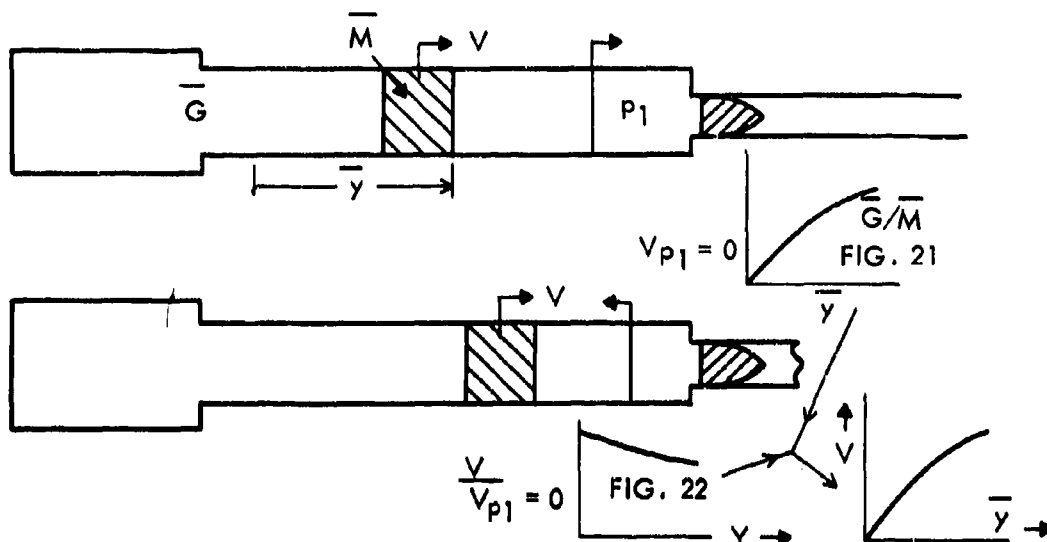
(b) The piston position $\bar{y}_3$, velocity v_3, when the reflected shock has traveled back to the piston can be calculated, as can the conditions in front of the piston, by using the V-$\bar{y}$ curve and the shock equations. (See Appendix Q).


$$\rho_1 L_1 = \rho_3(L_1 - \bar{y}_3)$$
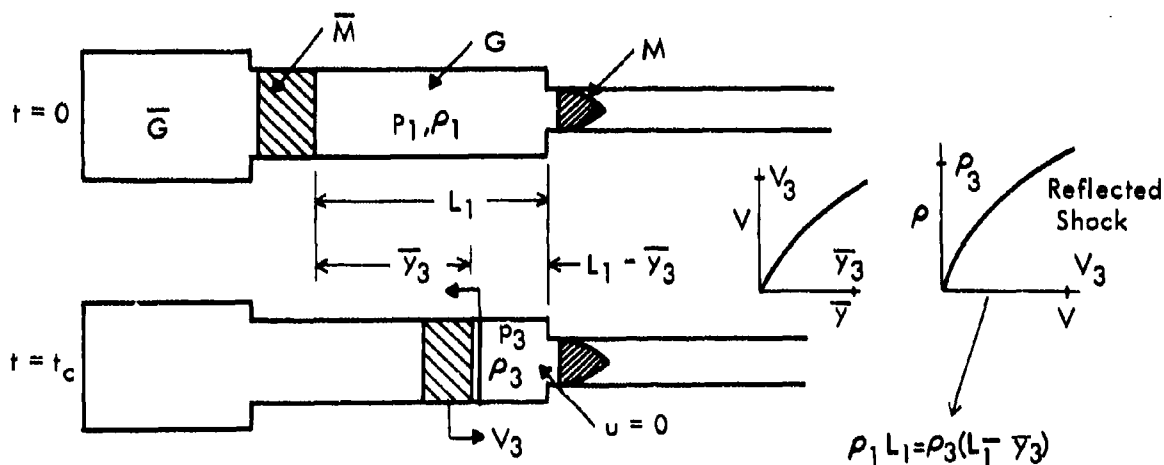
(c) Since at this time the velocity of the gas in state 3 is zero (and thus the gas kinetic energy is zero), it is convenient to apply the first law of thermodynamics

to the system consisting of the piston and gas in front of the piston*; the
first law is applied between the state existing in diagram C of Figure 27
(time t_c) and any subsequent state (say, state 4) of the system until the
projectile is released. Several simplifying assumptions are made:

(i) The gas in front changes state isentropically after t_c (see previous
footnote*).

(ii) The kinetic energy of the gas at any time after t_c is equal to $GV^2/6$.

(iii) The work due to the pressure behind the piston is negligible.

Assumption (i) is a good approximation because the irreversibility association
with the second and third shock reflections is small, as may be calculated by
the methods of Reference 32. Assumption (ii) is deduced from the approximation
of a linear velocity distribution which is valid for low gas velocities (see
Appendix F). Assumption (iii) agrees well with numerical results from electronic
computing machines (see Figure 28).
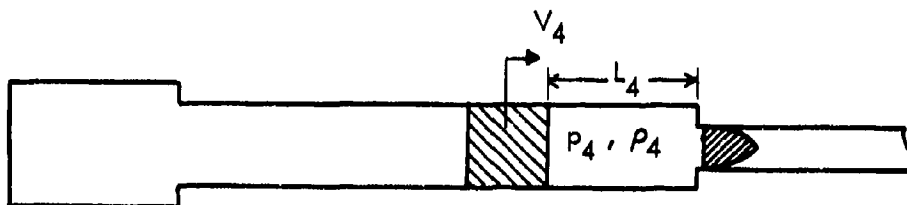
First Law: $\bar{M}V_3^2/2 + Gc_pT_3 = MV_4^2/2 + Gc_pT_4 + GV_4^2/6$

Isentropic
Equations:
$$p_4 L_4^\gamma = p_3 L_3^\gamma$$
$$(p_4/p_3)^{\frac{\gamma-1}{\gamma}} = T_4/T_3$$

From these three equations, the three unknowns T_4 , p_4 , and V_4 may be obtained,
the state 4 being at any time subsequent to time t_c but before the projectile has
been released.

(d) The next phase of the calculation is for the time period after projectile release.
It is assumed for simplicity that sonic flow exists in the barrel entrance. The
piston motion is determined with the aid of Newton's equation by a step-by-step
numerical process, as shown below.

---

* In some cases (e.g., for light piston cases) it may be desirable to calculate the conditions
at the time when the shock has gone forth and back a second time.
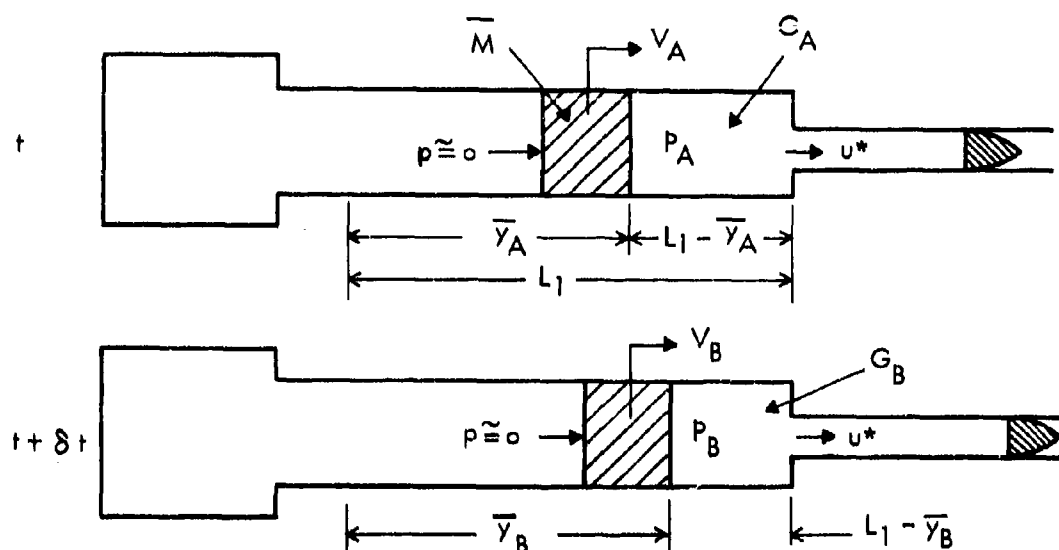
The applicable equations are

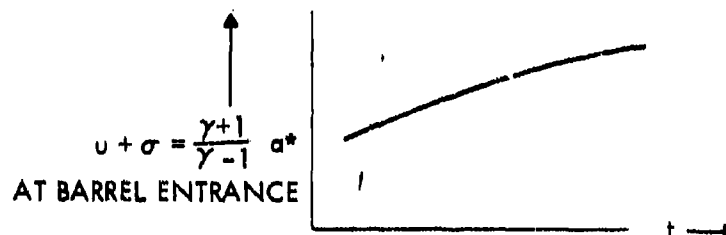$$\bar{M}[V_B^2 - V_A^2]/2 = -p_A A_0(\bar{y}_B - \bar{y}_A)$$

$$G_B = G_A - (\rho^* u^* A_1)\delta t$$

$$p_B/p_A = (\rho_B/\rho_A)^\gamma = [G_B(L_1 - \bar{y}_A)/G_B(L_1 - \bar{y}_B)]^\gamma .$$

The three equations permit, for a given δt, the solution for the three unknowns G_B, $\bar{y}_B$, and V_B.

(e) Finally, from (d) one may obtain the value for the barrel entrance condition of the sum $u + \sigma$ as a function of time. Since sonic conditions are assumed to exist there,

$$u + \sigma = u^* + \sigma^* = \frac{\gamma + 1}{\gamma - 1} a^*$$

This sum remains constant along $u + a$ disturbances which reach the projectile at a time Δt after they leave the barrel entrance position.
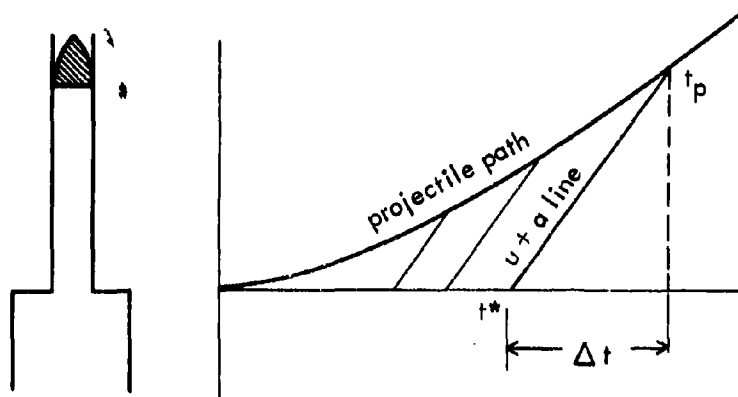
The time interval Δt is approximated by assuming the $u + a$ characteristic to be a straight line. Thus,

$$t_p - t^* - \Delta t = \frac{x_p}{\frac{1}{2}\{[u^*(t^*) + a^*(t^*)] + [u(t_p) + a(t_p)]\}}$$

$$= \frac{2x_p}{\frac{\gamma+1}{2}\sigma^*(t^*) + u_p(t_p) + \frac{\sigma_p(t_p)}{2/(\gamma-1)}} \quad .$$

Newton's equation is applicable to the projectile.

$$M\frac{du_p}{dt_p} = Mu_p\frac{du_p}{dx_p} = p_p A_1 = p_0\left(\frac{\sigma_p}{\sigma_0}\right)^{\frac{2\gamma}{\gamma-1}} A_1 \quad .$$

Along the $u + a$ characteristic

$$u^* + \sigma^* = u_p + \sigma_p = \frac{\gamma+1}{2}\sigma^* \quad .$$

The complete projectile motion may be obtained by a step-by-step numerical procedure using the three equations above. The effect of friction may be accounted for by using Figure 22.

The approximate method outlined in this section yields projectile velocities which agree well with the results of more sophisticated methods. For a heavy piston case the method above becomes equivalent to that described by Charters in Reference 83 (or Reference 86). However, not only is the calculation very time-consuming, it does not yield needed information about the details of the pressure experienced by the projectile. In the actual situation shocks, neglected in the approximation after the projectile is released, travel back and forth between piston and projectile.

These shocks, although sometimes weak, cause sharp pressure peaks which may cause projectile mechanical failure. In some cases predictions by approximate methods of the type outlined here for the peak pressure experienced by the projectile have been found to be in error by a factor as high as four. This is one reason that the use of electronic computers to calculate more exactly the performance of a two-stage gun becomes highly desirable.

<div style="text-align:center">

Section 46

The Two-Stage Gun – Performance Calculation
by Electronic Computing Machines

</div>

To avoid the tediousness of hand calculation and to better determine the actual pressure variations occurring, it is necessary to use electronic computers for two-stage gun calculations. The speed of these machines is particularly advantageous when it is necessary to select loading conditions to yield a maximum projectile velocity. In a given two-stage gun which is to propel a given mass projectile of given pressure capability, it becomes necessary to select the following parameters:

(a) The back chamber conditions.

(b) The pump tube conditions.

and

(c) The piston mass.

(d) The projectile release pressure.

The number of possibilities makes the electronic computer invaluable to use to select the optimum parameters. This is particularly so because as of the present time there are few general rules for guidance in the selection of these parameters, the optimum values depending on the particular two-stage gun geometry and pressure capabilities.

(If, however, one is designing a two-stage gun "from scratch" to propel a given projectile at a given velocity, the use of the "constant base pressure" ideas outlined in Section 47 yields a two-stage gun design without the necessity of as many trials.)

The most suitable scheme to the present for the electronic computer application to the two-stage gun is the one-dimensional Lagrangian scheme discussed in Section 27. It is based on the "q" method, as devised by von Neumann and Richtmyer[12, 13]. The code solves quasi-one-dimensional hydrodynamic problems, i.e., it will handle cases of one-dimensional flow through ducts of varying cross section. Automatic treatment of the shock by the "q" method lends itself nicely to the solution of multiple shock systems such as occur in the two-stage light gas gun. Any equation of state may be used for the gas. This scheme is presently being used at the US Naval Ordnance Laboratory[14, 106] and Aberdeen Proving Ground[33].

Another computer scheme using the method of characteristics and the shock equations is in use by Republic Aviation Corporation[93]. This scheme appears applicable to the two-stage gun problem.

For a given two-stage gun, firing a given projectile, the types of results one obtains by using the computing machine when attempting to optimize performance are as shown in the following sketch.
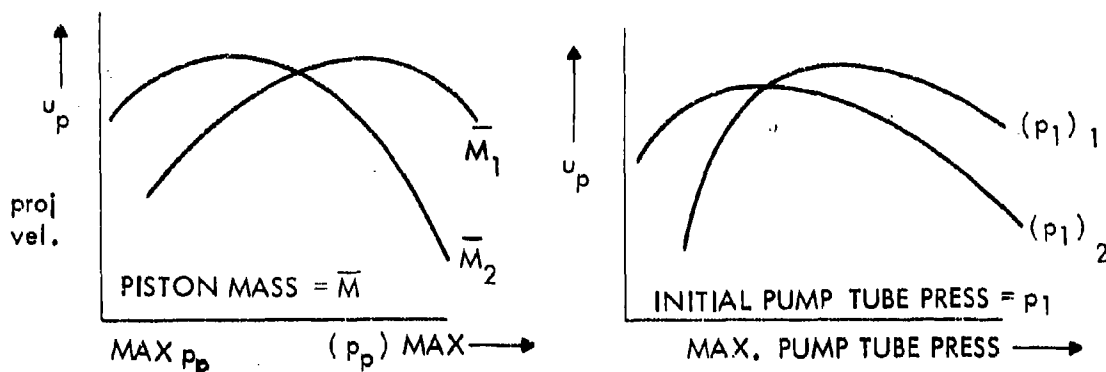
As mentioned before, the form of these curves varies greatly with the geometry of the two-stage gun. Therefore, each gun system geometry will have specific characteristics. *In general, the larger the pump tube, the better will be the performance* of a two-stage gun.

The calculations also indicate that preheating an ideal propellant gas in the pump tube is advantageous (see for example, References 82 or 95).
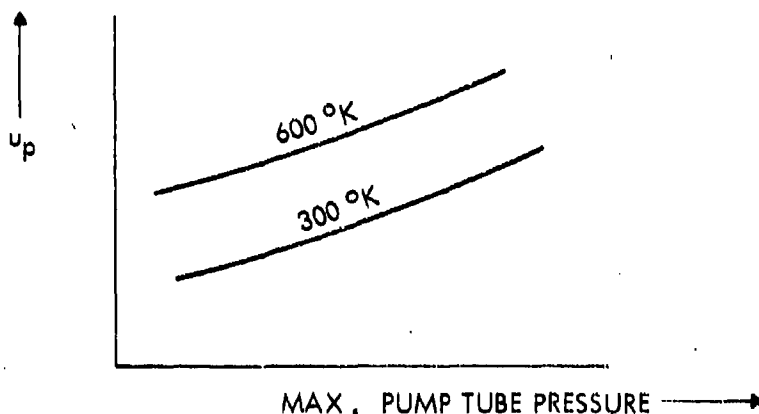

Experimental results to date are not conclusive as to the advantage of preheating the propellant gas. AEDC reported[82] an increase in projectile velocity from 27,500 ft/sec to 30,000 ft/sec by doubling the propellant gas initial temperature. In contrast, Cable[108] reported no gain by heating to about 400°K. (Thus, the increase in experimental projectile velocity due to preheating is often less than predicted by calculation. It is here speculated that this deficit is partially* due to the

---

* For long pump tubes there may occur convective heat losses which would contribute to the degradation of gun performance.

assumption that the propellant gas is an ideal gas. Actually, in many cases the propellant gas is sufficiently dense that the intermolecular forces are significant; in these instances, as shown below (see, e.g., Sections 5T and 64) the dense real-gas propellant produces a higher projectile velocity than an ideal gas propellant. By preheating the propellant the effects of the intermolecular forces are reduced; consequently, less gain in velocity is experimentally achieved by preheating than expected from the calculations done for an ideal-gas propellant.)

One may, in principle attain the benefits of preheating by increasing the pump tube volume as seen in the following sketch.
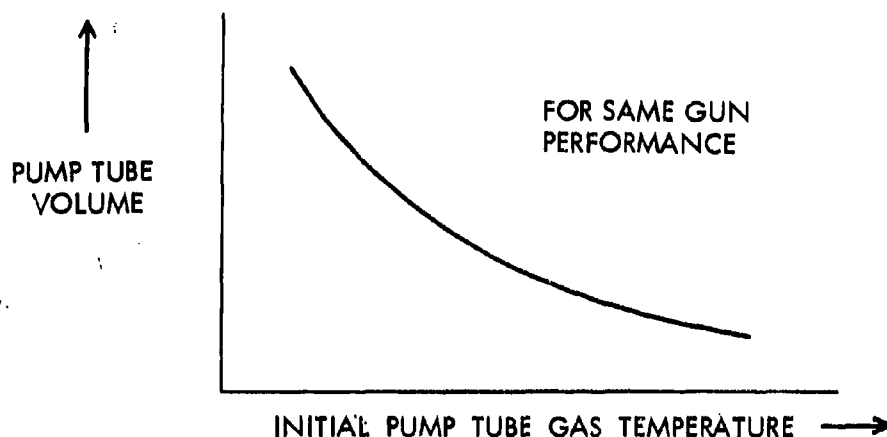
Typical calculated and experimental performance curves for two-stage guns are shown in Figure 28; other performance curves are given by Baer[33], Stephensen[80, 81, 82] Piacesi[14] and Swift[95]. A sketch of one of the US Naval Ordnance Laboratory two-stage guns is shown also in Figure 28. The barrel of this gun is two inches in internal diameter.

As mentioned before, almost every laboratory has successfully, and in its own individual manner, fitted its own experimental two-stage gun results to its own theory. Thus, for example, good agreement between theory and experiment have been reported in References 81, 82, 94, 27, 83, 37, 33, 103, and 14 (See Fig. 28). However, as previously noted, these comparisons, in almost all cases, lack the necessary accuracy to assess the validity of the theory used.

X. THE CONSTANT BASE PRESSURE GUN

Section 47

The Concept of Maintaining a Constant Base Pressure

In a preburned propellant gun the value of the maximum pressure experienced by the projectile is the same as the value of the maximum pressure experienced in the chamber. In such a gun the pressure of the gas behind the projectile decreases as the projectile accelerates in the gun barrel. This is seen from the equation

$$p_p = p_0 \left\{ 1 + \epsilon - \frac{u_p(\gamma - 1)}{2a_0} \right\}^{\frac{2\gamma}{(\gamma-1)}} \qquad (47\text{-}1)$$

which expresses the pressure as a function of the projectile velocity in the preburned propellant gun.
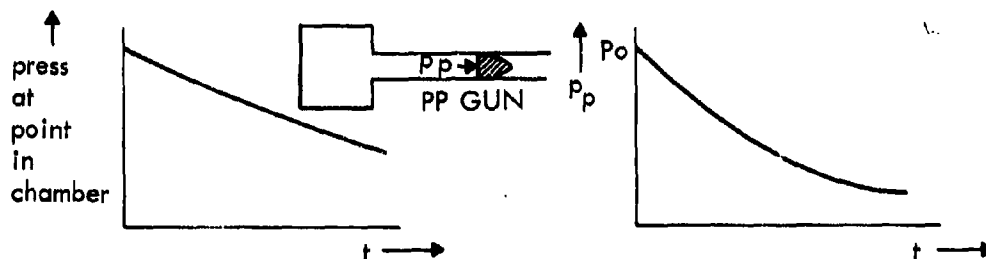
Only in the unattainable limit of infinite initial sound speed does the pressure not decrease behind the projectile in a PP gun.

It would be, of course, extremely desirable to maintain the pressure behind the projectile at a constant value. Such a possibility exists for a gun in which the pressure in the chamber is not limited to the maximum value experienced by the projectile, but could be increased as desired during the travel of the projectile.
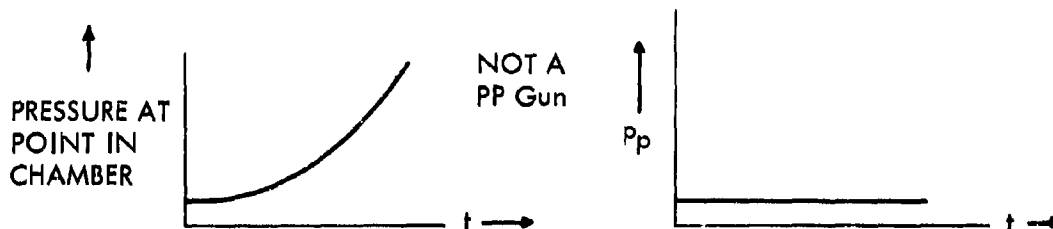
Such a gun would not be a preburned propellant gun; it might be a gun in which the propellant continued to burn during the projectile motion; it might be a two-stage gun in which the piston continued to increase the pump tube pressure during the projectile motion. The latter concept has been suggested by Curtis[38], Wilenius[97], and independently by Winkler[37].

Section 48

Deducing a Gas Flow Which Maintains the Base Pressure Constant (The "Similarity Solution")

How should the pressure vary in the chamber so as to maintain the pressure constant behind the projectile? A partial answer to this query is provided by the "similarity solution" of Stanyukovitch[34]; also see Smith[35], Curtis and Charters[38,39,57,94], Wilenius[37,92], and Winkler[36]. This solution assumes that the gas velocity in the constant diameter barrel is only a function of time (not of distance). Thus,

$$u = u(t) \tag{48-1}$$

It may be demonstrated that this assumption yields a constant base pressure gas flow as desired. A different and more logical approach than starting from the assumption of Equation (48-1) is given below.

The quest is for a gas flow which will yield a constant pressure behind the projectile. One possibility is to consider the situation in which the pressure is not only constant for the gas layer directly behind the projectile, but is constant (although a different constant) for each gas layer. Thus, for this situation it is assumed that in the constant diameter flow

$$\frac{\partial p}{\partial t} + u \frac{\partial p}{\partial x} = 0 \tag{48-2}$$

which states that the *pressure does not change along a particle path.* (See Appendix A). This then is the basic assumption made.

If it is now assumed that the gas changed state isentropically, then

$$\rho = \rho(p)$$

alone, and

$$a = a(p) \tag{48-3}$$

alone, etc. Thus, *since p does not change along a particle path, each of the other thermodynamic properties does not change* along a particle path. This is expressed in equation form from (48-2) and (48-3) to yield

$$\frac{\partial \rho}{\partial t} + u \frac{\partial \rho}{\partial x} = 0 \tag{48-4}$$

$$\frac{\partial a}{\partial t} + u \frac{\partial a}{\partial x} = 0 \qquad\qquad (48\text{-}5)$$

and so on for all the other thermodynamic properties.

The applicable one-dimensional unsteady equations of continuity and momentum are

$$\frac{\partial \rho u}{\partial x} + \frac{\partial \rho}{\partial t} = 0 \qquad\qquad (48\text{-}6)$$

$$\frac{\partial u}{\partial t} + u \frac{\partial u}{\partial x} = -\frac{1}{\rho}\frac{\partial p}{\partial x} \quad . \qquad\qquad (48\text{-}7)$$

Inserting the requirement for constant density of a gas layer Equation (48-4) into the continuity Equation (48-6) results in

$$\rho \frac{\partial u}{\partial x} = 0 \quad . \qquad\qquad (48\text{-}8)$$

Thus, from Equation (48-8), either the gas density is zero,

$$\rho = 0 \qquad\qquad (48\text{-}9)$$

or the gas velocity is a function of time alone, i.e.,

$$u = u(t) \quad . \qquad\qquad (48\text{-}10)$$

Either possibility will yield a constant base pressure gun.

Obtaining a zero density gas (and hence an infinite sound speed gas) is not realizeable in practice and this possibility will not be further considered.

The second possibility, that the gas velocity be a function of time alone, constitutes the similarity solution of Stanyokovitch and Smith and will be further considered.

If Equation (48-10) is inserted into the momentum Equation (48-7), there is obtained

$$\frac{du}{dt} = -\frac{1}{\rho}\frac{\partial p}{\partial x} \quad . \qquad\qquad (48\text{-}11)$$

Since the left hand side of this equation, by Equation (48-10), is a function of time t alone and the right side, in general, would be a function of x and t, it must be that each side of Equation (48-11) is equal to a constant, say, "α". Thus,

$$\frac{du}{dt} = -\frac{1}{\rho}\frac{\partial p}{\partial x} = \alpha \qquad\qquad (48\text{-}12)$$

and, hence, by integration with $u = 0$ at $t = 0$

$$u = \alpha t \quad . \tag{48-13}$$

Thus, the gas velocity is proportional to time in this case in which the thermodynamic properties do not change along a particle path.

In particular, the path of the particle which originates at $x = 0$, $t = 0$ may be chosen as the path of a projectile. The unchanging pressure and sound speed of the gas behind this projectile are denoted as p_0 and a_0, respectively. With the assumption that the barrel is evacuated in front of the projectile, the propelling pressure is constant (equal to p_0), resulting in a constant base pressure projectile. Newton's law for the projectile becomes

or

$$\left. \begin{aligned} M \frac{du_p}{dt} &= p_0 A \\ \\ u_p &= p_0 A t / M \end{aligned} \right\} \quad . \tag{48-14}$$

By comparing this result with the Equation (48-13) for velocity for any gas particle, it is seen that

$$\alpha = p_0 A / M \quad . \tag{48-15}$$

The travel-time history of the projectile is obtained directly by the integration of Equation (48-14)

$$x_p = \frac{p_0 A t^2}{2M} = \frac{\alpha t^2}{2} \tag{48-16}$$

and

$$x_p = \frac{u_p^2}{2} \quad . \tag{48-17}$$

The essential thermodynamic property which determines the magnitude of the pressure drop between the projectile and the $x = 0$ point may be deduced from the momentum equation (48-12). If this equation is integrated, there is obtained for any given time

$$\int_{p_0}^{p_1} \frac{dp}{\rho} = \alpha x_p \tag{48-18}$$

where p_1 is the pressure at the $x = 0$ point.

PRESSURE IN BARREL
AT A GIVEN TIME
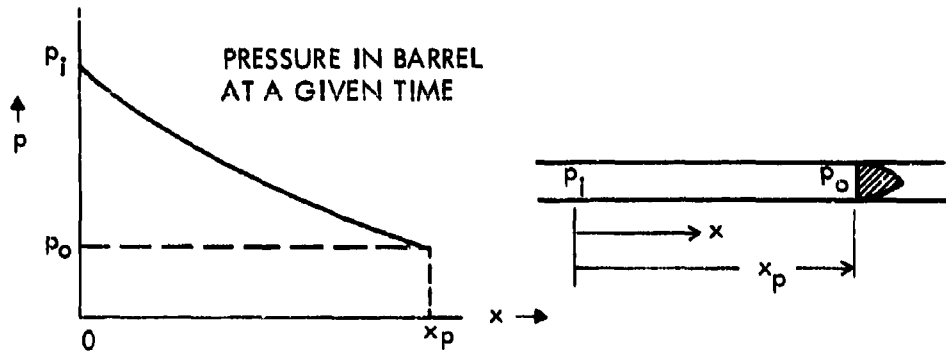
With Equation (48-17) this becomes

$$\int_{p_0}^{p_1} dp/\rho = u_p^2/2 \quad . \tag{48-19}$$

Equation (48-19) demonstrates that a propellant with a *low ρ as a function of* p *is desired* in order to have a low pressure p_1 at $x = 0$. (This is the same characteristic desired for a propellant in a steady flow expansion from a preburned gun chamber to the barrel).
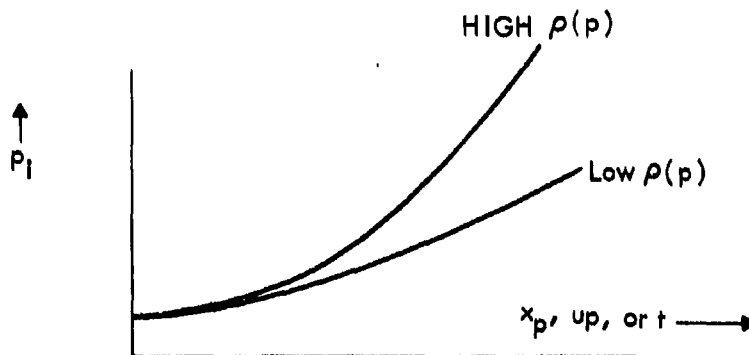

This is true for an ideal or non-ideal gas. In the case of an ideal gas, low density is equivalent to a high initial sound speed (or low initial density).

One might also integrate Equation (48-12) differently to determine the pressure difference between the projectile and the $x = 0$ position. Thus,

$$p - p_0 = \int_0^{x_p} \rho\alpha \, dx = \frac{G\alpha}{A} \tag{48-20}$$

where G is the gas mass between $x = 0$ and the projectile. It is seen that the pressure difference is proportional to the mass of gas behind the projectile.
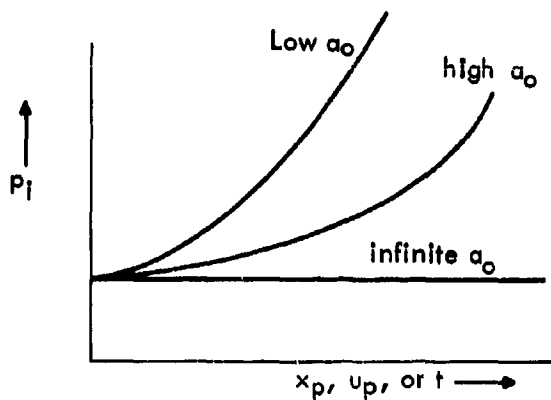
Section 49

The Variation of Gas Properties for the
Similarity Solution

The fact that pressure does not change along a particle path is expressed by the equation

$$\frac{\partial p}{\partial t} + u \frac{\partial p}{\partial x} = 0 \quad , \tag{49-1}$$

The expression for the differential pressure change

$$dp = \frac{\partial p}{\partial t} dt + \frac{\partial p}{\partial x} dx \tag{49-2}$$

becomes, by substitution of Equation (49-1),

$$dp = - u \frac{\partial p}{\partial x} dt + \frac{\partial p}{\partial x} dx \quad . \tag{49-3}$$

If the Equation (48-12) for the spacial pressure gradient and Equation (48-13) for the velocity u are substituted into Equation (49-3), there results

$$\frac{dp}{\rho} = \alpha^2 t dt - \alpha dx \quad . \tag{49-4}$$

Upon integration from $x = 0$ at $t = 0$, Equation (49-4) becomes

$$\int_{p_0}^{p} \frac{dp}{\rho} = \frac{\alpha^2 t^2}{2} - \alpha x \quad , \tag{49-5}$$

For an isentropic process

$$dh = dp/\rho \qquad (49\text{-}6)$$

so that Equation (48-12) becomes, in terms of enthalpy,

$$h - h_0 = \frac{\alpha^2 t^2}{2} - \alpha x \qquad (49\text{-}7)$$

where h_0 is the value of enthalpy at $x = 0$, $t = 0$. Equation (49-7) describes the variation of enthalpy necessary for the similarity solution. *It applies to any gas with any equation of state.*

Unless otherwise noted, the discussion will now be restricted to ideal gases. It is to be remarked, however, that real gas effects will change the quantitative results below. (See Section 57 below; also see Smith[35], for discussion of the effect of covolume). For an ideal gas the enthalpy may be readily put in terms of sound speed, pressure, or temperature. Thus, Equation (49-7) becomes

$$\left(\frac{a}{a_0}\right)^2 = 1 + \frac{(\gamma-1)\alpha}{a_0^2}\left[\frac{\alpha t^2}{2} - x\right] \qquad (49\text{-}8)$$

$$\frac{p}{p_0} = \left\{1 + \frac{(\gamma-1)\alpha}{a_0^2}\left[\frac{\alpha t^2}{2} - x\right]\right\}^{\frac{\gamma}{\gamma-1}} \qquad (49\text{-}9)$$

$$\frac{T}{T_0} = 1 + \frac{(\gamma-1)\alpha}{a_0^2}\left[\frac{\alpha t^2}{2} - x\right] \qquad (49\text{-}10)$$

where p_0, a_0, and T_0 are values of pressure, sound speed, and temperature at $t = 0$, and $x = 0$.

It becomes apparent that a constant base pressure equal to p_0 may be achieved on the back of a projectile if the enthalpy is altered as dictated by Equation (49-7), or equivalently if the pressure or the other variables are altered as shown in Equations (49-8), (49-9), and (49-10). Thus, for the position in the barrel where $x = 0$, which shall be designated by the subscript "1", pressures should increase with time in the manner prescribed by Equation (49-9).

$$\frac{p_1}{p_0} = \left[1 + \frac{(\gamma-1)\alpha^2}{2a_0^2} t_1^2\right]^{\frac{\gamma}{\gamma-1}} \qquad (49\text{-}11)$$

It is noted that the magnitude of the rise in pressure as a function of time is dependent on the sound speed a_0.
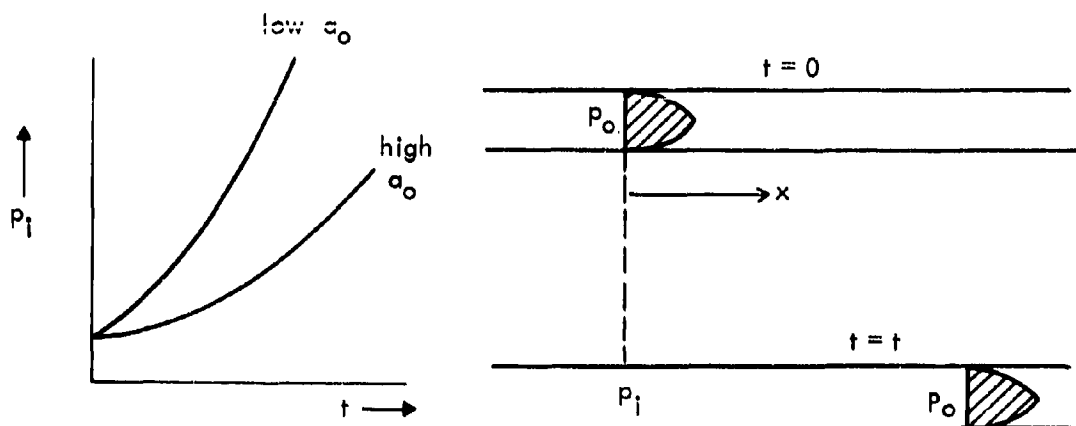
Sound speed and temperature will correspondingly increase with time at the position x = 0 .

$$\left(\frac{a_1}{a_0}\right)^2 = \frac{T_1}{T_0} = 1 + \frac{(\gamma-1)\alpha^2}{2a_0^2} t_1^2 \qquad (49\text{-}12)$$

where the subscript "1" designates the position x = 0 .

Other possibilities exist for attaining a constant base pressure gun than varying conditions at x = 0 . Thus, conditions may be varied at any given x or any given time t so as to satisfy Equations (49-8) through (49-10). For example, the pressure may be varied along the barrel at the time t = 0 to satisfy Equation (49-9).

$$\frac{p}{p_0} = \left[1 - \frac{(\gamma-1)\alpha}{a_0^2}x\right]^{\frac{\gamma}{\gamma-1}} \qquad . \qquad (49\text{-}13)$$

However, in practice the method employed has been to attempt to vary pressure at a given point (x = 0) as prescribed by Equation (49-11).

Section 50

The Path of Characteristics in Eulerian Coordinates for an Ideal Gas

The equations for the characteristic lines may be obtained by integrating the equations describing the slopes. Thus, letting the symbols ξ and τ denote the x , t coordinates of the characteristic lines, one has for the "u + a" characteristic lines
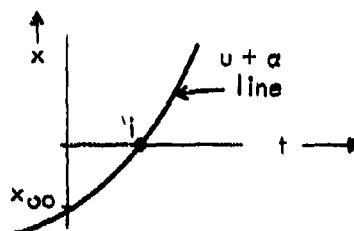
$$u + \sigma = \frac{2}{\gamma-1} a_{00} = u_1 + \sigma_1 \qquad (50\text{-}1)$$

$$\frac{d\xi}{d\tau} = u + a = \frac{3-\gamma}{2}u + a_{00} \qquad (50\text{-}2)$$

and

$$\xi - \frac{a_0^2}{(\gamma-1)\alpha} + \frac{2a_{00}^2}{(\gamma-1)\alpha(3-\gamma)} = \frac{(3-\gamma)\alpha}{4}\left[\tau + \frac{2a_{00}}{(3-\gamma)\alpha}\right]^2 \qquad (50\text{-}3)$$

where the subscript i denotes the conditions along $x = 0$, and where a_{00} is defined as the sound speed of the gas on the characteristics at $t = 0$ and is a function of the coordinate x_{00} of the characteristic at this time. Thus, from Equation (50-3) with $t = 0$,

$$x_{00} = \frac{a_0^2 - a_{00}^2}{\alpha(\gamma-1)} \qquad (50\text{-}4)$$

It is noted from Equation (50-3) that *every characteristic line is an identical parabola* whose vertex is displaced from characteristic to characteristic. (This was first noted by Winkler[34]). The equation for the vertex is

$$x_v = \frac{a_0^2}{(\gamma-1)\alpha} - \frac{(3-\gamma)\alpha}{2(\gamma-1)}t_v^2 \qquad (50\text{-}5)$$

where

$$t_v \leq 0$$

Similarly, for the "u - a" characteristics one finds

$$u - \sigma = -\frac{2}{\gamma-1}a_{00} = u_i - \sigma_i \qquad (50\text{-}6)$$

$$\frac{d\xi}{d\tau} = u - a = \frac{3-\gamma}{2}u - a_{00} \qquad (50\text{-}7)$$

und

$$\xi - \frac{a_0^2}{\alpha(\gamma-1)} + \frac{2a_{00}^2}{\alpha(\gamma-1)(3-\gamma)} = \frac{\alpha(3-\gamma)}{4}\left[\tau - \frac{2a_{00}}{(3-\gamma)\alpha}\right]^2 \qquad (50\text{-}8)$$

where a_{00} is the sound speed of the gas on the "u - a" characteristic at $t = 0$ at which point $x = x_{00}$ (described also by Equation (50-3)). It is seen that the

"u − a" characteristic lines are also identical paraboles which are displaced so that the verteres lie along the parth

$$x_v = \frac{a_0^2}{\alpha(\gamma-1)} - \frac{3-\gamma}{2(\gamma-1)}\,\alpha t_v^2 \qquad (50-9)$$

where $t_v \geqslant 0$. Moreover, most remarkably, the "u − a" parabolas are *identical* to the "u + a" parabolas.
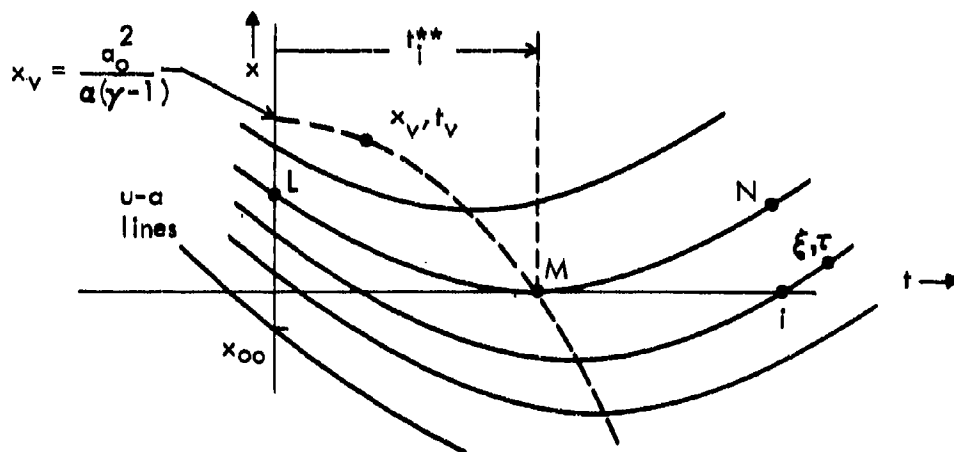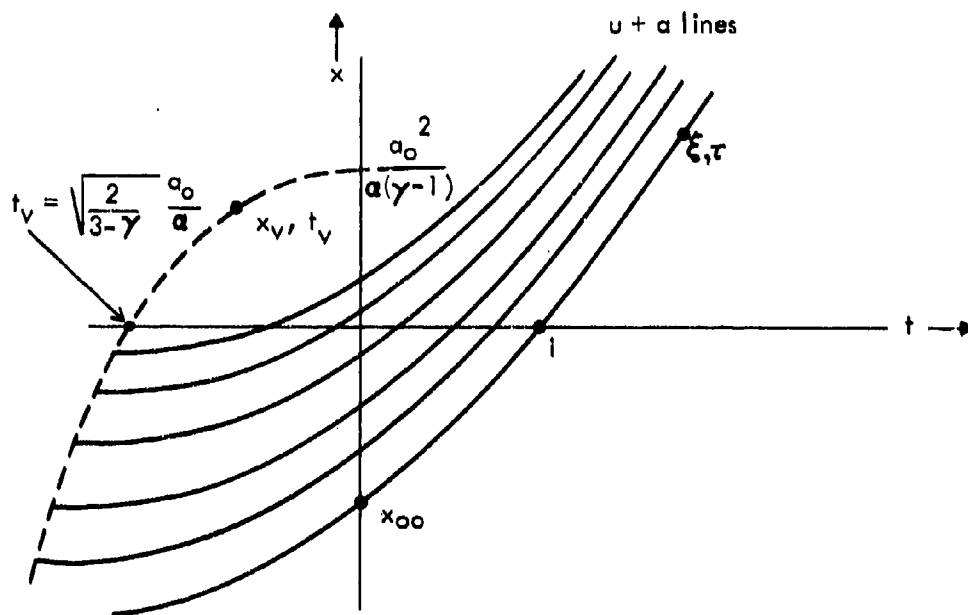
Of interest in later discussion will be the "u – a" characteristic (L-M-N) which is tangent to the t axis ($x = 0$) at a time which will be designated at t^{**}. Since the slope of the "u – a" line is zero at this point, M, the flow is sonic.

$$u_1^{**} = a_1^{**} \quad . \tag{50-10}$$

Inserting into this equation the expressions for u (Equation (48-10)) and for a_1 (Equation (49-12)) at $x = 0$, one obtains

$$t_1^{**} = \sqrt{\frac{2}{3 - \gamma}} \frac{a_0}{\alpha} \tag{50-11}$$

at which time

$$u_1^{**} = a_1^{**} = \alpha t_1^{**} = \sqrt{\frac{2}{3 - \gamma}} a_0 \quad . \tag{50-12}$$

The value of a_{00} for this characteristic is obtained by inserting Equation (50-12) into Equation (50-6).

$$a_{00} = a_0 \sqrt{\frac{3 - \gamma}{2}} \quad . \tag{50-13}$$

Substituting this into Equation (50-7) yields

$$\xi = \frac{a_0^2}{2\alpha} \left[\frac{3 - \gamma}{2} \frac{\alpha \tau}{a_0} - 1 \right]^2 \tag{50-14}$$

as the equation for this characteristic. For this "u – a" characteristic, $u - \sigma$ is a constant which may be evaluated from Equation (50-12) as
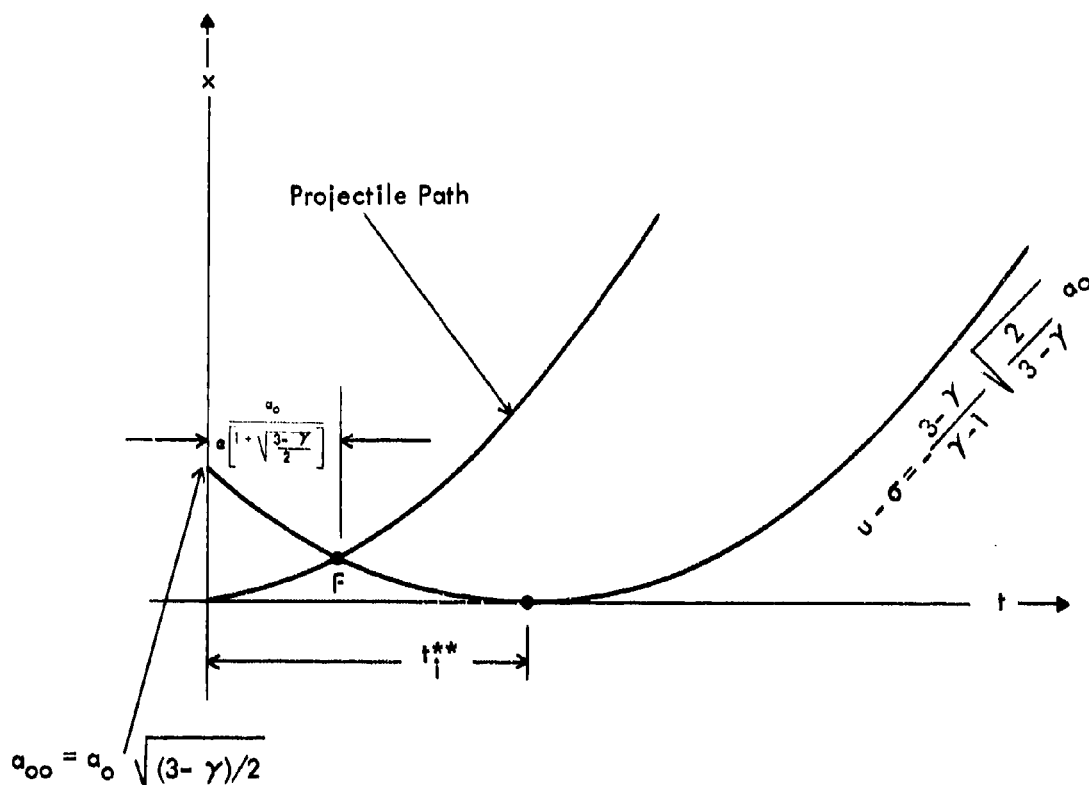
$$u - \sigma = u_1^{**} - \sigma_1^{**} = \frac{(\gamma - 3) a_1^{**}}{\gamma - 1} = -\frac{3 - \gamma}{\gamma - 1} \sqrt{\frac{2}{3 - \gamma}} a_0 \quad . \tag{50-15}$$

The pressure at time t_1^{**} is evaluated from Equation (49-9) as

$$p_1^{**} = p_0 \left[\frac{2}{3 - \gamma} \right]^{\frac{\gamma}{\gamma - 1}} \quad . \tag{50-16}$$

This characteristic intersects the projectile path at a time equal to

$$t_F = \frac{a_0}{\alpha \left[1 + \sqrt{\frac{3 - \gamma}{2}} \right]} \quad . \tag{50-17}$$

x

Projectile Path

$a\left[1+\sqrt{\frac{3-\gamma}{2}}\right]$

a_o

F

$u-\sigma=-\frac{3-\gamma}{\gamma-1}\sqrt{\frac{2}{3-\gamma}}\ a_o$

t

t_1^{**}

$a_{oo} = a_o \sqrt{(3-\gamma)/2}$

Section 51

Do Shocks Occur?

It is seem from an examination of the expression for the slope of the "u + a" characteristics line (Equation (50-2)) that these characteristics tend to converge. (This is also evident from a sketch in the x-t plane). Hence, it becomes of interest to determine if the characteristics lines will intersect to form a shock.

Examination of the equations for the characteristics in the case when no projectile is present reveals that a shock is not formed. (This conclusion is obvious if one looks at the characteristics in the Lagrangian coordinate system - see below).

Although the characteristics do not converge to form a shock, they do become tangent to a parabolic envelope; the equation of this envelope (obtained from the condition $(d\xi/da_{00})_\tau = 0$, is

$$\xi_{ENV} = \frac{\alpha\tau_{ENV}^2}{2} + \frac{a_0^2}{\alpha(\gamma-1)} \ , \qquad \begin{cases} \tau_{ENV} \geqslant 0 & \text{for} \quad u + a \ \text{lines} \\ \tau_{ENV} \leqslant 0 & \text{for} \quad u - a \ \text{lines} \end{cases} \ . \qquad (51\text{-}1)$$

Thus, part of this parabolic envelope is parallel to the path which the projectile would have if present and is the distance $a_0^2/a(\gamma-1)$ ahead of it.
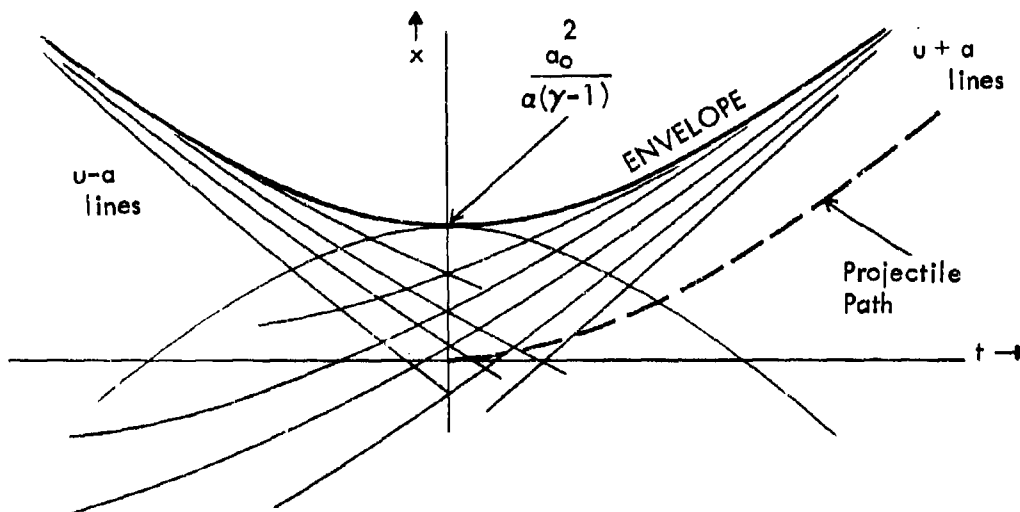
On this envelope the pressure p , sound speed a , temperature T , etc., are all zero. Calculation demonstrates that beyond the envelope the quantities p , T , a , etc., are imaginary or negative. Thus, the region beyond the envelope does not exist in reality.

$$\xi_{ENV} = \frac{a\,\tau_{ENV}^2}{2} + \frac{a_0^2}{a(\gamma-1)}$$
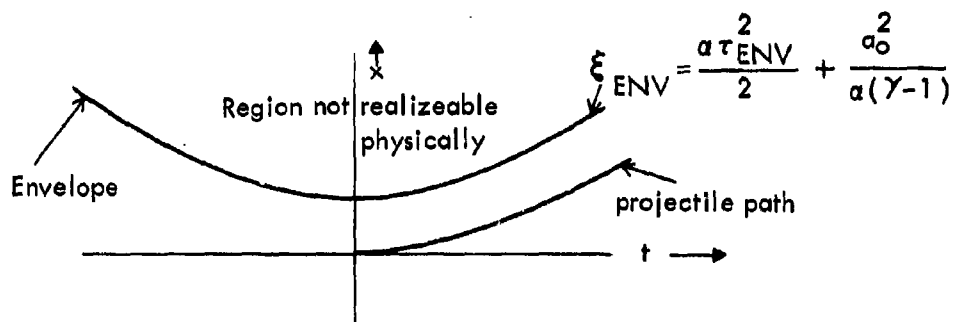
Section 52

Paths of Characteristics in Lagrangian Coordinates for the Ideal Gas

The equations of the characteristics are particularly simple when expressed in the Lagrangian coordinate system. The continuity, momentum and characteristics equations are the following (See Courant and Friedrichs[15]):

$$-\frac{1}{\rho^2}\left(\frac{\partial\rho}{\partial t}\right)_H = \left(\frac{\partial u}{\partial H}\right)_t \qquad (52\text{-}1)$$

$$\left(\frac{\partial u}{\partial t}\right)_H = -\left(\frac{\partial p}{\partial H}\right)_t \qquad (52\text{-}2)$$

$$\frac{\partial}{\partial t}(u \pm \sigma) \pm a\rho \frac{\partial}{\partial H}(u \pm \sigma) = 0 \qquad (52\text{-}3)$$

where

$$H = \int_{x(o,t)}^{x(H,t)} \rho \, dx$$

the mass per unit area of gas from a given point in the flow to any other point. It is noted that the slope of the characteristics in the H-t plane is equal to the acoustic impedance ($\pm a\rho$).

The assumption that density is unchanging for a particle is expressed as

$$\left(\frac{\partial\rho}{\partial t}\right)_H = 0 \qquad (52\text{-}4)$$

from which, by the continuity equation (52-1),

$$\left(\frac{\partial u}{\partial H}\right)_t = 0 \qquad (52\text{-}5)$$

or

$$u = u(t) \qquad \text{alone.} \qquad (52\text{-}6)$$

The momentum equation then becomes

$$\left(\frac{\partial u}{\partial t}\right)_H = -\left(\frac{\partial p}{\partial H}\right)_t = \alpha \qquad (52\text{-}7)$$

where α is a constant. Thus,

$$u = \alpha t \qquad (52\text{-}8)$$

and

$$p - p_0 = -H\alpha \qquad (52\text{-}9)$$

or

$$\frac{p}{p_0} - 1 = -\frac{HA}{M}$$
(52-10)

where H is taken equal to zero when $p = p_0$. Thus, the $H = 0$ gas layer is the layer adjacent to the projectile with pressure equal to p_0 . The mass of gas behind the projectile to the point in question, $-HA$, may be designated "G". Equation (52-10) then becomes

$$p/p_0 = 1 + G/M \quad .$$
(52-10)

The equations for the $u + a$ characteristics are obtained from the relevant relation

$$u + \sigma = \alpha t_p + \sigma_0$$
(52-11)

where t_p is the time that the $u + a$ characteristic intersects the projectile path (the $H = 0$ path). Since

$$\frac{\sigma}{\sigma_0} = \left(\frac{p}{p_0}\right)^{\frac{\gamma-1}{2\gamma}} = \left(1 - \frac{HA}{M}\right)^{\frac{\gamma-1}{2\gamma}}$$
(52-12)

for the "$u + a$" characteristic, Equation (52-11) becomes

$$1 - \frac{AH}{M} = \left[1 + \frac{\alpha}{\sigma_0}(t_p - t)\right]^{\frac{2\gamma}{\gamma-1}} \quad .$$
(52-13)

It is interesting to note that in a system of Lagrangian coordinates, using a linear coordinate (e.g., x_{00}) rather than H , these characteristic curves would be parabolas. This equation may be differentiated to obtain the slope of the characteristic on the H-t diagram

$$\frac{dH}{dt} = a_0 \rho_0 \left[1 + \frac{\alpha}{\sigma_0}(t_p - t)\right]^{\frac{\gamma+1}{\gamma-1}} = a\rho$$
(52-14)

$$= a_0 \rho_0 \left[1 - \frac{AH}{M}\right]^{\frac{\gamma+1}{2\gamma}} \quad .$$
(52-15)

The "$u + a$" characteristics are thus seen to be *identical curves* which are displaced one from the other in the t direction by an amount equal to Δt_p .
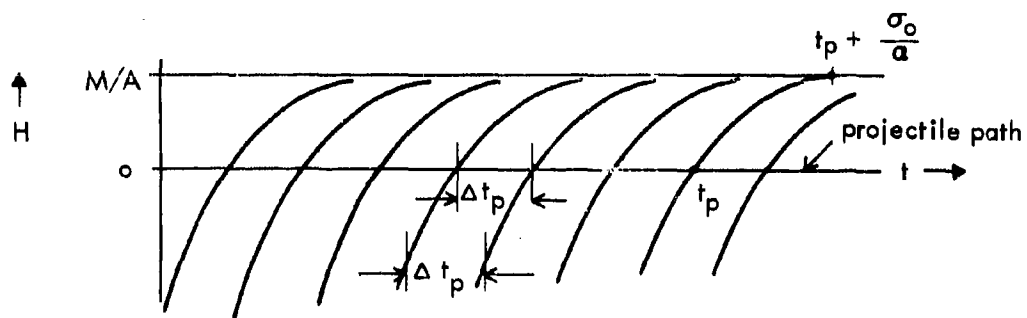
Similarly, the equation for the $u - a$ characteristics is obtained from the equation

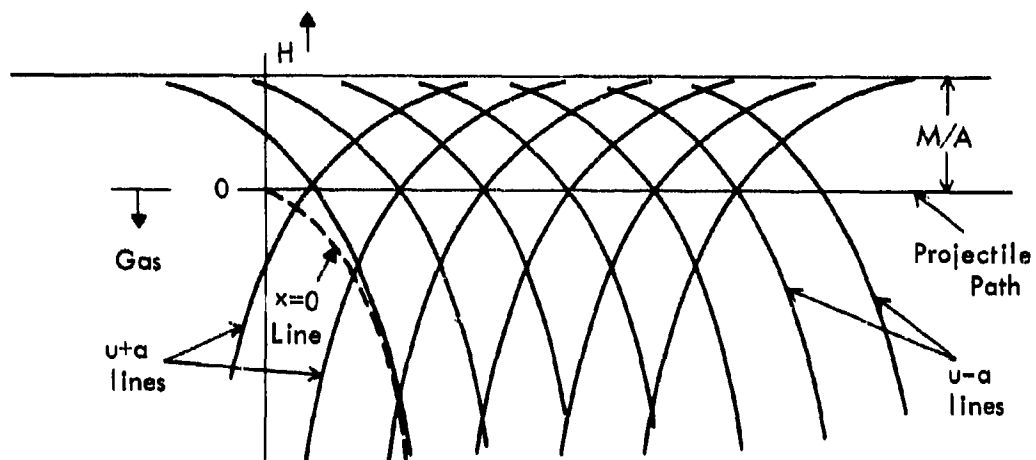$$u - \sigma = \alpha t_p - \sigma_0 \qquad (52\text{-}16)$$

and is

$$1 - \frac{AH}{M} = \left[1 - \frac{\alpha}{\sigma_0}(t_p - t) \right]^{\frac{2\gamma}{\gamma-1}} . \qquad (52\text{-}17)$$

The slope is

$$\frac{dH}{dt} = -a\rho = -a_0\rho_0 \left[1 - \frac{\alpha}{\sigma_0}(t_p - t) \right]^{\frac{\gamma+1}{\gamma-1}} \qquad (52\text{-}18)$$

$$= -a_0\rho_0 \left[1 - \frac{AH}{M} \right]^{\frac{\gamma+1}{2\gamma}} . \qquad (52\text{-}19)$$

Thus, the "u – a" characteristics are identical curves displaced in the t direction by Δt_p . Moreover, they are seen to be the same curve as the "u + a" curve but reflected about the H axis.

Both sets of characteristics form an envelope about the line H = M/A on which pressure, temperature, density, and sound speed are zero. In the sketch of the characteristics are also shown the projectile path (H = 0) and the path of the x = 0 line.

Section 53

Pressure Requirements in a Chambered Gun to Obtain a Constant Base Pressure – Subsonic Flow, Ideal Gas

It appears that one practical method of partially satisfying the requirements of the similarity solution is to use a chambered gun; the endeavor could then be made to increase the pressure in the chamber so as to increase the pressure at the entry to barrel as prescribed by the similarity solution, Equation (49-11).

$$\frac{p_i}{p_0} = \left[1 + \frac{(\gamma - 1)\alpha^2}{2a_0^2} t_i^2 \right]^{\frac{\gamma}{\gamma - 1}} \qquad (53\text{-}1)$$

Correspondingly, the temperature and sound speed at the barrel inlet would vary as given by Equation (49-12).

$$\frac{T_i}{T_0} = \frac{a_i^2}{a_0^2} = 1 + \frac{(\gamma - 1)\alpha^2}{2a_0^2} t_i^2 \qquad (53\text{-}2)$$

where the subscript "o" refers to the constant conditions behind the projectile.
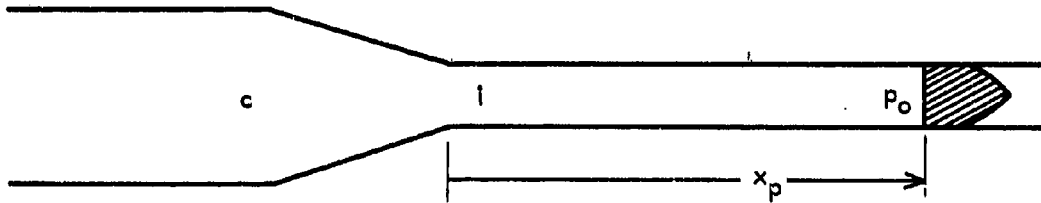
The conditions in the chamber, denoted by the subscript "c", may be related to those at the barrel inlet by the quasi-steady equations of energy and continuity. If the area ratio A_c/A_i is sufficiently large

$$\frac{2}{\gamma - 1} a_i^2 + u_i^2 = \frac{2}{\gamma - 1} a_c^2 \qquad (53\text{-}3)$$

From (53-2) and $u_1 = \alpha t_1$, Equation (53-3) becomes

$$a_c^2 = a_0^2 + (\gamma - 1) \ \alpha^2 t_1^2 \tag{53-4}$$

from which, by the isentropic relations, the chamber pressure variation is obtained as

$$\frac{p_c}{p_0} = \left[1 + \frac{(\gamma - 1)\alpha^2}{a_0^2} \ t_1^2 \right]^{\frac{\gamma}{\gamma - 1}} \quad . \tag{53-5}$$

The flow at the entry to barrel becomes sonic (see Equations (50-10) and (50-11)) at

$$t_1^{\star\star} = \sqrt{\frac{2}{3 - \gamma}} \ \frac{a_0}{\alpha} \tag{53-6}$$

at which time

$$u_1^{\star\star} = a_1^{\star\star} = \alpha t_1^{\star\star} = \sqrt{\frac{2}{3 - \gamma}} \ a_0 \tag{53-7}$$

and

$$p_1^{\star\star} = p_0 \left[\frac{2}{3 - \gamma} \right]^{\frac{\gamma}{\gamma - 1}} \tag{53-8}$$

and

$$p_c^{\star\star} = p_0 \left[\frac{\gamma + 1}{3 - \gamma} \right]^{\frac{\gamma}{\gamma - 1}} \quad . \tag{53-9}$$
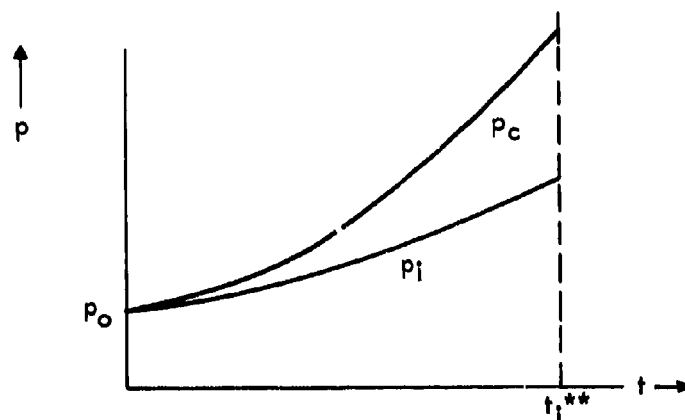
When the conditions at "i" become sonic, further pressure increases in the chamber will cause the velocity to increase at "i" but *the flow will remain sonic* for isentropic flow[*]. The similarity solution, however, assumes that the flow becomes supersonic at the barrel inlet, as seen from the equation for the inlet Mach number.

$$\left(\frac{u_i}{a_i}\right)^2 = \frac{1}{(a_0/\alpha t_i)^2 + (\gamma - 1)/2} \quad . \tag{53-10}$$

Similarity solution
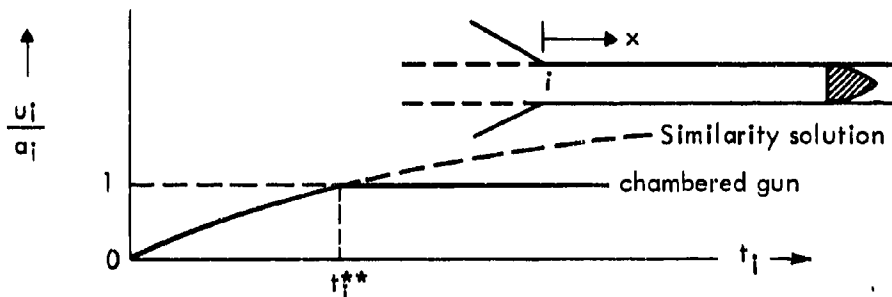
chambered gun

Thus, for isentropic flow in a chambered gun, the similarity solution requirements cannot be satisfied after sonic flow has been reached. Thus, Equations (53-6) through (53-9) hold only for times less than t_i^{**} for a chambered gun.

Section 54

Pressure Requirements in a Chambered Gun to Obtain a Constant Base Pressure After Sonic Flow is Reached for an Ideal Gas

The requirements for constant base pressure in a chambered gun after sonic flow is reached at the barrel entry may be obtained by use of the method of characteristics. The x-t diagram sketched on the following page shows a few characteristics.

The similarity solution applies to the region A-B-t[**]. The path of the "u + a" characteristic B-C-t[**] which is the boundary of this region may be obtained, if desired, from Equations (50-1) and (50-3). The time t_B, when this characteristic intersects the projectile path, may be directly calculated from the characteristic relation

$$u^{**} + \frac{2}{\gamma - 1} a^{**} = u_B + \sigma_B = \alpha t_b + \frac{2}{\gamma - 1} a_0 \tag{54-1}$$

from which, by equation (50-11),

$$t_B = \frac{2a_0}{(\gamma - 1)\alpha} \left[\frac{\gamma + 1}{2} \sqrt{\frac{2}{3 - \gamma}} - 1 \right] \quad . \tag{54-2}$$

---

[*] This is not necessarily true for non-isentropic flow. It is possible to obtain supersonic flow at the inlet by raising the pressure so as to cause shocks which enter the barrel.
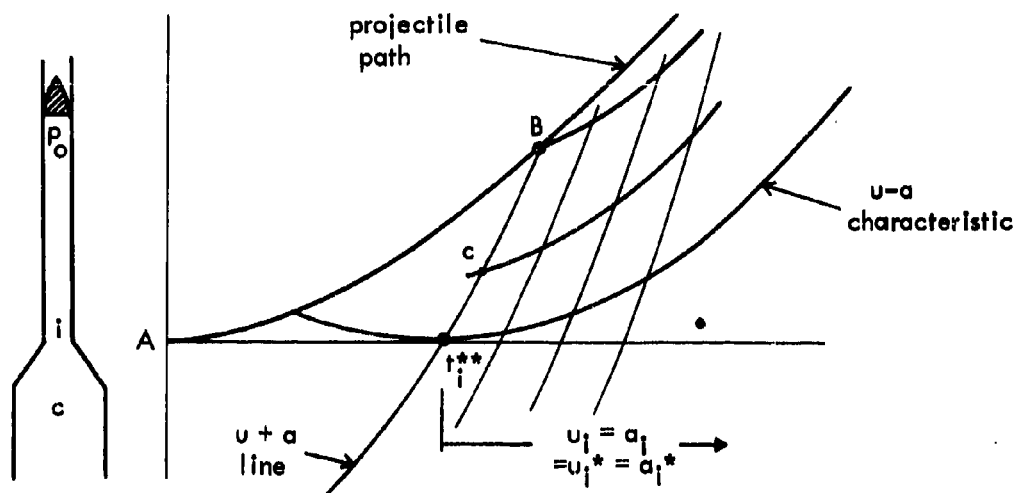
It is to be noted that at this time t_B the projectile is traveling at a speed equal to

$$u_B = \alpha t_B \tag{54-3}$$

with a "Mach number" u_B/a_0 equal to

$$\frac{u_B}{a_0} = \frac{2}{(\gamma - 1)} \left[\frac{\gamma + 1}{2} \sqrt{\frac{2}{3 - \gamma}} - 1 \right] . \tag{54-4}$$

For a $\gamma = 1.4$ gas this Mach number is 1.70. The similarity solution is thus satisfied until the projectile reaches this Mach number.

The flow conditions outside of the region A-B-t^{**} may be obtained using the characteristic equations

$$\frac{D(u \pm \sigma)}{Dt} = 0 \tag{54-5}$$

and the following boundary conditions:

At $\qquad x = 0 , \quad t_i \geqslant t_i^{**} : \qquad u_i = u_i^* = a_i = a_i^* \tag{54-6}$

and at the projectile

$$u_p = \alpha t_p , \qquad \sigma = \sigma_p = \sigma_0 \tag{54-7}$$

The star (*) indicates sonic flow; the subscript "p" indicates the projectile.

112

After time t^{**}, the conditions at the inlet are related to those at the projectile by consideration of the "u + a" characteristics. For each such characteristic the sum of $u + \sigma$ at the barrel inlet may be related to that directly behind the projectile

$$u_1^* + \sigma_1^* = u_p + \sigma_p = \frac{\gamma + 1}{\gamma - 1} a_1^* = u_p + \sigma_0 \qquad (54\text{-}8)$$

or

$$\frac{a_1^*}{a_0} = \frac{\gamma - 1}{\gamma + 1}\left(\frac{u_p}{a_0} + \frac{2}{\gamma - 1}\right) = \frac{\gamma - 1}{\gamma + 1}\left(\frac{\alpha t_p}{a_0} + \frac{2}{\gamma - 1}\right) \quad . \qquad (54\text{-}9)$$

From this follows

$$\frac{p_1^*}{p_0} = \left[\frac{\gamma - 1}{\gamma + 1}\left(\frac{\alpha t_p}{a_0} + \frac{2}{\gamma - 1}\right)\right]^{\frac{2\gamma}{\gamma - 1}} \quad . \qquad (54\text{-}10)$$

Equation (54-10) expresses the relation between barrel inlet pressure p_1^* and the corresponding time along the $u + a$ disturbance at the projectile t_p. However, it is desired to obtain the value of this pressure versus time, t_1, at the barrel inlet. Thus, the problem resolves itself into determining the relationship between the barrel inlet time t_1 and the projectile time t_p on each $u + a$ characteristic.
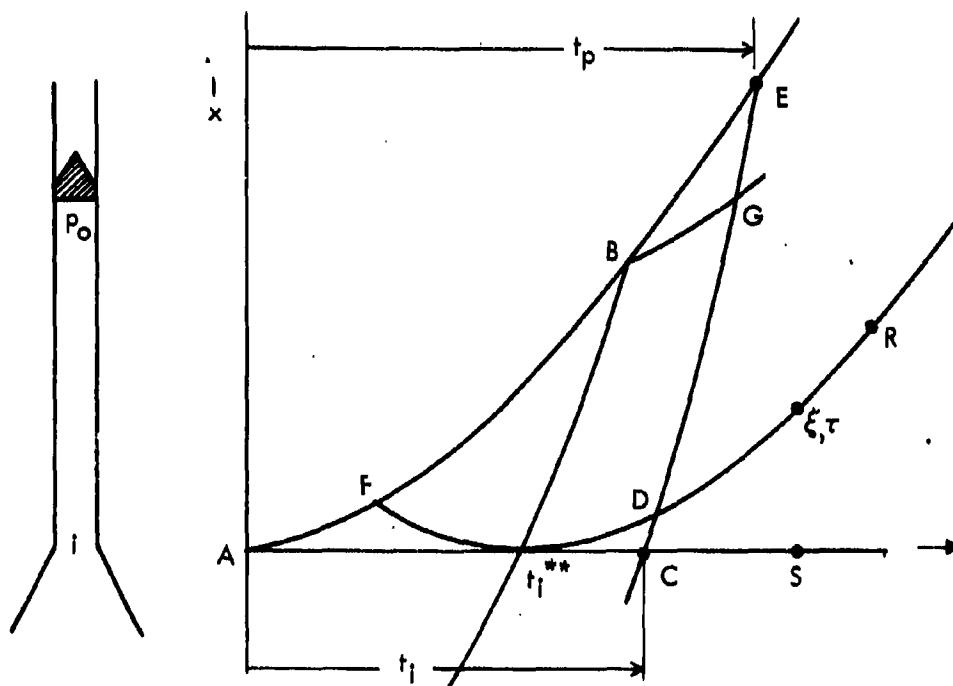
The sketch shows the x-t diagram applicable to a chambered gun. The line t^{**}-R is the u - a characteristic going through the point t^{**} . The line C-E is the path of a u + a characteristic.

If one attempts a numerical solution by the method of characteristics in the region E-B-t^{**}-R , it becomes quickly obvious that the conditions in this region are those of the similarity solution. For example, point G is determined from points E and B , both of which follow the similarity solution. Hence, so also will point G . (Smith[35], refers to the characteristic t^{**}-R as the "limiting characteristic"). Thus, the problem reduces itself to a numerical characteristics solution in the region R-t^{**}-S . The solution includes the sought-after relation between t_i and t_p . This relation has been obtained numerically in Reference 35 and also, approximately in Reference 37. An exact analytical solution for the region R-t^{**}-S has been obtained by Somes[96], for a $\gamma = 5/3$ propellant gas (see Equation (54-15)).

The results for pressure at the barrel inlet p_i and in the chamber p_0 , assuming large chambrage, are given in Figures 29 and 30 for various γ's . It is to be noted that after t^{**} the pressure required at the barrel inlet is higher than would have been required by the similarity solution in a gun with no chambrage.

114
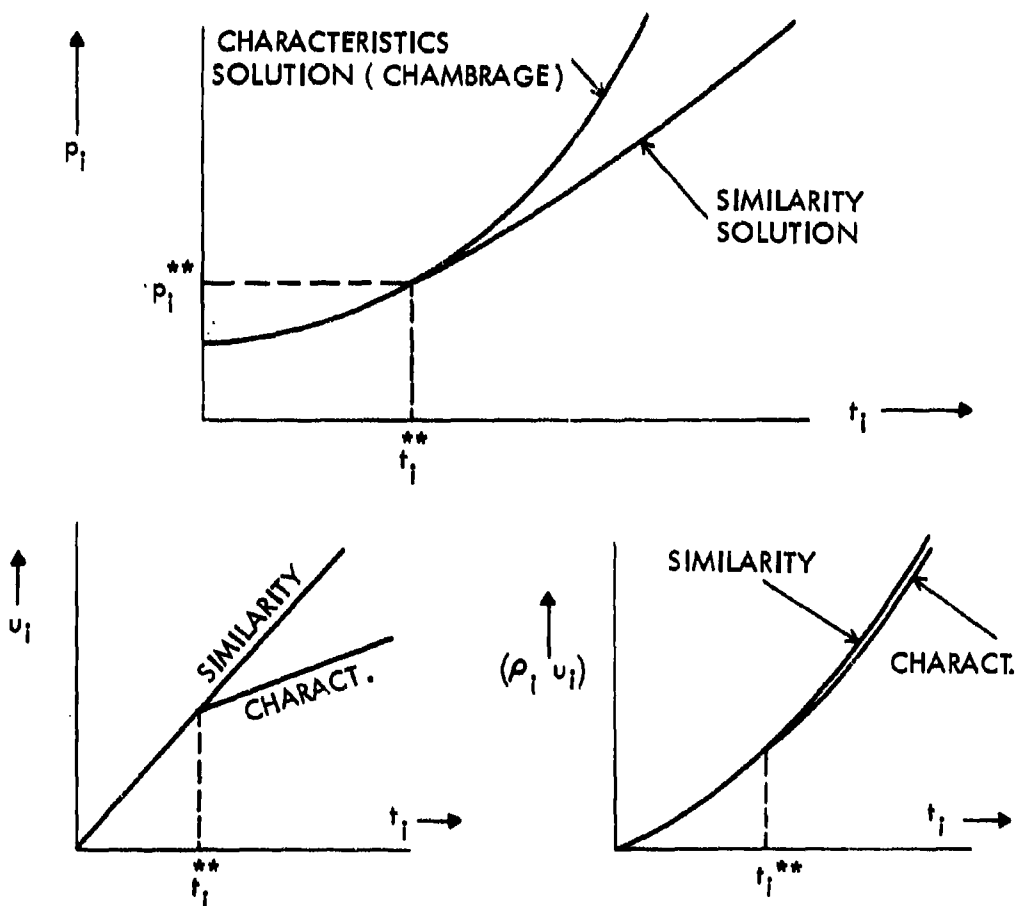
Calculation also indicates that after t_i^{**} the velocity at the barrel inlet becomes quite a bit less than given by the similarity solution and that the mass flow into the barrel is only slightly less than the similarity solution result.

It is again seen that, if the initial sound speed for an ideal gas propellant is high, the pressure rise in the chamber is correspondingly low.
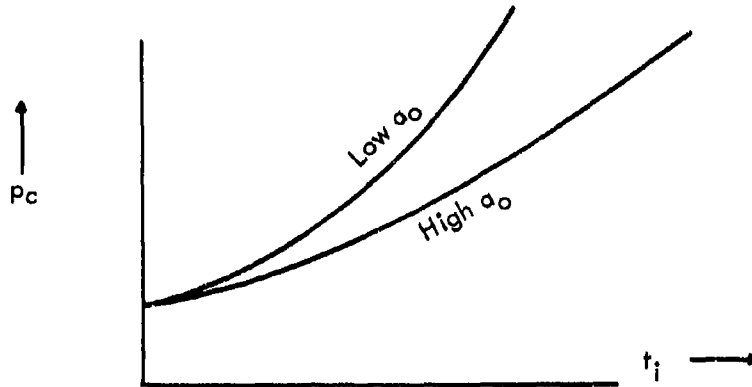
The results cited above for the ideal gas may be obtained in an approximate manner as related in Reference 37. There it is pointed out that the determination of the relation between t_i and t_p on the same $u + a$ characteristic may be obtained approximately without resort to a numerical characteristics solution by either of the following:

(i) assuming the $u + a$ line C-D (see sketch) to have the same path as the characteristic through point D in the similarity solution, or

(ii) assuming the line C-D to be a straight line of slope equal to the average of those at D and C .

The first assumption yields

$$\frac{\alpha t_p}{a_0} = \frac{\alpha t_i}{a_0} + \frac{2}{\gamma - 1}\left[1 + \frac{\gamma - 1}{2}\left(\frac{\alpha t_i}{a_0}\right)^2\right]^{\frac{1}{2}} - \frac{2}{\gamma - 1} \qquad (54\text{-}11)$$

from which is obtained

$$\frac{p_i^*}{p_0} = \left\{\left[\frac{2}{\gamma + 1}\right]\left[\frac{\gamma - 1}{2}\frac{\alpha t_i}{a_0} + \left(1 + \frac{(\gamma - 1)\alpha^2}{2a_0^2}t_i^2\right)^{\frac{1}{2}}\right]\right\}^{\frac{2\gamma}{\gamma - 1}} \qquad (54\text{-}12)$$

The second assumption yields

$$\frac{\alpha t_1}{a_0} = \frac{\alpha t_0}{a_0} - \frac{2\left[\sqrt{\frac{3-\gamma}{2}}\,\frac{\alpha t_D}{a_0} - 1\right]^2 (\gamma+1)}{(\gamma^2 + 10\gamma - 7)\,\frac{\alpha t_D}{a_0} + (\gamma+5)\,\sqrt{(3-\gamma)2}} \qquad (54\text{-}13)$$

where

$$\frac{\alpha t_D}{a_0} = 2\,\frac{\alpha t_D}{a_0} - \frac{2}{(\gamma-1)}\left[1 - \sqrt{\frac{3-\gamma}{2}}\right] \quad . \qquad (54\text{-}14)$$

The approximate results obtained by using the first assumption, Equation (54-12), have been compared to the exact analytical solution of Somes for a $\gamma = 5/3$ gas which may be expressed as

$$\frac{\alpha t_1}{a_0} = \left[\frac{48}{11}\eta - \frac{1}{5\eta} - \frac{(6)^{1/6}}{220}\eta^{-6/3}\right] \qquad (54\text{-}15)$$

where

$$\eta = \frac{u_1^\star}{3a_0} = \frac{a_1^\star}{3a_0} = \frac{1}{3}\left(\frac{p_1^\star}{p_0}\right)^{1/5} \quad \text{and} \quad t_1 \geqslant t_1^{\star\star} \quad .$$

The approximation is excellent, as seen from the values of $p_1^\star/p_0$ in the table (a plot would show almost no difference).

$\dfrac{\alpha t_1}{a_0} \rightarrow$	$\sqrt{1.5}$ $(= t_1^{\star\star})$	1.5	1.75	2.0	4.1575	10
Exact From Reference 17 Equation (54-15)	2.755	4.777	7.694	12.097	243.0	16,040
Approx. From Reference 37 Equation (54-12)	2.755	4.776	7.687	12.069	239.0	15,579
% error	0	0.02	0.09	0.23	1.65	2.87

Thus, all the barrel entry conditions ($u_1^\star$ equal to $a_1^\star$, $\rho_1^\star$, etc.) may be calculated from Equation (54-12) for the times beyond $t_1^{\star\star}$.

Section 55

### Required Motion of the Pump Tube Piston
When it Enters the Barrel

Heretofore, the possibility has not been considered that the piston, being deformable, might enter the barrel during the projectile travel.

Deformable Piston

Projectile

Pump Tube   **Propellant Gas**

Piston Front End
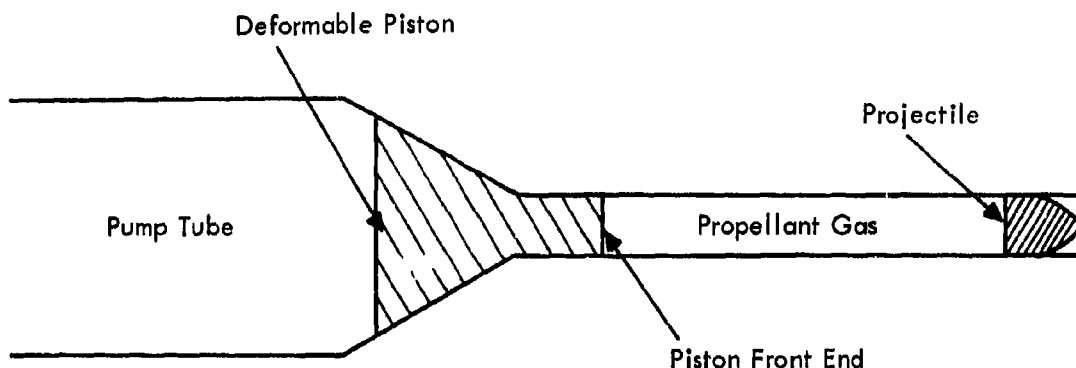
This situation can occur, for example, if the initial pressure in the pump tube is sufficiently low. The question arises: Is this an advantageous method of maintaining constant base pressure? An answer to this query is provided by determining the velocity required of the piston front end when it enters the barrel. The motion of the piston front end, when in the barrel, is to be that required to continue to maintain the pressure constant behind the projectile. Hence, the piston front end must travel at the velocity of the gas particles in the barrel as determined from the constant base pressure gun solution[*].

x

PROJECTILE PATH

Particle paths

t

t_i^{**}

$u_i = \alpha t_i$ $u_i = a_i = a_i^*$

---
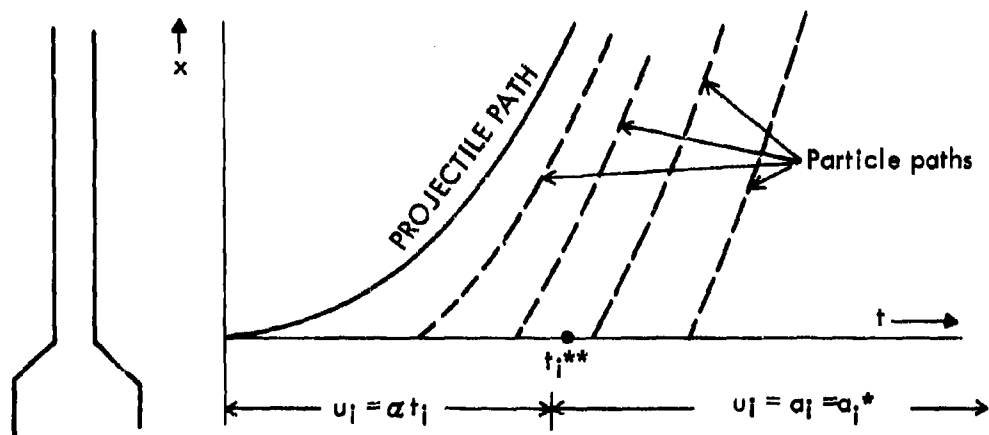
[*] This discussion assumes that the $u + a$ disturbance initiated from the piston front end will arrive at the projectile before it is out of the barrel.

Thus, a plot of velocity of piston front end as a function of time would appear as in the sketch.
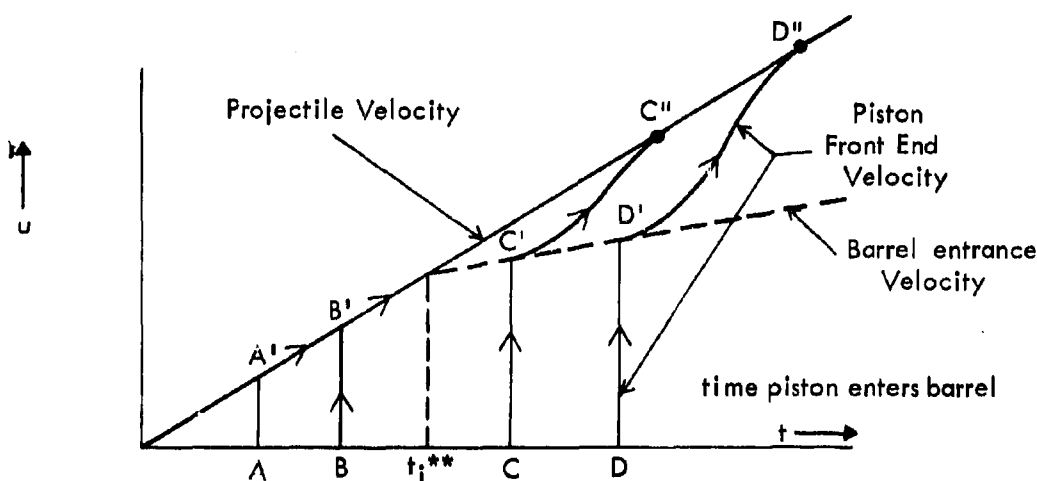
The required velocity time history of the piston front end is indicated by the arrows. If the piston enters at a time before t_i^{**} , the front end must travel at the projectile velocity. Thus, the velocity-time for piston entry at time t_A is the line A'-B'-C''-D''. If the piston enters at a time after t_i^{**} , its velocity will initially be the velocity of the gas at the barrel entrance; thereafter, the piston front end must accelerate until it reaches the velocity of the projectile. Thus, for example, let the case in the sketch where the piston enters the barrel at time t_C be considered; the velocity-time history of the front end of this piston will then be the path C'-C''.

It is obvious that to attain and control the needed very high piston velocity that is required as shown above, is probably not possible. It is therefore concluded that the entry of the piston into the barrel is undesirable as a means to maintain the base pressure constant behind the projectile. This conclusion seems to be in agreement with comments of Charters and R.N. Cox (page 403 of Reference 94).

Section 56

Methods of Achieving the Desired Chamber
Pressure Variation

It has been demonstrated that the pressure in the pump tube must change with time as indicated in Figure 29 for an ideal gas to attain a constant base pressure behind the projectile. Methods of obtaining the desired pressure-time variation in the chamber, or "matching", are discussed in References 35, 36, 37, and 40. The final words are yet to be written. In all cases the pressure of the gas in the pump tube is increased by means of the piston motion in a two-stage gun.

The following schemes have been proposed to match the pressure rise in the pump tube with that required for a constant base pressure behind the projectile.

(i) Matching by the proper selection of piston mass, pump tube geometry, and pump tube initial loading conditions. (See Smith[35], Winkler[36] and Wilenius[37]).
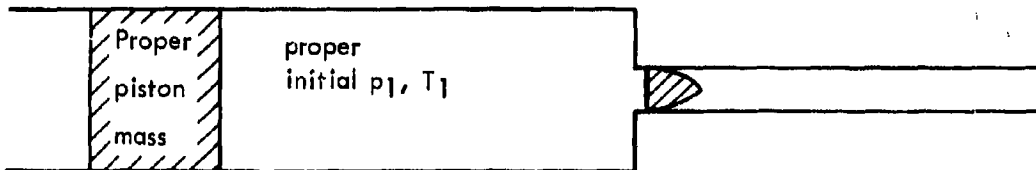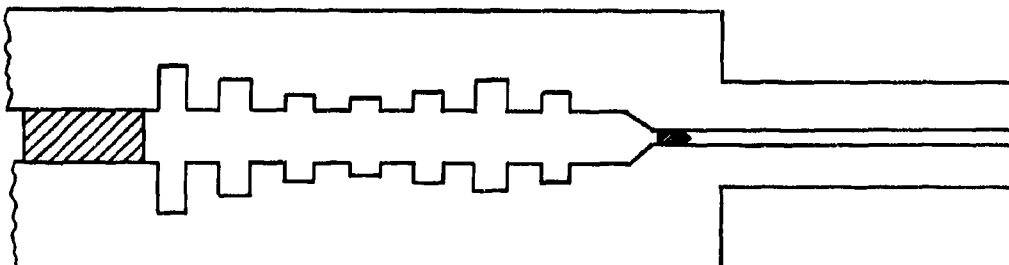

By judicious selection of the above parameters a reasonable match may be obtained.
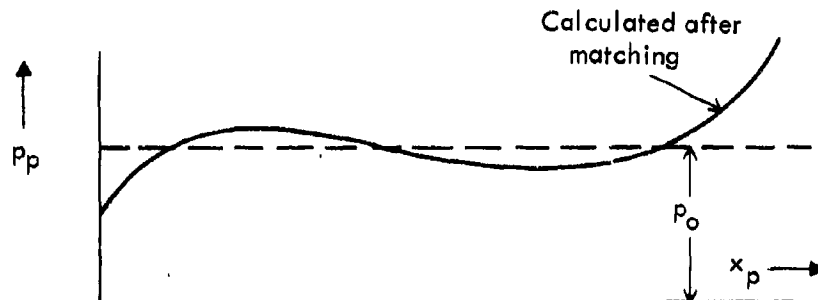
On difficulty of this method is an undesired rapid rise of pressure in the pump tube after the matching has ended.

(ii) Matching by the provision of available pump tube volume (grooves) which are excluded during piston travel.

This method of matching has the disadvantage that the number and size of grooves required make it impractical[36].

(iii) Matching by having orifices along the length of the pump tube to allow part of the pump tube gas to leak.
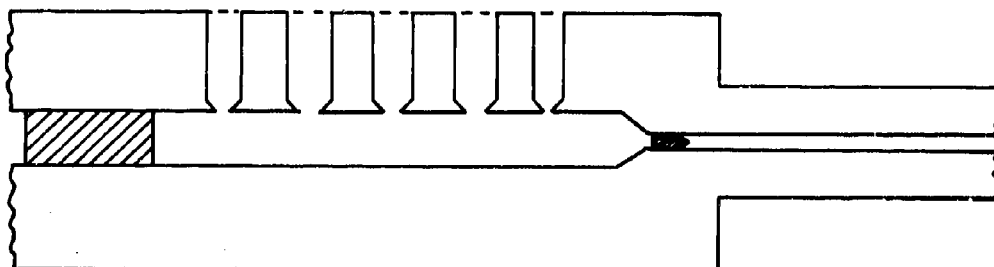
This modification of the pump tube appears to offer the possibility of perfect matching and seems mechanically feasible. (See References 35 and 36).

(iv) Matching by the use of a conical taper to control the end of the piston motion.
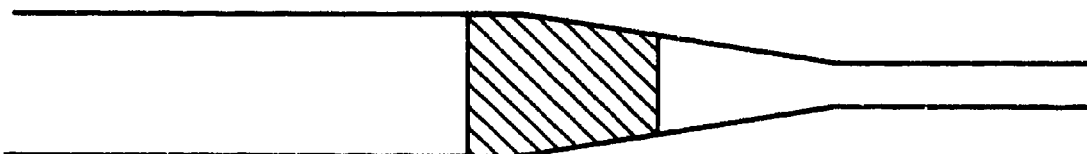

This method does not permit perfect matching, as seen from the analysis of Smith[35]. However, it has experimentally yielded the highest projectile velocities (Charters[94] - sketch of the gun used is shown in Section 70). It offers the advantage of permitting the piston to be stopped without unacceptable damage to the pump tube. (See also Curtis and Charters[38,39], and Cable[108]). The angle of conical taper which seems to have yielded the best experimental results is around 4-degree half-angle[94,108]).

(v) Matching by the use of a taper whose cross-sectional area is varied as a function of its length to effect the match.
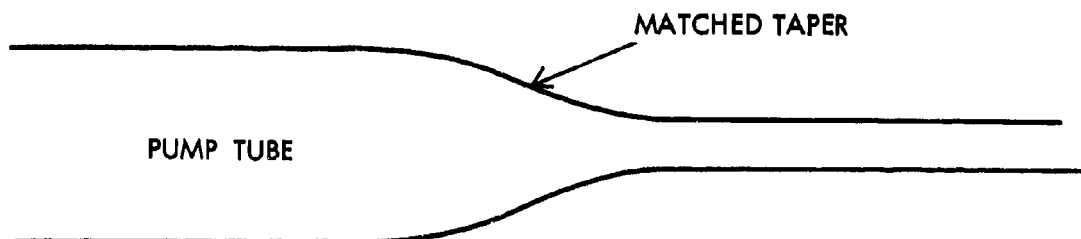
This method seems to offer promise but more study is required to determine its feasibility.

(vi) Matching by the use of orifices in the piston.
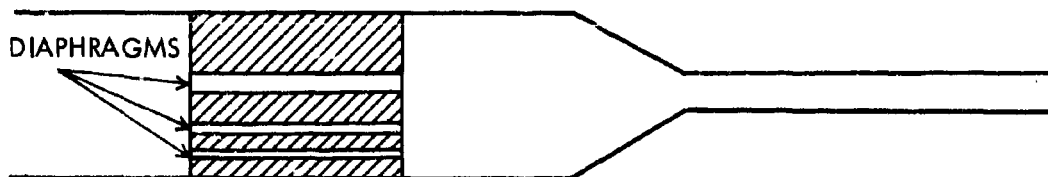
This method offers the possibility of matching for many different firing conditions without having to remodify the pump tube.

(vii) Matching by use of two pistons in the pump tube. Piacesi[98], describes this possibility of using two pistons separated by gas in the pump tube to maintain the pressure behind the projectile. This scheme, used in conjunction with one of the methods discussed above, may be advantageous.

In all of the methods described above, pistons are used to compress the pump tube propellant gas. When the piston accelerates to compress the gas in the pump tube, shocks will actually form, their strength being proportional to the square of the piston speed. These shocks may well cause "spikes" of pressure to be superimposed on the otherwise constant pressure at the base of the projectile.
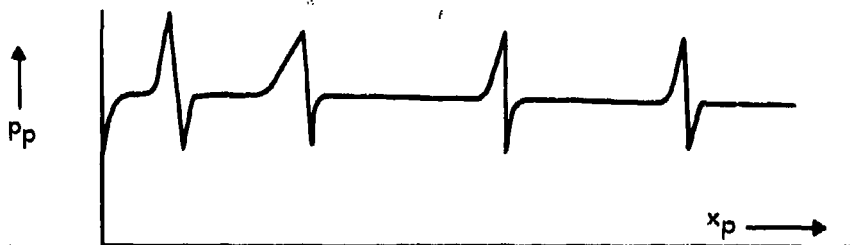
Thus, in the design of a constant base pressure gun, it is recommended that, after using one of the methods to select the gun system parameters, the actual performance be obtained from a computation which accounts for shocks such as described in Section 46.

Large pump tube diameters would avoid the occurrence of strong shocks by permitting the piston velocity to be decreased. However, this may not be a practical remedy.

At the present time the best method of matching has not been decided. However, the matching requirements of all of the above methods seem to demand relatively large pump tube volumes; also, the constant base pressure gun takes advantage of having long caliber barrels (e.g., 400 calibers), whereas, conventional gas gun barrels are relatively short (around 200 calibers) before frictional effects dominate.

The above methods allow one to design guns on paper to fire projectiles at velocities around 50,000 ft/sec*. Whether such velocities will be realizeable in practice will require experimental trial. The pressure capability of the pump tube becomes the limiting factor in the design. An expendable, deformable, part of the pump tube which will withstand perhaps a million lb/in^2 offers the possibility of achieving even higher velocities. Confidently, it is predicted that such velocities will be attained by use of the constant base pressure concept.

Section 57

Remarks on the Effects of Non-Idealities on the Performance of the Constant Base Pressure Gun

The effects of non-idealities on preburned propellant gas behavior are discussed in Part XI. Here these effects on the constant base pressure gun performance will be examined.

The discussion has largely been limited to the use of ideal gas propellants in the constant base pressure gun. However, the *actual real gas isentropic behavior must be used* to determine the performance of the gun. The constant base pressure requirements for a gas with any equation of state satisfy Equation (49-5), viz.

$$\int_{p_0}^{p} \frac{dp}{\rho} = \alpha^2 t^2/2 - \alpha x \quad . \tag{57-1}$$

In particular (see Equation (48-19))

$$\int_{p_0}^{p_1} \frac{dp}{\rho} = \frac{u_p^2}{2} \quad . \tag{57-2}$$

The real gas p-ρ isentropic relation may be inserted into Equation (57-1) to obtain the required pressure-time relation for the real gas. The energy relation between chamber and barrel is

$$\int_{p_1}^{p_c} \frac{dp}{\rho} = \frac{u_i^2}{2} \tag{57-3}$$

and again real gas data may be used. Smith[35] has inserted the equation of state of the Abel co-volume gas into these equations to obtain the similarity solution for the Abel gas.

---

* Of course, in any design real gas equation of state effects must be accounted for; see Section 57.

It is shown in Section 63 that real gases at high density, where the repulsive intermolecular field predominates, yield a larger $\int dp/\rho$ (which is equivalent to enthalpy change) than ideal gases. Thus, it is seen from Equation (57-2) and (57-3) that the performance of a dense propellant gas (such as the covolume gas) will be better than the ideal in the constant base pressure gun.

As pointed out below, another way to understand this gain in velocity in a quasi-steady expansion of a dense real gas relative to an ideal gas is to note that the enthalpy is greater for the real gas. Thus, for an Abel gas the enthalpy is

$$\int dp/\rho \;=\; h \;=\; C_p T + pb \quad .$$

The additional term pb , which the ideal gas does not have, is an additional energy term yielding better gun performance in a constant base pressure gun for the Abel gas. Smith's computed results[35] confirm this.

It happens, therefore, that if high densities occur in the propellant gas, the effects of non-idealities must be accounted for in calculating the requirements for a constant base pressure gun; the actual real gas data must be used.

As a result of the real gas effects of a dense propellant, preliminary calculated results indicate that, for a given projectile velocity and maximum pump tube pressure, the two-stage constant base pressure gun using a real gas has a significantly smaller pump tube than calculated for an ideal gas.
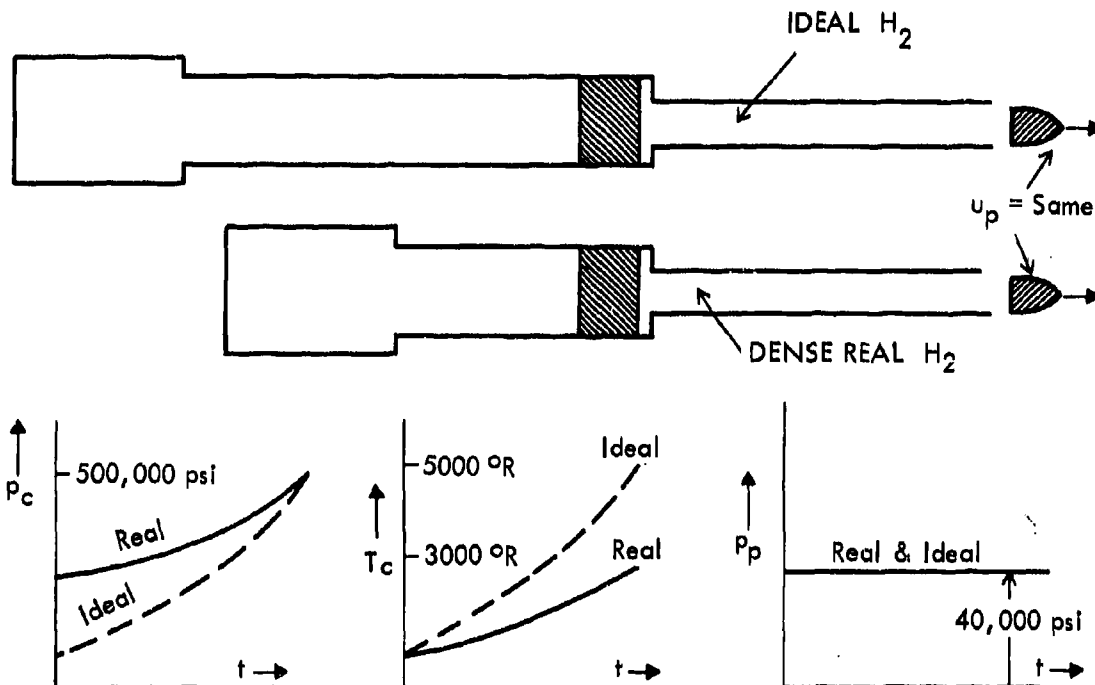
it is also noted that the temperature rise for the real propellant gas is less than for the ideal propellant gas.

To account for the non-ideal effects, it is convenient to approximate, as pointed out in Section 66, the behavior of the real gas by the following semi-empirical entropic equation:

$$p^{(\beta-2)/\beta} \left(\frac{1}{\rho} - f \right) = \kappa \tag{57-4}$$

where β, f, and κ are *functions only of entropy*. (This equation was used by Seigel[47] to describe dense gas behavior). It is seen that this equation is equivalent to the Abel equation for a given entropy if $\beta/(\beta-2)$ is replaced by γ, and if f is replaced by b; these constants, however, will change for each different entropy. The expression for enthalpy becomes for an isentrope

$$h - h_0 = \int_{p_0}^{p} \frac{dp}{\rho} = p_0 f \left[\frac{p}{p_0} - 1 \right] + \frac{\beta}{2} \left[p_0 \left(\frac{1}{\rho_0} - f \right) \right] \left[\left(\frac{p}{p_0} \right)^{\frac{2}{\beta}} - 1 \right] . \tag{57-5}$$

The similarity solution requirements for maintaining constant pressure become, from (57-5) and (57-1),

$$p_0 f \left[\frac{p}{p_0} - 1 \right] + \frac{1}{2} \beta p_0 \left(\frac{1}{\rho_0} - f \right) \left[\left(\frac{p}{p_0} \right)^{\frac{2}{\beta}} - 1 \right] = \frac{\alpha^2 t^2}{2} - \alpha x \tag{57-6}$$

from which the variation of pressure p_i at the barrel inlet ($x = 0$) as a function of time is

$$p_0 f \left[\frac{p_i}{p_0} - 1 \right] + \frac{1}{2} \beta p_0 \left(\frac{1}{\rho_0} - f \right) \left[\left(\frac{p_i}{p_0} \right)^{\frac{2}{\beta}} - 1 \right] = \frac{\alpha^2 t_i^2}{2} . \tag{57-7}$$

The relation between the barrel inlet conditions and the chamber pressure is, from (57-5) and (57-3),

$$\frac{u_i^2}{2} = p_i f \left[\frac{p_0}{p_i} - 1 \right] + \beta p_i \left(\frac{1}{\rho_i} - f \right) \frac{\left[\left(\frac{p_0}{p_i} \right)^{\frac{2}{\beta}} - 1 \right]}{2} = \frac{(\alpha t_i)^2}{2} . \tag{57-8}$$

Smith[35] has evaluated these equations for an Abel gas to apply to a hydrogen propellant[*]. He points out that the effect of the molecular volume is to increase the sound speed above its ideal gas value and thus in most cases the flow never reaches sonic at the

---

[*] Smith's results for hydrogen are in doubt, since he uses a constant covolume, whereas the available hydrogen isentropic data cannot be fitted with a constant covolume in the high density region.

barrel inlet. Hence, the similarity solution equation (57-6) is sufficient; the characteristics solution beyond the limiting characteristic is unnecessary. Of course, if the flow does become sonic, a characteristic solution must be computed.

Since the density reached by the propellant gas in a constant base pressure gun is relatively very high, it is particularly important to use the true gas data. Unfortunately, reliable isentropic data for hydrogen at high densities are not presently available. Wooley's hydrogen data[99] have been extended to high density and the results fitted, in reference 100 to Seigel's semi-empirical equation (57-4). A plot of the fitted constants is given in Figure 45. Until more reliable data are forthcoming, it is recommended that Equation (57-4), with the data of Figure 45, be used to approximate the behavior of dense hydrogen.

XI. THE EFFECTS OF PROPELLANT GAS NON-IDEALITY ON THE PERFORMANCE OF PREBURNED PROPELLANT GUNS[*]

Section 58

The Criteria for Propellant Gas Performance In an $x_0 = \infty$, PP Gun

The assumption that a propellant gas behaves as an ideal gas implies that the following conditions are true during the expansion of the gas:

(a) The number of degrees of freedom which are energized remains constant.

(b) The number of gas particles does not change.

(c) The forces between the gas particles are negligible.

However, if the temperature of the propellant gas is sufficiently high, conditions (a) and (b) are not satisfied; if the density is sufficiently high, condition (c) is not satisfied. In these instances the behavior of the propellant gas (and hence of the projectile) may deviate significantly from that for the ideal gas case. (It has already been noted in Section 57 that the non-ideality of hydrogen in a constant base pressure gun must be taken into account).

In comparing the performance of the actual or real propellant gas to that of an ideal gas, the view is taken here that before expansion the two propellant gases are at the same initial pressure (p_0) and the same initial temperature (T_0)[†]. During the expansion the pressure-velocity (p-u) curves of each of the propellant gases behind the projectile may be compared; the propellant gas with the higher curve will yield a higher projectile velocity.
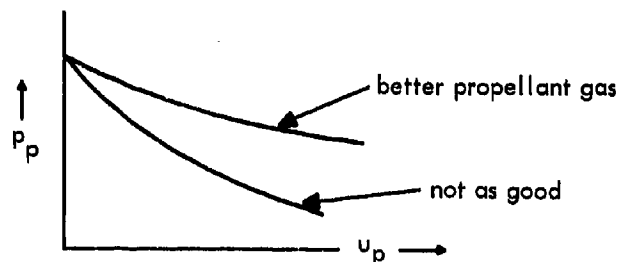
The determination of which gas properties control the velocity increase for a given pressure decrease may be obtained from an examination of some of the previously obtained fundamental gas dynamic equations which characterize the propellant gas expansion.

---

[*] A similar analysis has been applied to shocktubes by Seigel[41].

[†] Of course, there are other possible initial conditions to be used for a comparison (e.g., the comparison may be made for the same initial pressure and initial internal energy, or for the same initial pressure and initial sound speed, and so on).

126

A chambered, $x_0 \cdot \infty$ gun will be considered; the gas flow will be assumed isentropic. For the constant diameter chamber section and for the constant diameter barrel tube section the one-dimensional unsteady flow theory yields the results that (see Section 7).

$$du + dp/a\rho = 0 \quad . \tag{58-1}$$

This equation applies to both real and ideal gases.

The conditions within the transition section are approximated by the quasi-steady flow energy equation and the isentropic condition to yield in the differential form (see Section 15)

$$udu + dp/\rho = 0 \quad . \tag{58-2}$$

Here, again, the equation applies to both real and ideal gases.

Equations (58-1) and (58-2) are the fundamental equations of the propellant gas flow in a chambered $x_0 = \infty$ gun. They are derived on the premise that the flow in the constant diameter sections is one dimensional and that the flow throughout the gun is isentropic; *no assumption as to the equation of state of the fluid has been made.*

As discussed previously, it is evident from equations (58-1) and (58-2) that the velocity gain for a given pressure drop in a constant diameter $x_0 = \infty$, PP gun is inversely proportional to "$a\rho$" (the acoustic impedance). Hence, for such a gun the requirement for a good propellant is one in which $a\rho$ is low as a function of p for the isentrope.

The situation is different in a chambered gun; flow occurs both in the constant diameter chamber and barrel sections, and in the varying diameter transition section; in the latter section the velocity gain by Equation (58-2) for a given pressure drop is inversely proportional, not to $a\rho$, but to ρ (the gas density).

To review the situation in a $x_0 = \infty$, PP chambered gun, let us consider the sketch.

It may firstly be reasoned, as in Section 16, that the use of chambrage with a given driver gas increases the projectile velocity relative to that in a constant diameter $x_0 = \infty$ gun, since

$$u_i + \sigma_i > \sigma_0 \quad .$$

(See Equation (16.4)).

In the chamber the velocity increase for a given pressure drop is inversely proportional to $a\rho$; in the transition section the velocity increase for a given pressure drop is inversely proportional to ρ . In the barrel it is seen that *for* u + a *disturbances* traveling from the barrel entrance "i" to the projectile "p", the velocity gain is inversely proportional to $a\rho$.

Thus, the requirements for a good propellant in an $x_0 = \infty$, PP chambered gun of fixed geometry become apparent; to minimize the pressure drop for a given velocity gain, the following may be stated:

(i) In the $x_0 = \infty$ constant diameter chamber section a low $a\rho$ as a function of p is desired.

(ii) In the transition section a low ρ as a function of p is desired.

(iii) In the constant diameter barrel section what is desired is probably a low $a\rho$ as a function of p . (This requirement cannot be stated with certainty since a low $a\rho$ only insures minimum pressure drop along a "u + a" disturbance. As the flow conditions at the barrel entry become more steady, then the entire flow in the barrel is described by the equation

$$u + \sigma = u_i + \sigma_i = u_p + \sigma_p$$

and then a low $a\rho$ as a function of p is definitely desired)[*].

From the above, requirements for minimizing the pressure drop for a given velocity gain in an $x_0 = \infty$, PP chambered gun are seen to be different, depending on which part of the gun is being considered. However, in most instances the *qualitative* performance of an $x_0 = \infty$, PP gun with large chambrage is characterized by the flow in the transition section without regard to the flow in the uniform sections.

Thus, the characteristic of low ρ becomes the criterion for the best flow in a gun with large chambrage.

Accordingly, the *criteria for a qualitative comparison of an* $x_0 = \infty$, *PP gun propellant gas performance are the following:*

(i) The lowest $a\rho$ as a function of p for the isentrope for best constant diameter gun performance.

---

[*] It is to be noted that this result is not necessarily true for guns which are not preburned propellant guns. For example, it develops that for a constant base pressure gun a low "ρ" as a function of p is desired in the barrel to minimize the pressure drop (see Section 48).

(ii) The lowest ρ as a function of p for the isentrope for best infinitely chambered gun performance.

In most instances an examination of these thermodynamic quantities $a\rho$ and ρ for the isentrope in accordance with criteria (i) and (ii) is sufficient to determine the relative merits of propellant gases (and thus to determine the real gas effects on their performance).[*] These criteria are used below to compare the qualitative behavior of real gases with that of ideal gases at the same initial temperature T_0 and pressure p_0. For this purpose, it is convenient to record the equations for the ideal gas relating ρ and $a\rho$ to the pressure p for an isentrope. (See Appendix J).

$$a\rho = \left(\sqrt{\frac{\gamma}{RT_0}}\right)p_0 \left(\frac{p}{p_0}\right)^{\frac{\gamma+1}{2\gamma}} \tag{58-3}$$

$$\rho = \frac{p_0}{RT_0}\left(\frac{p}{p_0}\right)^{\frac{1}{\gamma}} . \tag{58-4}$$

Section 59

The Method of Calculating the PP Gun Performance With a Non-Ideal Propellant Gas

The characteristics equations previously derived in terms of the Riemann Function "σ" for the constant diameter sections are

$$\frac{\partial}{\partial t}(u \pm \sigma) + (u \pm a)\frac{\partial}{\partial x}(u \pm \sigma) = 0 , \tag{59-1}$$

The conditions at the exit and entrance to the transition section are related by the quasi-steady equations

$$\frac{u_c^2}{2} - \frac{u_1^2}{2} = \int_{p_c}^{p_1} dp/\rho = h_1 - h_c \tag{59-2}$$

$$(\rho uA)_c = (\rho uA)_1 . \tag{59-3}$$

Newton's equation for the projectile is

$$M\frac{du_p}{dt} = p_p A . \tag{59-4}$$

---

[*] In some cases the qualitative determination may require some calculation. For example, if $a\rho$ of one gas is lower in one region of p than the $a\rho$ of the other gas, and is higher in another region of p, an estimate of the relative areas $\int dp/a\rho$ must be made to compare the gases.

The evaluation of

$$p = p(\sigma)$$
$$a = a(\sigma)$$
$$\rho = \rho(\sigma)$$
$$h = h(\sigma)$$

$$(59-5)$$

for the isentrope of the gas may be done from tabular values of gas data. If possible, these tabular values may be fitted to empirical equations, as outlined in Section 66, to facilitate the calculations.

The equations above, with the given gun geometry and the initial conditions of the propellant gas may be solved in a step-by-step fashion to yield the complete behavior of gas and projectile. In the general case of a finite length chamber the calculation becomes too lengthy for hand computation; an electronic computer is required.

If $x_0 = \infty$, and $D_0/D_1 = 1$, quasi-steady equations (59-2) and (59-3) are unnecessary; the pressure-velocity relation behind the projectile may be obtained from the simple wave equation

$$u + \sigma = \sigma_0 \qquad (59-6)$$

or

$$u = \int_p^{p_0} dp/a\rho \quad . \qquad (59-7)$$

Hence, an integration of thermodynamic gas properties alone is enough to obtain a p-u relation for the real gas expanding in a constant diameter, $x_0 = \infty$, gun.

However, in the case of an $x_0 = \infty$, chambered PP gun the p-u relation behind a projectile can only be obtained by use of all the equations above. Thus, the pressure at the beginning of the barrel, p_1, may be obtained as a function of the velocity u_1 from the simple wave equation

$$u_0 + \sigma_0 = \sigma_0 \qquad (59-8)$$

and the quasi-steady equations (59-2) and (59-3) with the state equations (59-5). But conditions at barrel entry, 1, may be related to those at the projectile, p, only by use of the characteristic equations and the knowledge of the projectile motion (i.e., Newton's equation). Hence, a p-u curve for a chambered gun requires the complete gun calculation, whereas for the constant diameter gun only a knowledge of the gas data is required.

130
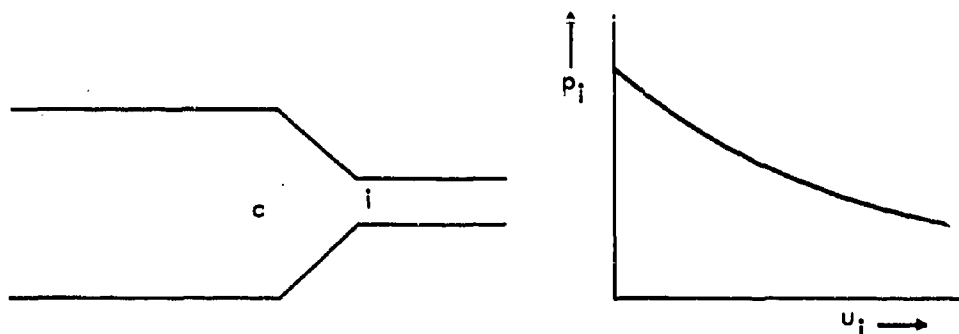
To avoid the required calculation, the approximation that the gas is at sonic velocity at the beginning of the barrel is sometimes made for high velocity guns. In that case

$$u_i = a_i \tag{59-9}$$

and

$$u_i + \sigma_i = u_p + \sigma_p . \tag{59-10}$$

The pressure behind the projectile may then be evaluated as a function of the velocity.
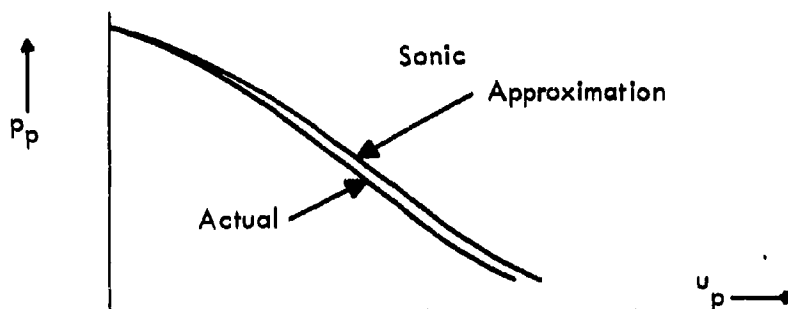
(In the case of the shocktube, the contact surface remains at a constant velocity; consequently, the p-u relation may be obtained for a chambered or unchambered shocktube from the thermodynamic properties of the gas alone.)

Section 60

The Application of the Criteria to a Propellant Gas at High Temperature

At room temperature the molecules of a gas are in translational and perhaps rotational motion. As the temperature is elevated, energy is imparted not only to the translational motion and rotational motion but to vibrate the molecules, to excite

and ionize the atoms, and to dissociate the molecules. When energy is imparted to these additional energy "sinks" as the temperature is elevated, the specific heats increase and the ratio of specific heats, γ, decreases. However, after elevated temperatures have been reached, further energy transferred to the gas again is imparted only to translational motion, and the ratio of specific heats, γ, will increase. The decrease and increase of γ may occur again if at still higher temperatures further energy sinks (e.g., ionization) become available. Eventually, when all the possible dissociation and ionization have occurred, the value of γ will be that of a monatomic gas, 5/3. The γ variation for hydrogen gas is sketched for a constant pressure and for a constant entropy.
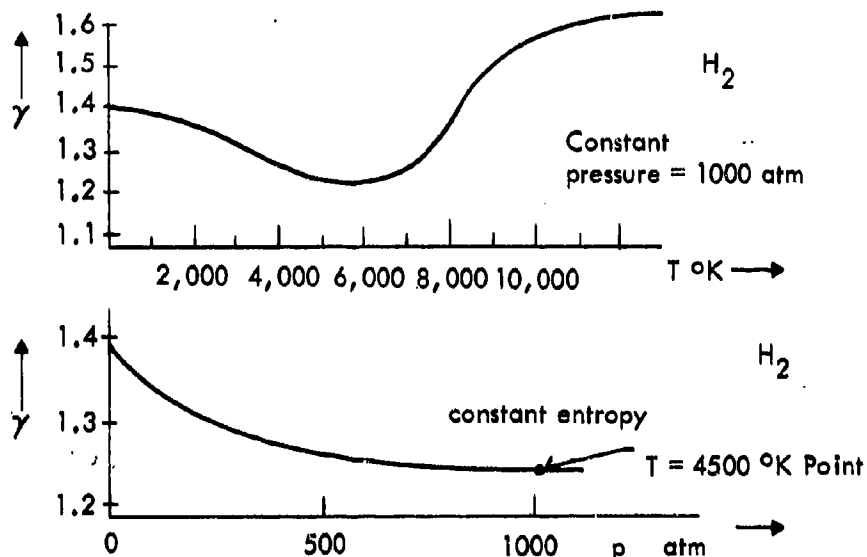
In general, for heated propellant gases the value of γ is less than it would be at room temperature.

An approximate method of accounting for this change in γ during the expansion of the propellant gas is to assume the isentropic relation

$$p = \rho^n K(s) \tag{60-1}$$

where K is a constant for a given isentrope and the exponent "n" is fitted by the equation to the actual isentropic p-ρ relation. Thus, n is not equal to the ratio of specific heats γ, but is an "effective γ" for the isentropic expansion. Bjork[42] has pointed out that a constant n value for hydrogen isentropes fits the calculated data very well (see Section 66)*.

---

* However, the hydrogen data Bjork uses does not take into account the non-idealities due to high density.

132

ISENTROPES

$p = \rho^n (p_o / \rho_o^n)$
ref. (42)

$P_o = 100{,}000$ psi

ρ_o AMAGAT

T_o °K →

n

1.6 1.5 1.4 1.3 1.2

1000 400 280 180 130 90

2,000 °K 4,000 °K 6,000 °K 8,000 °K 10,000 °K 12,000 °K
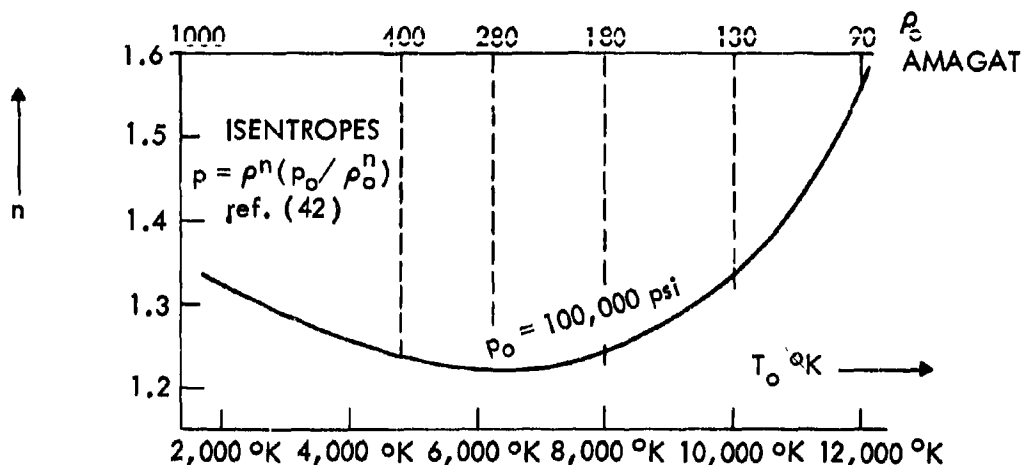
Since at the high temperatures the γ is generally lower than that of an ideal gas at lower temperature, the exponent "n" is also generally less than the γ of the ideal gas.

Because of the ionization and dissociation that occurs at elevated temperatures, the number of particles (atoms, molecules, ions, and electrons) is increased. As the propellant gas expands the number of particles decreases. Thus, the thermal equation of state takes the form

$$p = \rho(1 + \bar{\alpha})RT \tag{60-2}$$

where $\bar{\alpha}$ is the fraction of the additional particles and is obtained from a fit of this equation to the real gas over the range of the gas expansion. The variation of $\bar{\alpha}$ for hydrogen gas is shown in the sketch.

$\bar{\alpha}$

Pressure = 1000 atm

1.0 0.5 0

0 5,000 °K 10,000 °K

T →

$\bar{\alpha}$

Constant Entropy

1.0 0.5 0

10,000 °K
6,000 °K

0 500 1000

p atm →
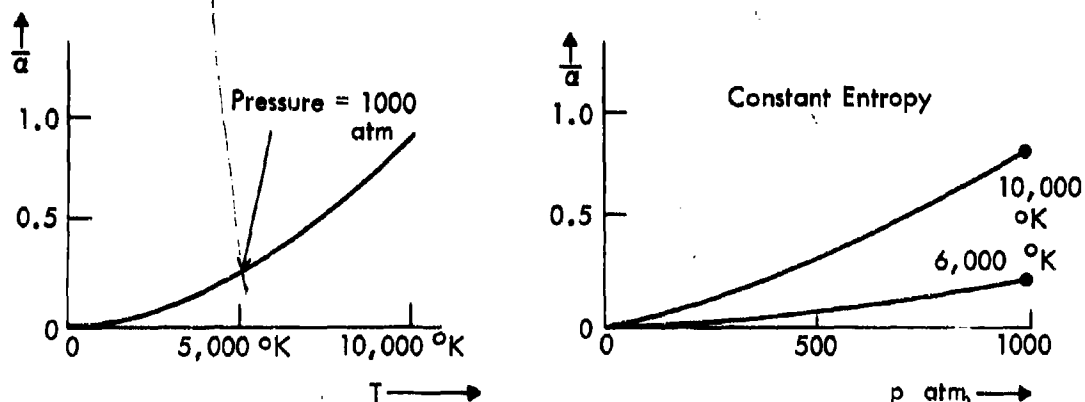
Equations (60-1) and (60-2) thus approximate the behavior of a real gas expanding from a high temperature.

From these equations one finds for the isentrope

$$a\rho \;=\; \frac{\sqrt{n}\;\nu_0}{\sqrt{(1+\bar{\alpha})RT_0}} \left(\frac{p}{p_0}\right)^{\frac{n+1}{2n}} \tag{60-3}$$

and

$$\rho \;=\; \frac{p_0}{(1+\bar{\alpha})RT_0} \left(\frac{p}{p_0}\right)^{\frac{1}{n}} \tag{60-4}$$

where the subscript "0" refers to the initial state.

If $a\rho$ and ρ are compared to the corresponding expressions for an ideal gas at the same initial pressure and temperature, the following ratios are obtained:

$$\frac{(a\rho)_{real,\ high\ T}}{(a\rho)_{ideal}} \;=\; \sqrt{\frac{n}{\gamma(1+\bar{\alpha})}}\;\left(\frac{p}{p_0}\right)^{\frac{n+1}{2n}-\frac{\gamma+1}{2\gamma}} \tag{60-5}$$

$$\frac{(\rho)_{real,\ high\ T}}{((\rho)_{ideal}} \;=\; \frac{1}{1+\bar{\alpha}}\left(\frac{p}{p_0}\right)^{\frac{1}{n}-\frac{1}{\gamma}} \;. \tag{60-6}$$

Upon examination of these equations, it becomes obvious, since n is less than γ and $\bar{\alpha}$ is positive, that these ratios are both less than one; that is, $a\rho$ and ρ for the real gas are less than the corresponding quantities for the ideal gas. (This is true even if $\bar{\alpha}$ is equal to zero, which is the case for no ionization and dissociation). Verification of this is seen in Figure 31, where these ratios are plotted as a function of p for the expansion of an air isentrope with initial conditions of pressure equal to 100 atmospheres and temperature equal to 8684°K. A sketch of Figure 31 is shown here. The data for real air were obtained from References 43 and 44.

Thus, according to the criteria (i) and (ii), a real gas at high temperature will be a better propellant than an ideal gas at the same temperature and pressure in both the chambered and constant diameter guns[*].

It is to be remarked, however, that a simplification in calculation is possible in the case of a gun in which the propellant is raised in temperature by a given amount of energy (or, for example, by being compressed by a moving piston of given kinetic

---

[*] It may be that during expansion of the propellant gas, some of the modes are not in equilibrium and lag the translational mode; then, as a first approximation, the "n" and "$\bar{\alpha}$" would be adjusted to reflect this condition. Such lags would tend to increase $\bar{\alpha}$ and decrease n , producing better propellant performance.

energy as in a two-stage gun) if only moderate amounts of dissociation occur. In this case, experience has shown that the calculated results with the assumption that the propellant gas is ideal are very nearly the same as obtained by taking into account the effects of high temperature on the gas behavior. This is true because, for a given energy input, the ideal gas would rise to a higher temperature than the vibrating, dissociating, ionizing real gas; hence, the higher temperature ideal gas would tend to behave as the lower temperature, lower γ, more particle, real gas. An example comparing the performance of a dissociating propellant gas to that of the propellant gas if undissociated is given in Appendix II of Reference 28.
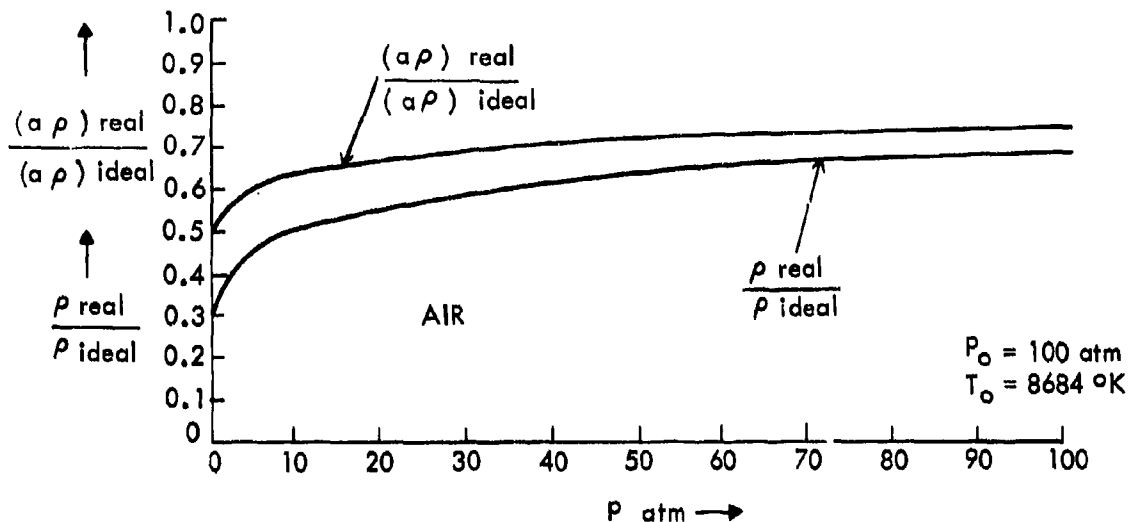
Section 61

Introductory Remarks Concerning
a Dense Propellant Gas

If the density of the propellant gas in a gun is sufficiently high, the gas molecules will be close enough to each other so that the intermolecular forces between them will influence their behavior. Under these circumstances the ideal equation of state does not describe the gas, and there is a possibility that the behavior of the propellant gas upon expansion will be substantially different from that of an ideal gas. If the gas is highly compressed, the intermolecular forces which exist are predominantly repulsive in nature and tend to push the molecules further apart; if the gas is allowed to expand to a less dense state, the forces between the molecules become predominately attractive in nature and tend to pull the molecules closer together. If the gas is still further expanded, the intermolecular forces become negligibly small, and the gas behavior may be described by the equations for an ideal gas.

It seems reasonable to suppose that repulsive forces between molecules would tend to accelerate the gas flow compared to a gas with no intermolecular forces (that is, compared to an ideal gas), and that attractive forces would tend to retard the gas flow. Thus, by this supposition, a highly compressed dense propellant gas upon expanding would flow more rapidly than an ideal gas until it reached the region where its density was low enough so that the attractive field predominated; then, the gas would expand at a slower rate than an ideal gas until its density was sufficiently low so that the intermolecular forces would be negligible; thereafter, it would expand as an ideal gas.

This simple picture of the effects of intermolecular forces on the expansion of the driver gas does not, however, take into account two important factors. One is the difference in nature between repulsive forces and attractive forces; the repulsive forces between molecules are "short range" forces and act only over short distances relative to the longer range attractive forces which exert influence over relatively much longer distances. Thus, the influence of repulsive forces on the expansion may well be different in magnitude than that of the attractive forces. The second factor not taken into account by the simple picture above is the relation between intermolecular forces and the geometry of the gun. In a non-uniform cross-section gun the driver gas expands from a chamber to a smaller tube; during the expansion the flow is basically steady in the transition section between chamber and tube and unsteady elsewhere. It is difficult to ascertain the effects of the intermolecular forces on the combined steady and unsteady flow which results from the non-uniformity of the shocktube.

It is the purpose of the following sections to discuss the effects of this type of non-ideality due to high density on the behavior of the expanding propellant gas. The expansion in both the constant diameter gun and the chambered gun will be examined.

Section 62

The Moderately Dense Propellant Gas in an $x_0 = \infty$, PP Gun

(a) *The van der Waals Gas — A model for a Moderately Dense Gas*

The van der Waals equation of state will be used to approximate a real gas at moderate density. This equation is

$$(p + \tilde{\alpha}\rho^2)\left(\frac{1}{\rho} - b\right) = RT \quad . \tag{62-1}$$

The terms $\tilde{\alpha}\rho^2$ and b are corrections to the ideal equations of state which account for the attractive and repulsive forces between molecules, respectively. If it is assumed that C_v at zero pressure is a constant ($C_{v\,\infty}$ = constant), then the isentrope may be derived from Equation (62-1) as

$$(p + \tilde{\alpha}\rho^2)\left(\frac{1}{\rho} - b\right)^{\gamma} = K$$

136

where K is a function of entropy only, and γ is defined as $(C_{v\ \infty} + R)/C_{v\ \infty}$.

Since the values of $\tilde{\alpha}\rho^2/p$ and $b\rho$ are small relative to one at moderate densities, the expressions for ρ and $\tilde{\alpha}\rho$ as functions of p may be simplified to yield

$$a\rho = \left\{ \frac{\gamma p_0^2}{RT_0} \left(\frac{p}{p_0} \right)^{\frac{\gamma+1}{\gamma}} \right\}^{\frac{1}{2}} \cdot \left\{ 1 + \frac{\tilde{\alpha}(\gamma-1)p_0}{\gamma(RT_0)^2} \left[1 + \left(\frac{p}{p_0} \right)^{\frac{2-\gamma}{\gamma}} \right] \right\}^{\frac{1}{2}} \tag{62-2}$$

$$\rho = \left(\frac{p}{p_0} \right)^{\frac{1}{\gamma}} \frac{p_0}{RT_0} \left\{ 1 - \frac{bp_0}{RT_0} \left(\frac{p}{p_0} \right)^{\frac{1}{\gamma}} \right\} \left\{ 1 + \frac{\tilde{\alpha}p_0}{\gamma(RT_0)^2} \left[(\gamma-1) + \left(\frac{p}{p_0} \right)^{\frac{2-\gamma}{\gamma}} \right] \right\} \tag{62-3}$$

In the derivation of these equations, terms containing the square of the terms $\tilde{\alpha}\rho^2/p$ and $b\rho$ and higher (or their product) were dropped as being small relative to these terms themselves.

The effects of the intermolecular forces are evident from the equations for $a\rho$ and ρ . It is seen that in the expression for $a\rho$ there *are no repulsive terms present* (i.e., there are no terms containing b), but attractive force terms (involving $\tilde{\alpha}$) are present[*]. These attractive terms increase $a\rho$ from the ideal value, and therefore act to retard the expansion rate relative to an ideal gas (according to criterion (i)) as expected. Since the repulsive field exerts no influence, it is seen to be ineffective in improving gun performance in a constant diameter gun.

From an examination of the expression for ρ , it is seen that the density as a function of p for a given initial pressure and temperature is altered from that of the ideal gas by both the attractive force term (containing $\tilde{\alpha}$) and repulsive force term (containing b). The attractive force term increases the density ρ , and thus the expansion is retarded relative to an ideal gas according to criterion (i)); the repulsive force term decreases the density ρ , and thus the expansion is accelerated relative to an ideal gas. It is further seen from the equation for density that when the initial density (approximately p_0/RT_0) is increased, the density ρ is decreased. Thus, the effect of the repulsive forces becomes greater than that of the attractive forces with increasing initial density.

It is apparent that the dominating effect for the chambered gun (repulsive or attractive) would depend on the relative magnitudes of the constants "$\tilde{\alpha}$" and "b" and the initial density ρ_0 . For a gas such as helium (and to a lesser extent hydrogen) the attractive field is weak relative to the repulsive field, and the b term would

---

[*] If second-order terms are taken into account, repulsive terms (with b) do appear in the expression for $a\rho$ for the van der Waals gas; thus, in the case of extreme densities, there would be an effect of the repulsive field on the expansion in a uniform tube (as shown by Dawson and Slawsky[45]).

dominate. Other gases, such as nitrogen or carbon disulfide, have a relatively strong attractive field. The van der Waals constants which are indicative of the relative strength of the repulsive and attractive fields are given in the table for a few gases[*].

Propellant Gas	$\tilde{\alpha}$ atm (liters/mole)^2	b (liters/mole)
Helium	0.034	0.024
Hydrogen	0.24	0.010 to 0.027
Nitrogen	1.39	0.039
Carbon disulfide	11.62	0.077

It may be concluded from the above discussion that at moderate density the effects of molecular forces on the expansion in a uniform cross-sectional area tube is to retard the expansion. In the transition section the effects of the attractive and repulsive forces tend to cancel each other; the gas flow may be retarded or accelerated by these forces; which effect dominates depends on the relative magnitudes of the van der Waals constants and the density; the higher the density, the more the repulsive field dominates.

(b) *The Moderately Dense Real Propellant Gas in an*
   $x_0 = \infty$, *PP Gun*

The above conclusions may be verified by examining pressure-velocity (p-u) curves for real (actual) gases in guns. These curves are calculated using Equations (59-1) through (59-4) with the gas tabular isentropic data fitted to a semi-empirical equation, as explained in Section 66. The p-u curve for nitrogen at moderate density ($p_0 = 340$ atm, $T_0 = 25^\circ C$) expanding in a gun is shown in Figure 32. It is noted that, for $D_0/D_1 = 1$, the real nitrogen curve falls below that of the ideal nitrogen. This is in accord with our qualitative result. For a diameter ratio of infinity (infinite chambrage) the curves are very nearly coincident, indicating the cancelling effects of the repulsive and attractive fields – again in accord with our qualitative conclusions. (The tendency for lower p at a given u in the lower region of pressure is due to the fact that the gas state approaches the strongly attractive two-phase region).

It would seem from the above discussion that at a higher density the effect of the repulsive field may more than cancel that of the attractive field in an expansion in a chambered gun. This is seen in Figure 33 to be the case with nitrogen at an initial pressure of 1,000 atmospheres and an initial temperature of $25^\circ C$. *Here is seen the remarkable results that the* p-u *curve for the real nitrogen falls below that of the ideal gas for the constant diameter shocktube and is above that of the ideal gas for the infinite diameter ratio case.*

---

[*] The relative strength of the repulsive and attractive fields may also be seen from an examination of the force constants σ and ϵ/k which occur in the Leonard-Jones equation of state.
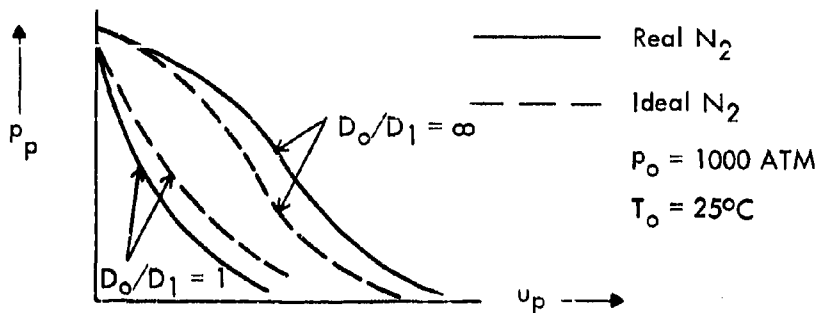
That this result agrees with criteria (i) and (ii) is seen from Figure 34, where $\theta\rho$ and ρ are plotted as functions of p for this case. It is seen from this figure that the real nitrogen should expand more rapidly than the ideal in the transition section (since $(\rho)_{real}/(\rho)_{ideal} < 1$) and less rapidly in the constant area section (where $(\rho a)_{real}/(\rho a)_{ideal} > 1$).

The effects of diameter ratios other than one and infinity have also been investigated. From calculated results it is concluded that the $D_0/D_1 = 5$ curve is practically the same as the $D_0/D_1 = \infty$ curve, and that a diameter ratio curve somewhat less than the $D_0/D_1 = 2$ curve (say, $D_0/D_1 = 1.5$) would lie midway between the one and infinity curves.
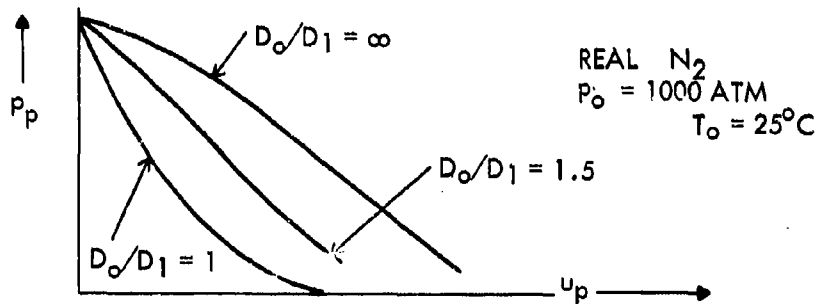
(These conclusions are true for ideal gases, and, as will be seen below, are approximately true for real gases except at extremely high density).

Section 63

The Highly Dense Propellant Gas in an
$x_0 = \infty$, PP Gun

(a) *The Abel-Noble Gas – A Model for a Highly Dense Gas*

In the very dense gas the molecules are so close together that the repulsive field is extremely large relative to the attractive field. To describe approximately the behavior of such a dense gas, the attractive term $(\tilde{\alpha}\rho^2)$ in the van der Waals equation is neglected and the equation

$$p \left(\frac{1}{\rho} - b \right) = RT \qquad (63\text{-}1)$$

is often used. The terms "Abel-Noble", "Abel", or "covolume" are used for this equation or for the gas that the equation describes.

From Equation (63-1) and the thermodynamic relation

$$C_v = C_{v\,\infty,T} + \int_0^\rho \frac{T}{\rho^2} \left(\frac{\partial^2 p}{\partial T^2} \right)_\rho d\rho \qquad (63\text{-}2)$$

where $C_{v\,\infty,T}$ is C_v are zero pressure and temperature T, it is found that

$$C_c = C_{v\,\infty,T} \qquad (63\text{-}3)$$

for the Abel-Noble gas. Then from the Gibbs Law equation expressed as

$$ds = \frac{C_v}{T} dT + \frac{1}{\rho^2} \left(-\frac{\partial p}{\partial T} \right)_\rho d\rho \qquad (63\text{-}4)$$

and the assumption that $C_{v\,\infty,T}$ is constant, the isentrope for the Abel-Noble gas is obtained as

$$p \left(\frac{1}{\rho} - b \right)^\gamma = K \qquad (63\text{-}5)$$

where K is a function only of entropy. This isentropic equation (63-5) is especially useful in interior ballistics calculations and is very convenient to use. (In Section 66 a similar equation applicable to actual propellants is discussed).

The expressions for $a\rho$ and ρ as a function of p may be obtained from Equations (63-1) and (63-5) as

$$a\rho = \left[\frac{\gamma p_0^2}{RT_0} \left(\frac{p}{p_0} \right)^{\frac{\gamma+1}{\gamma}} \right]^{\frac{1}{2}} \qquad (63\text{-}6)$$

$$\rho = \left[\left(\frac{p_0}{p} \right)^{\frac{1}{\gamma}} \frac{RT_0}{p_0} + b \right]^{-1} . \qquad (63\text{-}7)$$

By comparing Equation (63-6) for $a\rho$ with the corresponding expression for an ideal gas (Equation (58-3)), it is seen that the two expressions are identical. *The pressure-velocity history during an expansion of an ideal gas and that of an Abel-Noble gas from the same initial temperature and pressure in a constant diameter tube are therefore identical; from this point of view there is no effect of the repulsive field on the expansion in a constant diameter gun.*
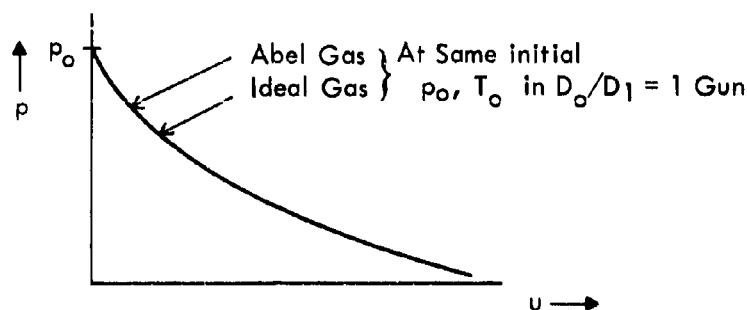
This result is as expected from the previous result with the van der Waals equation at moderate density. (However, in the case of extremely high density there probably would be some effect of the repulsive field, as evidenced by the theoretical work of Reference 45). Thus, repulsive forces are again seen to be inefficient in improving driver gas performance in a constant diameter section.

In the case of an ideal propellant gas, the initial sound speed a_0 was found to be a criterion for the merit of the gas. The sound speed of an Abel gas is much above that of an ideal gas at the same temperature and pressure.

$$a = \sqrt{\gamma R T_0} \left[\frac{p}{p_0}\right]^{\frac{\gamma-1}{2\gamma}} \left[1 + \frac{b}{v_0 - b} \left(\frac{p}{p_0}\right)^{\frac{1}{\gamma}}\right]$$

$$a_0 = \sqrt{\gamma R T_0} \left[1 + \frac{b}{v_0 - b}\right] = \sqrt{\gamma R T_0} \left[1 + \frac{p_0 b}{R T_0}\right] .$$

Yet, as shown above, the ideal propellant gas and the Abel propellant gas at the same initial temperature and pressure would produce the same constant diameter gun performance. Hence, *the acoustic velocity is not an indicator of the merit of a real propellant gas* [*].

The Abel-Noble expression for ρ is different from that of the ideal gas Equation (58-4) by the presence of the covolume term b which decreases it as a function of p for given initial p_0 and T_0. Therefore, *in an expansion (from a given pressure and temperature) in a transition section, a highly dense real gas will expand more rapidly than an ideal gas* [†]. Thus, the repulsive field is again seen to be efficient in improving gun performance in the transition section.

---

[*] However, it should be noted that initial temperature still retains a dominant role for the Abel gas in an $x_0 = \infty$, pp chambered or unchambered gun. This is seen from an examination of Equations (63-7) and (63-6); from these equations it is evident that a higher initial T_0 yields a higher projectile velocity for a given b and p_0.

[†] Another way to understand the gain in velocity in a covolume gas in a steady expansion is to note that the enthalpy has an additional term, pb, which the ideal gas does not; thus $h = C_{0_{\infty, T}} T + pb + RT$ for the covolume gas.

These remarks are borne out in Figure 35 where the p-u curves are shown for a
$\gamma = 7/5$ gas with and without covolume; the diameter ratio one case (no chambrage
case) and the diameter ratio infinity (infinite chambrage case) are illustrated.   A
covolume parameter $b/(v_0 - b)$ equal to 100 is used for this curve[*].
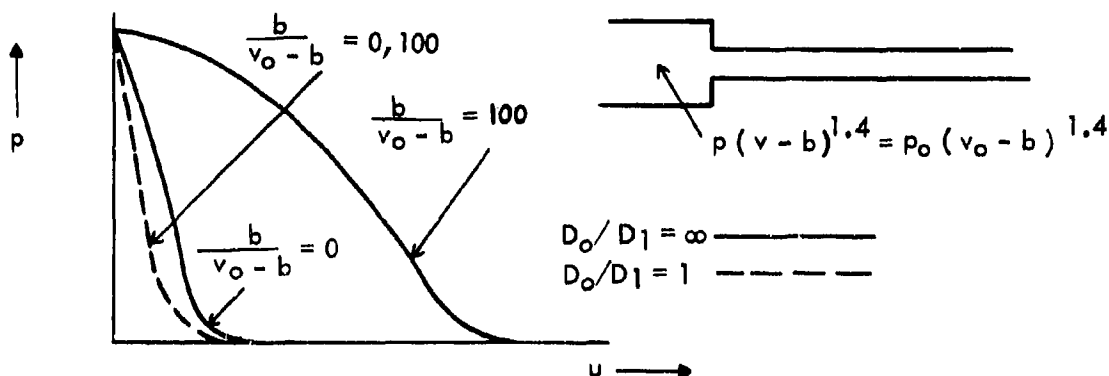
It is seen that, for the constant diameter gun, the p-u curve of the ideal gas
(i.e., the gas with $b/(v_0 - b) = 0$) is coincident with that of the covolume gas
($b/(v_0 - b) = 100$). However, for the infinite chambrage case the effect of covolume
is seen to increase the pressure for a given velocity by a huge amount.

(It is to be remarked that the velocity in these and other curves for the Abel-Noble
gas is made dimensionless by dividing by a parameter which has a factor $\sqrt{\gamma p_0(v_0 - b)}$.
This factor would equally well be expressed as $\sqrt{\gamma RT_0}$ by use of the thermal equation,
Equation (63-1).   Thus, a given dimensionless velocity indicates a given velocity for
a given initial temperature.   The reason the factor $\sqrt{\gamma p_0(v_0 - b)}$ is used is to
emphasize the fact that the p-u curve is derived only from the isentropic equation,
Equation (63-5); thus, when real gas data are fitted to an isentropic equation similar
to the Abel-Noble equation, the p-u curve for it may be calculated without regard
to the thermal equation of state and the velocity made dimensionless in a like manner).

The effects of a value of the covolume parameter equal to 8.09 for the $\gamma = 7/5$
gas is seen in Figure 36 where p-u plots are shown.   Here again the repulsive forces
(which are accounted for by the covolume) are seen not to affect the uniform diameter
expansion, but do increase the pressure for a given velocity (or increase the velocity
for a given pressure) in the chambrage cases.

It has been observed from other calculated results that the diameter ratio curve
which is midway between the $D_0/D_1 = 1$ and $D_1/D_2 = \infty$ curves is 2 for the
$b/(v_0 - b) = 8.09$ (very dense) gas and 3 for the $b/(v_0 - b) = 100$ (extremely dense)
gas case.

---

[*] This dimensionless parameter is the ratio of volume occupied by gas molecules to the volume
not occupied by gas molecules — the larger this ratio is, the larger is the covolume.   This
parameter occurs conveniently in the equations of an Abel gas.   A value of this parameter
equal to 100 is an extremely large value; a value equal to about 10 is what nitrogen or
hydrogen gas at a pressure of around 10,000 atmospheres and room temperature would possess as
seen from Bridgman's data[46].

The escape velocity (the velocity that the propellant gas attains when it expands into a vacuum)[*] is seen from Figure 37 to be increased by the repulsive forces in the cases with chambrage. In this figure the dimensionless escape velocity is plotted as a function of the parameter b/v_0 (the covolume divided by the total volume). For the no-chambrage case ($D_0/D_1 = 1$) the escape velocity is unaffected by the repulsive forces – it is the same as for an ideal gas; however, for chambered guns the enormous influence of these forces is evident in the figure.
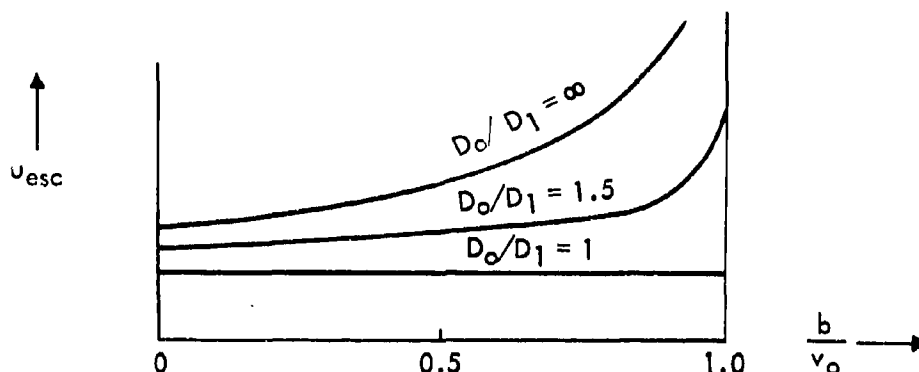
In fact, for large b/v_0 the escape velocity may be shown to be equal to the product of the area ratio and the escape velocity of a covolume gas in a gun with no chambrage; viz.,

$$u_{esc} = \left(\frac{D_0}{D_1}\right)^2 \sqrt{\gamma p_0(v_0 - b)}\ \frac{2}{\gamma - 1} = \frac{A_0}{A_1}\sqrt{\gamma RT_0}\left[\frac{2}{\gamma - 1}\right] \qquad (63\text{-}8)$$

and becomes infinite for infinite chambrage.

(b) The Highly Dense Real Gas

The same effects of the intermolecular forces as appeared in the Abel-Noble gas are evident in real (actual) gases at very high densities. Figures 38 and 39 show a comparison between real nitrogen and ideal nitrogen. In Figure 38 the pressure-velocity curves are compared for an initial condition of nitrogen at a pressure of 3,000 atmospheres and temperature of 25°C. For the no-chambrage case ($D_0/D_1 = 1$) the ideal and real curves are very close together[†]. For the infinite chambrage case, the real gas curve as for the Abel gas model is much above that of the ideal curve and demonstrates the expected increase due to the repulsive forces.

---

[*] The escape velocity is evaluated from the equation

$$u_{esc} = \left\{\left[\int_{p_0}^{p_0} dp/a\rho\right]^2 + \left[2\int_{p_1^*}^{p_0} dp/\rho\right]\right\}^{\frac{1}{2}} + \int_{p=0}^{p_1^*} dp/a\rho$$

with the condition that the flow is sonic at the barrel entrance, i.e.,

$$u_1 = u_1^* = a_1^*$$

[†] Since in the lower region of pressure the influence of the two-phase region is felt, the attractive forces predominate and cause the real gas curve to fall below the ideal gas curve.

Like effects are evident in Figure 39, where ideal and real nitrogen are compared at a higher initial pressure, 6,000 atmospheres, at 25°C. Here the repulsive effect is seen in the no-chambrage case as well as in the infinite chambrage case where it is most striking.
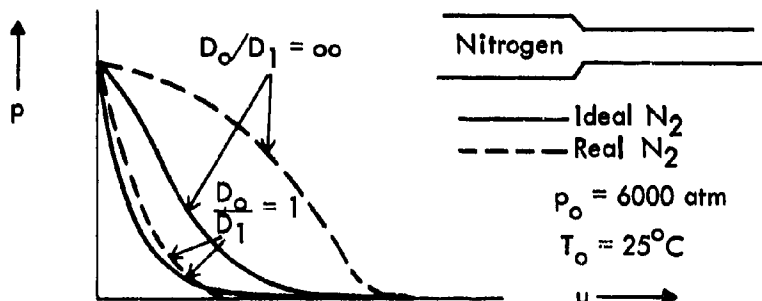
Similar evidence of the real gas effects on the expansion in guns is shown in Figure 40 where p-u curves for ideal and real hydrogen are compared at initial conditions of p_0 = 2190 atmospheres, T_0 = 150°C. The repulsive effect is apparent.

The effect of chamber diameter on the dense real gas has been calculated. It has been found that the D_0/D_1 = 5 case is almost the same as the D_1/D_2 = ∞ case, and that a D_0/D_1 equal to slightly less than 2 (about 1½) is halfway between the 1 and ∞ cases.

Section 64

Summarizing Remarks on Dense Propellant Gases in an x_0 = ∞, PP Gun

It has been demonstrated that the behavior of a dense propellant gas in an x_0 = ∞, PP gun may be considerably different from that of an ideal gas. This difference is due to the existence of attractive and repulsive forces which act between the gas molecules. The attractive forces tend to decelerate the expansion rate relative to an ideal gas and thus adversely affect gun performance; the repulsive forces tend to accelerate the expansion rate relative to an ideal gas and thus improve gun performance.

At very low gas densities the intermolecular forces which exist are negligible; at higher densities the forces are predominately attractive. At still higher densities the repulsive forces predominate. The effectiveness, however, of these forces on gun performance depends on the geometry of the gun. It is found that the attractive forces are much more effective relative to the repulsive forces during an expansion in a uniform cross-sectional area gun; whereas, both types of forces, attractive and repulsive, are effective when expanding in a non-uniform gun. It is to be noted that *acoustic velocity is not a measure of the merit of a real propellant gas as it is for an ideal propellant gas.* Qualitatively low $a\rho$ (acoustic impedance) as a function of pressure for the isentrope is desirable for good propellant performance in a constant diameter gun; for a chambered gun, low ρ (density) as a function of pressure for the isentrope is desired.

The effects of the propellant gas density on gun performance are summarized in the table.

Propellant Gas Density	Relative Magnitude of Attractive and Repulsive Intermolecular Forces	$x_0 = \infty$, PP Gun Performance of Real Gas Relative to Ideal Gas	
		$D_0/D_1 = 1$ Uniform Gun	Chambered Gun
Low	Both negligible	Same	Same
Moderate	Attractive predominates	Much worse	Somewhat worse, or same, or somewhat better
Moderately high	Both of same order	Worse	Better
Very high	Repulsive predominates	Same or somewhat better	Much better

It is remarkable that at moderately high density the performance of a real gas may be worse than that of an ideal gas in a uniform diameter gun, but better in a chambered gun (as seen in Figure 33). Thus, the gun in this region of density becomes a discriminator between the attractive and repulsive intermolecular forces. At very high densities, the performance of a real gas is about the same as that of an ideal gas in a uniform gun, but is much better in a chambered gun. This result agrees with that obtained from the Abel-Noble equation of state to approximate the behavior of a very dense real gas.

To describe accurately real gas behavior a semi-empirical entropic equation (similar to the Abel-Noble equation) has been fitted to tabular data with success (see Section 66). From the isentrope the velocity (and thus the performance) of a driver is evaluated from the $\int (dp/a\rho)_s$ for the expansion in a uniform gun, and $\int (dp/\rho)_s$ for the nonuniform gun.

<div align="center">

Section 65

**Expansion of a Real Propellant Gas in a PP Gun
With Finite Length Chamber**

</div>

It is reasonable to assume that the effect on gun performance of the gas non-idealities when the chamber length x_0 is not infinite is qualitatively the same as when x_0 is infinite. Each such finite x_0 case requires a calculation involving all the Equations (59-1) through (59-5).

An interesting result may be obtained for the expansion of an Abel gas in the preburned propellant gun for which x_0 is finite and D_0/D_1 is equal to one. This is then the classical Lagrange ballistics problem with a propellant whose isentropic equation of state is

$$p(v - b)^\gamma = K \tag{65-1}$$

and whose thermal equation is

$$p(v - b) = RT \quad . \tag{65-2}$$

It is demonstrated in Appendix I that for a given propellant gas mass to projectile mass (G/M), a given ratio of specific heats γ, and the same initial pressure and temperatures, the *projectile behavior for the Abel gas is precisely the same as that for the ideal gas in a* $D_0/D_1 = 1$ *gun.*

Thus, in general, for constant diameter guns ($D_0/D_1 = 1$), dense real gases will yield the same performance as ideal gases at the same p_0 and T_0 if the mass of gass G is the same; however, for a given $D_0/D_1 = 1$ gun of fixed finite volume, the dense real gas will yield *poorer* performance, since the mass of real gas in that case is less than the mass of the ideal propellant gas.

$$u_p \,(\text{ideal}) > u_p \,(\text{Real})$$
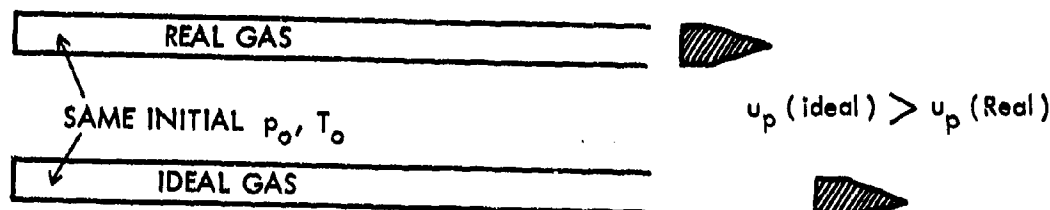
Another way to rationalize in this instance is to think in terms of the sound speed; the sound speed in the real gas is larger than in the ideal gas. Consequently, the pressure lowering rarefactions are reflected more quickly to the projectile in the case of the real gas.

For $x_0 < \infty$ chambered guns, dense real propellant gases will yield better performance than ideal propellant gases at the same p_0 and T_0 if the mass of gas G is the same; this is true for the reasons discussed above, that is, the greater $\int dp/\rho$ for the real gas. However, for a chambered gun having a fixed finite volume, the real gas propellant may or may not be superior to the ideal gas propellant, depending on whether the real gas $\int dp/\rho$ advantage is greater or not than the real gas small G disadvantage.

FASTER GUN = ?

146
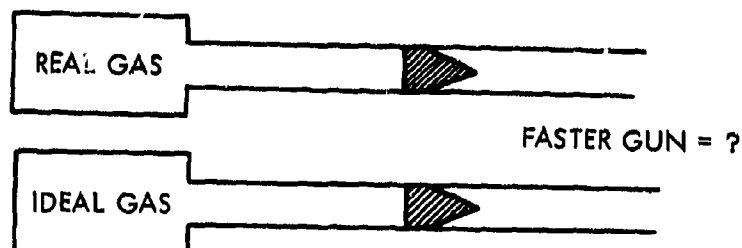
In this instance a calculation is required to determine the better propellant.

For the constant base pressure two-stage guns the required volumes of the gun may be considerably smaller for the real gas than for the ideal gas to obtain the same performance (see the discussion in Section 57).

Section 66

The Use of a Semi-Empirical Entropic Equation
To Approximate Actual Propellant Gas Behavior

In general, the gas thermodynamic properties are given in tabular form; in this situation the fundamental equations of Section 59 may be solved numerically. This is a long and tedious process. It has been found by Seigel[5,47] that the isentropic data of dense real gases at temperatures between 150°C and -150°C and pressures up to 6,000 atmospheres may be fitted accurately by a semi-empirical entropic equation of the form

$$p^{(\beta-2)/\beta} (v - f) = \kappa \tag{66-1}$$

where β, f, and κ are functions only of entropy. This equation has been fitted to nitrogen, argon, and hydrogen data at temperatures below 150°C (Reference 41). This equation is similar to the Noble-Abel (covolume) equation of state used for many years by ballisticians to describe propellant powder gas.

$$p^{1/\gamma} (v - b) = \text{constant} . \tag{66-2}$$

The semi-empirical Equation (66-1) may be fitted to real gas data with much greater accuracy than the Abel equation because of the fact that the parameters β, f, and κ may vary with entropy.

Evidence to date indicates that this equation may also be applied to propellant gases at high temperature as well as high density. Bjork[42] was able to fit high temperature hydrogen gas data to the more restrictive equation

$$p^{1/n} (v) = K' \tag{66-3}$$

where n, and K' are functions of entropy. His fit covered the region of hydrogen data from 100,000 lb/in² and 12,000°K and below. (However, the effect of molecular attraction was not accounted for in the data.)

An advantage of the semi-empirical equation is that it may be conveniently applied to the preburned propellant gun. Thus, from

$$p^{(\beta-2)/\beta} (v - f) = \kappa$$

the Riemann function σ may be evaluated as

$$\sigma/\sigma_0 = (p/p_0)^{1/\beta} , \tag{66-4}$$

The characteristic equations which apply to the constant diameter chamber and barrel are, as before,

$$\frac{\partial}{\partial t}(u \pm \sigma) + (u \pm a)\frac{\partial}{\partial x}(u \pm \sigma) = 0 \quad , \tag{66-5}$$

The sound speed a may be expressed as

$$a = \frac{\sigma}{\beta - 2}\left[1 + F\left(\frac{\sigma}{\sigma_0}\right)^{\beta-2}\right] \tag{66-6}$$

where F is defined as

$$F \equiv \frac{f}{v_0 - f} \quad . \tag{66-7}$$

The quasi-steady energy and continuity equations relating the transition section exit and entrance become

$$u_0^2 + \frac{\sigma_0^2}{\beta-2}\left[1 + \frac{2}{\beta}F\left(\frac{\sigma_0}{\sigma_0}\right)^{\beta-2}\right] = u_i^2 + \frac{\sigma_i^2}{\beta-2}\left[1 + \frac{2}{\beta}F\left(\frac{\sigma_i}{\sigma_0}\right)^{\beta-2}\right] \tag{66-8}$$

$$u_0 A_0\left[1 + \frac{1}{F}\left(\frac{\sigma_0}{\sigma_i}\right)^{\beta-2}\right] = u_i A_i\left[1 + \frac{1}{F}\left(\frac{\sigma_0}{\sigma_0}\right)^{\beta-2}\right] \tag{66-9}$$

These equations may be applied to the preburned propellant gun and solved numerically by hand or machine. In such a calculation it is usually convenient to make the equations dimensionless by dividing σ, u, and a by σ_0, and dividing p by p_0. It is interesting to note Appendix I, where it is shown that for the case of a constant diameter gun ($D_0/D_i = 1$), the above equations when expressed in Lagrangian coordinates become equivalent to those of an ideal gas.

If the gas described by the semi-empirical entropic equation is shocked, it is necessary to use an expression for the internal energy v (or the enthalpy). From the thermodynamic identity

$$\left(\frac{\partial v}{\partial v}\right)_s = -p \tag{66-10}$$

and Equation (66-1) is obtained

$$v = g + \tfrac{1}{2}p(v - f)(\beta - 2) \tag{66-11}$$

where g is a function only of entropy.

One need at the present time is for tabular data for propellant gases such as helium and hydrogen which include the non-idealities due to temperature and density. (Some hydrogen data will soon be available from the National Bureau of Standards,

Washington, DC, according to Dr. H.Wooley.) These data are required, for example, in
order to design a constant base pressure, two-stage gun; in such a design, as discussed
in Section 57, the effects of the non-idealities are extremely significant in determining
the size of the gun. Toward this end the available hydrogen data of Wooley[99] has been
extended to higher density and the results fitted in Reference 100 to Seigel's Equations
(66-1) and (66-11). A plot of the fitted constants is given in Figure 45. Until more
reliable data are calculated, it is recommended that the information in Figure 45 be
used to approximate the behavior of hydrogen.

Section 67

Remarks on Expansion of Liquids and Solids

The criteria of driver gas performance applied above to gases may be equally well
applied to liquids or solids; such substances under huge pressures behave like very
dense non-ideal gases and expand in a "propellant gas" fashion. It is to be expected
that extremely large repulsive forces would exist within the liquid or solid when in
this highly compressed dense state. Therefore, the expansion even in a constant
diameter tube of a liquid or solid would be more rapid than such an expansion of an
idealized like substance, and the expansion in a chambered gun would be a great deal
more rapid than that of the ideal substance.

These views are borne out by a p-u plot of the expansion of high density water
(T_0 = 26°C, and p_0 = 100,000 atmospheres) in a gun. The plot, seen in Figure 41,
shows the pressure-velocity relation for water expanding in a gun as an ideal gas
(no intermolecular forces) and as real water.
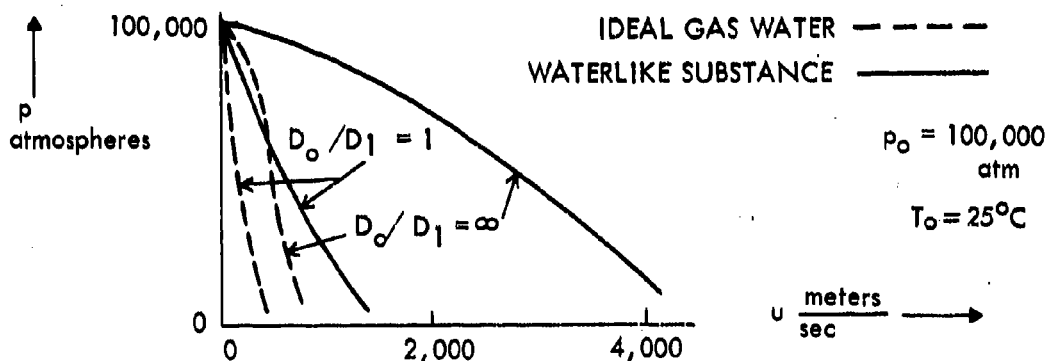
The effects of the repulsive forces are manifest and are, as expected, much larger
for the chambered than the uniform gun.

It is to be remarked that the isentropic behavior of solids and liquids has
often been approximated by the Murghnahan equation of state

$$p + A = \left(\frac{v_0}{v}\right)^n A \qquad (67-1)$$

where A and n are empirically fitted constants[*]. This is a very convenient equation to use, since the expressions for the thermodynamic quantities are similar to an ideal gas; thus

$$a^2 = \frac{n(p + A)}{\rho} \tag{67-2}$$

$$\sigma = \frac{2}{n - 1} \, a \tag{67-3}$$

$$h = \frac{a^2}{n - 1}. \tag{67-4}$$

where σ and h are taken to be zero at $a = 0$. To make Equation (67-1) more flexible, the parameters A and n could be functions of entropy.

Finally, an isentropic equation of state could be written which would describe the behavior of any substance, gas, liquid, or solid:

$$(p + A)(v - B)^n = c$$

where A , B , c , and n are functions of entropy.

---

[*] This equation was used to obtain Figure 41.

PART XII. REMARKS CONCERNING PROJECTILE
VELOCITIES – PRESENT AND FUTURE

Section 68

The Selection of a Propellant

It is not always obvious which propellant is best to use. For example, a preburned propellant gun having relatively small chamber volume may perform better with air than hydrogen as a propellant.
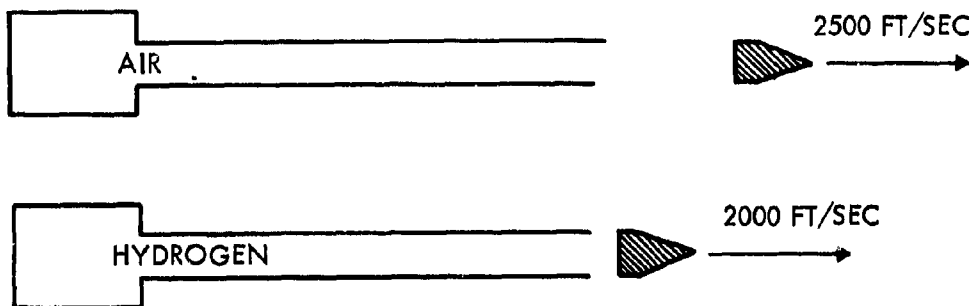
(This results from the fact that the larger G/M of air, weight of propellant to projectile, being much greater than for the hydrogen, may offset the disadvantage of air's low sound speed relative to hydrogen's. The calculation for a given case may be performed using Figures 20 and 21. Of course, for relatively large chamber volumes hydrogen becomes far superior.)

If high velocity is desired (say, about 15,000 ft/sec) the choice of propellants is restricted to either heated hydrogen or heated helium. This results from the fact, as has been pointed out, that the achievable velocity in a gun is practically limited to velocities corresponding to a $\gamma u_p/a_0$ equal to about 2.5 to 3 (or about 30 to 40% of the escape velocity). Moreover, to achieve the required a_0, a two-stage gun is necessary.

As between hydrogen and helium, hydrogen gives, in general, higher projectile velocities relative to helium; its temperature is lower; this results in less heat loss and less erosion.

One must, however, exercise caution in the use of hydrogen. It is explosive when reacted with the oxygen in air. In addition, hydrogen embrittles many steels when it is contained at pressures above 500 atmospheres; at these pressures materials (like certain stainless steels) not subject to hydrogen embrittlement should be used. In the case of a two-stage gun the embrittlement problem usually does not occur since the initial loading pressures are low and the peak pressures are only held for milliseconds. If hydrogen is to be heated and maintained at high temperature, one must ascertain that the containing vessel is not attacked by the hydrogen ("hydrogen attack").

Section 69

Proposed Schemes to Increase Projectile Velocities

There have been a number of schemes attempted in order to increase the projectile velocities in guns. (See, for example, the survey made by Knapp[113].) A few will be listed below:

(a) *The Traveling Charge Gun or Rocket Projectile*

In this scheme the projectile is propelled in part or entirely as a rocket. (See, for example, References 67 and 68.) It carries a propellant attached to its back end which burns during its travel in the barrel.

BURNING PROPELLANT
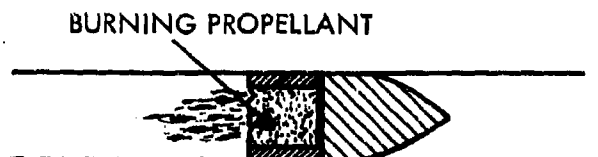
Up to date this scheme has not produced significant velocity increases due to the difficulty of burning the propellant rapidly enough.

(b) *The Addition of Energy Along the Barrel*

At successive locations along the barrel energy (electrical or chemical) is put into the barrel immediately after the passage of the projectile. (See, for example, References 69, 104 and 111.)
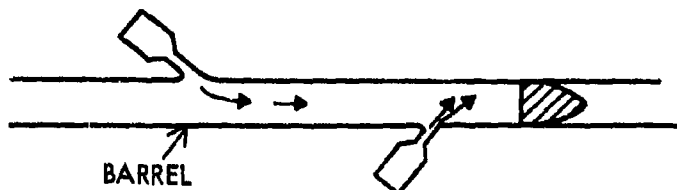
BARREL

This scheme has not been successful to date.

(c) *The Varying of Barrel and Projectile Geometry to Augment the Velocity*

The use of tapered gun barrels, either sudden or gradual, has been considered with various arrangements of projectile and projectile-sabot geometry.

Howell, using the scheme sketched on the following page (right), reports achieving a velocity of 34,000 ft/sec consistently with a 0.02 gm sphere.
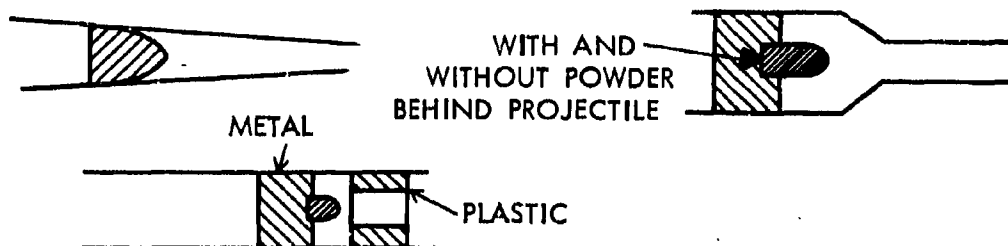
(d) *Use of Electromagnetic and Electrostatic Concepts to Increase the Projectile Velocity*

Various schemes to accelerate projectiles by electromagnetic and electrostatic devices have been proposed and tried for at least the past fifteen years. (See, for example, References 65, 66, and 109.) These include attempts to directly accelerate the projectile electromagnetically, and also to indirectly accelerate the projectile by accelerating the ionized propellant gas. To the present time the use of electromagnetic concepts does not offer much promise of producing velocities above 15,000 ft/sec for heavy projectiles. However, for small masses (less than 0.01 gm) these types of accelerators have achieved velocities[72] up to 50,000 ft/sec and give promise of higher velocities.

(e) *Heating the Gas in the Pump Tube of a Two-Stage Gun*

Calculation indicates a velocity gain if the helium or hydrogen gas in the pump tube of a two-stage gun is initially heated, or heated during the compression stroke (see, for example, References 48, 63, 64, 82, and 85). Results to date by Arnold Engineering Development Center indicate that gains of 2000-3000 ft/sec have been achieved in this manner at a projectile velocity of 30,000 ft/sec; however, Cable[108], reports no gain by heating.

In summary, the various proposed schemes (a) through (e) may prove to be useful in conjunction with a two-stage light gas gun to augment projectile velocity. None of the schemes, it is felt, will increase the projectile velocity by more than 15%.

One must not overlook the possible use of shaped charge or explosive concepts. Such concepts have resulted in the acceleration of small projectiles to very high velocities (up to 50,000 ft/sec). (See, for example, References 73 through 75, Reference 84, and Reference 109.) These concepts are being advanced with two promising new schemes: the "implosion driven" launcher of Glass[76] and the "gas injector" of Godfrey[77]. (See also Reference 71.) In application of all of these concepts the projectiles must be rugged to withstand the high pressures which occur. A discussion of strength limitations on projectiles is given by Curtis[108].

Section 70

Presently Obtained Maximum Projectile Velocities

The maximum velocities obtained experimentally from light gas guns are shown in Figure 46; this figure updates the information contained in a plot by Lukasiewicz[60]. The figure is shown in the following sketch.
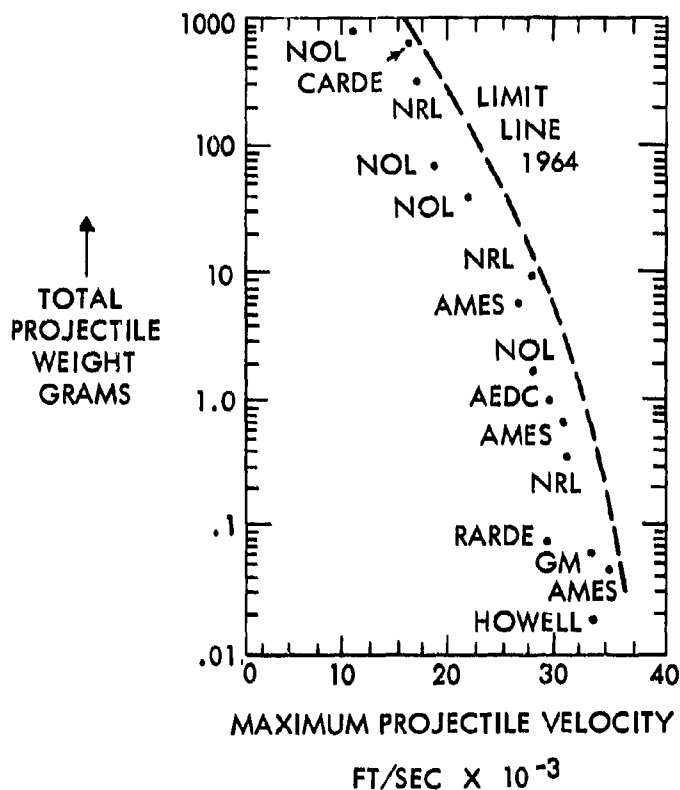
A listing of some of the velocity data used for Figure 46 with the pertinent gun characteristics is given in Table I.

It is seen that the highest velocities are obtained for the smallest mass projectiles. Thus, Charters[94] has reported a velocity of 32,800 ft/sec for a 0.07 gm cylindrical model. A sketch of the two-stage gun used by Charters is shown on page 155.

Howell has reported[101] consistent 34,000 ft/sec velocities with 0.02 gm projectiles using a two-stage gun with an augmenter technique[69]. NASA (Ames) has achieved a velocity of 37,060 ft/sec with a 0.040 gm projectile[113]. The performance of the NASA (Ames) light gas guns is shown in Figure 47.

TABLE I

Maximum Projectile Velocities

Organization	Projectile Muzzle Velocity (ft/sec)	In-Gun Projectile Weight (gm)	Barrel Diameter (in)	Pump Tune Diameter (in)
Arnold	25,600	0.27	0.30	1.5
Engineering	24,800	0.41	0.30	1.5
Development	26,700	1.0	0.5	1.58
Center (AEDC),	29,900	1.12	0.5	1.58
Tennessee	26,100	1.5	0.5	1.58
Royal Armament	30,100	0.08	0.25	1
Research and	27,800	0.106	0.25	1
Development	28,400	0.145	0.25	1
Establishment	27,000	0.2	0.25	1
(RARDE), Kent	26,200	0.24	0.25	1
England				
US Naval	26,900	1.3	0.50	2
Ordnance	22,000	30	1.6	5
Laboratory (NOL),	19,000	77	1.6	5
White Oak,	17,800	141	2	5
Silver Spring,	15,200	265	2	5
Maryland	10,600	1170	4	5
Canadian Armament	25,000	0.20	0.25	1.66
Research and	16,000	8-14	0.78	2.28
Development	17,600	55-75	1.5	4
Establishment	15,900	850-1000	4	10
(CARDE),				
Quebec, Canada				
US Naval	31,200	0.535	0.3	1.14
Research	28,600	10	0.83	3.25
Laboratory (NRL),	24,500	13.54	0.83	3.25
Washington, DC	18,200	24.0	0.83	3.25
	18,300	253	2.5	8.2
	16,400	462	2.5	8.2
NASA	35,600	0.052	0.22	1.77
Ames Research	32,300	0.091	0.22	1.77
Center,	31,600	0.100	0.22	1.25
Moffett Field,	28,800	0.19	0.28	0.78
California	30,500	0.90	0.50	2.13
	26,800	6.9	1.00	4.00
	37,060	0.040	0.22	1.77
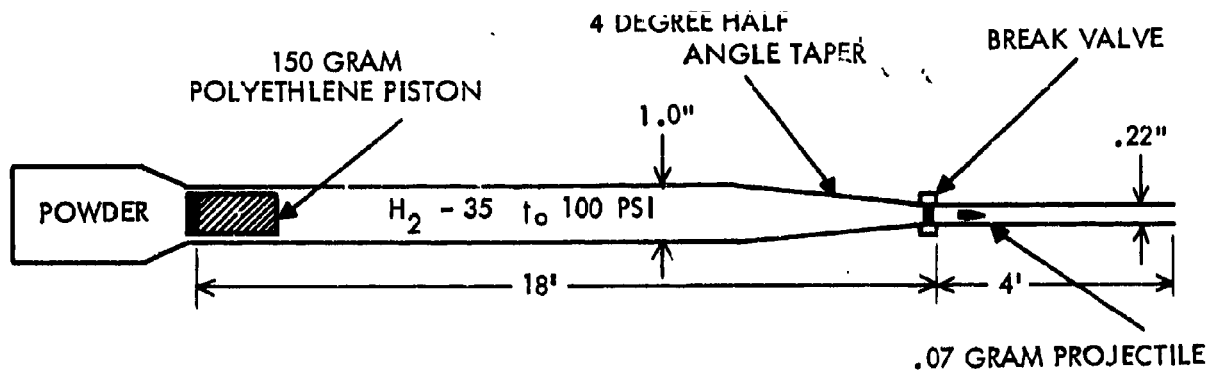
Obtaining these high velocities with larger projectiles is certainly possible in principle by scaling up the gun system. However, the cost and sizes involved may make such scaling impractical. (Thus, the gun sketched would be 250 ft long if scaled up by a factor of ten to fire a 70 gm 2.2 in projectile at 32,800 ft/sec.)

The plot of data in Figure 46 and in the sketch does not indicate the present lesser velocity capabilities of propelling fragile projectiles, for example, cones; such fragile projectiles often must be saboted and designed to be aerodynamically stable. Charters[102], has reported the repeated successful launching of cone models at velocities up to 24,000 ft/sec; these cones had half angles between 6¼ degrees and 12½ degrees. He also has launched saboted glass spheres at about 27,000 ft/sec. T. Canning of Ames Research Center (NASA) has launched saboted aluminum spheres at 32,000 ft/sec.

Section 71

Future Possibilities

Although the increase of projectile velocities from guns has been rather phenomenal in the last 20 years, it is predicted that the increase will continue and that projectile velocities in excess of 60,000 ft/sec will be obtained for projectiles weighing more than 0.1 gm by 1985.

156
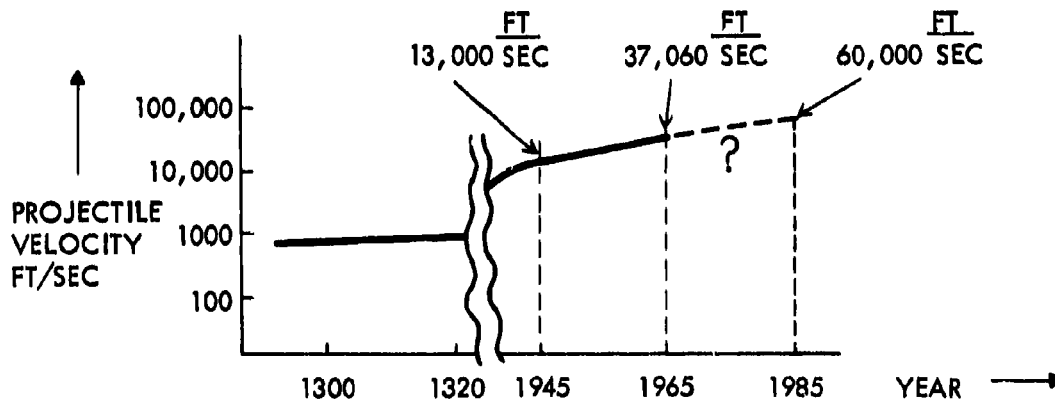
This increase in velocity will result from the following advances:

(i) Application of the constant base pressure principle.

(ii) Improvement in the design and strength of projectiles and guns.

(iii) Perhaps some augmentation by one of the techniques discussed in Section 89.

Derivation of the Expression for the Time
Rate of Change of a Quantity

Let P denote a quantity which depends *only* on position x and time t . This is
expressed by the equation

$$P = P(x, t) \qquad\qquad (A\text{-}1)$$

P is called the dependent variable; it depends on the values of x and t , which
are thus called the independent variables. For every value of x and t , Equation
(A-1) states there is a determined, definite value of P . This may be shown by
looking at an x-t plane as in the sketch.
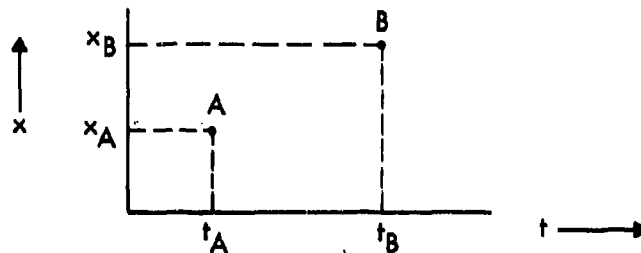
For point A the x and t values are x_A and t_A . Corresponding to this point
is a value of P , that is, P_A . Similarly the x and t values of point B
determine a value of P_B .

Let it be desired to determine the change in P in going from point 1 to a point
2 very close (differentially close) to point 1.
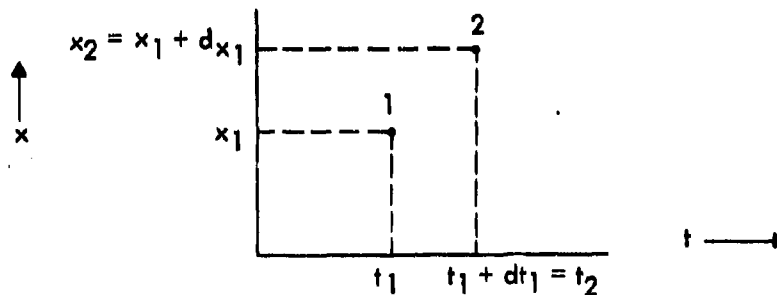
The change in P , in going from 1 to 2, will be designated as dP .

$$dP = P_2 - P_1 \qquad . \qquad\qquad (A\text{-}2)$$

* This elementary discussion is to be omitted by the reader familiar with partial derivatives.

158

To obtain the change in P , one may think of starting at point 1 and proceeding to
point 2, noting the change in P during the movement. It matters not which path is
chosen to go from point 1 to 2; the difference dP will always be the same; this is
true because the value of P at each of the points 1 and 2 depends only on the values
of x and t at each of the points 1 and 2 by Equation (A-1). Hence, their difference
dP depends not on the path chosen to go from one point to the other, only on the end
points.

It is convenient to choose a path between points 1 and 2 which is first a constant
x line and then a constant t line, as indicated in the sketch.
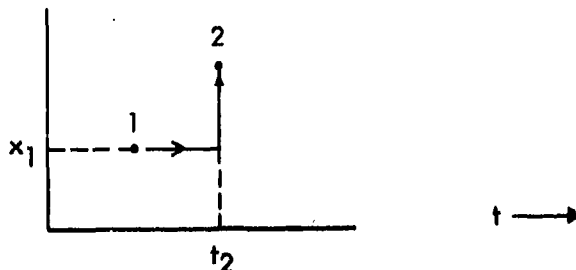
The selection of this path allows a simple calculation of the desired dP . For this
path

$$dP \; = \; \left(\begin{array}{c} dP \text{ due to change in } t \\ \text{at constant } x \end{array} \right) \; + \; \left(\begin{array}{c} dP \text{ due to change in } x \\ \text{at constant } t \end{array} \right) \; . \qquad (A\text{-}3)$$

Let the first term on the right of the equation be found by the following procedure.
From a knowledge of P = P(x,t) , one could plot P as a function of t for a number
of given x's as sketched.
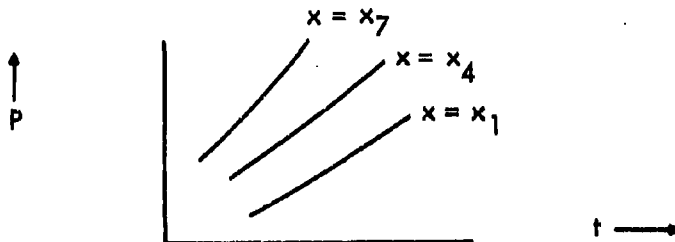
Let the constant x_1 line which is the path of interest be considered.
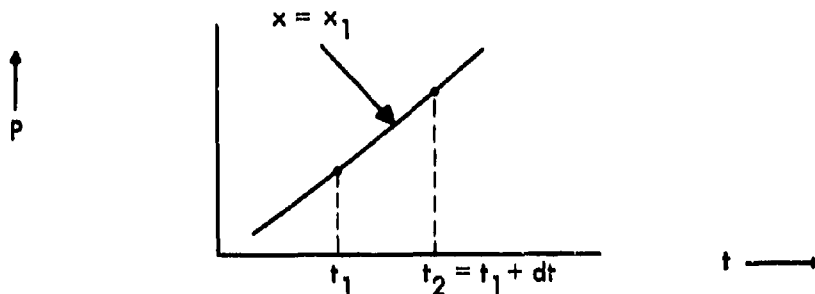
The part of this line to be examined is the differential segment between $t = t_1$ and $t = t_2$. This part of the line, being only of differential length, may be considered a straight line of slope $\tan \theta$.
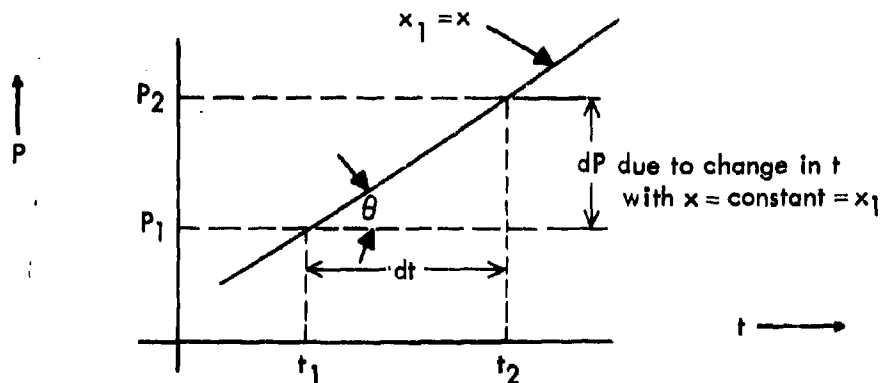
Then from the sketch

$$\frac{dP \text{ due to change in t}}{dt} = \tan \theta \quad . \tag{A-4}$$

What is $\tan \theta$? It is the slope of the x-equal-constant line in the x-t plane, or

$$\tan \theta = \frac{dP}{dt} \text{ at constant } x = x_1$$

which is written by convention as a partial derivative,

$$\tan \theta = \left(\frac{\partial P}{\partial t}\right)_{x=x_1} = \frac{\partial P}{\partial t} \tag{A-5}$$

where, as indicated, the subscript on the partial derivative is sometimes omitted. Equation (A-4) thus becomes

$$\left(\begin{array}{c} dP \text{ due to change in t} \\ \text{at constant x} \end{array}\right) = \left(\frac{\partial P}{\partial t}\right)_x dt \quad . \tag{A-6}$$

Similarly, it will be found by considering the constant $t = t_2$ line that

$$\left(\begin{array}{c} dP \text{ due to change in x} \\ \text{at constant t} \end{array}\right) = \left(\frac{\partial P}{\partial x}\right)_t dx \quad . \tag{A-7}$$

160

The expression Equation (A-3) for the total change in P in going from point 1 to point 2 becomes

$$dP = \frac{\partial P}{\partial t} dt + \frac{\partial P}{\partial x} dx \qquad \text{(A-8)}$$

where the derivatives are evaluated at point 1 (or, equivalently, at 2 which is infinitesimally close to 1). Equation (A-8) follows from the fact that

$$P = P(x, t)$$

and is often written directly in an elementary calculus course.

If the rate of change of P with time is desired, i.e., dP/dt , the equation (A-8) becomes after division by dt

$$\frac{dP}{dt} = \frac{\partial P}{\partial t} + \frac{dx}{dt} \frac{\partial P}{\partial x} \qquad \text{(A-9)}$$

This expression is meaningless unless dx/dt is specified; dx/dt is a direction or velocity in the x-t plane. Therefore, if one desired the dP/dt in a direction dx/dt equal to V (that is, if going at a velocity equal to V) the expression for dP/dt becomes

$$\left(\frac{dP}{dt}\right)_{\frac{dx}{dt} = V} = \frac{\partial P}{\partial t} + V \frac{\partial P}{\partial x} \qquad \text{(A-10)}$$

V may specify any desired velocity. For example, the rate of change of P with time when moving in a fluid with a velocity V = 10 miles per hour is

$$\left(\frac{dP}{dt}\right)_{\frac{dx}{dt} = 10} = \frac{\partial P}{\partial t} + 10 \frac{\partial P}{\partial x} \qquad \text{(A-11)}$$

If one desired the time rate of change in P experienced by a gas particle moving in the flow, the value of dx/dt would be the velocity of the gas particle, u . Thus,

$$\left(\frac{dP}{dt}\right)_{\frac{dx}{dt} = u} = \frac{\partial P}{\partial t} + u \frac{\partial P}{\partial x} \qquad \text{(A-12)}$$

Such a time rate of change when going along with a gas particle is thus the rate of change for a "material" particle or "substance" and, hence, is often termed the "material" or "substantial" derivative.

Material or substantial derivative $= \dfrac{d}{dt}$

$$= \frac{\partial}{\partial t} + u \frac{\partial}{\partial x} \quad . \qquad \text{(A-13)}$$

For three dimensions the material derivative becomes

$$\frac{d}{dt} = \frac{\partial}{\partial t} + u \frac{\partial}{\partial x} + v \frac{\partial}{\partial y} + w \frac{\partial}{\partial z} \quad . \qquad \text{(A-14)}$$

It is of interest to obtain the time rate of change of P along a disturbance path which has a velocity equal to the particle speed plus the sound speed

$$\frac{dx}{dt} = u \pm a \quad . \qquad \text{(A-15)}$$

Then Equation (A-9) becomes

$$\frac{DP}{Dt} = \frac{\partial P}{\partial t} + (u \pm a) \frac{\partial P}{\partial x} \qquad \text{(A-16)}$$

where

$$\frac{D}{Dt} = \frac{\partial}{\partial t} + (u \pm a) \frac{\partial}{\partial x} \qquad \text{(A-17)}$$

represents the rate of change along a disturbance path.

APPENDIX B

The Derivation of the One-Dimensional
Unsteady Characteristics Equations

The gas flow in a constant diameter tube will be examined. Let a layer of gas of differential length dx be considered. Across this layer the gas thermodynamic properties and gas velocity all change by differential amounts as shown in the sketch.
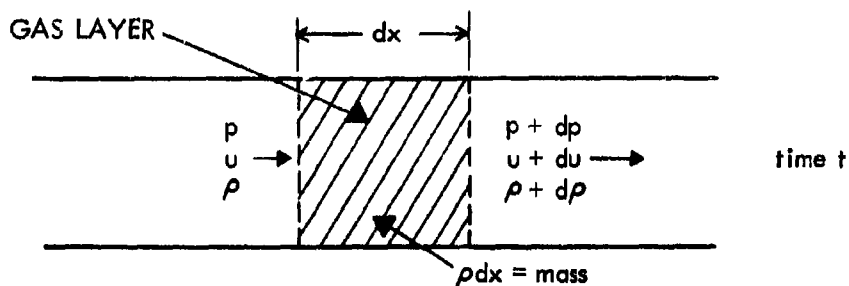
These differential amounts are all small changes due to a change in x at a given t ; thus

$$dp = (\partial p/\partial x)\ dx$$
$$du = (\partial u/\partial x)\ dx \qquad\qquad\text{(B-1)}$$
$$d\rho = (\partial \rho/\partial x)\ dx$$

and the differential change in products may be similarly expressed

$$d(\rho u) = \frac{\partial(\rho u)}{\partial x}\ dx \quad . \qquad\qquad \text{(B-2)}$$

The continuity equation applied to this layer is

$$\rho u = \rho u + d(\rho u) + \frac{\partial \rho}{\partial t} = \rho u + \frac{\partial \rho u}{\partial x}\ dx + \frac{\partial \rho}{\partial t}$$

or

$$\rho \frac{\partial u}{\partial x} + u \frac{\partial \rho}{\partial x} + \frac{\partial \rho}{\partial t} = 0 \quad . \qquad\qquad \text{(B-3)}$$

The acceleration of the gas layer is

$$\frac{du}{dt} = \frac{\partial u}{\partial t} + u \frac{\partial u}{\partial x}$$

where d/dt represents the "material" or "substantial" derivative (see Appendix A).
The momentum equation may thus be written in terms of the acceleration as

$$\rho \frac{du}{dt} = p - (p + dp) = p - \left(p + \frac{\partial p}{\partial x} \, dx \right)$$

or

$$\frac{\partial u}{\partial t} + u \frac{\partial u}{\partial x} = - \frac{1}{\rho} \frac{\partial p}{\partial x} \quad . \tag{B-4}$$

The assumption is now made that the process occurring in the tube *is isentropic.*
Thus, whereas, in general,

$$p = p(\rho, s) \tag{B-5}$$

this becomes

$$p = p(\rho) \quad \text{for} \quad s = \text{constant} \quad . \tag{B-6}$$

The sound speed a and Reimann Function σ are defined by

$$a^2 = \left(\frac{\partial p}{\partial \rho} \right)_s \tag{B-7}$$

$$d\sigma = \left(\frac{a}{\rho} \, d\rho \right)_s \tag{B-8}$$

or, from (B-7),

$$d\sigma = \left(\frac{1}{a\rho} \, dp \right)_s \quad . \tag{B-9}$$

For the constant entropy process assumed here the equations become

$$a^2 = \frac{dp}{d\rho} , \qquad s \text{ constant} \tag{B-10}$$

$$d\sigma = \frac{a}{\rho} \, d\rho = \frac{1}{a\rho} \, dp , \qquad s \text{ constant} \quad . \tag{B-11}$$

164

Equation (B-11) may be transformed to

$$d\rho = \frac{\rho}{a} d\sigma \qquad \text{(B-12)}$$

$$dp = a\rho \, d\sigma \quad . \qquad \text{(B-13)}$$

Equation (B-12) states that a differential change in ρ is equal to ρ/a times a differential change in σ. One may thus write

$$\frac{\partial \rho}{\partial t} = \frac{\rho}{a} \frac{\partial \sigma}{\partial t} \qquad \text{(B-14)}$$

$$\frac{\partial \rho}{\partial x} = \frac{\rho}{a} \frac{\partial \sigma}{\partial x} \quad . \qquad \text{(B-15)}$$

Similar reasoning yields

$$\frac{\partial p}{\partial x} = a\rho \frac{\partial \sigma}{\partial x} \quad . \qquad \text{(B-16)}$$

It is thus seen from these three equations that the gradient in the Riemann Function σ may be substituted for gradients in ρ and p. If this substitution is made in the continuity equation (B-3) and the momentum equation (B-4), the following set of equations results:

$$\frac{\partial u}{\partial t} + u \frac{\partial u}{\partial x} + a \frac{\partial \sigma}{\partial x} = 0 \qquad \text{(B-17)}$$

$$\frac{\partial \sigma}{\partial t} + u \frac{\partial \sigma}{\partial x} + a \frac{\partial u}{\partial x} = 0 \quad . \qquad \text{(B-18)}$$

By adding and subtracting equations (B-17) and (B-18) the "characteristics equations" are obtained.

$$\frac{\partial}{\partial t} (u + \sigma) + (u + a) \frac{\partial}{\partial x} (u + \sigma) = 0 \qquad \text{(B-19)}$$

$$\frac{\partial}{\partial t} (u - \sigma) + (u - a) \frac{\partial}{\partial x} (u - \sigma) = 0 \qquad \text{(B-20)}$$

With the notation

$$\frac{D}{Dt} = \frac{\partial}{\partial t} + (u \pm a) \frac{\partial}{\partial x} \qquad \text{(B-21)}$$

these equations may be written

$$\frac{D}{Dt} (u \pm \sigma) = 0 \quad . \tag{B-22}$$

The characteristics equations (B-22) are equivalent to the continuity and momentum equations provided the gas pressure is determined alone by density (as for an isentrope).

APPENDIX C

The Meaning of the Characteristic Theory

(a) The Meaning of the Characteristic Equations

The meaning of the characteristic equations derived in Appendix B becomes clear from the results of Appendix A. According to Appendix A, the time rate of change of a quantity P along a path of slope u + a is

$$\left(\frac{dP}{dt}\right)_{along \ \frac{dx}{dt} \ = \ u \ + \ a} = \frac{\partial P}{\partial t} + (u + a)\frac{\partial P}{\partial x} \quad . \tag{C-1}$$

If P is assumed to be the quantity (u + σ) ,

$$\left(\frac{d(u + σ)}{dt}\right)_{along \ \frac{dx}{dt} \ = \ u \ + \ a} = \frac{\partial(u + σ)}{\partial t} + (u + a)\frac{\partial(u + σ)}{\partial x} \quad . \tag{C-2}$$

The characteristic equation thus states that the time rate of change of u ± σ along a path of slope u ± a is zero. This is written for conciseness as (see Appendix A)

$$\frac{D(u ± σ)}{Dt} = 0 \quad . \tag{C-3}$$

The characteristic equations state that within the gas there is no change in the quantity u ± σ to an observer traveling with the velocity u ± a . Equivalently, one may state that along a characteristic line in the x-t plane (defined by a slope u ± a in this plane) the quantity u ± σ remains constant. Therefore, on the x-t plane two sets of "characteristic lines" are obtained: one with the slope u + a , along which u + σ is constant, the other with the slope u - a , along which u - σ is constant. The two sets intersect and form what is known as a characteristic net.
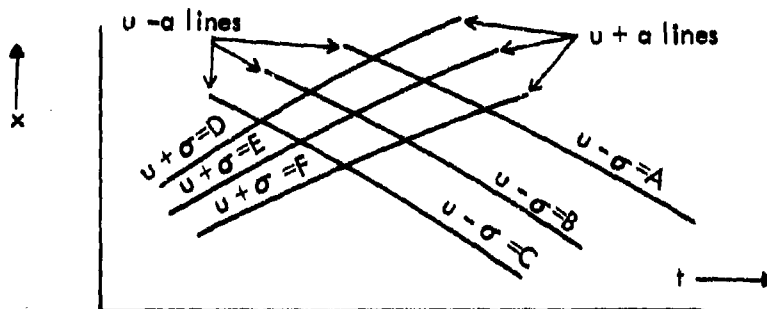
These characteristic lines may be interpreted as the paths of disturbance waves, since as one goes along a characteristics line, one travels at the same speed as an acoustic disturbance would, that is, at the local sound speed relative to the moving fluid. (See Equation (6-4) of the main text.) Thus, the characteristic net is quite naturally viewed as a net of interacting disturbances. The number of disturbances to be considered is arbitrary, depending only on the number of characteristics one desires to examine.

To make these ideas clearer, consider the case of an isentropic flow of a gas in a tube. For each and every point in the x-t plane which describes this flow there exist corresponding values of pressure, gas velocity, temperature, sound speed, etc. Let the area on the x-t plane be divided into an arbitrary number of squares; in each square let the value of "u + a" which exists at the middle of each of the squares be written as shown in the sketch, where numerical values have been written for illustration.
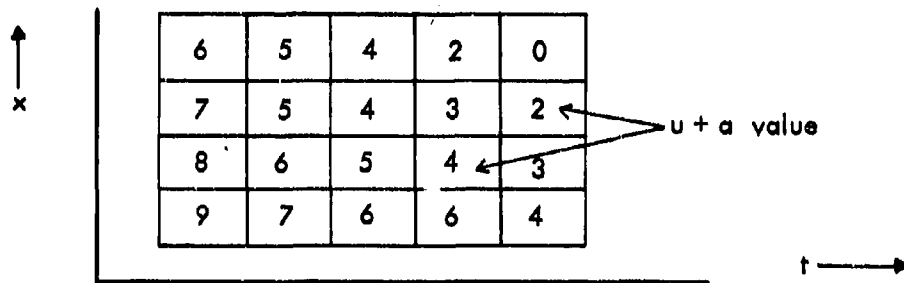
Let any mid-point of any square in the x-t plane be selected. From that mid-point, draw within the square a line of the slope equal to u + a in that square. When the line intersects the adjacent square, draw a new line in the adjacent square of slope equal to u + a in the adjacent square. Continue this process.
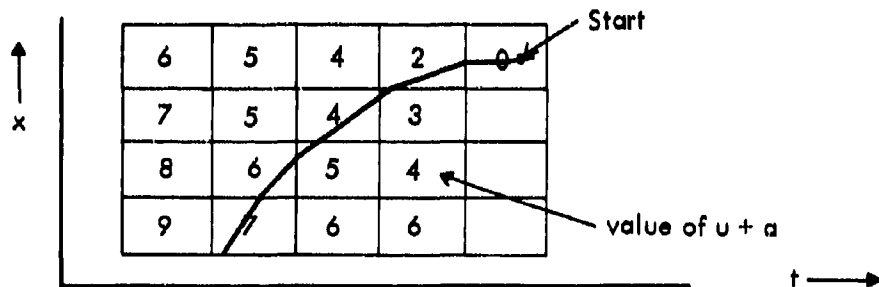
The path traced by the above procedure is a line of slope u + a . It may be made as smooth as desired by decreasing the size of the squares. It is a "u + a" characteristic line and along it the quantity $u + \sigma$ remains constant. This procedure may be repeated to yield as many u + a lines as desired.
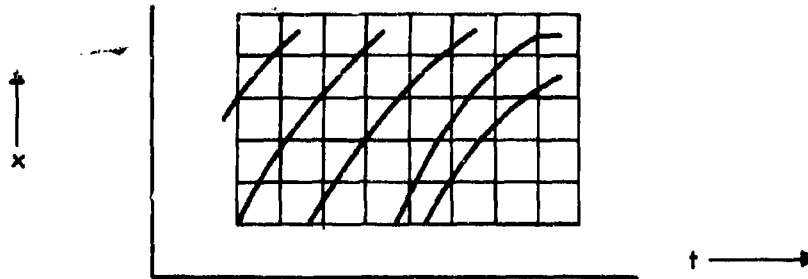
Along each u + a line, u + σ is a constant, in general, a different constant for each line.

A like procedure could be applied to squares containing values of u – a within each square; this would result in u – a lines.
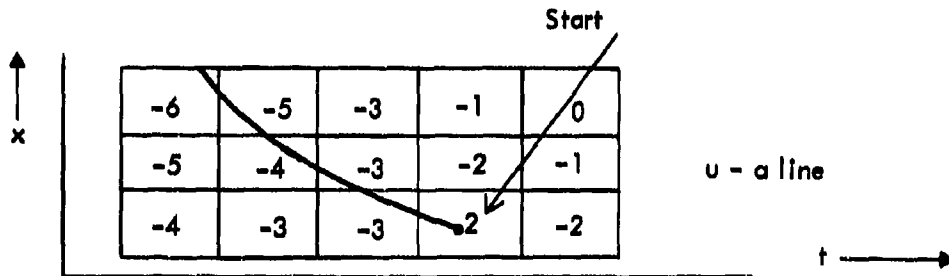
On each u – a line the quantity u – σ is a constant.

As a result of the property that the quantity u $\pm$ σ remains constant along the disturbance paths of slope u $\pm$ a , the behavior of the gas and projectile in constant diameter portions of a gun can be found by using the characteristics net; in general, a numerical procedure is necessary. In some instances an analytic solution occurs, as for the case of the simple wave region discussed in Appendix D.

APPENDIX D

The Simple Wave Region in a $D_0/D_1 = 1$, PP Gun

Let the relevant case of a preburned propellant gun of $D_0/D_1 = 1$ be considered. At the instant the projectile begins to move, a "u - a" disturbance is sent back towards the breech. This disturbance travels at a speed equal to $-a_0$, since it moves at a speed of $u - a$ into a gas at rest with sound speed a_0.
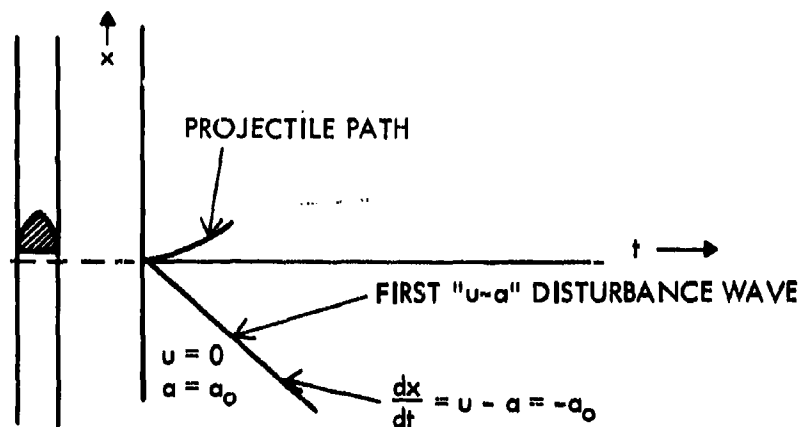
During each succeeding instant that the projectile moves, it sends back toward the breech $u - a$ disturbance waves. In the sketch the projectile path is represented as A-B-C-D-E.
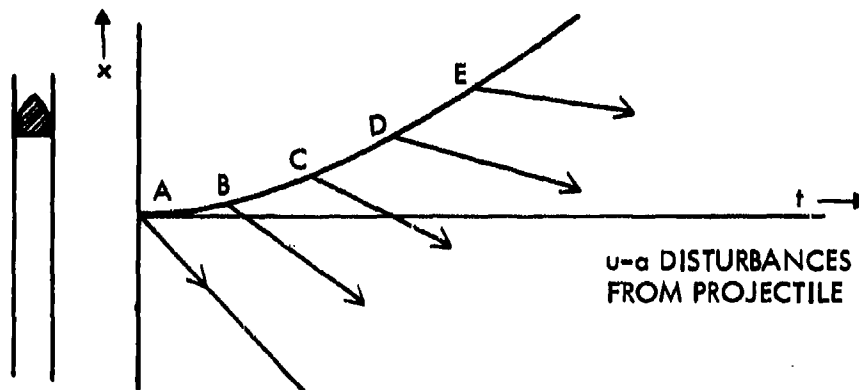
To determine more concerning the behavior of the gas let the "u + a" characteristic lines which extend from the region A-O-L be considered. These are shown dashed in the sketch.
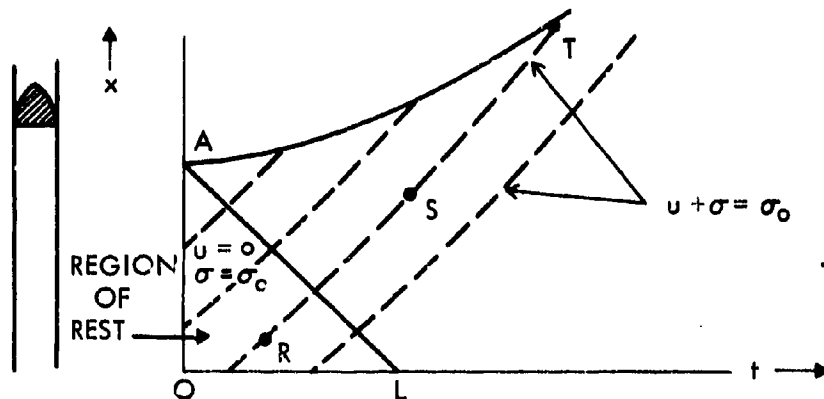
The region A-O-L is a "rest" region in which the gas has been undisturbed. Consequently, in this region $u = 0$ and $\sigma = \sigma_0$. For any $u + a$ characteristic which extends into this region, e.g., characteristic R-S-T, the sum of $u + \sigma$ is therefore

$$u + \sigma = 0 + \sigma_0 = \sigma_0 \quad .$$

Moreover, according to the characteristic equations, this sum is constant along the entire characteristic. Thus, for all the $u + a$ characteristics which extend into the rest region A-O-L,

$$u + \sigma = \sigma_0 \quad . \tag{D-1}$$

Hence, this equation, which is true for all $u + a$ characteristics in A-O-L, applies to the entire region into which these characteristics exist, the region A-O-L-E, where E is the point where the first reflected disturbance reaches the projectile.
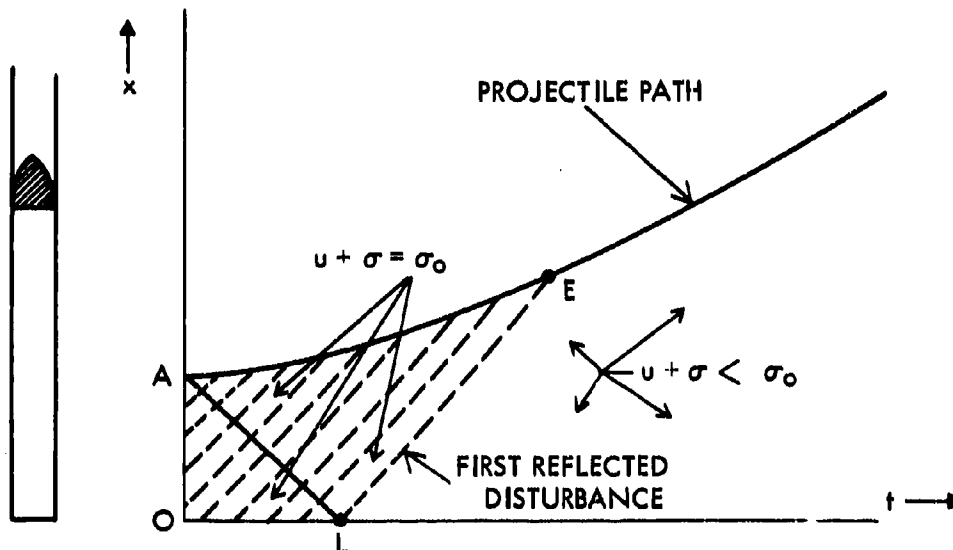
The region A-O-L-E is termed a "simple wave" region. It occurs because all the u + a characteristics within it extend into a region of constant state, in this case a rest state. The entire region is described by the equation

$$u + \sigma = \sigma_0 \quad .$$

It is to be noted that the u + a lines in the region A-L-E are not straight lines but are curved; in the rest region, however, the u + a lines are straight lines with slope equal to a_0 .
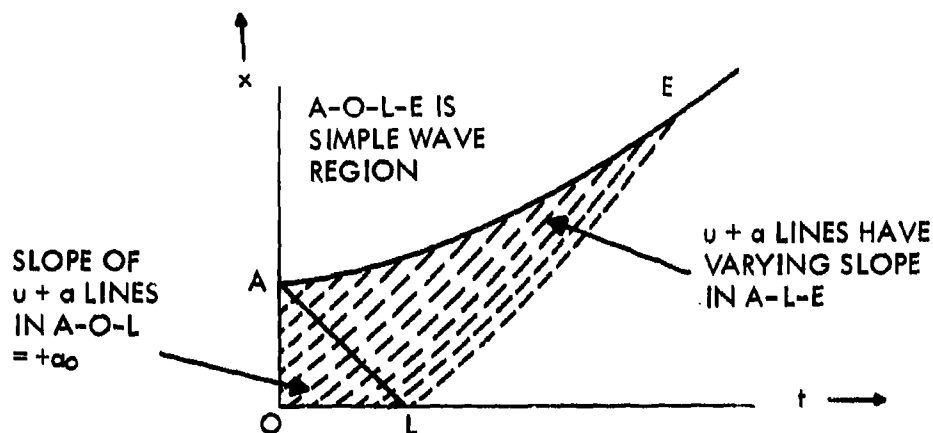
The u - a characteristics each have u - σ equal to a constant along them. For example, for the characteristic B-M in the sketch

$$u - \sigma = u_B - \sigma_B = \text{constant} \qquad (D-2)$$
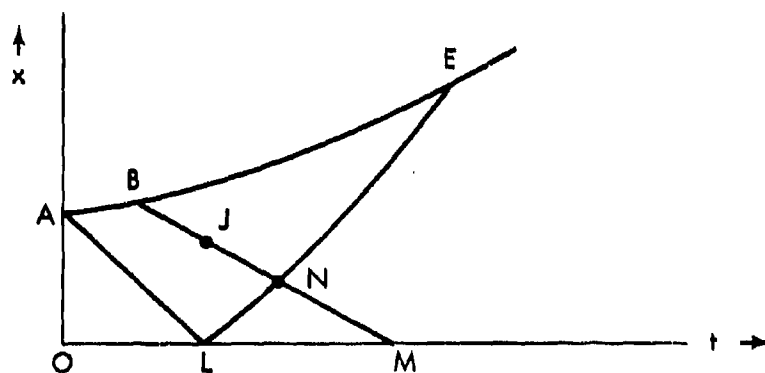
Let the portion of this characteristic B-N which is in the simple wave region be considered; for any point on this portion, e.g., point J, Equation (D-2) becomes

$$u_J - \sigma_J = u_B - \sigma_B = \text{constant} \quad . \qquad (D-3)$$

But since this point is in the simple wave region

$$u_J + \sigma_J \ - \ \sigma_0 \quad . \tag{D-4}$$

From Equations (D-3) and (D-4) it is found that along the u – a line B-N within the simple wave region,

$$u \ = \ constant \ = \ (\sigma_0 + u_B - \sigma_B)/2$$

$$\sigma \ = \ constant \ = \ [\sigma_0 - (u_B - \sigma_B)]/2$$

and, hence, the other thermodynamic properties a , p , ρ , etc., are each constants. The slope "u – a" is therefore a constant. Thus, the line B-N is a straight line. By the same argument all the u – a lines originating at the projectile are straight lines within the simple wave region.
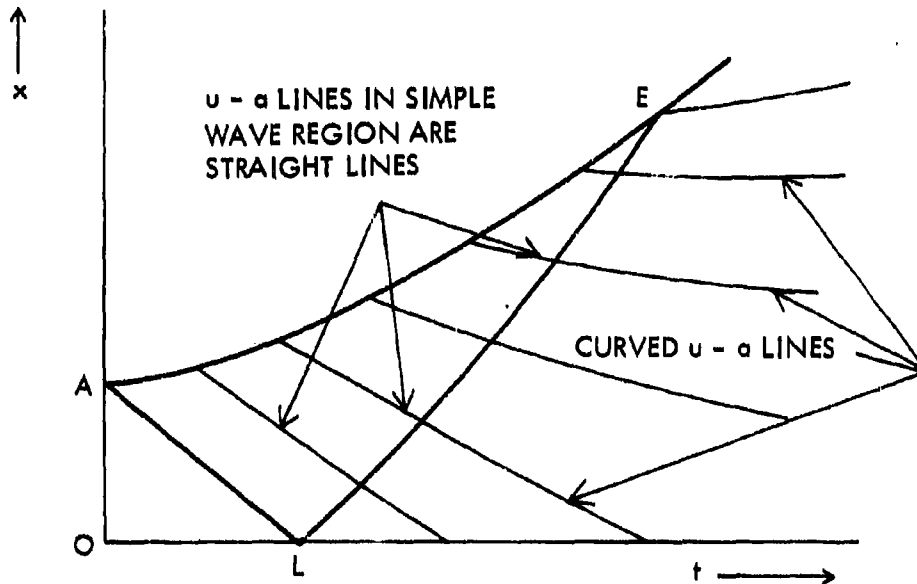
APPENDIX E

The Numerical Procedure to Determine
The Behavior in a PP Gun with $D_0/D_1 = 1$

The following equations will be employed

$$\frac{\partial}{\partial t}(u + \sigma) + (u + a)\frac{\partial}{\partial x}(u + \sigma) = 0 \tag{E-1}$$

$$\frac{\partial}{\partial t}(u - \sigma) + (u - a)\frac{\partial}{\partial x}(u - \sigma) = 0 \tag{E-2}$$

$$\frac{du_p}{dt} = \frac{A}{M}p_p \tag{E-3}$$

$$p = p(\rho) \text{ for the given entropy} \tag{E-4}$$

$$a = a(\rho) \text{ for the given entropy} \tag{E-5}$$

$$\sigma = \sigma(p) \text{ for the given entropy} . \tag{E-6}$$

The method used to obtain the last three isentropic relations from real gas thermo-dynamics data is discussed in Reference 5; these three relations are in graphical form. An x-t diagram is employed as a visual aid in the solution. The procedures outlined in (i) and (iii) below are essentially those described by Heybey[3], for a Noble-Able gas. (See also Foa[56] and Rudinger[91]).

(i) *Determining the conditions at an unknown point within the characteristic net*

It is assumed that the characteristic lines are composed of chains of connected straight segments; these straight segments, which connect points of the characteristic net in the x-t plane, replace the actual curved lines. (However, the solution may be made as accurate as desired by the use of smaller steps.) Thus, the characteristic net consists of quadrilaterals, the sides of which are parts of characteristic lines. If the conditions (u, σ, x, t, p, a) at the points A and B (see sketch) which are diagonally opposite corners of one of these quadrilaterals are known, then the conditions at point C, one of the other two corners of the quadrilateral, can be determined from the equations listed above.

By characteristic equations (E-1) and (E-2)

$$u_C - \sigma_C = u_A - \sigma_A , \qquad u_C + \sigma_C = u_B + \sigma_B .$$
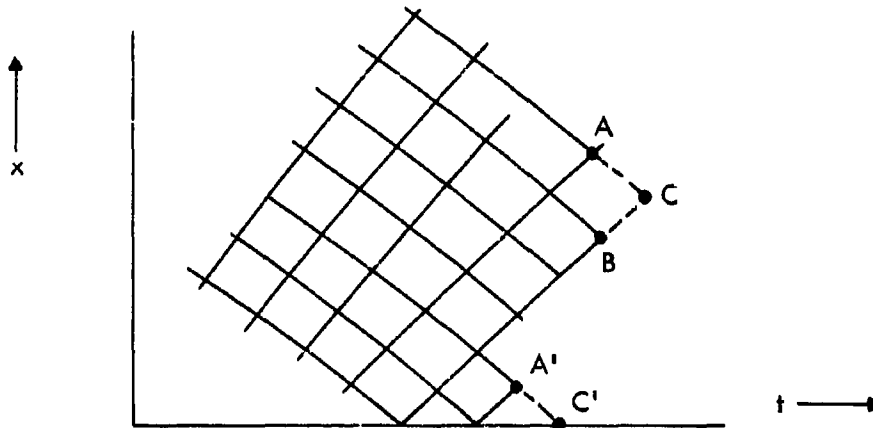
Therefore,

$$u_C = \tfrac{1}{2}(u_B + u_A + \sigma_B - \sigma_C)$$

$$\sigma_C = \tfrac{1}{2}(u_B - u_A + \sigma_B + \sigma_A) \quad . \tag{E-7}$$

By Equations (E-4), (E-5), and (E-6) the velocity of sound and the pressure at C, a_C and p_C, may be determined from σ_C. The slopes of lines A-C and B-C are taken as arithmetic means of the slopes at A and C, and the slopes at B and C:

$$(\text{slope})_A = S_A = \tfrac{1}{2}[(u_A - a_A) + (u_C - a_C)]$$

$$S_B = \tfrac{1}{2}[(u_B + a_B) + (u_C + a_C)] \quad .$$

Then the straight lines through A and B intersect at C with coordinates

$$x_C = \frac{S_A(x_B - S_B t_B) - S_B(x_A - S_A t_A)}{S_A - S_B}$$

$$t_C = \frac{(x_B - S_B t_B) - (x_A - S_A t_A)}{S_A - S_B} \quad . \tag{E-8}$$

Thus, all the conditions (u, σ, x, t, p, a) at C are known from the conditions of the two points A and B.

A special case of the above is when the unknown point (here C') is on the t-axis (at the breech). In this case conditions at only one adjacent point need to be known. From then $u_{C'} = 0$, $x_{C'} = 0$, and

$$\sigma_{C'} = (\sigma_{A'} - u_{A'})$$

$$S_{A'} = \tfrac{1}{2}(u_{A'} - a_{A'} - a_{C'}) \tag{E-9}$$

$$t_{C'} = t_{A'} - \frac{x_{A'}}{S_{A'}} \quad .$$

(11) *Determining the point at which the first reflected*
     wavelet reaches the projectile

By use of the simple wave equations, the piston path can be obtained until the
first reflected wavelet reaches the projectile. However, this point is unknown and
can be found by the procedure described here.
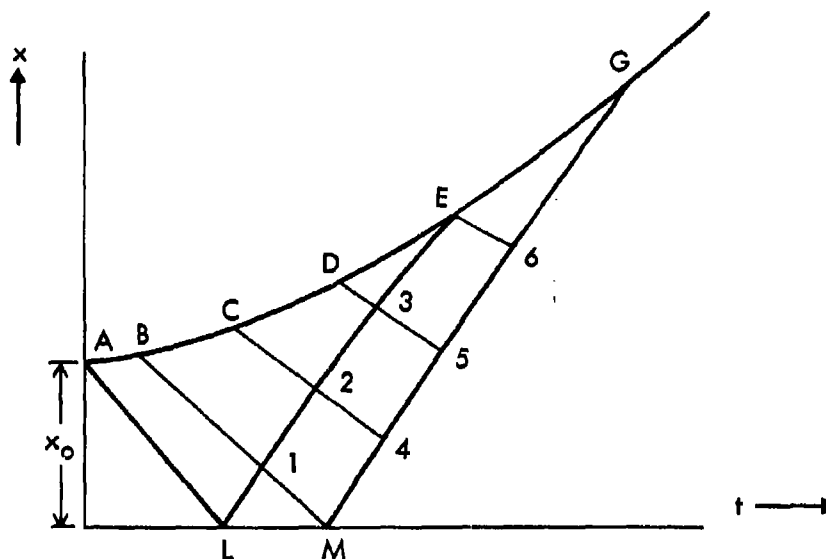
Point E in the sketch, at which the first reflected wavelet reaches the projectile,
is the intersection of the projectile path as determined by the simple wave equations
and the first wavelet A-L-E. From point A (the initial projectile position, $x = -x_0$)
the first wavelet's path to the breech may be drawn immediately, since it is a straight
line of slope equal to $u - a = 0 - a_0 = -a_0$. The intersection of the first wavelet
with the breech is at time equal to x_0/a_0 ; all the conditions at L are known

$$\sigma = \sigma_0 , \quad u = 0 , \quad x = -x_0 , \quad t = x_0/a_0 , \quad a = a_0 .$$

Now a point B on the projectile path adjacent to A should be selected[*]. The conditions
at B are known from the simple wave equations and Equations (E-4) through (E-6).
Therefore, the conditions at 1 (the intersection of the reflected wavelet ascending
from L and the wavelet descending from B) may be obtained by the method described
above in (1). Similarly, from C, a known point on the projectile path adjacent to B,
and from point 1, the conditions at point 2 may be calculated. In this manner the
reflected first wavelet is continued until it intersects the projectile path (at E).

---

[*] The spacing of point B from A (and C from B, etc.) is such that any smaller spacing would
yield the same results within the accuracy desired.

(iii) Determining the projectile path after the first reflection

The characteristic net must be continued in a step-by-step fashion to obtain the piston path and gas behavior after the first reflection point at E. Point M at the breech is obtained by the method outlined in (i). Point 4 is obtained from the conditions at 2 and M, and so on up the reflected wavelet M-4-5-6. From the conditions at point E on the projectile path and from the point 6, the desired point G may be obtained by an iterative process. The iterative process demands the following:

(a) Point G is the intersection of a line through E whose slope is the average of the slopes at E and G (on the line E-G), and a line through 6 whose slope is the average of the slopes at 6 and G (on the line 6-G). Thus,

$$\text{slope E-G} = s_E = 1/2\,(u_E + u_G)$$

$$\text{slope 6-G} = s_6 = 1/2\,(u_6 + a_6 + u_G + a_G)$$

(b) Newton's law applied to the projectile is satisfied in the interval of time between E and G. Thus,

$$\frac{u_G - u_E}{t_G - t_E} = \frac{A}{M}\,(p_G + p_E)\,(\tfrac{1}{2}) \quad .$$

The iterative process is illustrated below.

As a first approximation the time at point G, $t_G^{(1)}$, is obtained as the intersection of a line from point E with slope u_E and of a line from point 6 of slope $u_6 + a_6$; $a_G^{(1)}$ is provisionally assumed equal to a_E and the first approximation of the velocity at point G is found from

$$u_G^{(1)} = u_E + (t_G^{(1)} - t_E)\,(p_E)\,\frac{A}{M} \quad .$$

Then

$$s_E^{(2)} = \frac{u_E + u_G^{(1)}}{2}$$

$$s_6^{(2)} = \frac{(u_6 + a_6) + (u_G^{(1)} + a_G^{(1)})}{2}$$

$$t_G^{(2)} = \frac{(x_6 - s_6^{(2)} t_6) - (x_E - s_E^{(2)} t_E)}{s_E^{(2)} - s_6^{(2)}}$$

$$u_G^{(2)} = u_E + (t_G^{(2)} - t_E)\,\frac{p_E + p_G^{(1)}}{2}\,\frac{A}{M}$$

$$\sigma_G^{(6)} = (u_6 + \sigma_6) - u_G^{(2)}$$

$p_G^{(2)}$ and $a_G^{(2)}$ are obtained from Equations (E-5) and (E-6);

$$s_E^{(3)} \;=\; \frac{u_E + u_G^{(2)}}{2}\,, \qquad s_6^{(3)} \;=\; \frac{(u_6 + a_6) + (u_G^{(2)} + a_G^{(2)})}{2}$$

and so on. The process is quickly converging. If a counter-pressure is assumed acting on the projectile, the procedure may be slightly altered to account for this.

APPENDIX F

The Classical Approximate Solutions to the
Internal Ballistics Problem

(1) *Lagrange's Method of Assuming the Density to be a*
    Function of Time

As previously mentioned, the classical "Lagrange Problem of Internal Ballistics"
is the problem of what occurs when a projectile initially at rest in a constant cross-
sectional area gun is propelled by a propellant which burns instantaneously. The
process is considered as one-dimensional, frictionless, and adiabatic. Lagrange[49]
initiated the study of this problem in 1793, when he presented an approximate solution
to the problem. He assumed that the propellant gas density ρ was a function only of
time and not of distance x, i.e.,

$$\rho = \rho(t) \quad . \tag{F-1}$$

With this assumption, by use of the continuity and momentum equations, the following
relations are derived (as shown, for example, by Corner[16]) for the $D_0/D_1 = 1$ gun .

$$\frac{u}{u_p} = \frac{x + x_0}{x_p + x_0} \tag{F-2}$$

a linear velocity distribution.

$$\frac{p}{p_p} = 1 + \frac{G}{2M} - \frac{G}{2M} \left(\frac{x + x_0}{x_p + x_0} \right)^2 \tag{F-3}$$

a parabolic pressure distribution.

$$\frac{p_{x=-x_0}}{p_p} = 1 + \frac{G}{2M} \tag{F-4}$$

a constant ratio between pressure at the breech and projectile.

$$\frac{\bar{p}}{p_p} = 1 + \frac{G}{3M} \tag{F-5}$$

$$\text{kinetic energy of gas} = \frac{1}{3} \left(\frac{1}{2} G u_p^2 \right) \tag{F-6}$$

$$u_p^2 = \frac{2Ga_0^2}{\gamma M (\gamma - 1)} \left[1 - \left(\frac{x_0}{x_p + x_0} \right)^{\gamma - 1} \right] \quad . \tag{F-7}$$

Thus, the assumption $p - p(t)$ leads to the condition of a parabolic pressure distribution, with pressure ratio for the gas at the breech to that at the projectile a constant; obviously, this is not true for the Lagrange problem at the start when the pressure is uniform in the chamber. It is also noted that the projectile velocity becomes infinite for infinite G/M and infinite travel; this is, as known from the discussions of the main text, not true.

Nevertheless, this approximation accounts somewhat for the gas inertia, and for the case of low G/M (and, hence, low velocity, and many reflections of the first disturbance from the projectile) is a convenient approximation.

(2) The Special Solution of Pidduck and Kent

After Lagrange had initiated the study of the "Lagrange Problem", Hugoniot[50] extended Riemann's theory of waves of finite amplitude and applied it to the problem; he solved it to the point when the first expansion disturbance shed by the projectile reached the breech. Gossot and Louisville went still further and followed the first expansion disturbance after it had been reflected from the breech back to the projectile. The culmination of this method of attack (which did not use the method of characteristics) was the complete solution as far as the first disturbance traveling back and toward the breech for the third time by Love[51] in 1921.

Love replaced the system of hyperbolic quasi-linear partial differential equations which describe the problem by a single partial differential equation of second order for one single dependent variable and solved it separately for each wavelet. His solution contained lengthy and involved computations and was valid only for a Noble-Abel gas (with isentropic relation $p(v-b)^{\gamma} = $ constant) whose ratio of specific heats was of the form

$$\gamma = \frac{2n + 1}{2n - 1}$$

where n is an integer.

Pidduck, noted, from the results he had calculated with Love's equations, that the ratio of the breech pressure to the pressure of the gas directly behind the projectile oscillated as shown in the sketch.

180
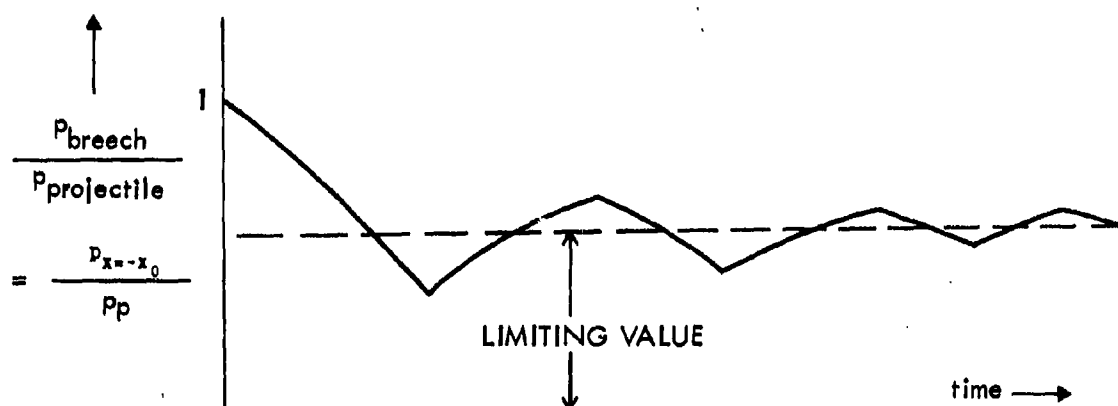
This oscillation is a result of the lowering of the pressure occurring as the first
disturbance reflects back and forth between breech and projectile. Pidduck found that
the oscillations damped out and that the pressure ratio approached a certain limiting
value. He then deduced a "special solution" to the governing differential equations
which indeed did yield the condition that the ratio p_B/p_p is a constant, not only in
a limit but at all times. This solution, an analytic one, did not satisfy the initial
conditions of the Lagrange problem; the initial conditions for the special solution
were a non-uniform distribution of density and pressure. Pidduck and all later
investigators have suspected, but not proved, that the accurate solution to the
Lagrange problem approached the special solution in the limit of large travel.

The special solution has also been derived by Kent[52] and by Vinti and Kravitz[53].
(See also Corner[16]). It is often referred to as "The Pidduck-Kent Special Solution"
or "Pidduck Special Solution". The essential results are as follows.

$$\frac{u}{u_p} = \frac{x + x_0}{x_p + x_0}$$

(F-8)

$$\frac{p_{x=-x_0}}{p_p} = (1 - \tilde{a}_0)^{-\frac{\gamma}{\gamma-1}}$$

(F-9)

or, for a $\gamma = 1$ gas,

$$\frac{p_{x=-x_0}}{p_p} = e^{\alpha_0}$$

(F-10)

where $\tilde{a}_0$ and α_0 depend on G/M and γ, as shown below and plotted in Figure 44.

$$\frac{G}{M} = \frac{2\gamma}{\gamma - 1} \tilde{a}_0 (1 - \tilde{a}_0)^{-\frac{\gamma}{\gamma-1}} \int_0^1 (1 - \tilde{a}_0\mu^2)^{\frac{1}{\gamma-1}} d\mu$$

(F-11)

or, for a $\gamma = 1$ gas,

$$\frac{G}{M} = 2\alpha_0 e^{\alpha_0} \int_0^1 e^{-\alpha_0\mu^2} d\mu .$$

(F-12)

For small G/M, $\tilde{a}_0$ may be approximated as

$$\tilde{a}_0 \simeq \frac{G(\gamma - 1)}{M(2\gamma)} \left\{ 1 - \frac{3\gamma - 1}{6\gamma}\frac{G}{M} + \left[\frac{1}{4} - \frac{1}{12\gamma} + \frac{1}{180\gamma^2}\right]\left(\frac{G}{M}\right)^2 + \ldots \right\}$$

(F-13)

The projectile velocity is obtained as

$$
\left.\begin{aligned}
u_p &= \frac{2a_0\sqrt{\tilde{a}_0}}{\gamma - 1}\left[1 - \left(\frac{x_0}{x_p + x_0}\right)^{\gamma-1}\right]^{\frac{1}{2}} \\[2mm]
&= \frac{2a_0\sqrt{\tilde{a}_0}}{\gamma - 1}\left[1 - \left(1 + \frac{\gamma\bar{x}_p}{G/M}\right)^{1-\gamma}\right]^{\frac{1}{2}}
\end{aligned}\right\}
\tag{F-14}
$$

and, for $\gamma = 1$,

$$
\begin{aligned}
u_p &= 2a_0\sqrt{\alpha_0}\left(\log_e \frac{x_p + x_0}{x_0}\right)^{\frac{1}{2}} \\[2mm]
&= 2a_0\sqrt{\alpha_0}\left[\log_e\left(1 + \frac{x_p}{G/M}\right)\right]^{\frac{1}{2}}
\end{aligned}
\tag{F-15}
$$

where

$$
\bar{x}_p = \frac{p_0 A_1 x_p}{M a_0^2} \quad .
\tag{F-16}
$$

Thus Figure 44 may be used in conjunction with Equations (F-14), (F-15), and (F-16) to to calculate the projectile velocity for any gun, even a chambered gun, although the solution was derived for a $D_0/D_1 = 1$ gun. Then, for the chambered gun, x_0 should be replaced by $x_0 A_0/A_1$ in the above equations.

The above results may be deduced for a $D_0/D_1 = 1$ gun with a covolume propellant gas, and have been applied as an approximation to even the case of a chambered gun with a covolume propellant gas. In the chambered covolume case the sound velocity a_0 in all the equations above should be replaced by $\sqrt{\gamma R T_0} = \sqrt{\gamma p_0(v_0 - b)}$ and x_0 should be replaced by $(A_0 x_0 - bG)/A_1$.

It is found that, when G/M becomes infinite, $\tilde{a}_0$ approaches one. In this case, for the $D_0/D_1 = 1$ gun, the projectile velocity becomes, from Equation (F-14),

$$
u_p = \frac{2a_0}{\gamma - 1}\left[1 - \left(\frac{x_0}{x_p + x_0}\right)^{\gamma-1}\right]^{\frac{1}{2}}
\tag{F-17}
$$

which, for infinite travel distance, becomes equal to $2a_0/(\gamma - 1)$; this is, as it should be, the escape velocity for a $D_0/D_1 = 1$, $x_0 = \infty$ gun*.

---

* However, the same result for escape velocity is arrived at for a chambered $x_0 = \infty$ gun, for which it is incorrect.

182

The special solution applies to the $D_0/D_1 = 1$ gun in which initially there is a pressure gradient in the propellant gas; the Lagrange ballistics problem (the PP gun problem), however, assumes no gradients initially. Pidduck and later investigators suspected, but never proved, that the special solution approaches the acurate solution the limit of large travel. The results of calculations made on the electronic computing machines (see Section 28) seem to confirm this suspicion.

The computed results indicate that, indeed, the special solution is an amazingly good approximation for the finite chamber length PP gun for any D_0/D_1 ; this is true for small projectile travel as well as large travel. A comparison of the special solution results with the computed results for the PPIG gun is shown in Figure 21.

APPENDIX G

Equations for a Shock Moving into a Gas
at Rest in a Closed End Cylinder

Let a shock moving into an ideal gas at rest be considered.
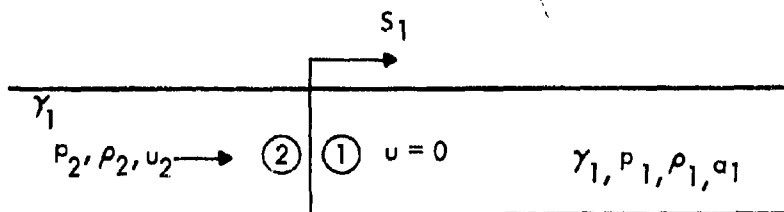
The equations describing this situation are summarized below (see, for example, Glass[110, 112] or Lukasiewicz[114]).

$$\frac{p_2}{p_1} = 1 + \frac{\gamma_1(\gamma_1 + 1)}{4}\left(\frac{u_2}{a_1}\right)^2 + \frac{\gamma_1 u_2}{a_1}\sqrt{1 + \left(\frac{\gamma_1 + 1}{4}\right)^2\left(\frac{u_2}{a_1}\right)^2} \tag{G-1}$$

$$= \frac{2\gamma_1}{\gamma_1 + 1}\left(\frac{S_1}{a_1}\right)^2 - \frac{\gamma_1 - 1}{\gamma_1 + 1} \tag{G-2}$$

$$\frac{\rho_2}{\rho_1} = \frac{1 + \dfrac{\gamma_1 + 1}{\gamma_1 - 1}\dfrac{p_2}{p_1}}{\dfrac{\gamma_1 + 1}{\gamma_1 - 1} + \dfrac{p_2}{p_1}} \tag{G-3}$$

$$= \left(\frac{S_1}{a_1}\right)^2 \bigg/ \left[\frac{\gamma_1 - 1}{\gamma_1 + 1}\left(\frac{S_1}{a_1}\right)^2 + \frac{2}{\gamma_1 + 1}\right] \tag{G-4}$$

$$\left(\frac{a_2}{a_1}\right)^2 = \frac{T_2}{T_1} = \frac{p_2/\rho_2}{p_1/\rho_1} \tag{G-5}$$

$$\frac{u_2}{a_1} = \frac{2}{\gamma_1 + 1}\frac{\left(\dfrac{S_1}{a_1}\right)^2 - 1}{\dfrac{S_1}{a_1}} \tag{G-6}$$

$$= \frac{\dfrac{2}{\gamma_1 - 1}\left[p_2/p_1 - 1\right]}{\sqrt{\dfrac{2\gamma_1}{\gamma_1 - 1}\left[\dfrac{\gamma_1 + 1}{\gamma_1 - 1}\dfrac{p_2}{p_1} + 1\right]}} \tag{G-7}$$

$$\frac{u_2}{a_2} = \frac{\dfrac{2}{\gamma_1 - 1}\left[p_2/p_1 - 1\right]}{\sqrt{\dfrac{2\gamma_1}{\gamma_1 - 1}\dfrac{p_2}{p_1}\left[\dfrac{p_2}{p_1} + \dfrac{\gamma_1 + 1}{\gamma_1 - 1}\right]}} \tag{G-8}$$

$$\frac{u_2}{S_1} = \frac{2}{\gamma_1 + 1}\left[1 - \left(\frac{a_1}{S_1}\right)^2\right] \tag{G-9}$$

or

$$S_1 = \frac{\gamma_1 + 1}{4}u_2\left\{1 + \sqrt{1 + \left[4a_1/(\gamma_1 + 1)u_2\right]^2}\right\} \quad . \tag{G-10}$$

If the shock is a strong one (i.e., $p_2/p_1 \gg 1$, $s_1/a_1 \gg 1$) these equations become

$$\frac{p_2}{p_1} \simeq \frac{\gamma_1(\gamma_1 + 1)}{2}\left(\frac{u_2}{a_1}\right)^2 \tag{G-11}$$

$$\simeq \frac{2\gamma_1}{\gamma_1 + 1}\left(\frac{S_1}{a_1}\right)^2 \tag{G-12}$$

$$\frac{\rho_2}{\rho_1} \simeq \frac{\gamma_1 + 1}{\gamma_1 - 1} \tag{G-13}$$

$$\frac{T_2}{T_1} \simeq \frac{\gamma_1 - 1}{\gamma_1 + 1}\frac{p_2}{p_1} \tag{G-14}$$

$$\simeq \frac{\gamma_1(\gamma_1 - 1)}{2}\left(\frac{u_2}{a_1}\right)^2 \tag{G-15}$$

$$\frac{u_2}{a_1} \simeq \frac{2}{\gamma_1 + 1}\frac{S_1}{a_1} \tag{G-16}$$

$$\simeq \sqrt{\frac{2p_2}{\gamma_1(\gamma_1 + 1)p_1}} \tag{G-17}$$

$$\frac{u_2}{a_2} \simeq \sqrt{\frac{2}{\gamma_1(\gamma_1 - 1)}} \tag{G-18}$$

$$\frac{u_2}{S_1} \simeq \frac{2}{\gamma_1 + 1} \quad . \tag{G-19}$$

When the shock reaches the end of the tube it is reflected as shown in the sketch.
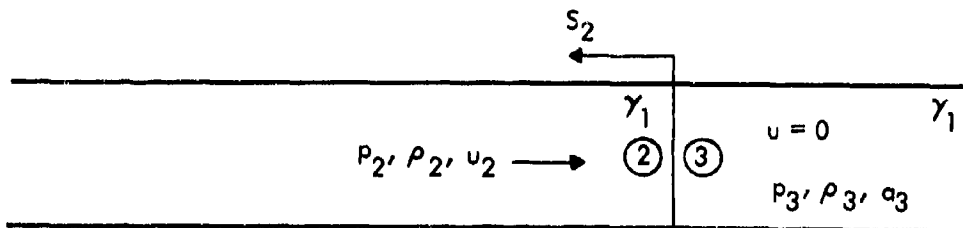
By superimposing the velocity u_2 to the left, this becomes the case of a shock moving into a gas at rest.
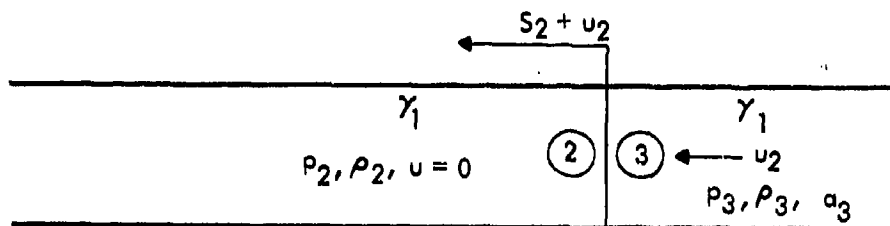
The following equations apply to this reflected case:

$$\frac{p_3}{p_2} = \frac{\left(\dfrac{\gamma_1 + 1}{\gamma_1 - 1} + 2\right)\dfrac{p_2}{p_1} - 1}{\dfrac{p_2}{p_1} + \dfrac{\gamma_1 + 1}{\gamma_1 - 1}} \qquad (G\text{-}20)$$

$$\frac{S_2}{a_3} = \sqrt{\frac{\dfrac{\gamma_1 + 1}{\gamma_1 - 1}\dfrac{p_2}{p_1} + 1}{\dfrac{2\gamma_1}{\gamma_1 - 1}}} \qquad (G\text{-}21)$$
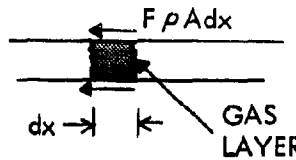
$$\frac{\rho_3}{\rho_2} = \frac{1 + \dfrac{\gamma_1 + 1}{\gamma_1 - 1}\dfrac{p_3}{p_2}}{\dfrac{\gamma_1 + 1}{\gamma_1 - 1} + \dfrac{p_3}{p_2}} \qquad (G\text{-}22)$$

$$\frac{T_3}{T_2} = \frac{p_3/\rho_3}{p_2/\rho_2} \qquad (G\text{-}23)$$

APPENDIX H

The One-Dimensional Unsteady Characteristic Equations
for the Case of Gas-Wall Friction and Heat Transfer

Here is irreversibility and inhomogeneity introduced by the gas-wall friction and heat transfer are assumed to be of a magnitude such that p, ρ, s, u, etc., may still be defined for each gas layer at position x and time t. Also, it is assumed that the second law equation, $Tds = du + pdv$, is valid within the gas layer. Then, with F the gas-wall friction force per unit mass, the force equation for the gas layer becomes

$$\frac{\partial u}{\partial t} + u \frac{\partial u}{\partial x} = -\frac{1}{\rho} \frac{\partial p}{\partial x} - F \quad . \tag{H-1}$$

The continuity equation and the gas law are

$$u \frac{\partial \rho}{\partial x} + \rho \frac{\partial u}{\partial x} + \frac{\partial \rho}{\partial t} = 0 \tag{H-2}$$

$$p = p(\rho, s) \quad . \tag{H-3}$$

These equations may be manipulated to yield the following characteristics equations:

$$\frac{Du}{Dt} \pm \frac{1}{a\rho} \frac{Dp}{Dt} = \pm \frac{1}{a\rho} \left(\frac{\partial p}{\partial s}\right)_\rho \left(\frac{ds}{dt}\right) - F \tag{H-4}$$

where a is the sound speed and D/Dt is defined as

$$\frac{D}{Dt} \equiv \frac{\partial}{\partial t} + (u \pm a) \frac{\partial}{\partial x} \tag{H-5}$$

and d/dt is

$$\frac{d}{dt} \equiv \frac{\partial}{\partial t} + u \frac{\partial}{\partial x} \quad . \tag{H-6}$$

To obtain the entropy change for each gas layer, use is made of the first law equation applied to the gas layer.

$$\frac{d\left(v + \frac{u^2}{2}\right)}{dt} = -\frac{1}{\rho} \frac{\partial(pu)}{\partial x} + \dot{q} \tag{H-7}$$

where v is internal energy and $\dot{q}$ is the rate of heat transfer into the layer per unit mass. The second law applied to the gas layer is

$$T \frac{ds}{dt} = \frac{dv}{dt} - \frac{p}{\rho^2} \frac{d\rho}{dt} \quad .$$

(H-8)

Equations (H-1), (H-2), (H-7), and (H-8) may be combined to yield

$$T \frac{ds}{dt} = Fu + \dot{q}$$

(H-9)

which is Equation (39-6) of the text.

APPENDIX I

The Equivalence of the Ideal and the Abel Equations of State in Application to the Lagrange Ballistic Problem

$$(D_0/D_1 = 1, \ x_0 = \infty)$$

In Reference 54, Heybey discusses the significant parameters of the Lagrange Ballistic Problem. This classical internal ballistics problem is the problem of what occurs when a projectile initially at rest *in a constant cross-sectional area gun* is propelled by a propellant which burns instantaneously (thus initially establishing a uniform high pressure gas behind the projectile). This process is considered as one dimensional, frictionless, and adiabatic. Heybey demonstrates that, for a given ratio of propellant gas mass to projectile mass (G/M) and a given ratio of specific heats (γ) the dimensionless projectile motion is the *same* function of dimensionless time for the Abel gas as for the ideal gas. However, the characteristic net (the interior of which must be used to obtain the behavior of the *gas* behind the projectile) is different for the two cases in the Eulerian coordinate system which Heybey uses; a new characteristic net must be calculated with the Abel equation of state for each value of the covolume (see Figure 6, Reference 54).

It will be shown here that if Lagrangian coordinates are employed to solve the Lagrange problem, a seemingly natural choice, the use of the Abel equation of state is equivalent to that of the ideal equation of state; the two cases become one w   one characteristic net.

It can be shown (see Courant and Friedrich[15]) that in Lagrangian coordinates the characteristic equations describing the isentropic unsteady one-dimensional flow are

$$\frac{\partial}{\partial t} (u \pm \sigma) \pm k \frac{\partial}{\partial H} (u \pm \sigma) = 0 \qquad (I-1)$$

where $H = \int_{x(0,t)}^{x(H,t)} \rho \, dx$ (the mass per unit area of gas from a given point in the flow to the breech of the gun) and k is the acoustic impedance of the gas, ρa. The dimensional variables become dimensionless by the following transformations:

$$
\begin{aligned}
\bar{u} &= \frac{(\gamma - 1)u}{2\sqrt{\gamma RT_0}}, & \bar{\sigma} &= \frac{(\gamma - 1)\sigma}{2\sqrt{\gamma RT_0}}, & \bar{k} &= \frac{2}{(\gamma - 1)} \frac{\sqrt{\gamma RT_0}}{p_0} k \\[2ex]
\bar{x} &= \frac{p_0 A x}{G\gamma RT_0 [2/(\gamma - 1)]^2}, & \bar{a} &= \frac{(\gamma - 1)a}{2\sqrt{\gamma RT_0}}, & \bar{p} &= \frac{p}{p_0} \\[2ex]
\bar{t} &= \frac{p_0 A t (\gamma - 1)}{2G\sqrt{\gamma RT_0}}, & \bar{\rho} &= \left(\frac{2}{\gamma - 1}\right)^2 \frac{\gamma RT_0 \rho}{p_0}; & \bar{H} &= \frac{HA}{G}
\end{aligned}
\qquad (I-2)
$$

With the use of (I-2) the characteristic equations become

$$\frac{\partial}{\partial \bar{t}} (\bar{u} \pm \bar{\sigma}) \pm \bar{k} \frac{\partial}{\partial H} (\bar{u} \pm \bar{\sigma}) = 0 \quad . \tag{I-3}$$

Newton's force law applied to the projectile becomes

$$\frac{d\bar{u}}{d\bar{t}} = \frac{G}{M} \bar{p} \quad . \tag{I-4}$$

The isentropic law yields, for both the ideal gas and for the Abel gas, the following relations:

$$\bar{k} = \frac{2\gamma}{\gamma - 1} \bar{p}^{\frac{(\gamma + 1)}{2\gamma}}$$

$$\bar{\sigma} = \bar{p}^{\frac{(\gamma - 1)}{2\gamma}} \quad . \tag{I-5}$$

The initial conditions for the Lagrange problem are

$$\left.\begin{array}{l} \bar{H} = 1 \ , \ \bar{t} = 0 \ \text{ at the projectile} \\[2mm] \bar{H} = 0 \ , \ \bar{t} = 0 \ \text{ at the breech} \end{array}\right\} \quad . \tag{I-6}$$

The entire behavior of the gas and projectile are determined by the dimensionless equations (I-3) through (I-6). A characteristic net on the $\bar{H}$-$\bar{t}$ plane can be calculated from the equations. Since these equations describe both cases (the ideal and Abel gas cases), only one solution for a given G/M and γ is necessary. The ideal and Abel gases are equivalent in this system of coordinates in application to the Lagrange Ballistic Problem.

PROJECTILE PATH

190
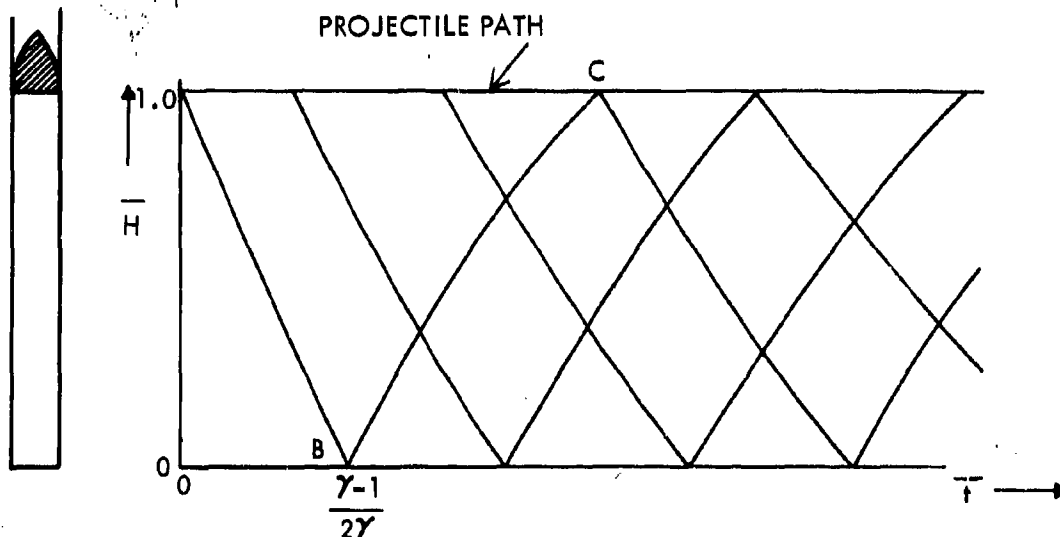
A characteristic net in the $\bar{H}$-$\bar{t}$ plane for the Lagrange problem is shown in the previous sketch.

It is interesting to note that the equation for the first reflected impulse (B-C) can be obtained analytically. This relation is

$$\bar{H} = \left[1 + \frac{2\gamma}{\gamma + 1}\frac{M}{G}\right]\left[1 - \frac{1 + \dfrac{\gamma + 1}{2\gamma}\dfrac{G}{M}}{1 + \dfrac{\gamma + 1}{\gamma - 1}\dfrac{G}{M}\bar{t}}\right] \, . \tag{I-7}$$

A comparison of the two propellants initially is shown in the sketch.
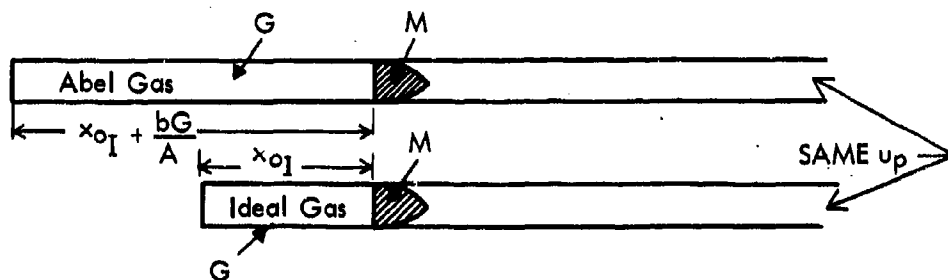
It is important to remember that, with a *chambered* gun, the performance of the Abel and ideal gases are no longer equivalent. Because of the increased enthalpy (or $\int dp/\rho$) of the Abel gas relative to the ideal gas, the Abel gas gives better performance for the same G/M.

APPENDIX J

Equations for the Thermodynamic Properties
of an Isentropically Expanding Ideal Gas

For an ideal (or perfect) gas the thermal equation and isentropic equation are, respectively,

$$p = \rho RT = \rho \frac{\bar{R}}{M} T \tag{J-1}$$

$$p = \rho^\gamma (p_0/\rho_0^\gamma) \tag{J-2}$$

where the subscript "0" indicates an initial state from which the gas expands. From these equations the following relations may be derived for the isentropic expansion of the ideal gas in terms of the Riemann Function σ (defined as $d\sigma = (dp/a\rho)_s$):

$$a = (\gamma - 1)\sigma/2 \tag{J-3}$$

$$h = a^2/(\gamma - 1) = (\gamma - 1)\sigma^2/4 \tag{J-4}$$

$$p = p_0(\sigma/\sigma_0)^{2\gamma/(\gamma-1)} \tag{J-5}$$

$$\rho = \rho_0(\sigma/\sigma_0)^{2/(\gamma-1)} \quad . \tag{J-6}$$

The expressions for $a\rho$ and ρ as functions of p during the isentropic expansion are

$$a\rho = p_0 \sqrt{\frac{\gamma}{RT_0}} \left(\frac{p}{p_0}\right)^{\frac{\gamma+1}{2\gamma}} = \frac{\gamma p_0}{a_0} \left(\frac{p}{p_0}\right)^{\frac{\gamma+1}{2\gamma}} \tag{J-7}$$

$$\rho = \frac{p_0}{RT_0} \left(\frac{p}{p_0}\right)^{\frac{1}{\gamma}} = \frac{\gamma p_0}{a_0^2} \left(\frac{p}{p_0}\right)^{\frac{1}{\gamma}} \quad . \tag{J-8}$$

192

GENERAL REFERENCES

The number of papers published on the subject of high velocity gas guns within the past twenty years is multi-tudinous. Dr. Glass, in Reference 24, recently has made a survey of constant diameter preburned propellant guns. It is suggested that reviewing the proceedings of the following two symposia, which are each held every year to two years, will quickly familiarize one with the field:

(1) Symposia on Hypervelocity Impact, sponsored by the US Army, US Air Force, and US Navy. The last symposium was held in Tampa, Florida, in November 1964.

(2) Symposia on Hypervelocity Techniques, sponsored by various groups. The last symposium was held in Denver, Colorado, on March 1, 1964.

The predominant number of publications in the field of high-speed guns has been produced by the following Laboratories in the United States:

(1) US Naval Research Laboratory, Washington, DC.

(2) Ames Research Center, NASA, Moffett Field, California.

(3) US Ballistic Research Laboratories, Aberdeen Proving Ground, Maryland.

(4) US Naval Ordnance Laboratory, White Oak, Silver Spring, Maryland.

(5) General Motors Defense Research Laboratories, General Motors Corporation, Santa Barbara, California.

(6) Arnold Engineering Development Center, Arnold Air Force Station, Tennessee.

(7) Denver Research Institute, University of Denver, Denver, Colorado.

(8) AVCO Corporation, Wilmington, Massachusetts and Everett, Massachusetts.

(9) Armour Research Foundation, Illinois Institute of Technology, Chicago, Illinois.

In addition, the following Laboratories outside of the United States have been active in this field:

(1) Canadian Armament Research and Development Establishment, Quebec, Canada.

(2) McGill University, Montreal, Canada.

(3) Royal Armament Research and Development Establishment, Fort Halstead, Kent England.

(4) Institute Franco-Allemand De Recherches De Saint-Louis, France.

(5) LRBA, Vernon, France.

A search of the high-speed gun literature under the names of these Laboratories will uncover much of the publications in the field.

CITED REFERENCES

1. Michels, A.   *The Rapid Expansion of Compressed Gases Behind a Piston.*
   et alii   *The Effect of Molecular Interaction, Part III.* Physica,
                    Vol.20, p.1157, 1954.

2. Seigel, A.E.   *A Study of the Applicability of the Unsteady One-
                    Dimensional Isentropic Theory to an Experimental Gun.*
                    NavOrd Report 2692, July 1952.

3. Heybey, W.   *A Solution of Lagrange's Problem of Interior Ballistics
                    by Means of its Characteristic Lines.* NOLM 10819,
                    March 1950.

4. Slawsky, Z.I.   *The Rapid Expansion of Compressed Gases Behind a Piston.*
   et alii   *The Effect of Molecular Interaction, Part I.* Physica,
                    Vol.20, p.210, 1954.

5. Seigel, A.E.   *The Rapid Expansion of Compressed Gases Behind a Piston.*
                    Doctoral Thesis, University of Amsterdam, January 1952.

6. de Haller, P.   Bulletin Tech. Swisse Romande No.1, 1, 1948, and Sulzer
                    Tech. Rev. No.1, 6, 1945.

7. Guderley, G.   Translation of ZWB, Forschungsbericht No.1744, October
                    1942. NACA TM 1196, December 1948.

8. Shapiro, A.H.   *The Dynamics and Thermodynamics of Compressible Fluid
                    Flow,* Ronald Press, New York, 1953.

9. Seigel, A.E.   *The Effect of the Optimum Chambrage on the Muzzle
                    Velocity of Guns With a Qualitative Description of the
                    Fundamental Phenomena Occurring During Gun Firing.*
                    NavOrd Report 2691, October 1952.

10. Seigel, A.E.   *Results of Chambrage Experiments on Guns with Effectively
    Dawson, V.C.D.   Infinite Length Chambers.* NavOrd Report 3636, April
                    1954.

11. Seigel, A.E.   *The Influence of Chamber Diameter on the Muzzle Velocity
                    of a Gun With an Effectively Infinite Length Chamber.*
                    NavOrd Report 3635, January 1954.

12. von Neumann, I. *A Method for the Numerical Calculation of Hydrodynamic
    Richtmyer, R.D. Shocks.* Journal of Applied Physics, Vol.21, p.232,
                    1932.

13. Richtmyer, R.D. *Difference Methods for Initial Value Problems.*
                    Interscience Publishers, New York, 1957.

194

14. Piacesi, R.   *Computer Analysis of Two-Stage Hypervelocity Model*
    et alii   *Launchers.* NOLTR 62-87, February 1963.

15. Courant, R.   *Supersonic Flow and Shock Waves.* Interscience Publishers,
    Friedrichs, K.O.   New York, 1948.

16. Corner, J.   *Theory of Internal Ballistics of Guns.* Wiley, New York,
                          1950.

17. Smith, F.   *The Development of a Hypersonic Launcher.* ARDE
                          Report (B) 18/58, Fort Halstead.

18. Seigel, A.E.   *Method of Calculating Preburned Propellant Gun
                          Performance with Special Application to Two-Stage Guns.*
                          NOLTR 61-29, June 1961.

19. Michels, A.   *The Rapid Expansion of Compressed Gases Behind a Piston.
    et alii   The Effect of Molecular Interaction, Part II.* Physica,
                          Vol.20, p.223, 1954.

20. Jacobs, S.J.   *ERMA and the Study of Rapid Gas Expansion.* Doctoral
                          Thesis, University of Amsterdam, June 1953.

21. Slawsky, Z.I.   *Comparison Study Between a Microwave Interferometer and
    et alii   an Electrical Contact System for Following the Motion of
                          High-Speed Projectiles.* Review of Scientific Instruments,
                          Vol.30, No.8, p.679-683, August 1959.

22. Ho, L.T.   *Determination of Isentropic Pressure-Density Curves for
    et alii   Argon from a Rapid Dynamic Process.* Physics of Fluids,
                          Vol.4, No.8, August 1961.

23. Seigel, A.E.   *An Experimental Solution to the Lagrange Ballistic
                          Problem.* NavOrd Report 2693, September 1952.

24. Glass, I.I.   *Hypervelocity Launchers. Part I: Simple Launchers.*
                          University of Toronto Institute of Aerophysics, UTIA
                          Review No.22, January 1963.

25. Williams, A.C.   *Propagation of the Effects of Wall Interaction in the
                          Rarefaction Region of Shock Tube Flow.* Lehigh
                          University, Tech. Report No.6, 1955.

26. Seigel, A.E.   *Effect of Gas-Wall Friction and Heat Transfer on the
    Piacesi, R.   Performance of High-Speed Guns.* To be published.

27. Bioletti, C.   *A High Velocity Gun Employing a Shock-Compressed Light
    Cunningham, B.   Gas.* NASA TN D-307, February 1960.

28. Seigel, A.E.   *A Hypervelocity Gun Using a Shock-Compressed Steam-
    Slawsky, Z.I.   Heated Propellant.* NavOrd Report 4345, July 1956.

29. Crozier, W.D.   *High-Velocity, Light-Gas Gun.* Journal of Applied
    Hume, W.   Physics, Vol.28, p.892, 1957.

30. Hunt, F.R.W.   *Internal Ballistics,* Philosophical Library, New York,
    1951.

31. Carriere, P.   *Proceedings of the Seventh International Congress on
    Applied Mechanics,* Vol.3, p.139, 1948.

32. Evans, C.   *Shock Compression of a Perfect Gas.* Journal of Fluid
    Evans, F.   Mechanics, Vol.I, p.399, October 1956.

33. Baer, P.G.   *Experimental and Theoretical Studies on the Interior
    Smith, H.C.   Ballistics of Light Gas Guns.* Sixth Symposium on Hyper-
    velocity Impact, Cleveland, Ohio, August 1963.

34. Stanyukovitch, K.   *Unsteady Motion of Continuous Media.* Pergamon Press,
    London, 1960.

35. Smith, F.   *Theory of a Two-Stage Hypervelocity Launcher to Give
    Constant Driving Pressure at the Model.* RARDE Report
    (B) 5/63. Also Journal of Fluid Mechanics, September
    1963.

36. Winkler, E.H.   *The Constant Acceleration Gas Gun Problem.* NOLTR
    64-111. *The Presentation of the Propellant Flow in a
    Constant Acceleration Gun by the method of Characteristics.*
    NOLTR 64-69. Both to be published.

37. Wilenius, G.P.T.   *The Constant Base Pressure Light Gas Gun.* Third
    et alii   Hypervelocity Techniques Symposium, Denver, Colorado,
    March 1964.

38. Curtis, J.S.   *An Accelerated Reservoir Light Gas Gun.* NASA TN D-1144,
    February 1962.

39. Charters, A.C.   *High Velocity Guns for Free Flight Ranges.* TM 62/207,
    Curtis, J.S.   General Motors Corporation, Defense Research Laboratory,
    1962.

40. Curtis, J.S.   *An Analysis of the Interior Ballistics of the Constant
    Base Pressure Gun.* Third Hypervelocity Techniques
    Symposium, Denver, Colorado, March 1964.

41. Seigel, A.E.   *Theoretical Study of the Effect of the Non-Ideality of
    a Dense Shocktube Driver Gas with Special Reference to
    Non-Uniform Shocktubes.* NavOrd Report 5707, US Naval
    Ordnance Laboratory, November 1957.

42. Bjork, R.L.   *The Atomic-Hydrogen Gun.* Rand Research Memorandum RM-1707,
    1961.

196

43. Hilsenrath, J.
    Beckett, C.W.

Tables of Thermodynamic Properties of Argon-Free Air to 15,000°K. Arnold Engineering Development Center Report, AEDC-TN-56-12, September 1956.

44. Feldman, S

Hypersonic Gas Dynamic Charts for Equilibrium Air. AVCO Research Laboratory, January 1957.

45. Dawson, J.M.
    Slawsky, Z.I.

The Effect of Intermolecular Forces on the Rapid Expansion of a Gas from an Initial Condition of Very High Density and Temperature. Bulletin of the American Physical Society, H3, Washington, DC, 29, 30 April and 1 May 1954.

46. Bridgman, P.W.

The Physics of High Pressure. Bell, London, 1949.

47. Seigel, A.E.

A Convenient and Accurate Semi-Empirical Entropic Equation for Use in Internal Ballistic Calculations. NavOrd Report 2695, February 1953.

48. Anderson, D.E.

Design of Light-Gas Model Launchers for Hypervelocity Research. Arnold Engineering Development Center, AEDC-TDR-62-97, May 1962.

49. Lagrange, J.L.

J. ècole polytech., Vol.21, p.13, 1832.

50. Hugoniot, H.

J. ècole polytech., Vol.58, p.1, 1889.

51. Love, A.E.H.
    Pidduck, R.P.

Philosophical Transactions of the Royal Society, A222, p.167, 1921.

52. Kent, R.H.

Some Special Solutions for the Motion of the Powder Gas. Physics, Vol.7, p.319, 1936.

53. Vinti, J.P.
    Kravitz, S.

Tables for the Pidduck-Kent Special Solution for the Motion of the Powder Gas in a Gun. BRL Report 693, January 1949.

54. Heybey, W.

Significant Parameters for the Expansion of Propellant Gases in an Idealized Gun. NavOrd Report 1582, February 1951.

55. Vasiliu, J.

Analysis of Chambered, Finite Length Hypervelocity Launchers by the Method of Characteristics. A Computer Solution. Republic Aviation Corporation Report No. RAC 1617, July 1963.

56. Zondek, Bernd

A Computing Program for the Interior Ballistics of a Hypervelocity Gun. US Naval Weapons Laboratory, Dahlgren, Virginia, NWL Report No.1743, November 1964. (Also Somes, J. and Herring A. of NWL for programing, coding, etc.).

57. Charters, A.C.   *The Free Flight Range: A Tool for Research in the Physics of High Speed Flight*. "Hypersonic Flow Research", edited by F.R. Riddell. Academic Press, 1962.

58. Foa, J.V.   *Elements of Flight Propulsion*. Wiley, New York, 1960.

59. Lukasiewicz, J.   *Status of Development of Hotshot Tunnels at the AEDC*.
    et alii   Chapter 19, "The High Temperature Aspects of Hypersonic Flow", AGARDograph 68, edited by Wilbur C. Nelson. Pergamon Press, 1964.

60. Lukasiewicz, J.   *The High Temperature Aspects of Hypersonic Flow*, p. 760. AGARDograph 68, Wilbur C. Nelson, Pergamon Press, 1964.

61. Lord, M.E.   *Performance of a 40mm Combustion-Heated Light Gas Gun Launcher*. AEDC-TN-60-176, October 1960.

62. Georgiev, Steven   *Hypervelocity Wake Studies Using an Electrically Heated Gas Gun*. AVCO-Everett Research Laboratory, Research Note 189, 1960.

63. Eckerman, J.   *Performance of a Three Stage Arc Heated Light Gas Gun*.
    McKay, W.L.   Vol. 1, *Proceedings of the Sixth Symposium on Hypervelocity Impact*, Cleveland, Ohio, August 1963.

64. Swift, H.F.   *A Study of Electrically Augmented Gas Guns*. Proceedings of the Seventh Symposium on Hypervelocity Impact, Tampa, Florida, November 1964.

65.   Proceedings of the Seventh Symposium on Hypervelocity Impact, Tampa, Florida, November 1964.

66.   Proceedings of the Second Hypervelocity Impact Symposium, December 1957.

67. Baer, Paul G.   *The Traveling Charge Gun as a Hypervelocity Launching Device*. Proceedings of the Fourth Hypervelocity Impact Symposium, April 1960.

68. Barbarek, L.A.C.   *Armour Research Foundation Traveling Charge Gun*. Proceedings of the Sixth Hypervelocity Impact Symposium, August 1963.

69. Howell, W.G.   *Electrical Augmentation of a Light Gas Hypervelocity*
    et alii   *Projector*. Proceedings of the Second Symposium on Hypervelocity Techniques, Denver, Colorado, March 1962.

70. Kottenstette, J.   *The Traveling Reservoir Light Gas Gun*. Proceedings of
    Howell, W.G.   the Seventh Symposium on Hypervelocity Impact, Tampa, Florida, November 1964.

198

71. Cooley, W.C.
The Shock Plasma Acceleration Technique for Velocity Augmentation. Proceedings of the Seventh Symposium on Hypervelocity Impact, Tampa, Florida, November 1964.

72. Scully, C.N. et alii
Exothermal Gun for Hypervelocity Ballistics Research. Proceedings of the Seventh Symposium on Hypervelocity Impact, Tampa, Florida, November 1964.

73. Kineke, J.H. Holloway, Lee S.
Macro-Pellet Projector with an Air Cavity High Explosive Charge for Impact Studies. BRL Memorandum Report No.1264, 1960.

74. Poulter, T.C.
The Acceleration of Small Particles with High Explosives. Proceedings of the Second Hypervelocity Impact Symposium, December 1957.

75. Kronman, S. Merendino, A.
Inhibited Jet Charge. Proceedings of the Sixth Symposium on Hypervelocity Impact, August 1963.

76. Glass, I.I. et alii
University of Toronto Institute of Aerophysics, UTIA Progress Reports, 1961, 1962, and 1963.

77. Godfrey, C.
Proceedings of the Seventh Symposium on Hypervelocity Impact, Tampa, Florida, November 1964.

78. Lemcke, Bo
An Investigation of the Performance of a Compression Heater for Use with Gun Tunnels or Hypervelocity Launchers.

79. Lukasiewicz, J. et alii
Development of Hypervelocity Range Techniques at AEDC. AEDC-TR-61-9, June 1961.

80. Stephenson, W.B.
Theoretical Light Gas Gun Performance. AEDC-TR-61-1, May 1961.

81. Stephenson, W.B. Anderson, D.E.
Design of a Large Two-Stage Light Gas Model Launcher. AEDC-TR-61-6.

82. Stephenson, W.B. Anderson, D.E.
Performance of Two Stage Light Gas Model Launchers. IAS 30th Annual Meeting, New York, January 1962. Also Aerospace Engineering, August 1962.

83. Charters, A.C. et alii
Development of a Piston-Compressor Type Light Gas Gun for Launching of Free Flight Models at High Velocity. NACA TN 4143, November 1957.

84. Kreyenhagen, K.N. et alii
Special Explosive Projectors. Proceedings of the Sixth Symposium on Hypervelocity Impact, August 1963.

85. Stephenson, W.B.
    Knapp, R.E.
    Performance of a Two-Stage Launcher Using Hydrogen.
    AEDC-TDR-62-32, March 1962.

86. Charters, A.C.
    et alii
    Development of a High-Velocity Free-Flight Launcher –
    The Ames Light-Gas Gun. NACA RM A55G11, December 1955.

87. Shepard, B.M.
    Design and Testing of NOL Hypervelocity Missile Launcher
    and Associated Apparatus. Industrial and Engineering
    Chemistry, 1957.

88. Crozier, W.D.
    High Velocity Gun. US Patent No. 2,872,846, 10 February
    1959.

89. Rinehart, J.S.
    Some Historical Highlights of Hypervelocity Research.
    Proceedings of the Hypervelocity Techniques Symposium,
    Denver, Colorado, October 1960.

90. Slawsky, Z.I.
    Survey of NOL Hyperballistics Research. NOLR 1238,
    May 1959.

91. Rudinger, G.
    Wave Diagrams for Nonsteady Flow in Ducts. Van Nostrand
    New York, 1955.

92. Wilenius, G.
    et alii
    A Theoretical Analysis of a Constant Base Pressure Light
    Gas Gun. CARDE TM 703/62.

93. Vasiliu, J.
    Piston Motion and Shock Wave Formation in a Free-Piston
    Cycle – A Computer Solution. Republic Aviation Corpora-
    tion Report RAC 2553, November 1964.

94. Charters, A.C.
    Curtis, J.S.
    High Velocity Guns for Free Flight Ranges. "The High
    Temperature Aspects of Hypersonic Flow". AGARDograph
    68, edited by Wilbur C. Nelson. Pergamon Press, 1964.

95. Swift, H.F.
    et alii
    NRL Hypervelocity Accelerator Development. Proceedings
    of Sixth Symposium on Hypervelocity Impact, Cleveland,
    Ohio, August 1963.

96. Somes, John.
    Analytic Solution of a Special Gun Problem. NWL Technical
    Memorandum No. K-47/64, US Naval Weapons Laboratory,
    Dahlgren, Virginia, July 1964.

97. Wilenius, G.P.T.
    Slow Piston Gun Development at CARDE. ARPA, CARDE,
    ARGMA Symposium on Aeroballistic Ranges, CARDE TM
    Q-646/61, 1961.

98. Piacesi, R.
    Waser, R.H.
    A Multiple Piston Two-Stage Light Gas Launcher. US Naval
    Ordnance Laboratory, NOLTR 64-96, May 1964.

99. Wooley, Harold W.
    et alii
    Compilation of Thermal Properties of Hydrogen in Various
    Isotopic and Ortho-Para Modifications. National Bureau
    of Standards Journal of Research, Research Paper RP
    1932, Vol. 41, November 1948.

200

100. Bixler, D.
et alii

Extrapolated Thermodynamic Properties at High Densities.
Naval Ordnance Laboratory Report. To be published.

101. Howell, W.

University of Denver, Denver Research Institute, Denver
Colorado, personal communication.

102. Charters, A.C.

General Motors Defense Research Laboratory, personal
communication.

103. Baker, J.R.

*Light Gas Gun Performance. Theoretical Analysis and
Experimental Comparison.* Proceedings of the Seventh
Symposium on Hypervelocity Impact, Tampa, Florida,
November 1964.

104. Volpe, V.F.
Zimmerman, F.J.

*An Experimental Variation of the Sequential Electrical
Discharge Light Gas Gun.* Proceedings of the
Hypervelocity Techniques Symposium, Denver, Colorado,
October 1960.

105. Curtis, John S.

*Some Limitations on the Performance of High-Velocity
Guns.* General Motors Research Laboratory Contract
Technical Note, CTN 64-03, August 1964.

106. Carter, H.
et alii

*The Design and Testing of the Naval Ordnance Laboratory's
2-in. Two-Stage Gun.* NOLTR 62-112, US Naval Ordnance
Laboratory, June 1962.

107. Benoit, André

*Thermodynamic and Composition Data for Constant-Volume
Stoichiometric Mixtures of Hydrogen-Oxygen Diluted with
Helium or Hydrogen.* UTIA Technical Note No.85, Aero-
space Studies, University of Toronto.

108. Cable, A.J.

*The Performance of the RARDE ¼-in. Calibre Hypervelocity
Launcher.* RARDE Memorandum 14/64, April 1964, Fort
Halstead.

109. Knapp, R.E.

*Survey of Literature Covering High Velocity Particle
Launchers.* Arnold Engineering Development Center,
Technical Memorandum No. AEDC-TM-63-7, March 1963.

110. Glass, I.I.
Hall, J.G.

Shock Tubes. Handbook of Supersonic Aerodynamics,
Section 18, Navord Report 1488 (Vol.6), US Government
Printing Office, Washington, DC, 1959.

111. Howell, W.G.
Kottenstette, J.P.

Electrical Augmentation of a Light Gas Gun. Arnold
Engineering Development Center, AEDC-TR-65-32, January
1965.

112. Glass, I.I.
et alii

Theoretical and Experimental Study of the Shock Tube.
UTIA Report No.2, University of Toronto, November 1953.

113. Knapp. R.E. *Survey of Literature Covering High Velocity Particle Launchers*. Arnold Engineering Development Center, AEDC-TM-63-7, March 1963.

114. Lukasiewicz, J. *Shock Tube Theory and Applications*. National Aeronautical Establishment, Canada, Report 15, 1952.

115. Baker, J.R. *A Comparison of Shock and Isentropic Heating in Light-Gas Gun Compression*. NRL Report 6063, April 1964.

116. De France,
  Smith, J. Personal communication, letter dated March 19, 1965.

117. Knystantas, R.
  Leftheris, B. *An Analysis of the Double Shock Compression Light Gas Gun Cycle*. CARDE T.R. 516/65, January 1, 1965.

202

Figure 1

The figure shows a plot of DIMENSIONLESS GAS PRESSURE $-\dfrac{p}{p_o}$ (vertical axis, from 0 to 1.0) versus DIMENSIONLESS GAS VELOCITY $-\dfrac{a_o}{\gamma u}$ (horizontal axis, from 0 to 4), with curves for $\gamma = 1$ and $\gamma = \dfrac{5}{3}$.

$$\frac{p}{p_o} = \left[1 - \frac{u\,(\gamma-1)}{2\,a_o}\right]^{\frac{2\gamma}{\gamma-1}}$$
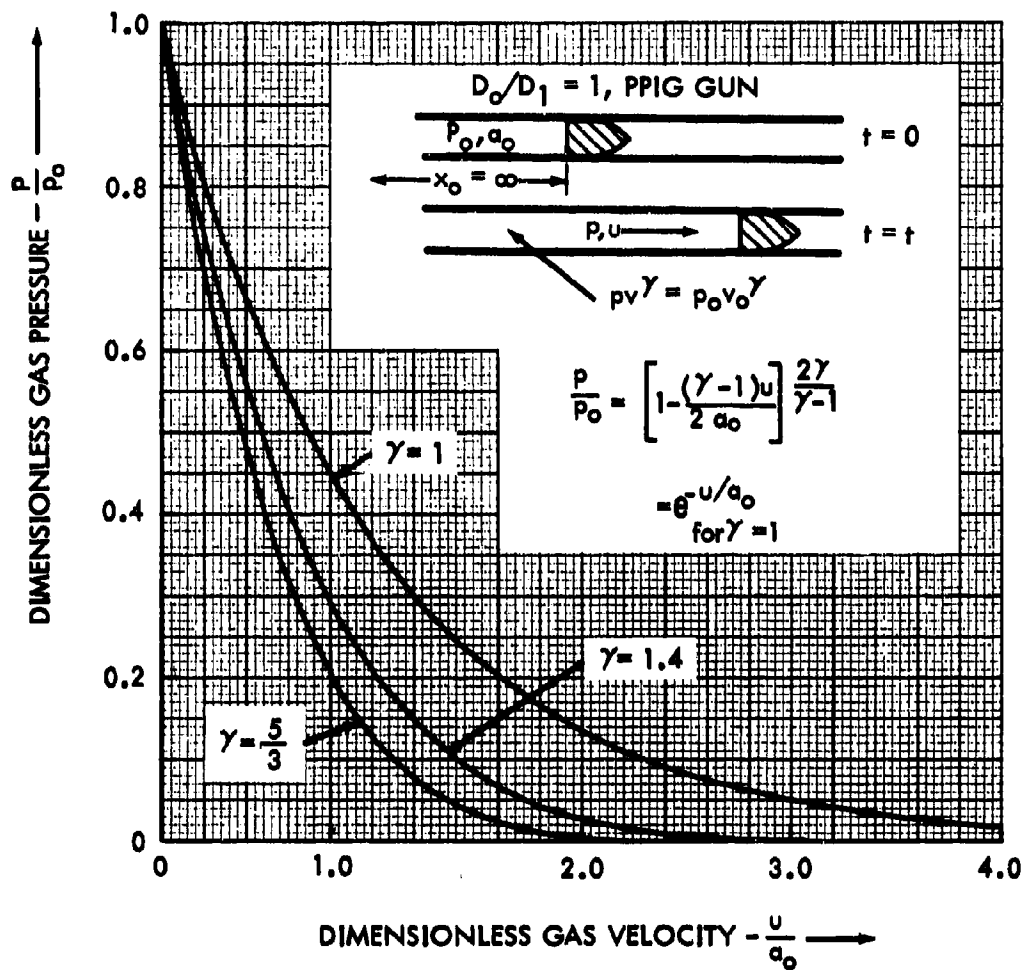
$$= e^{-u/a_o} \quad \text{for } \gamma = 1$$
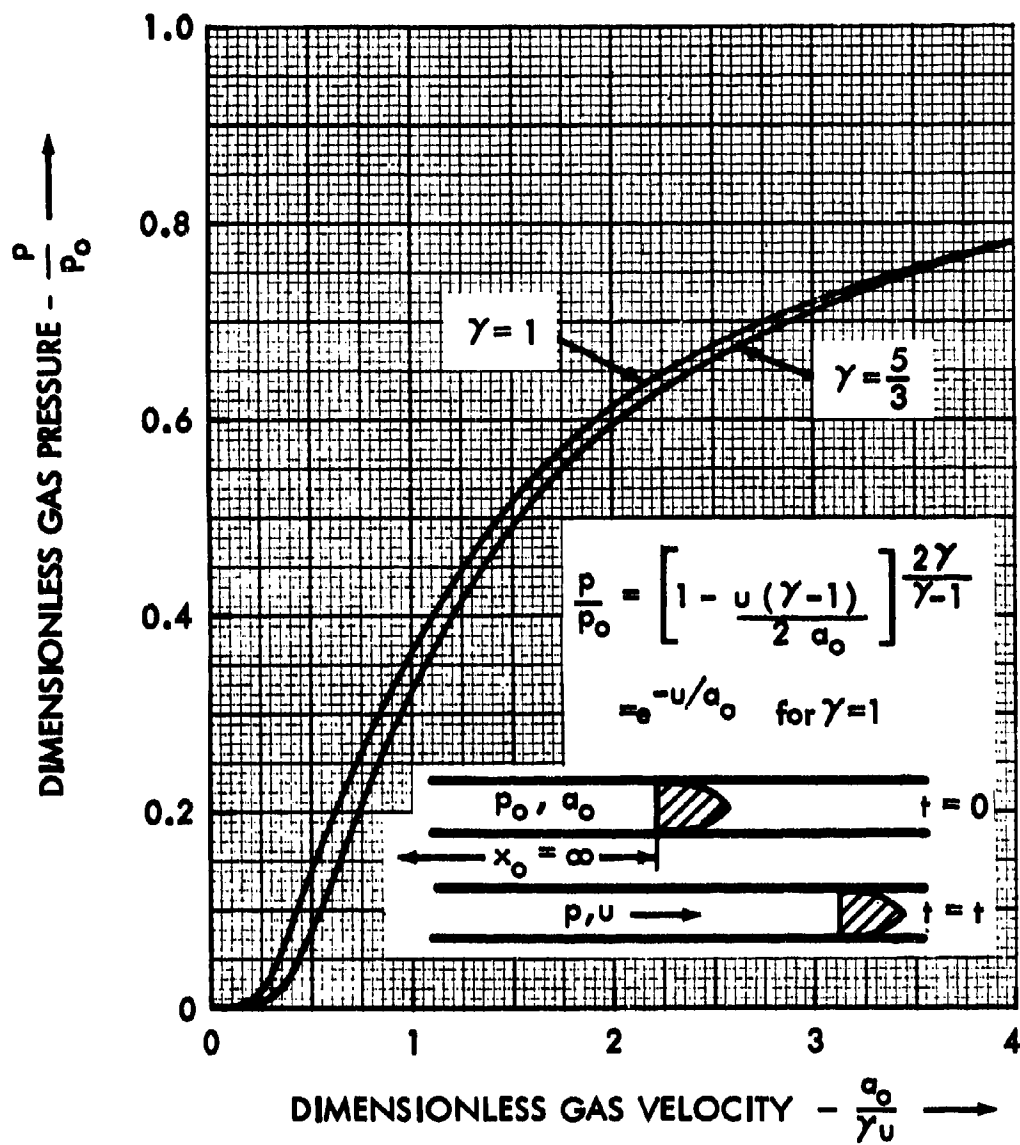
Figure 2

Figure 3

Figure 4

CHAMBER LENGTH TO BE EFFECTIVELY INFINITE

$$\frac{P_o \, A \, x_o}{M a_o^2} \longrightarrow$$
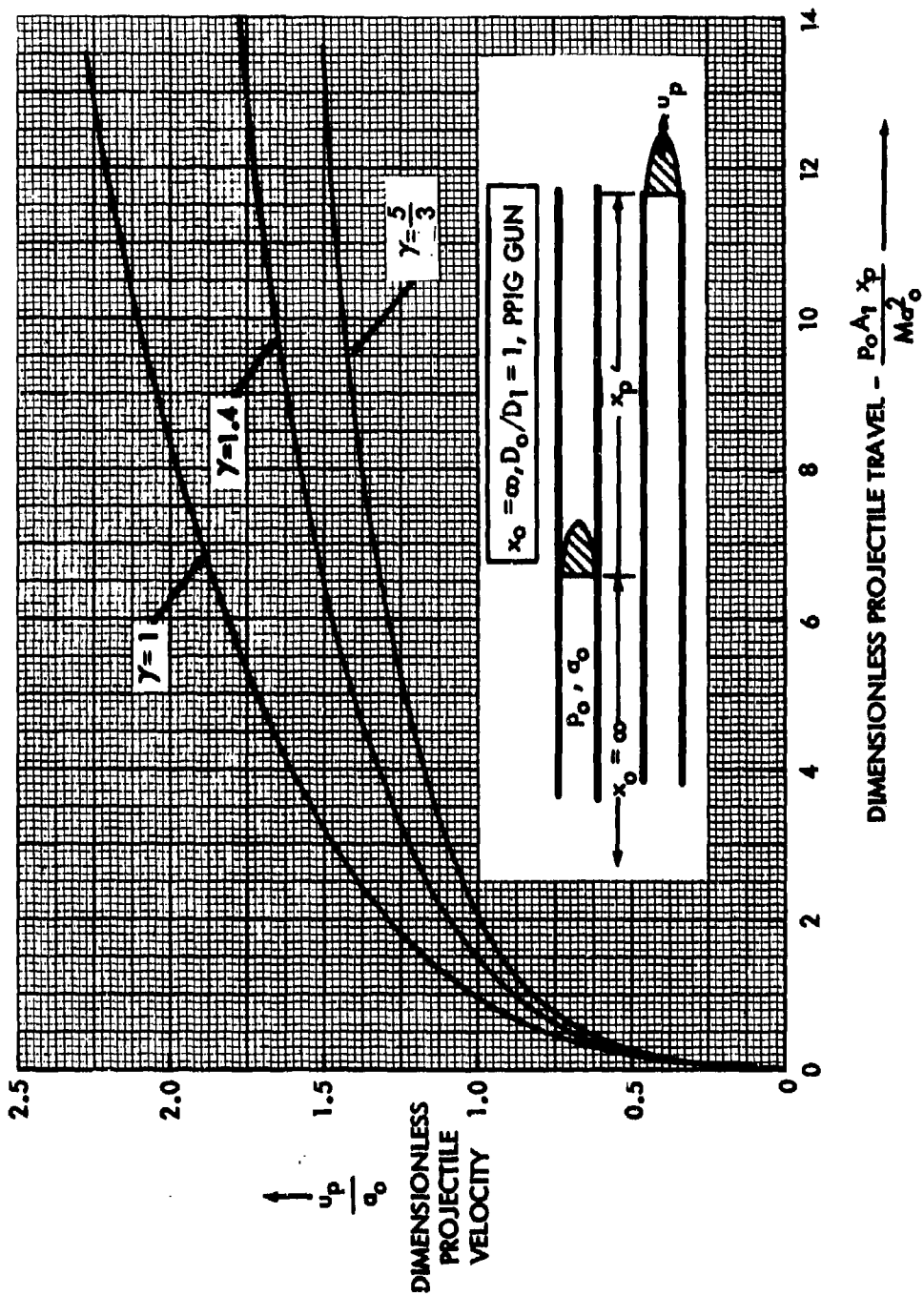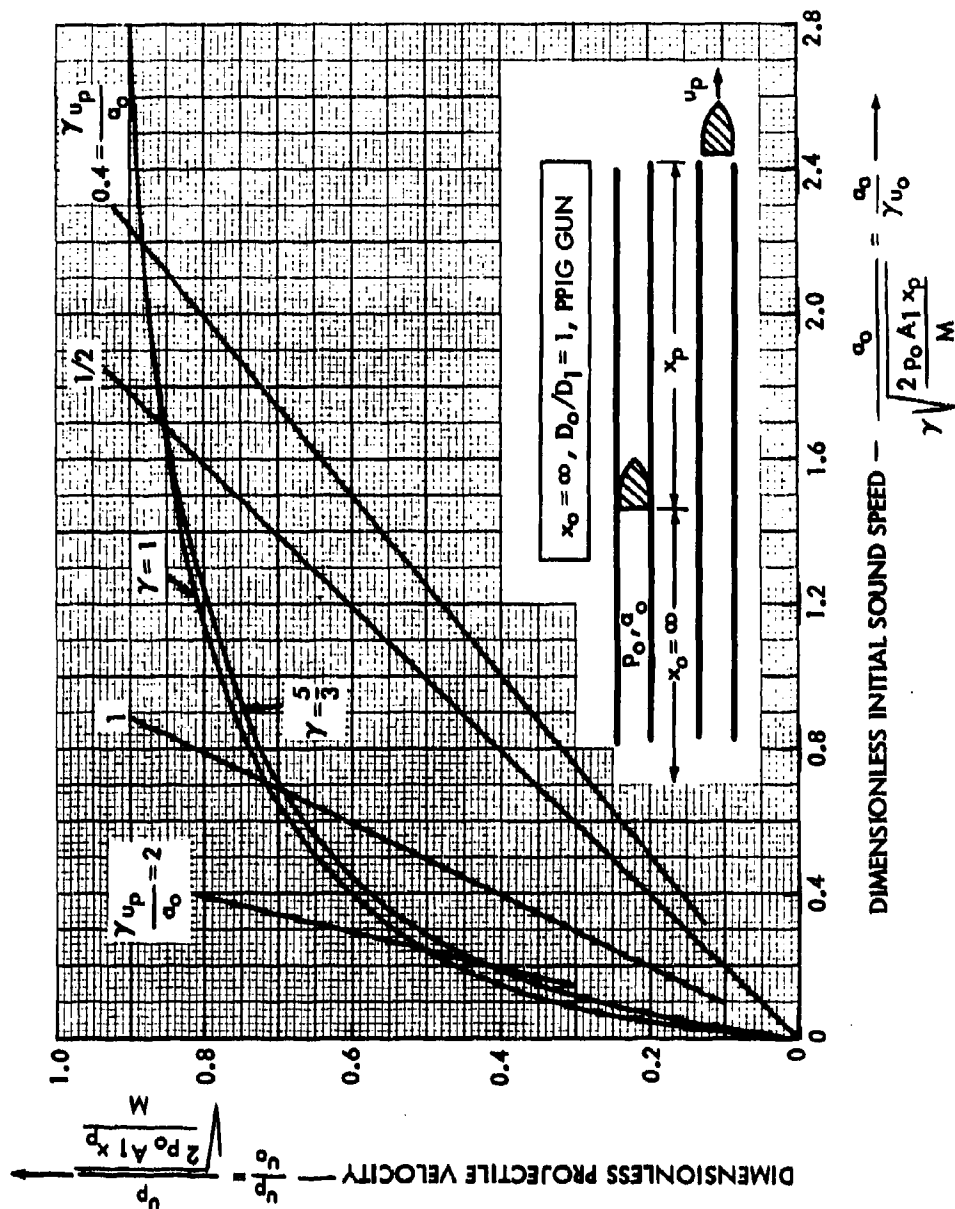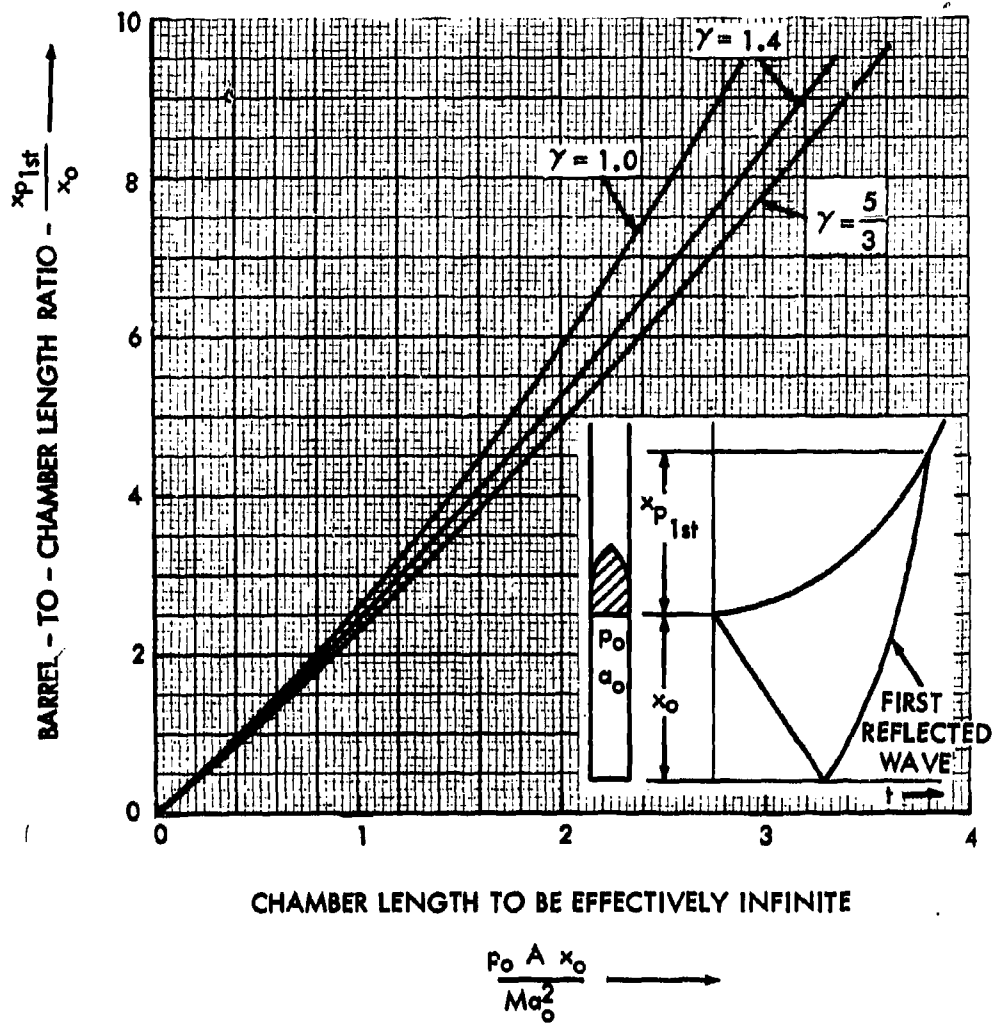
Figure 5

Figure 6

Figure 7

0.5" TO 2.5"

30° HALF-ANGLE TAPER

0.5"

BARREL

17" AND 30"

COUPLING

3000 psi AIR

CHAMBER

AIR INLET
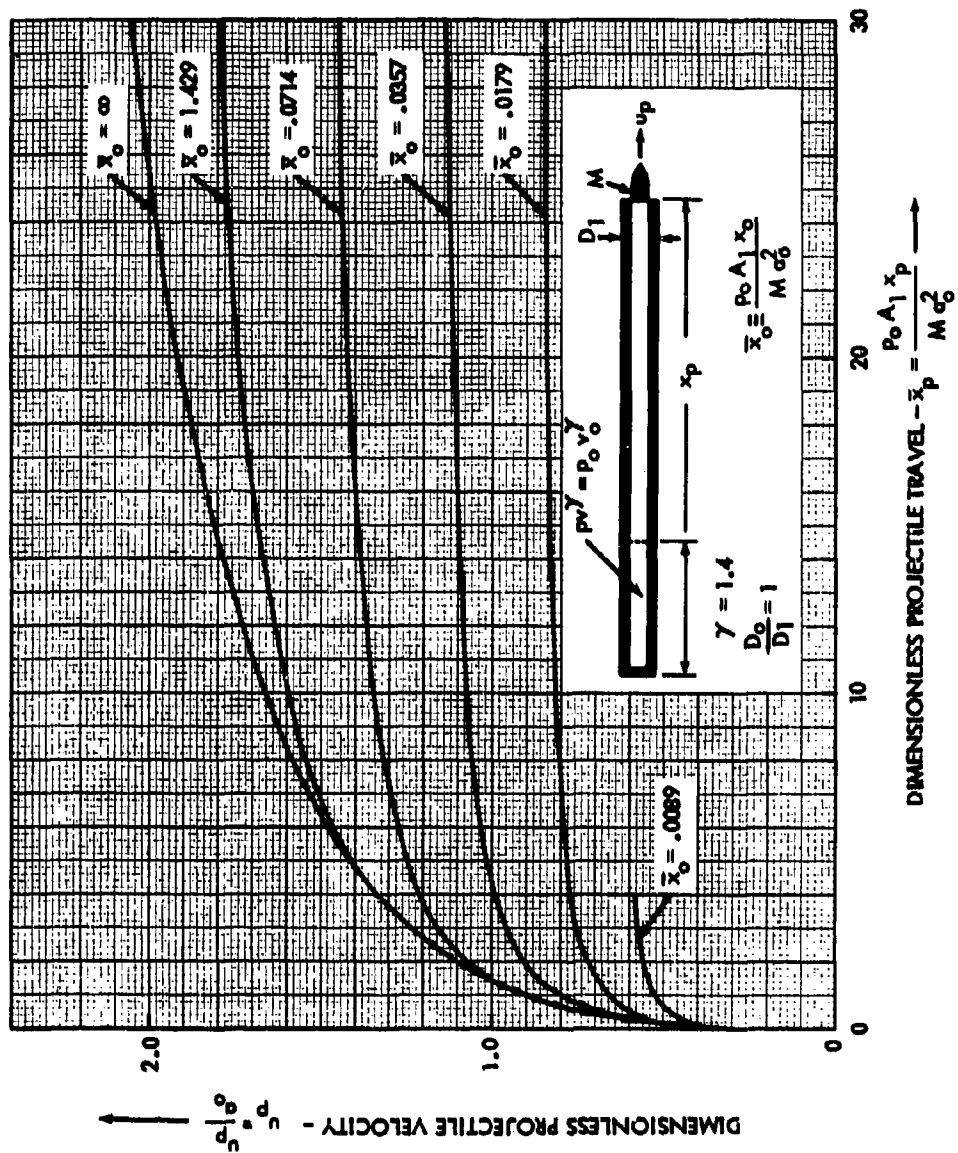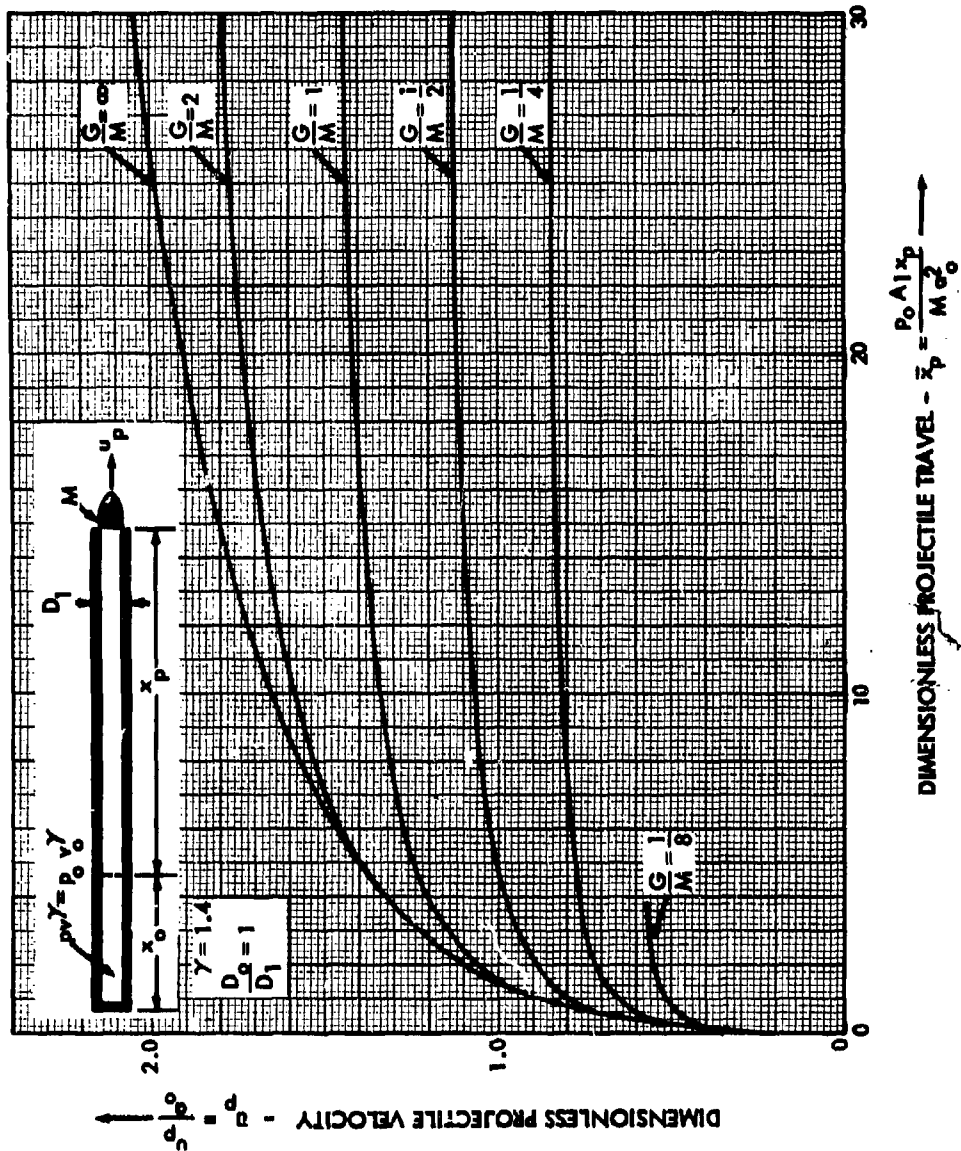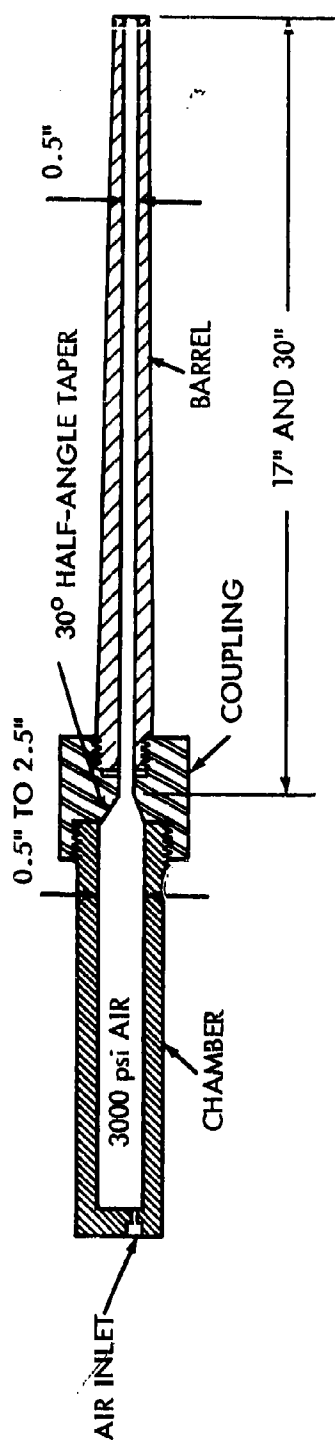
CHRONOGRAPH SCREEN ARRANGEMENT

50 CM

50 CM

50 CM

GUN MUZZLE

PROJECTILE
WEIGHT = 1 gm

PART 1

PART 2
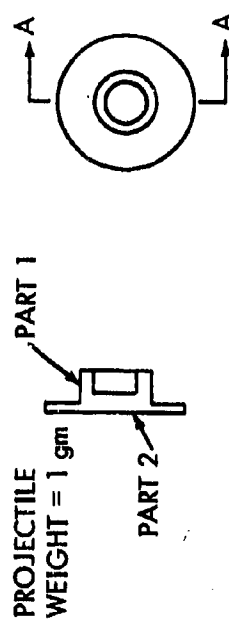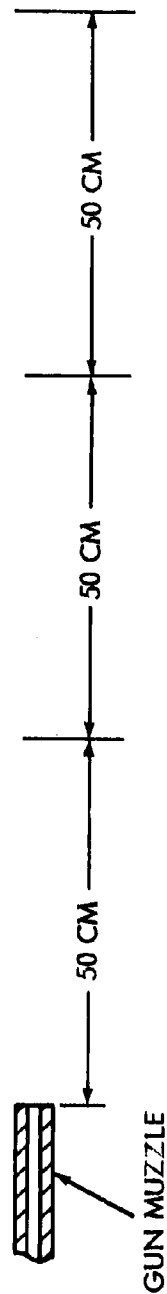
SECTION AA

A

A

Fig. 8(a) Schematic of NOL gun system for chambrage tests (ref. 10)
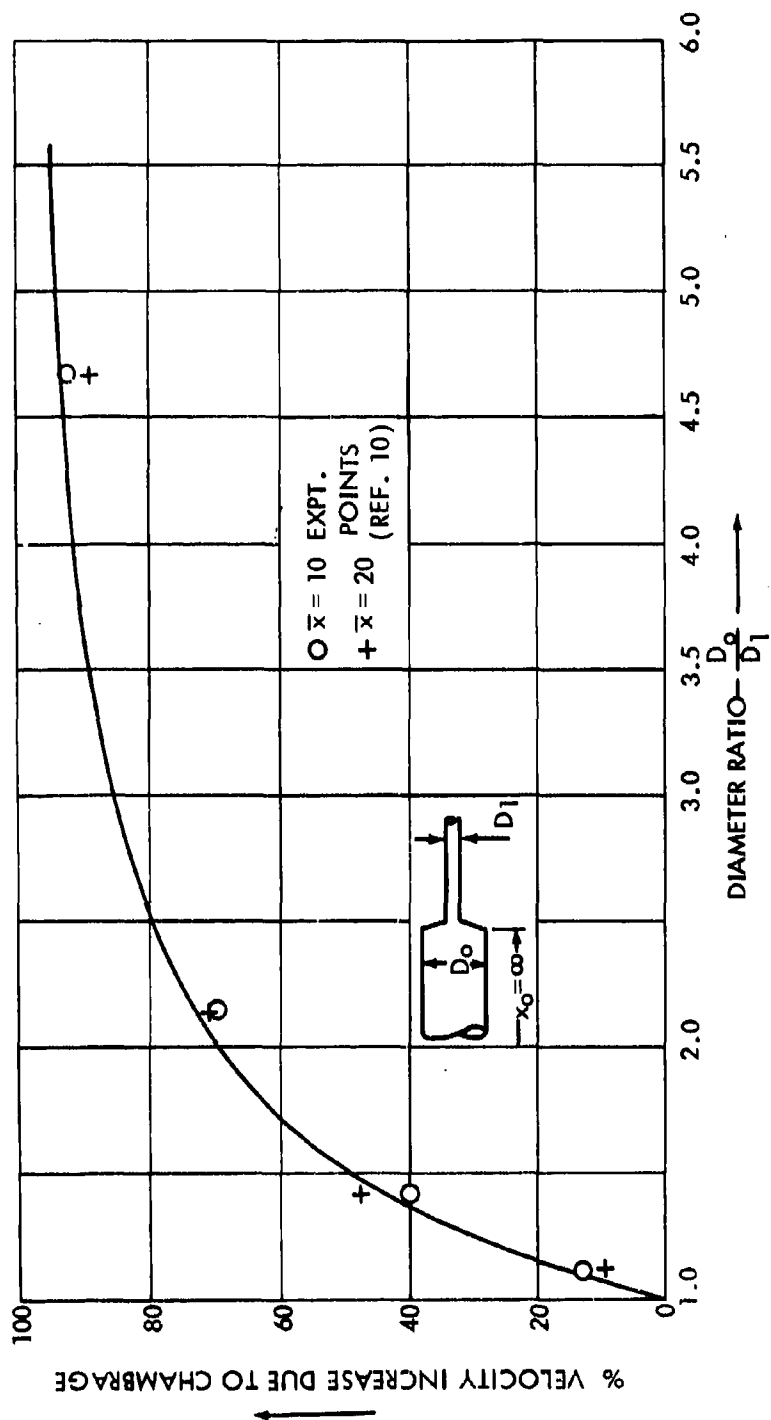
Fig. 8(b)   Comparison of experimental and theoretical velocity increase due to chambrage

211

Figure 9(a)

212

Figure 9(b)

Figure 10

214

Figure 11

Figure 12

INCREASE IN PROJECTILE VELOCITY DUE TO CHAMBRAGE

Δu_p

DIMENSIONLESS PROJECTILE VELOCITY

$$\left(\frac{\gamma u_p}{a_0} \right)_{D_o/D_1 = 1}$$

PPIG GUN
$x_0 = \infty$

$\gamma = 1.4$

$\gamma = 1$

Figure 13

217
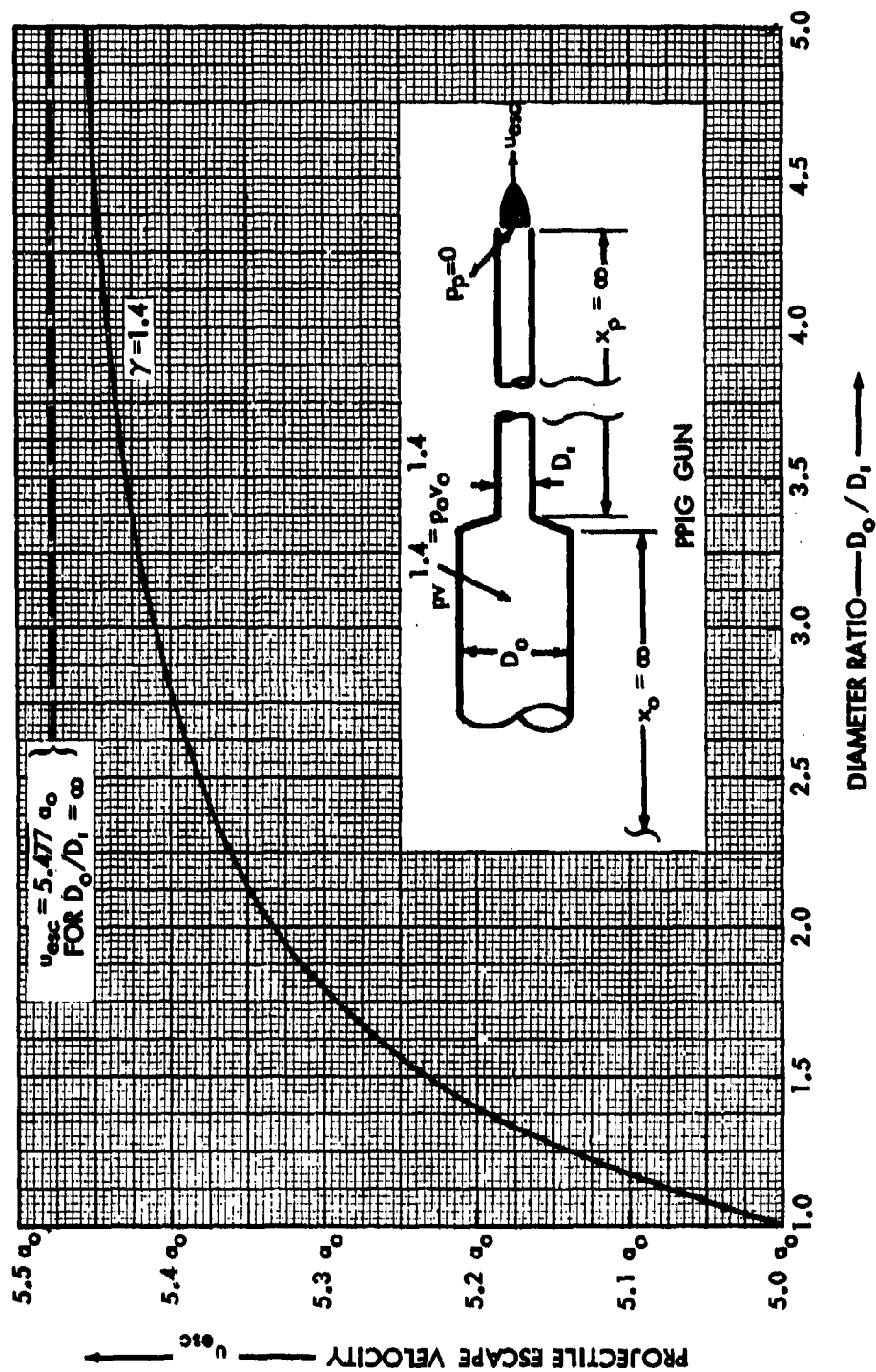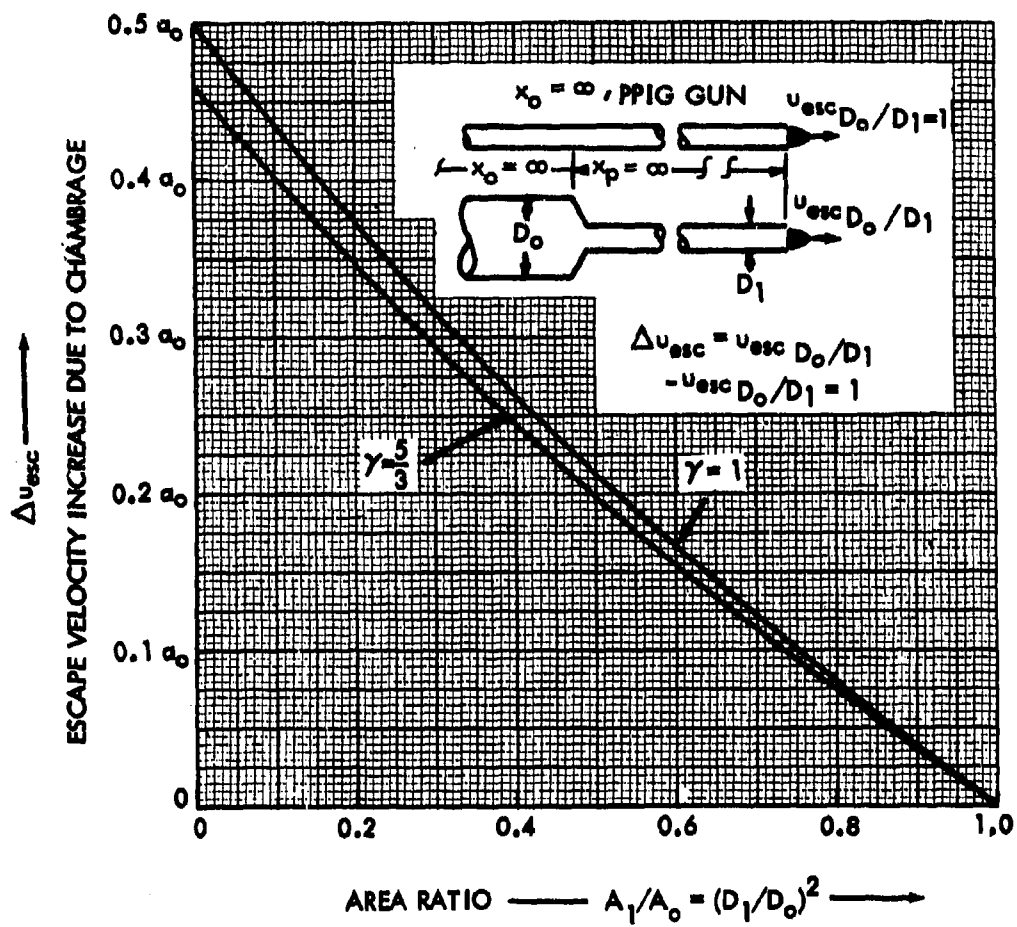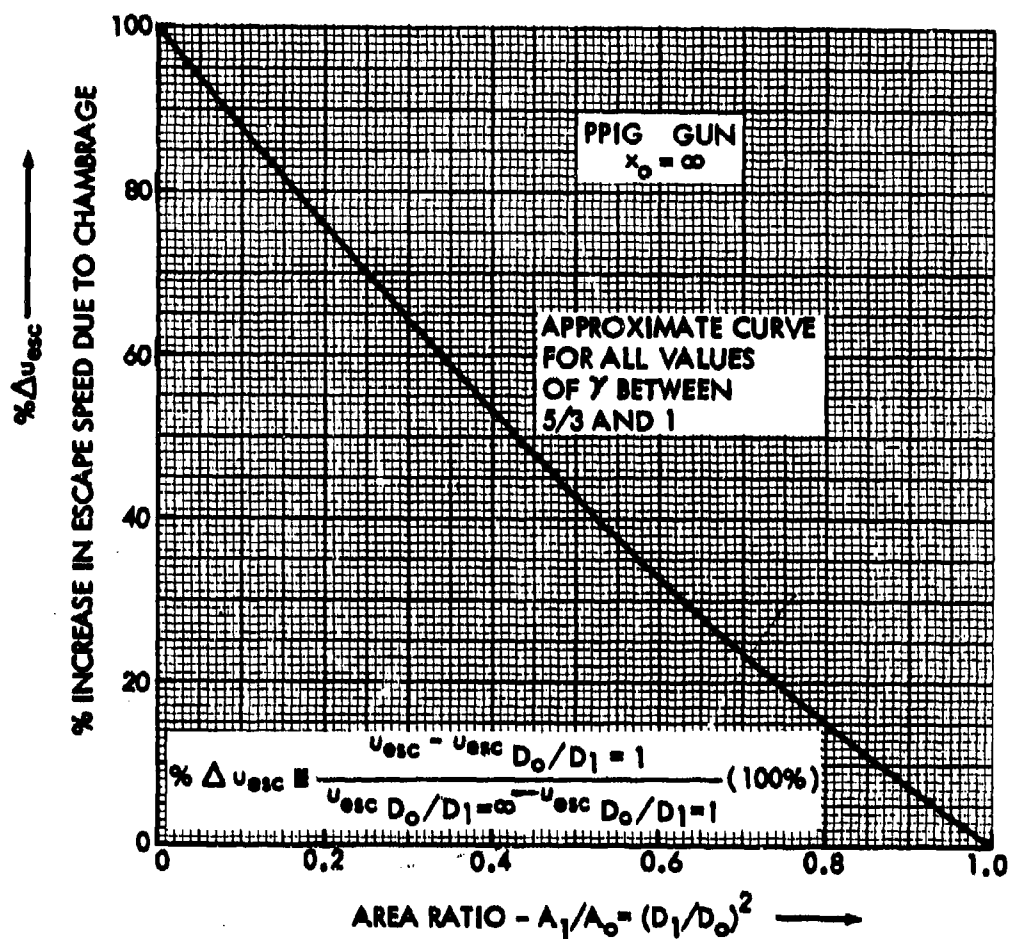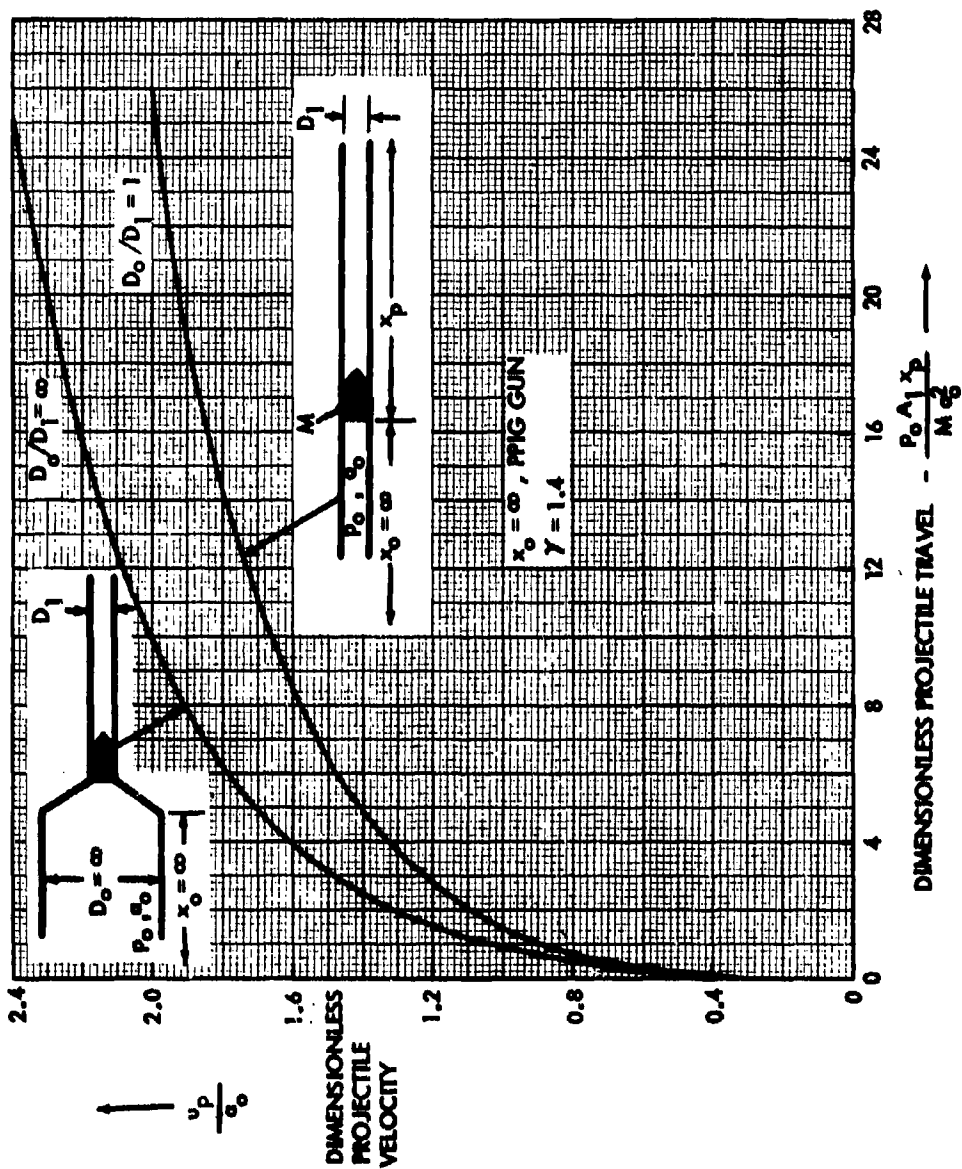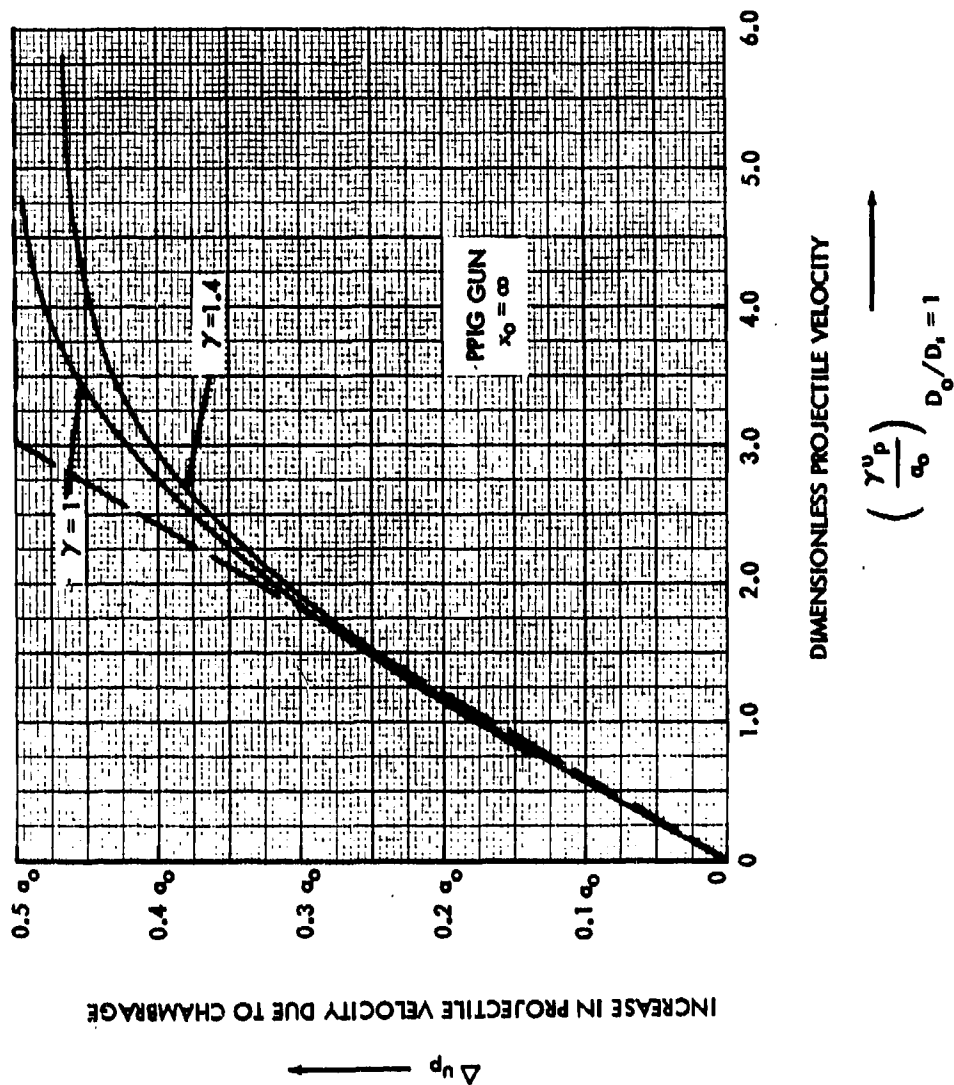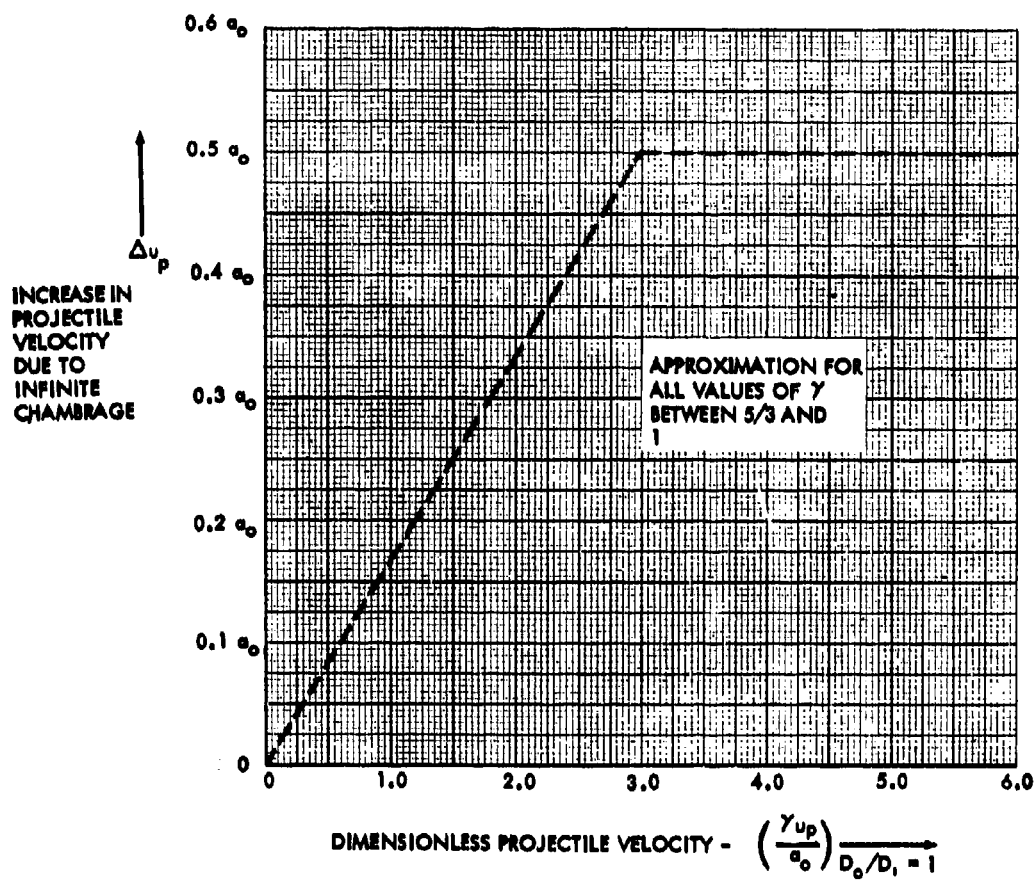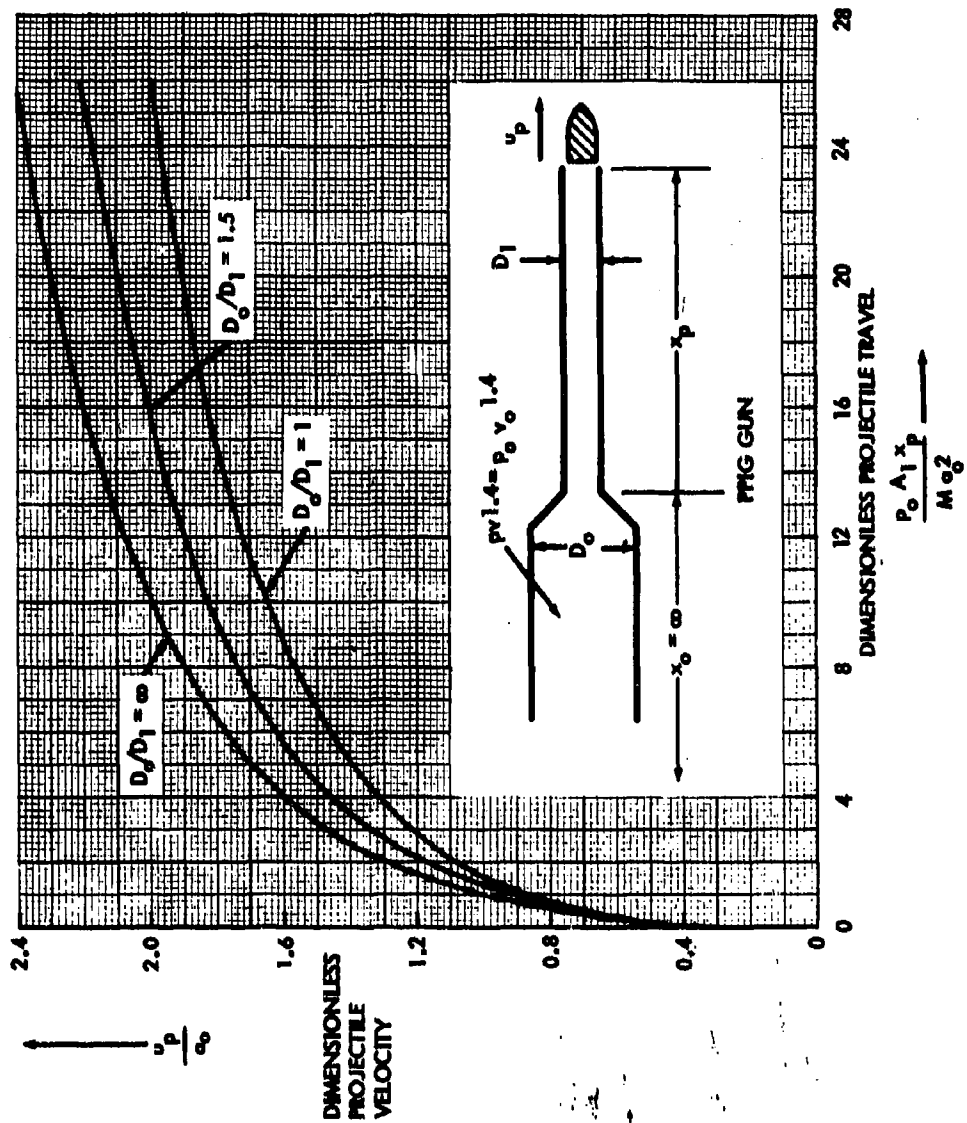
Figure 14

Figure 15

Figure 16

220

APPROXIMATE CURVE
FOR ALL VALUES
OF γ BETWEEN
5/3 AND 1

PPIG GUN
$x_o = \infty$

$$\frac{P_p}{P_o} = \left[1 + \epsilon \frac{u_p}{\frac{2}{\gamma-1} a_o} \right]^{\frac{2\gamma}{\gamma-1}}$$

$$\text{OR FOR } \gamma = 1, \frac{P_p}{P_o} = e^{(r - \frac{u_p}{a_o})}$$

Figure 17

PROJECTILE VELOCITY AS A FUNCTION OF THE
LENGTH OF CHAMBER TO BE EFFECTIVELY INFINITE

PPIG GUN
$\gamma = 1.4$

$\frac{D_o}{D_1} = \infty$

$\frac{D_o}{D_1} = 1.5$

$\frac{D_o}{D_1} = 1$

DIMENSIONLESS CHAMBER LENGTH

$\frac{P_o A_1 \, x_o}{M \, a_o^2}$

DIMENSIONLESS PROJECTILE VELOCITY

$\frac{U_{p1st}}{5 \, a_o}$

Figure 18

222

THE RELATION BETWEEN PROJECTILE TRAVEL AND
LENGTH OF CHAMBER TO BE EFFECTIVELY INFINITE

$$\frac{P_o A_1 x_{pist}}{Ma_o^2} \longrightarrow \text{DIMENSIONLESS PROJECTILE TRAVEL}$$

$$\frac{P_o A_1 x_o}{Ma_o^2} \longrightarrow$$

DIMENSIONLESS CHAMBER LENGTH

PPIG GUN
$\gamma = 1.4$

$\frac{x_o}{x_{pist}}$

$\frac{x_{pist}}{x_o}$

$\frac{D_o}{D_1} = \infty$

$\frac{D_o}{D_1} = 1.5$

$\frac{D_o}{D_1} = 1$

$\frac{D_o}{D_1} = \infty$

$\frac{D_o}{D_1} = 1.5$

$\frac{D_o}{D_1} = 1$

Figure 19

Figure 20(a)

224

Figure 20(b)

Figure 20(c)

Figure 20(d)

Figure 20(e)

228
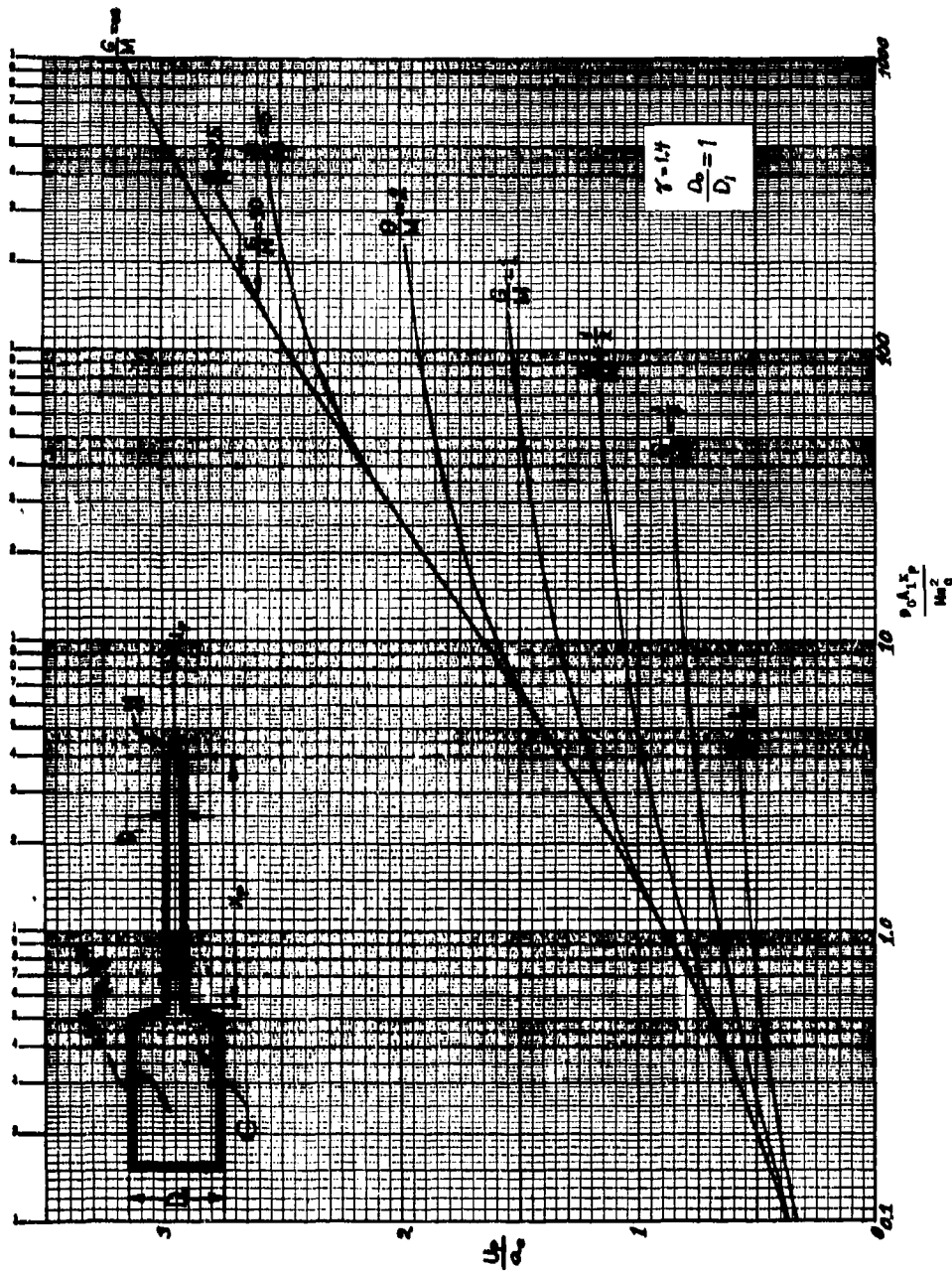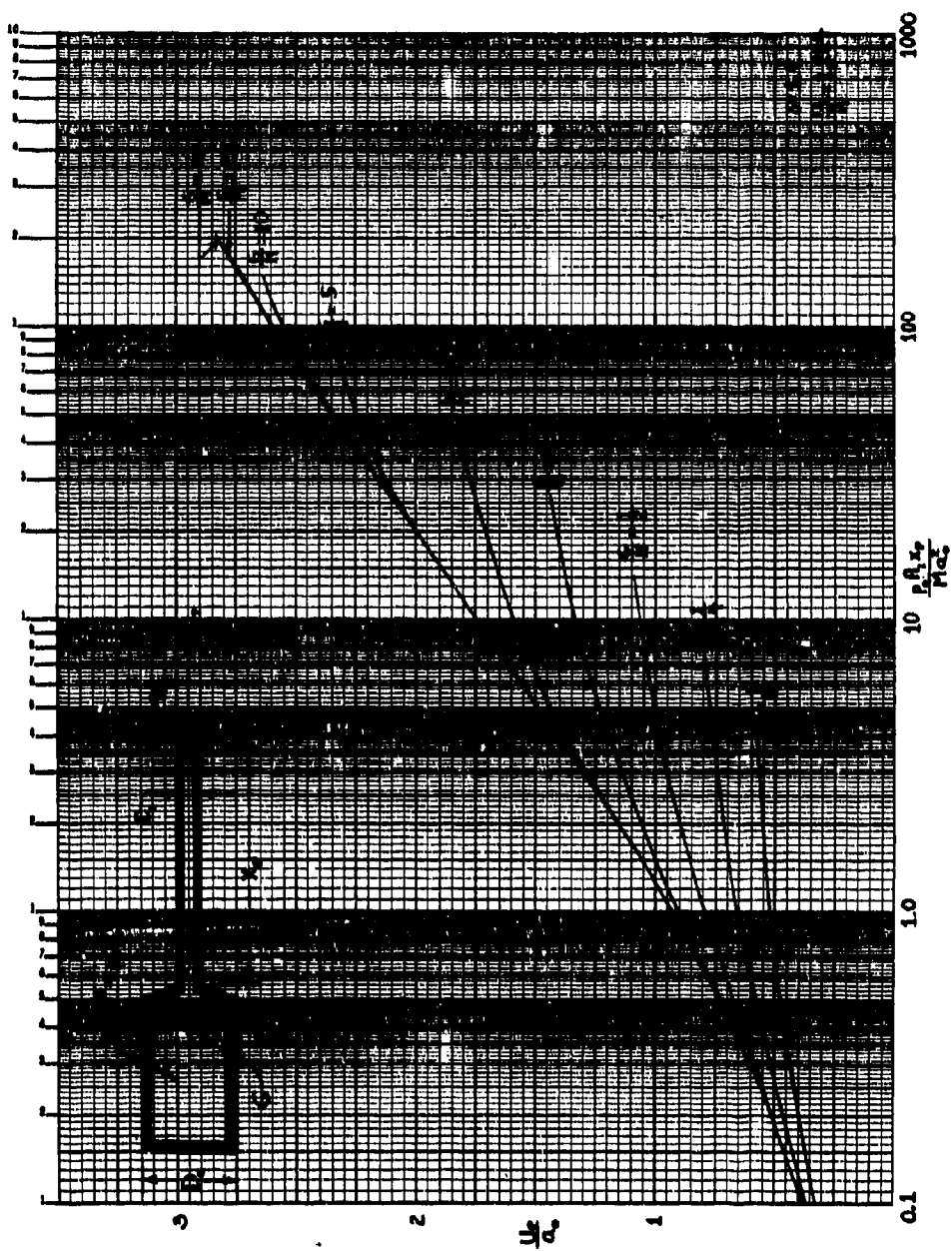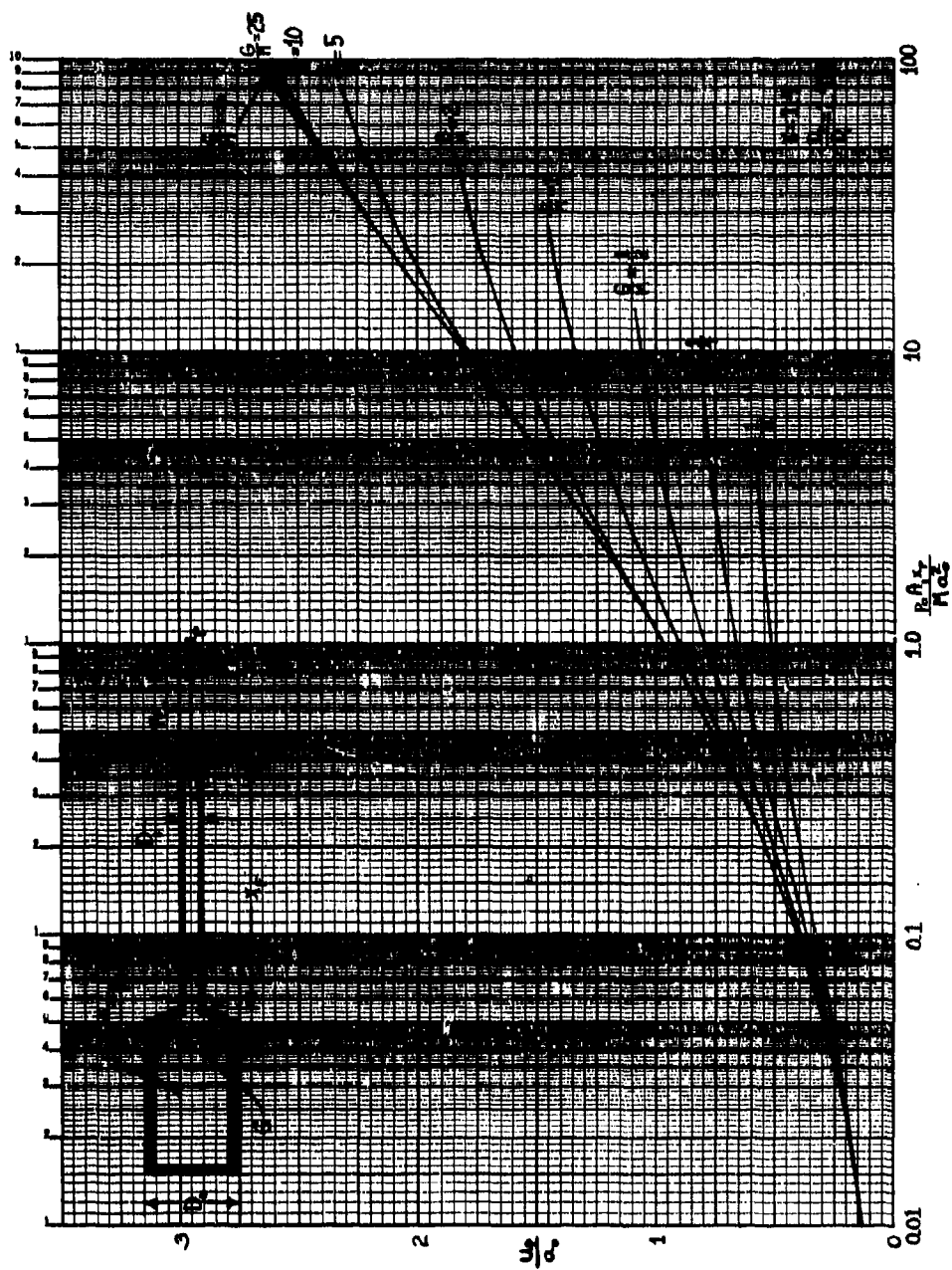
Figure 20(f)

Figure 20(g)
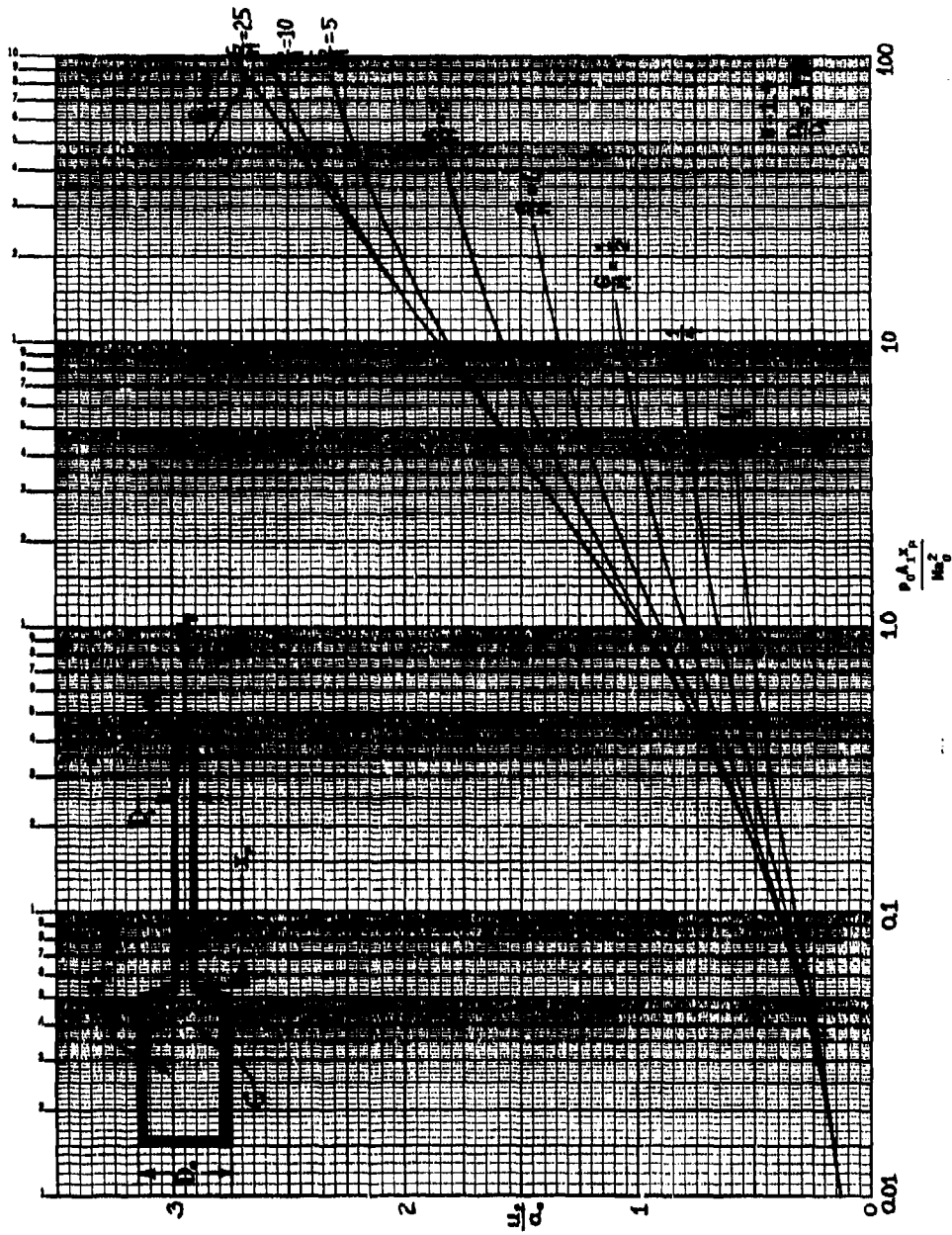
Figure 20(h)

Figure 20(i)

232

Figure 20(j)

Figure 20(k)

234

Figure 20(1)

235

Figure 20(m)

236

Figure 20(n)

$$\frac{p_o A_T x_p}{W_0^2}$$
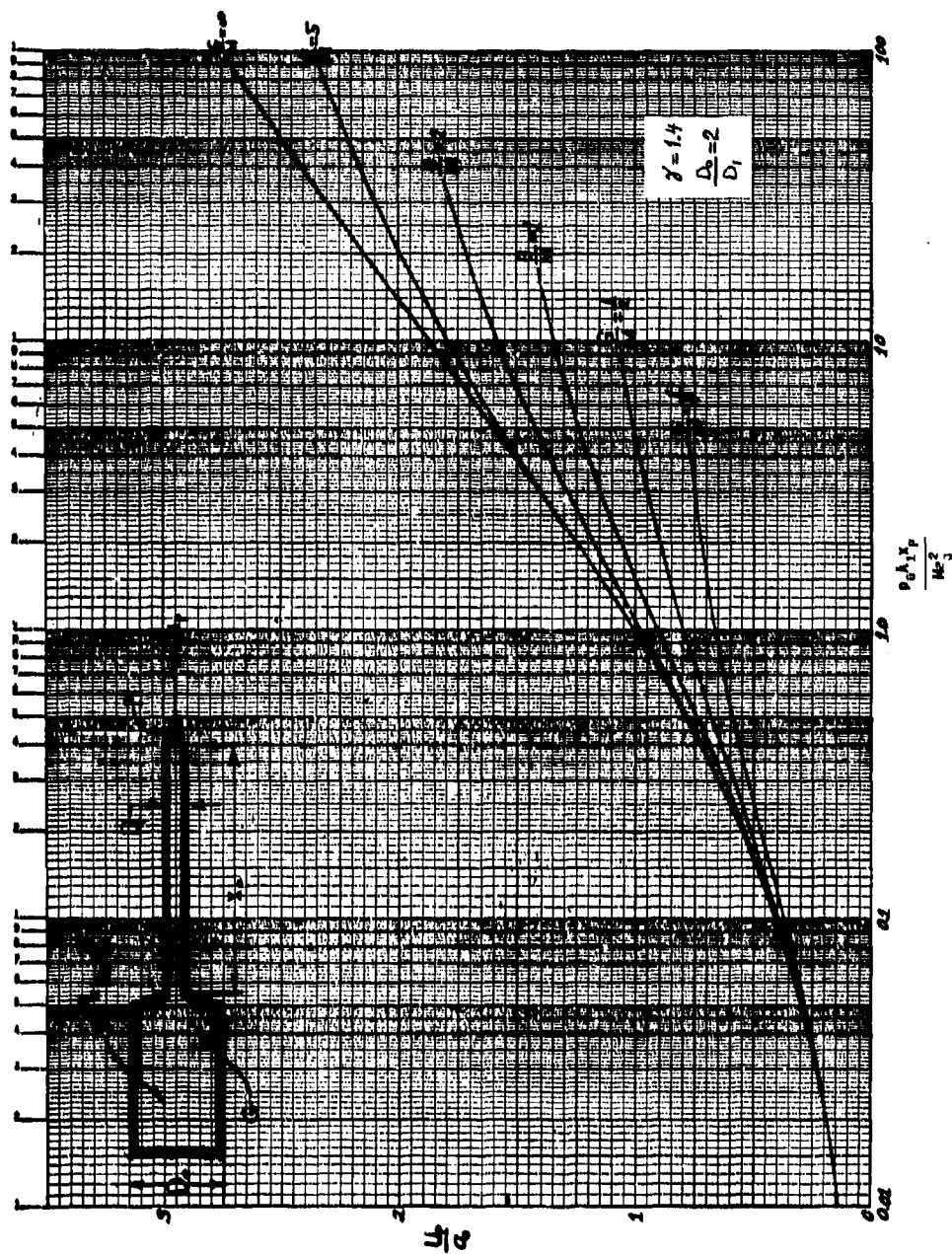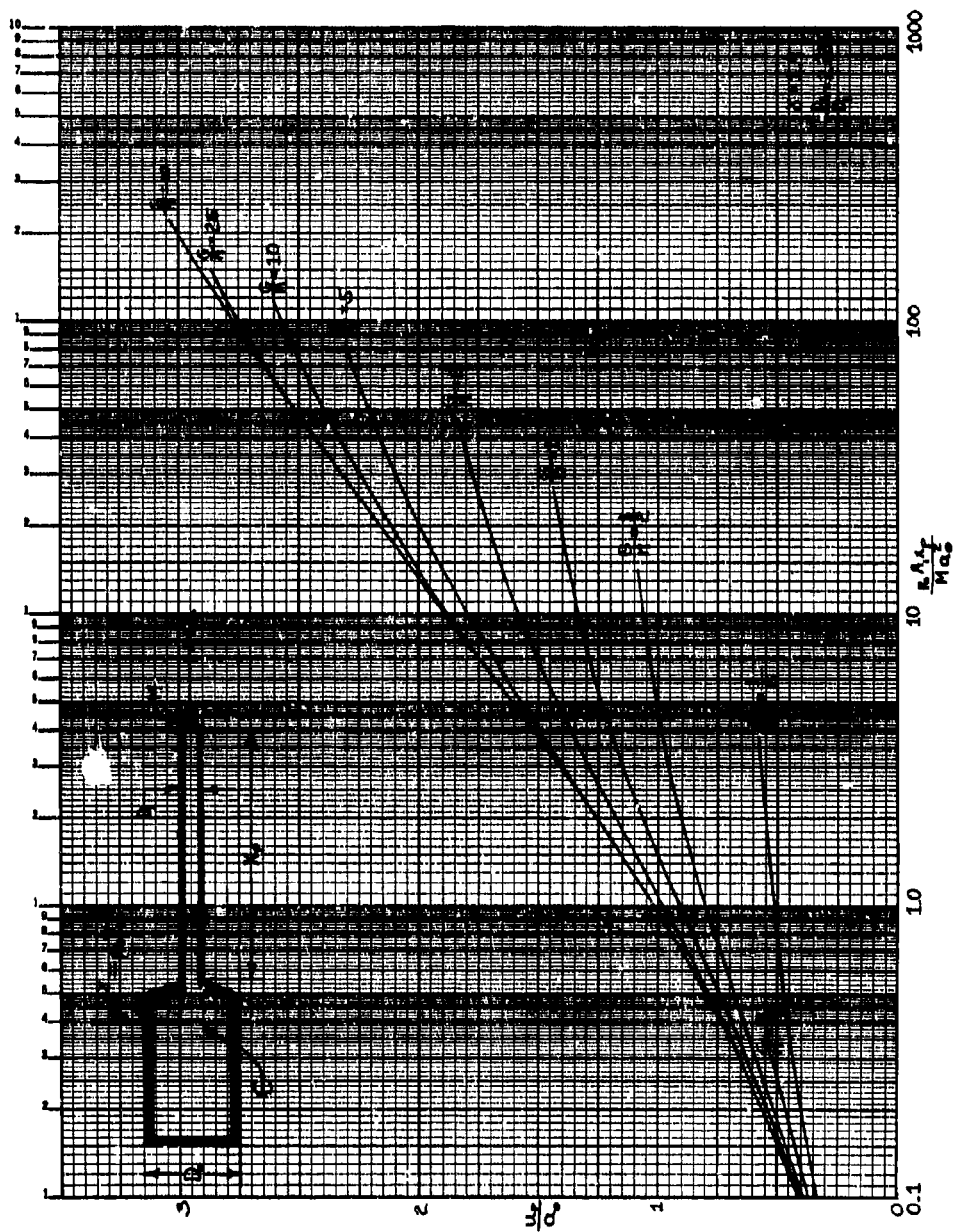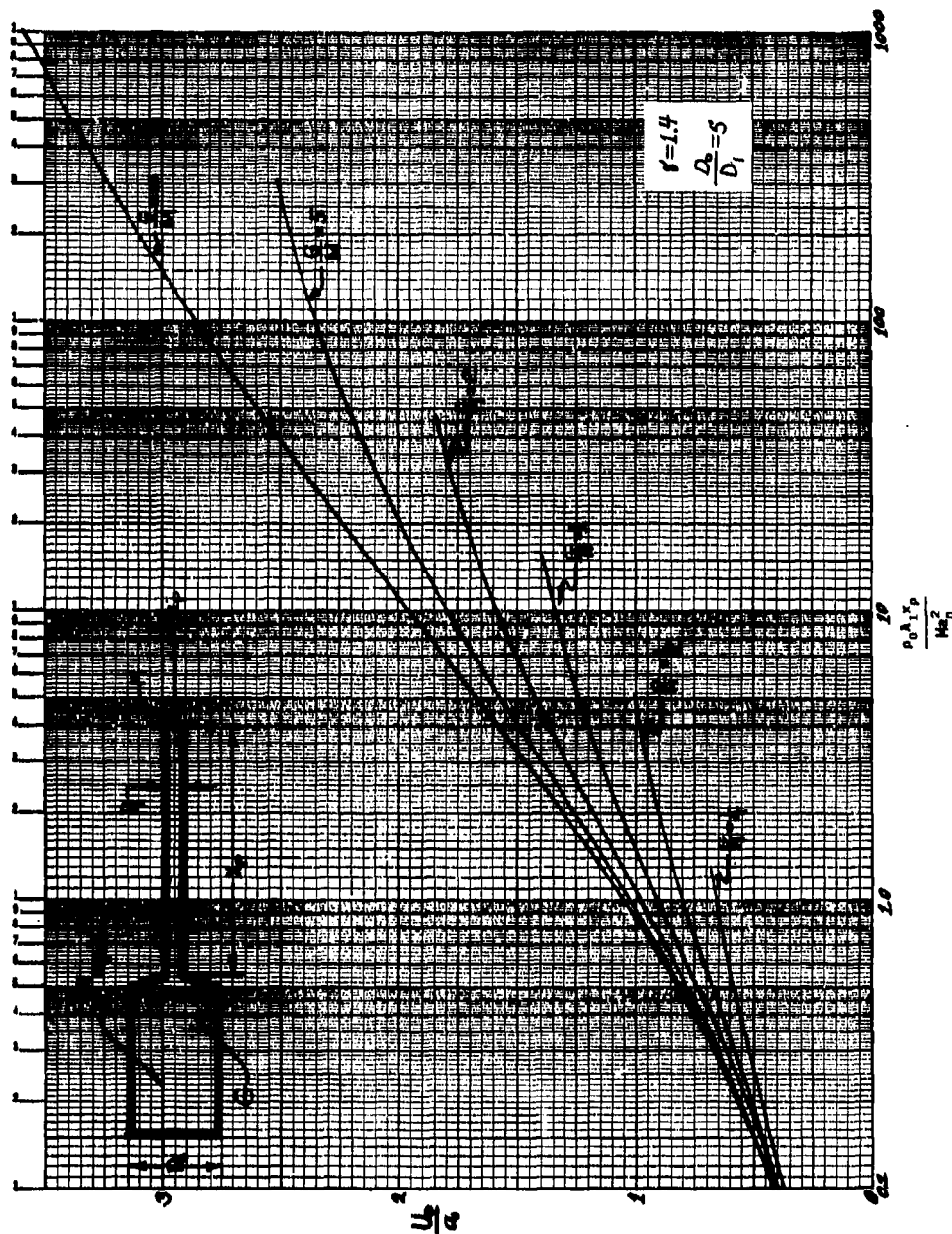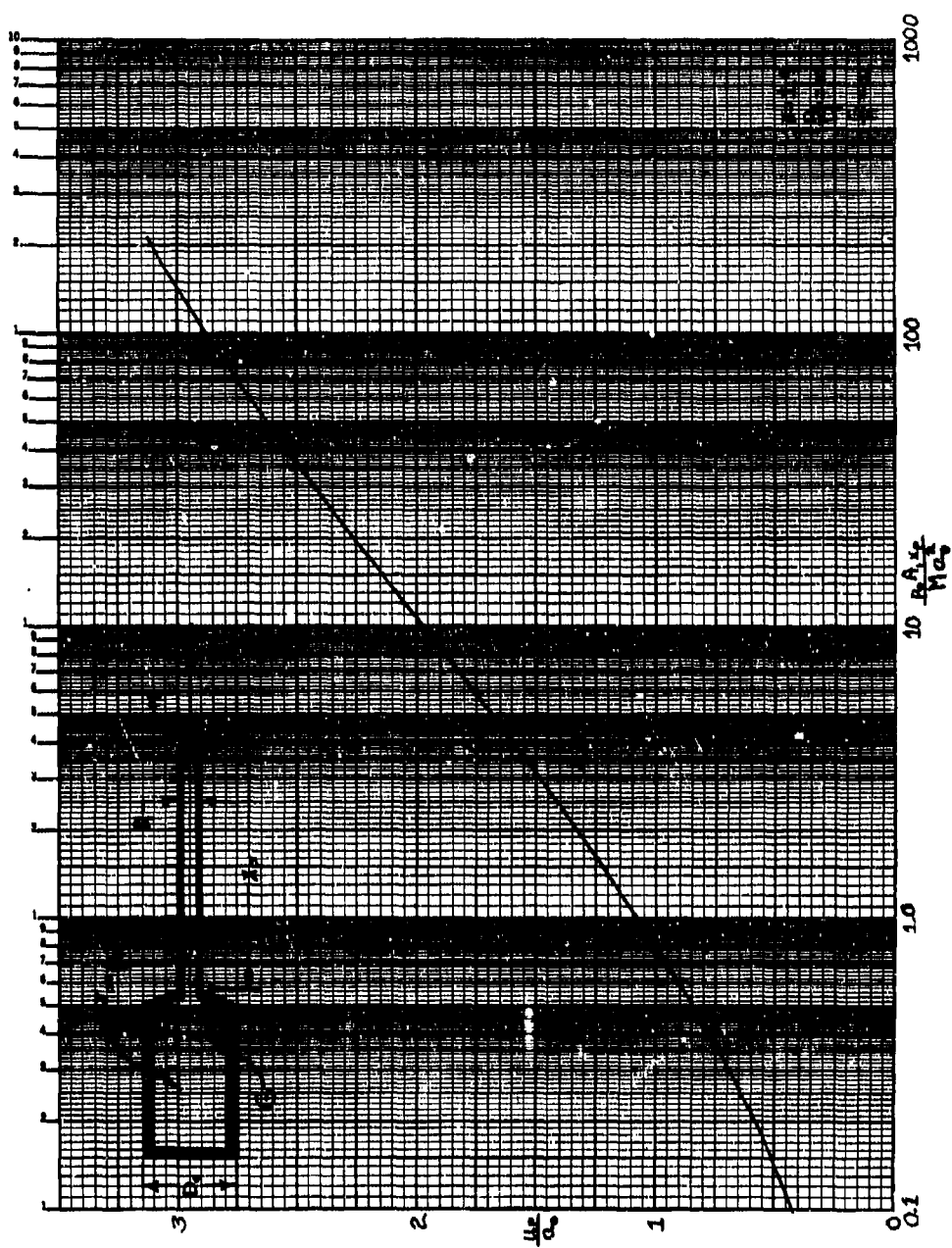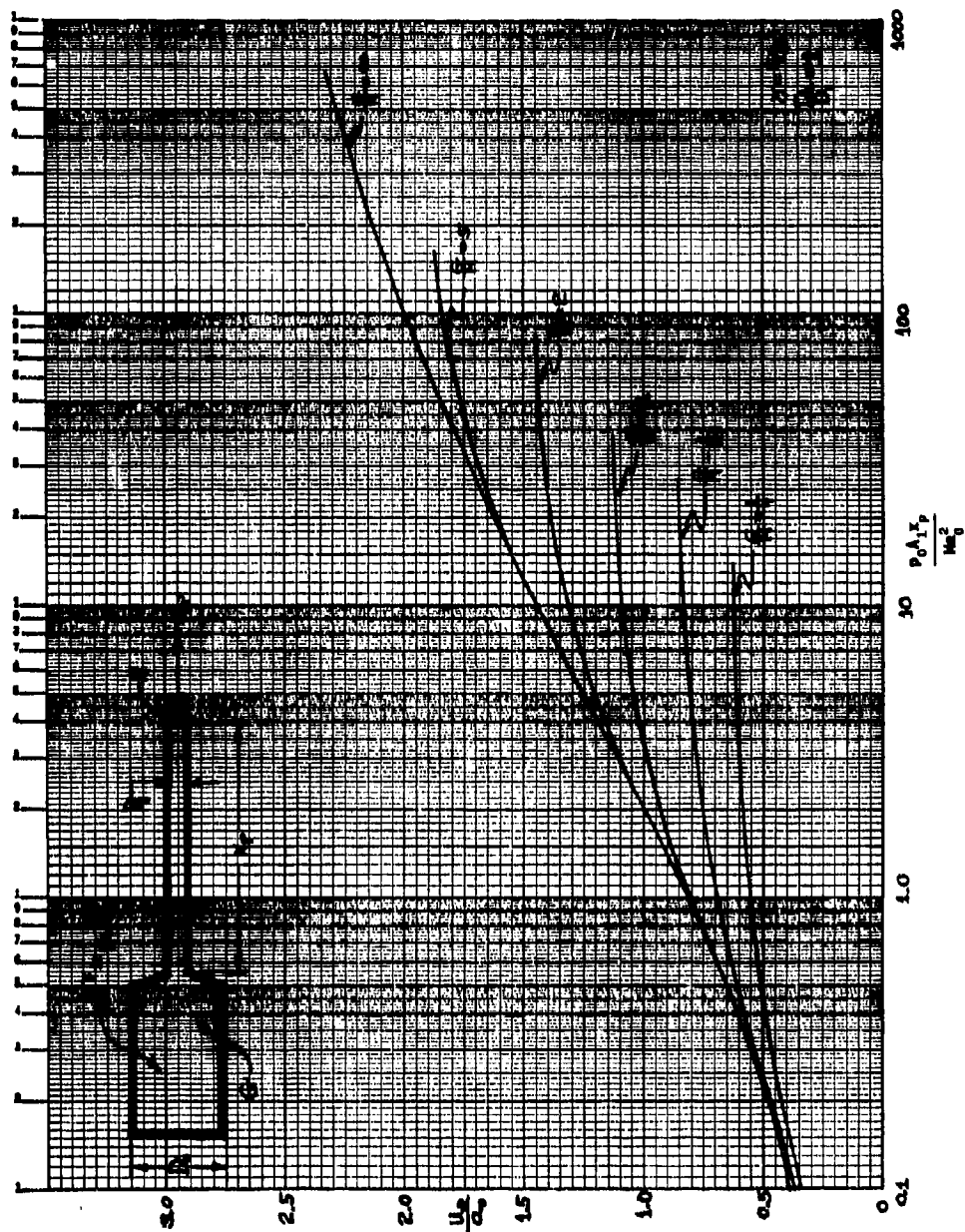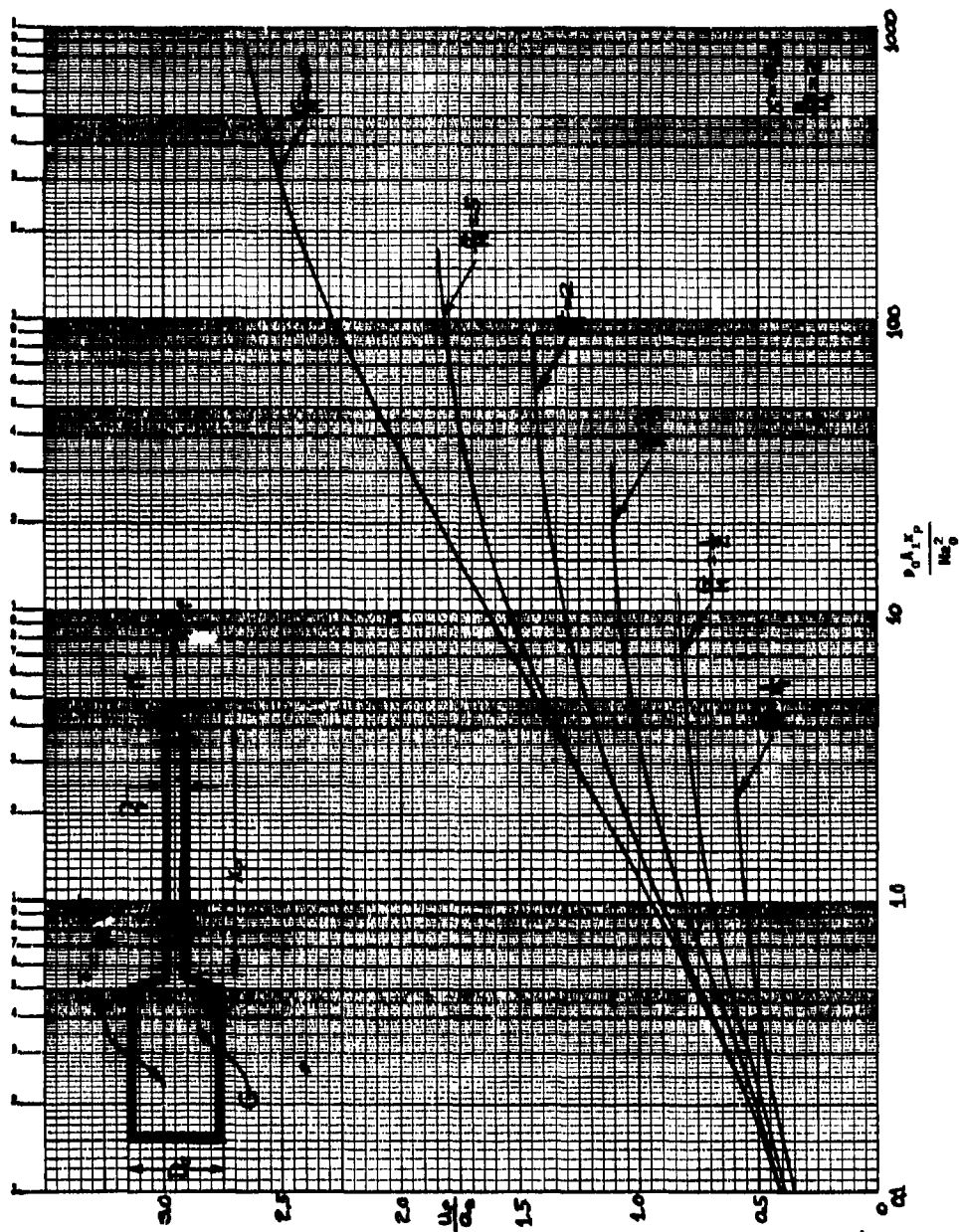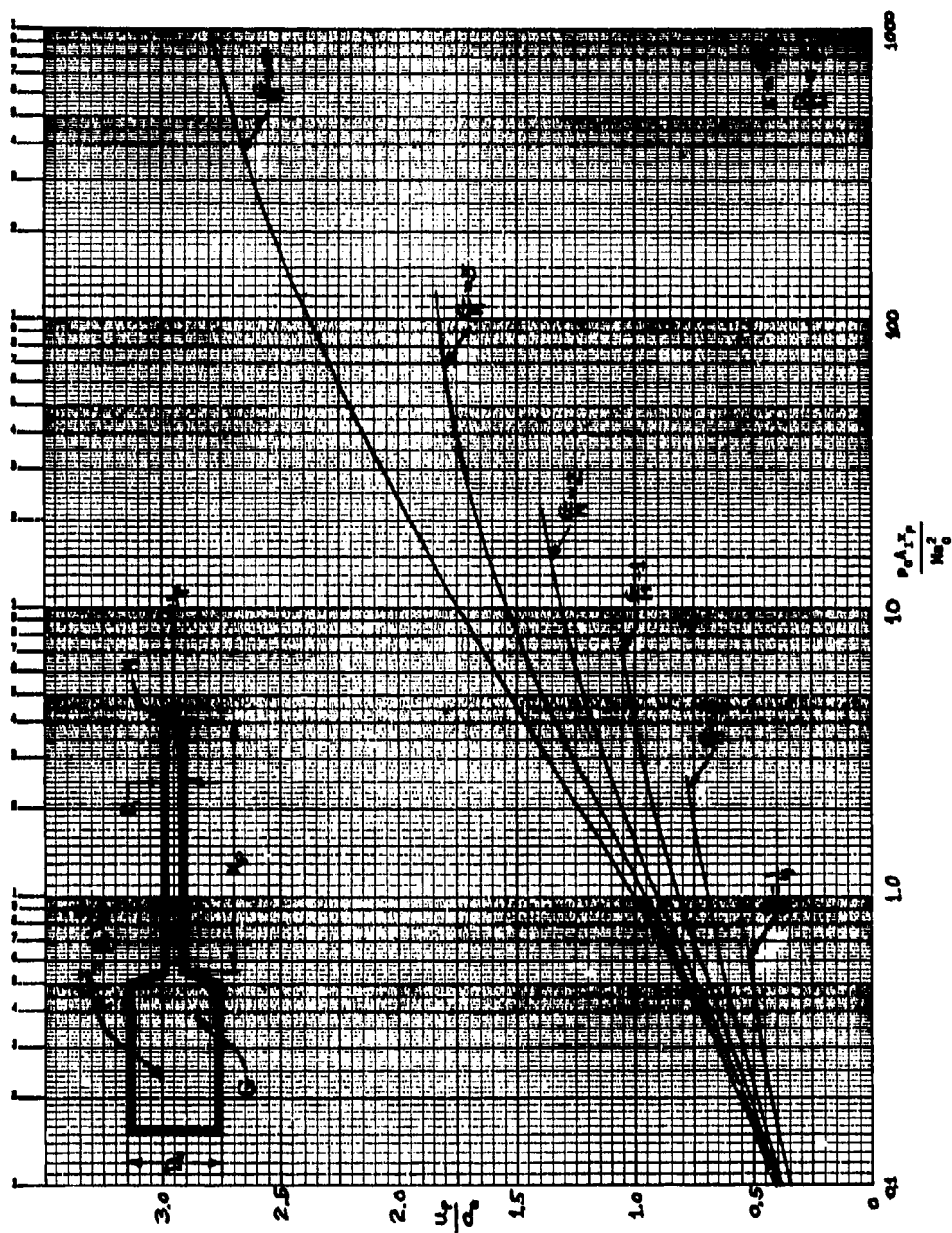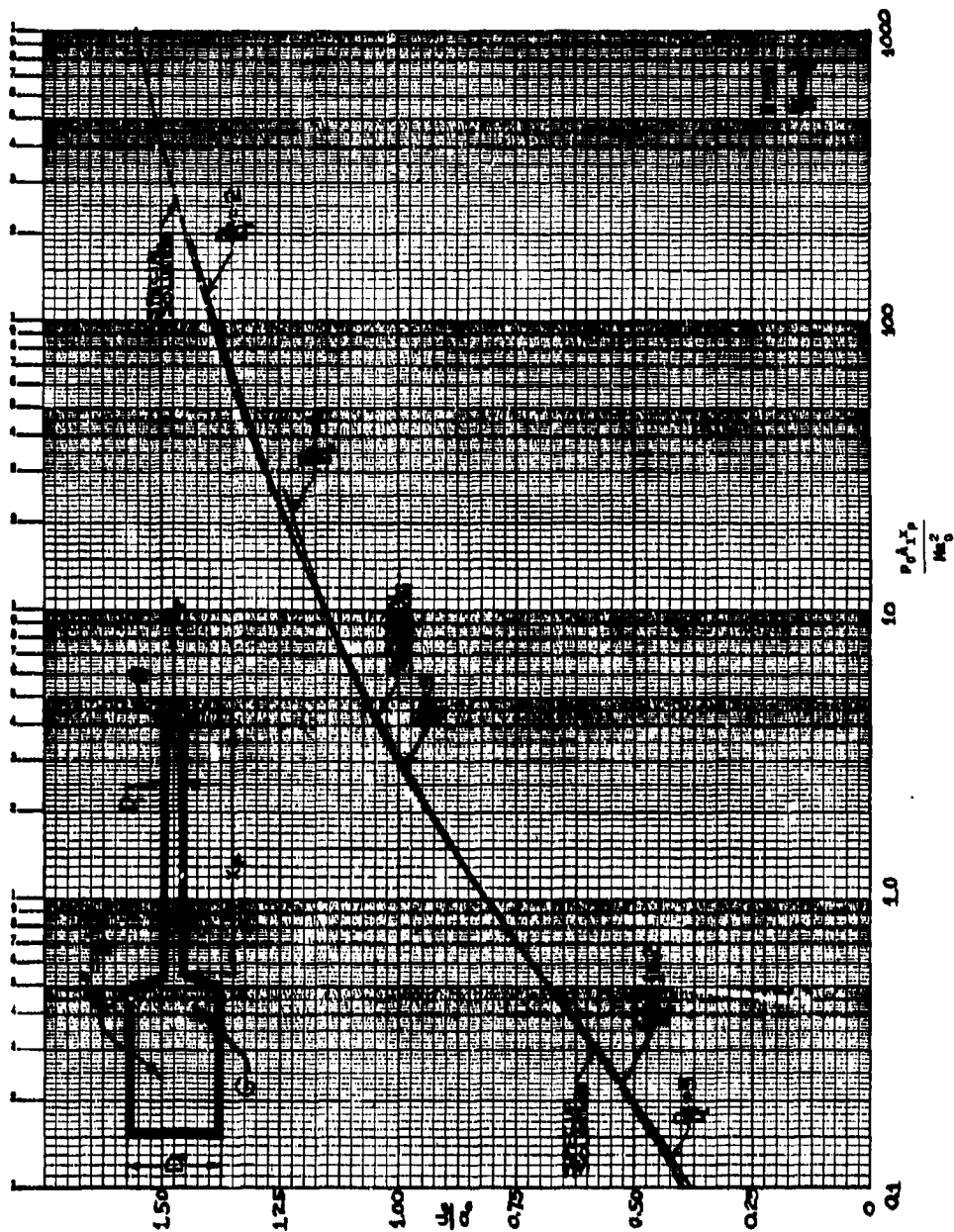
Figure 20(o)

Figure 21(a1)

Figure 21(a2)

240
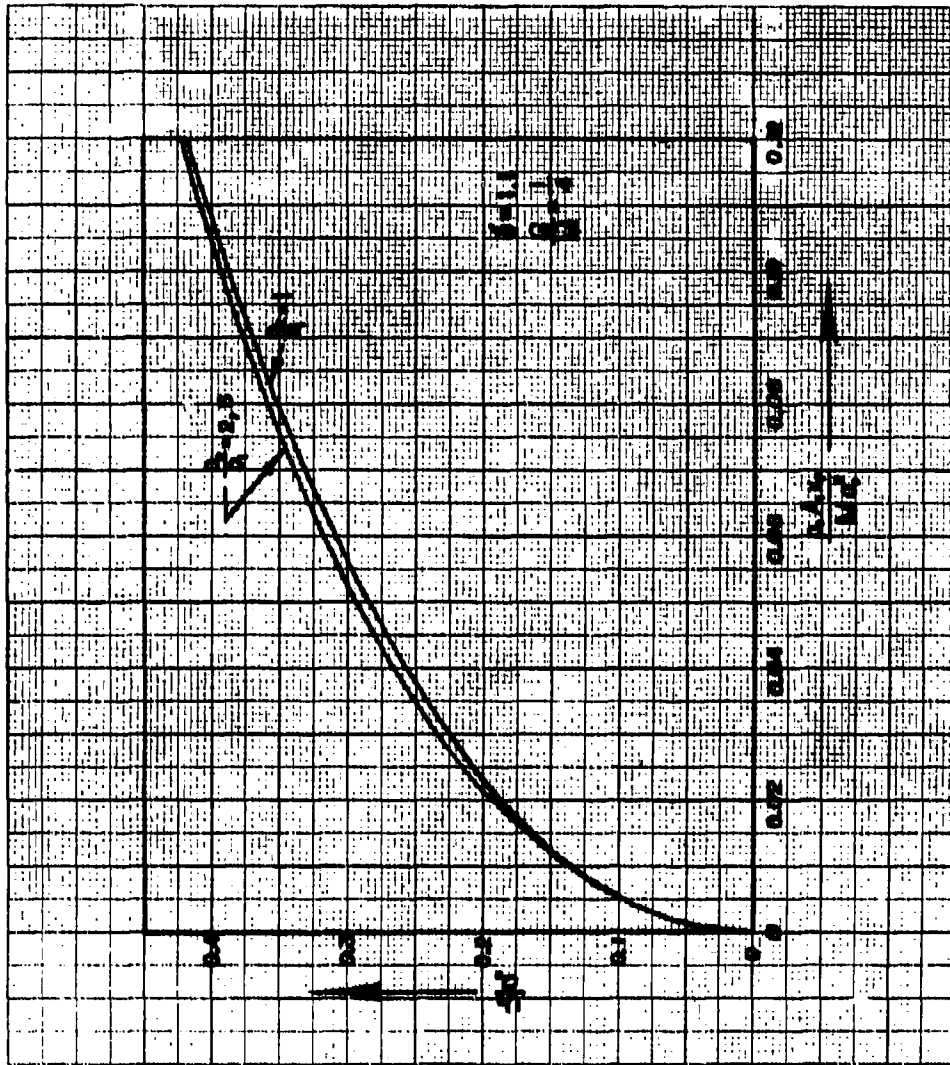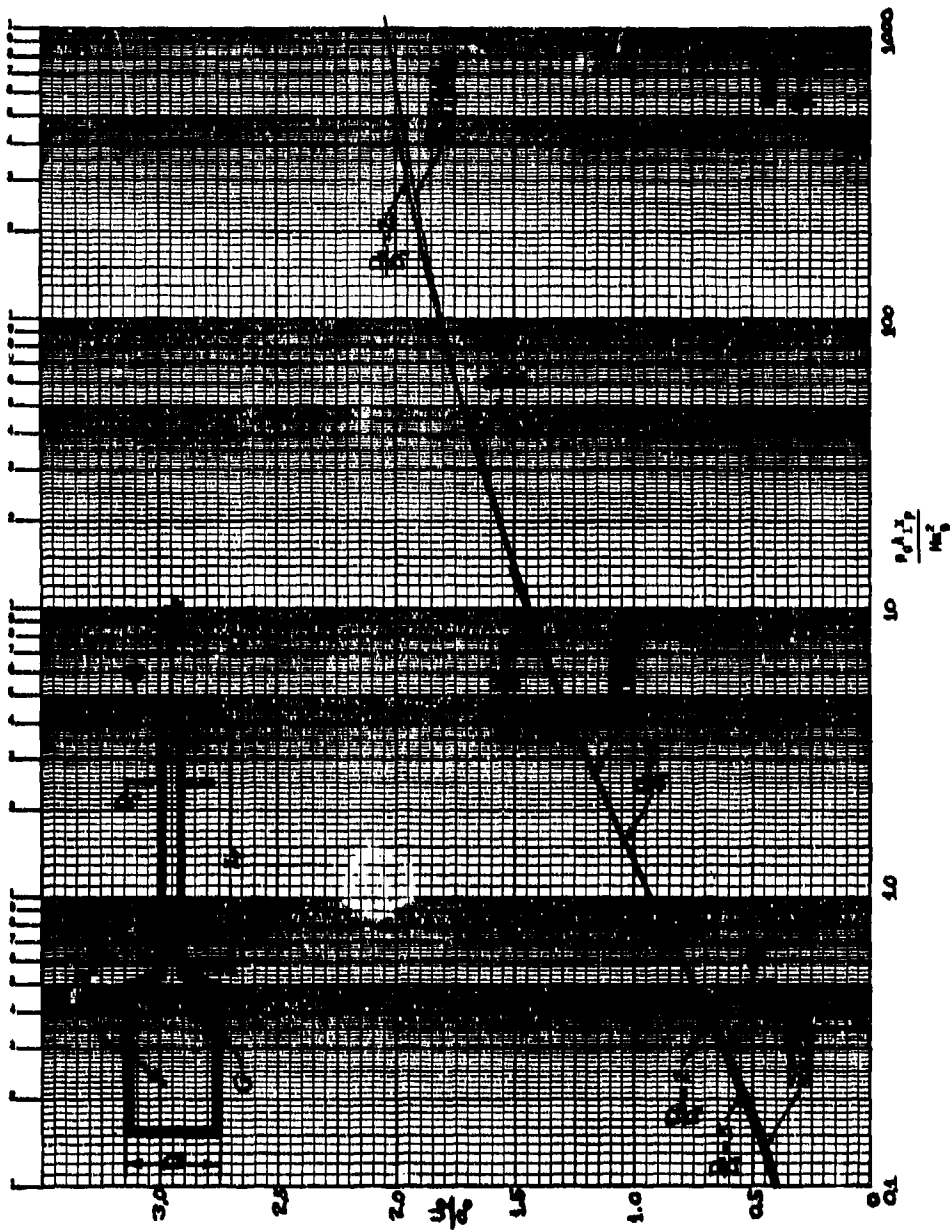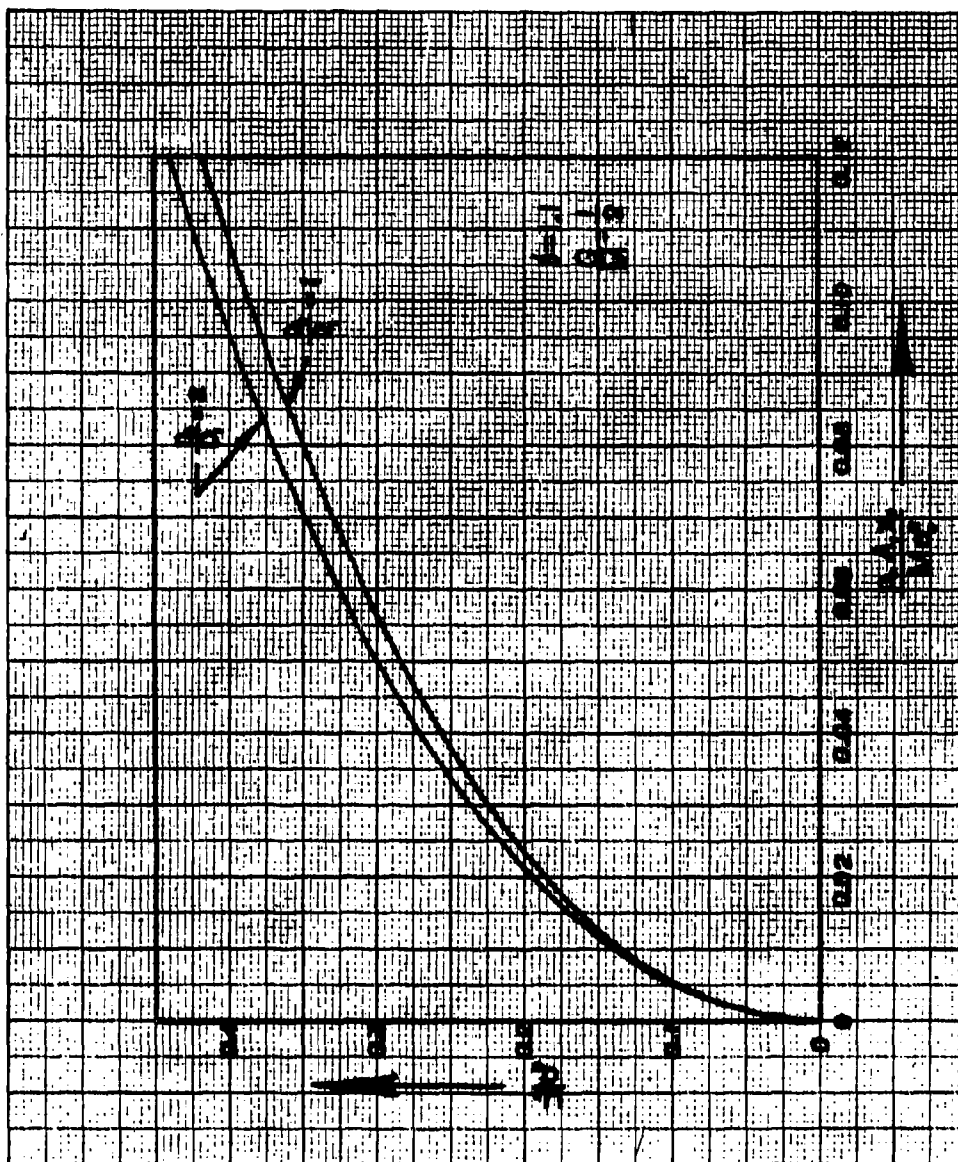
Figure 21(b1)

Figure 21(b2)
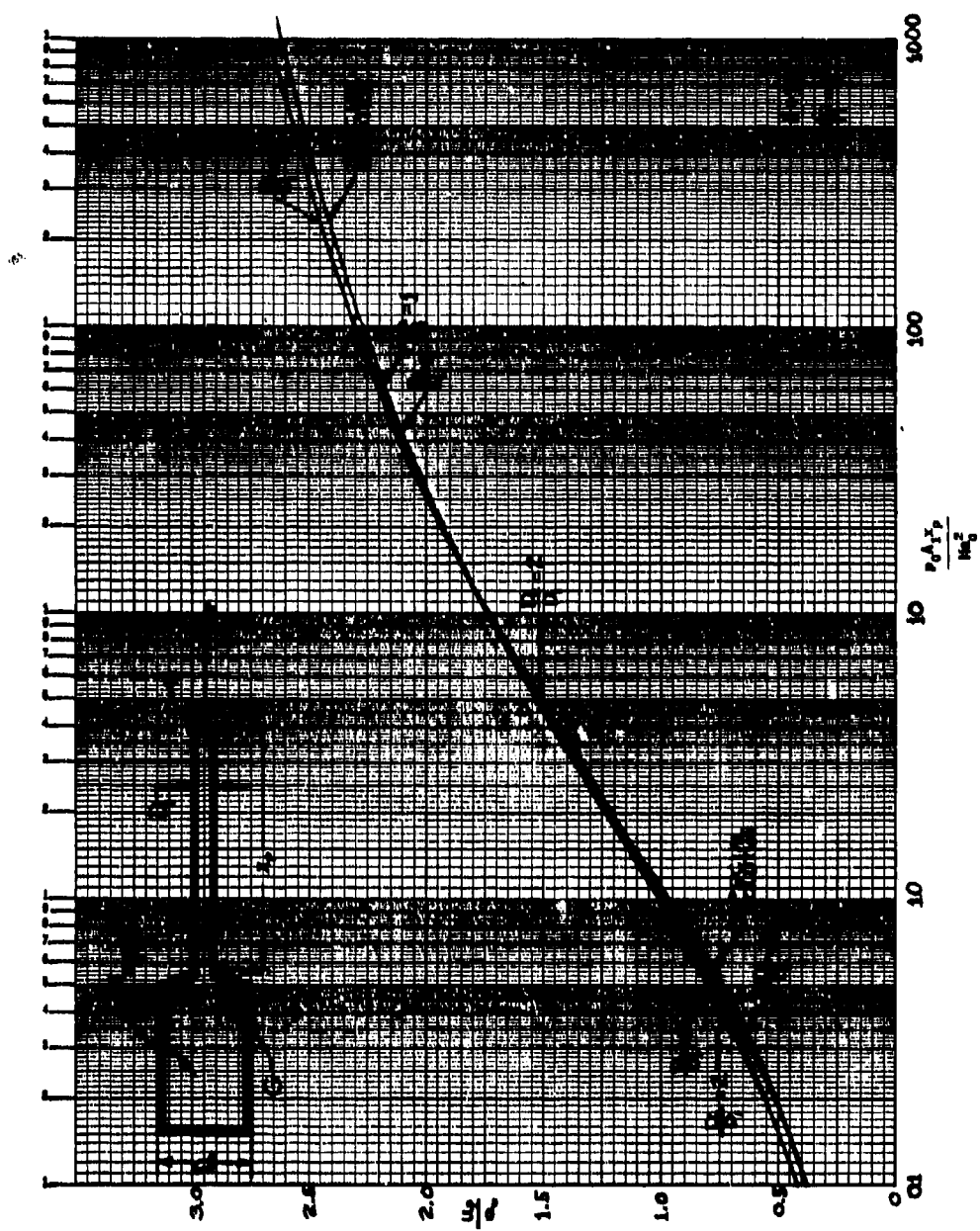
Figure 21(c1)

Figure 21(c2)

244

Figure 21(d1)

$$\frac{P_0 A_* x_p}{M_0^2}$$

Figure 21(d2)

246
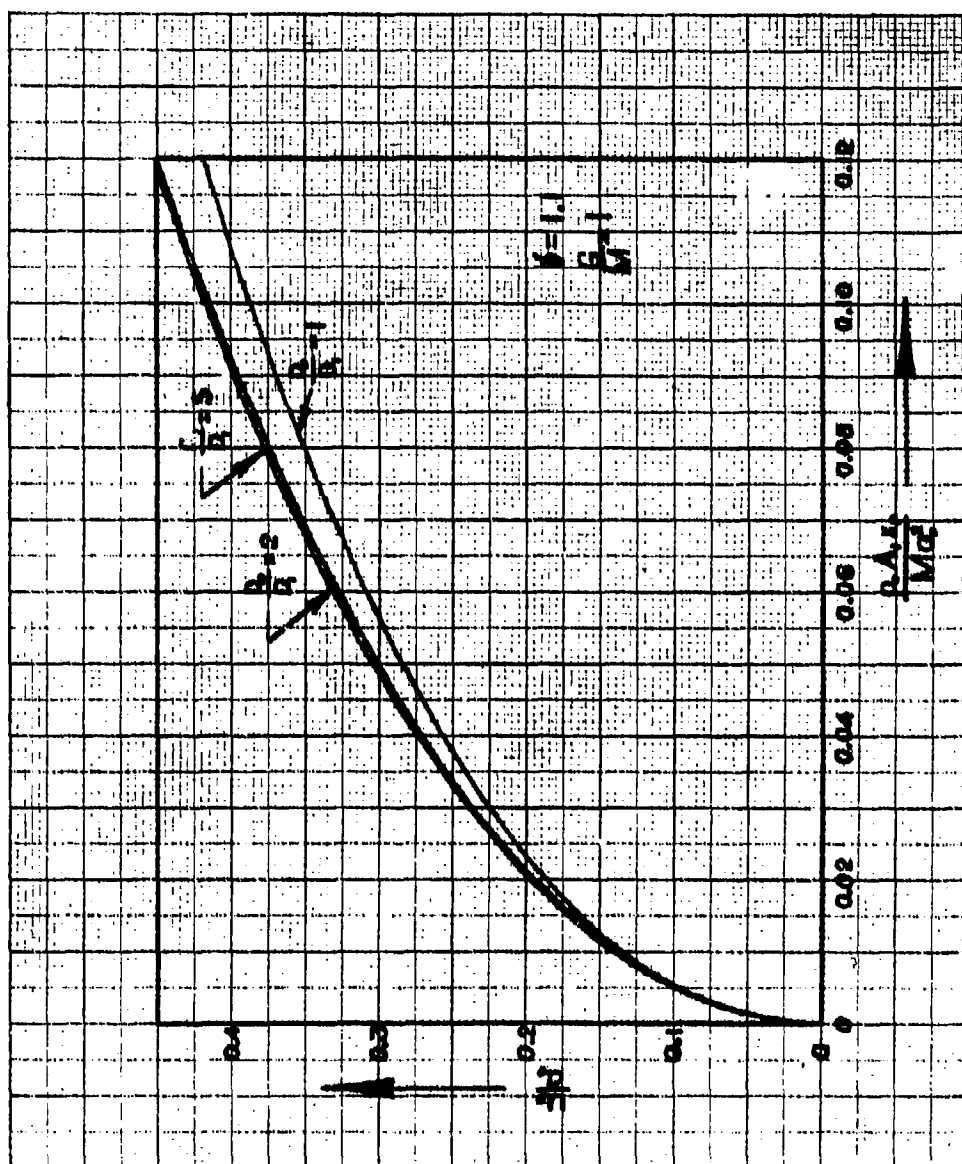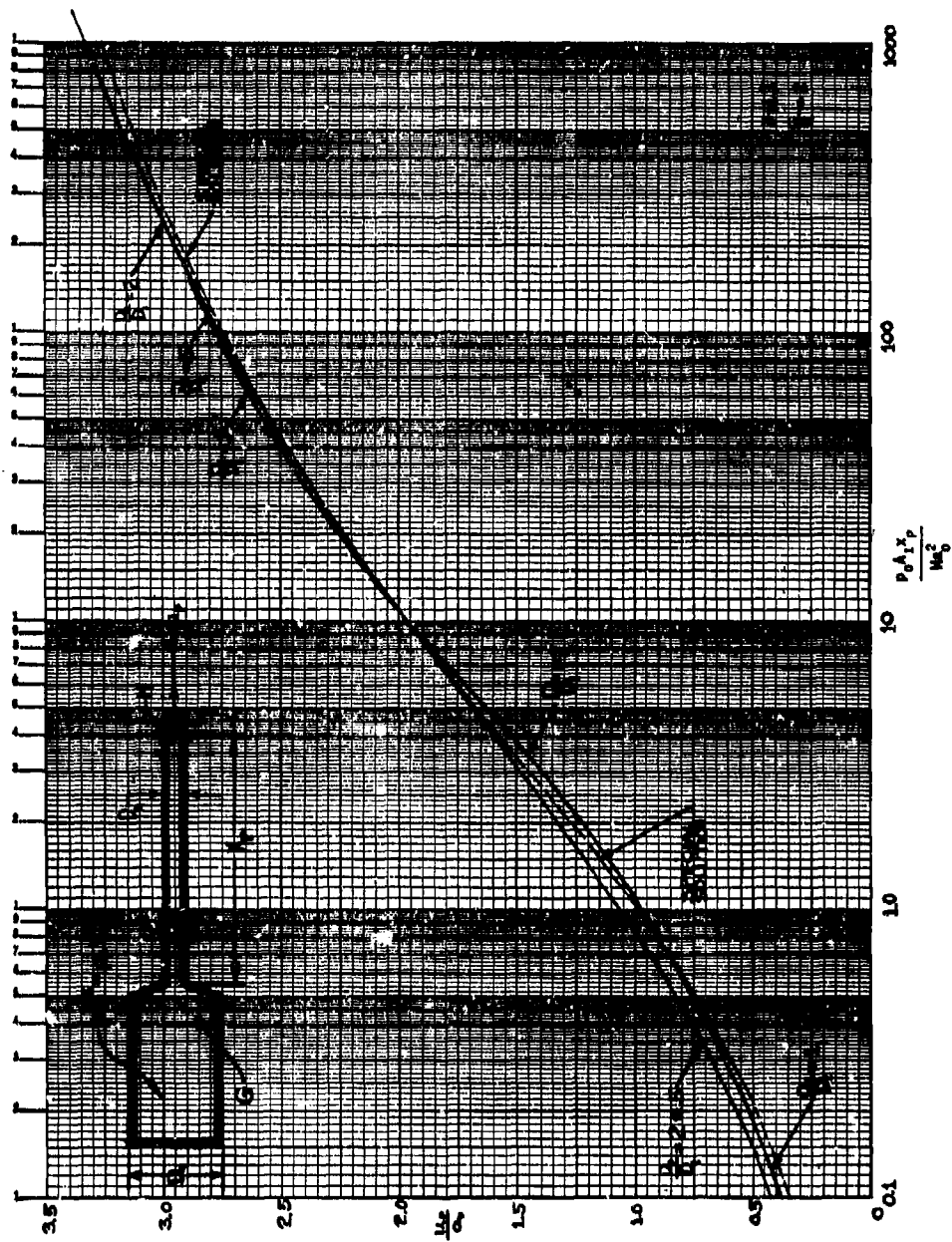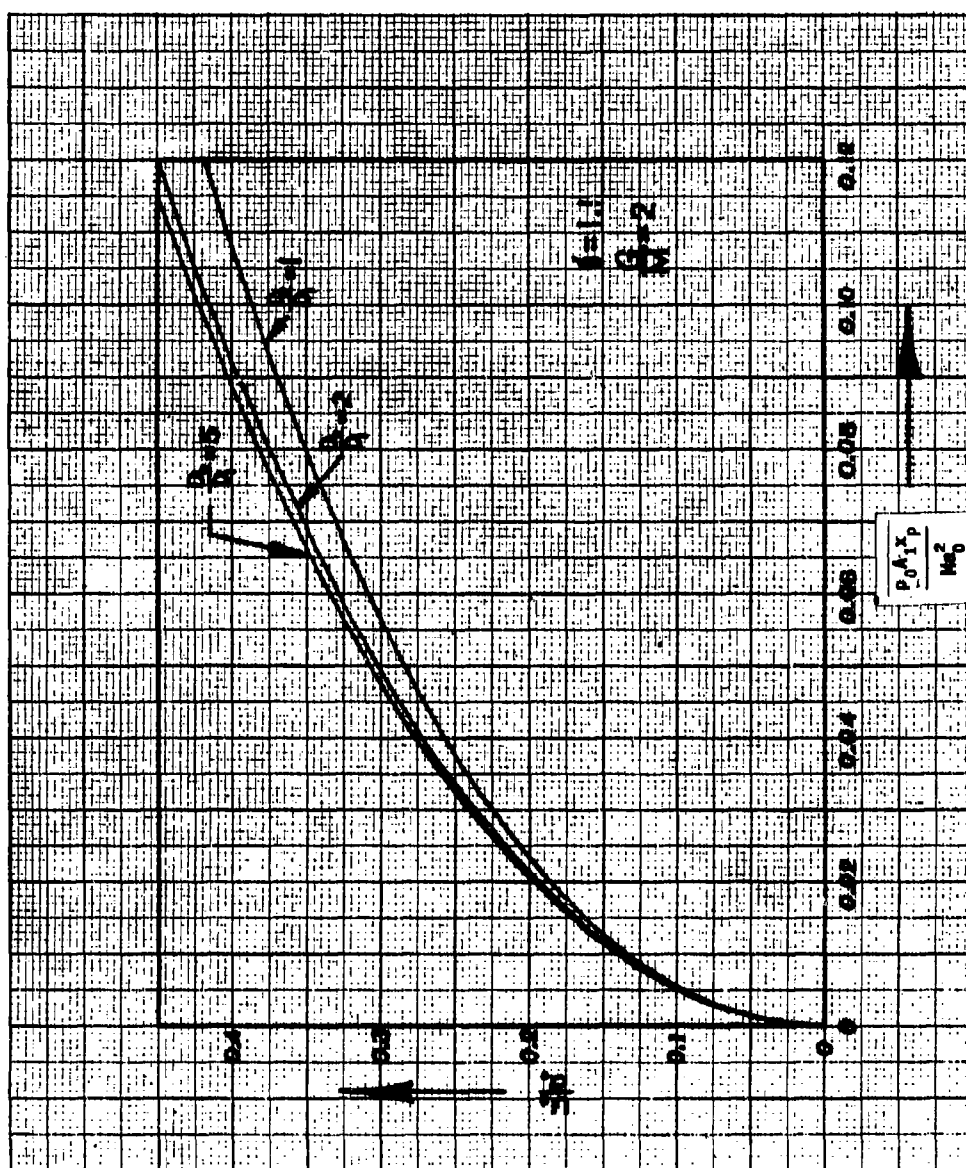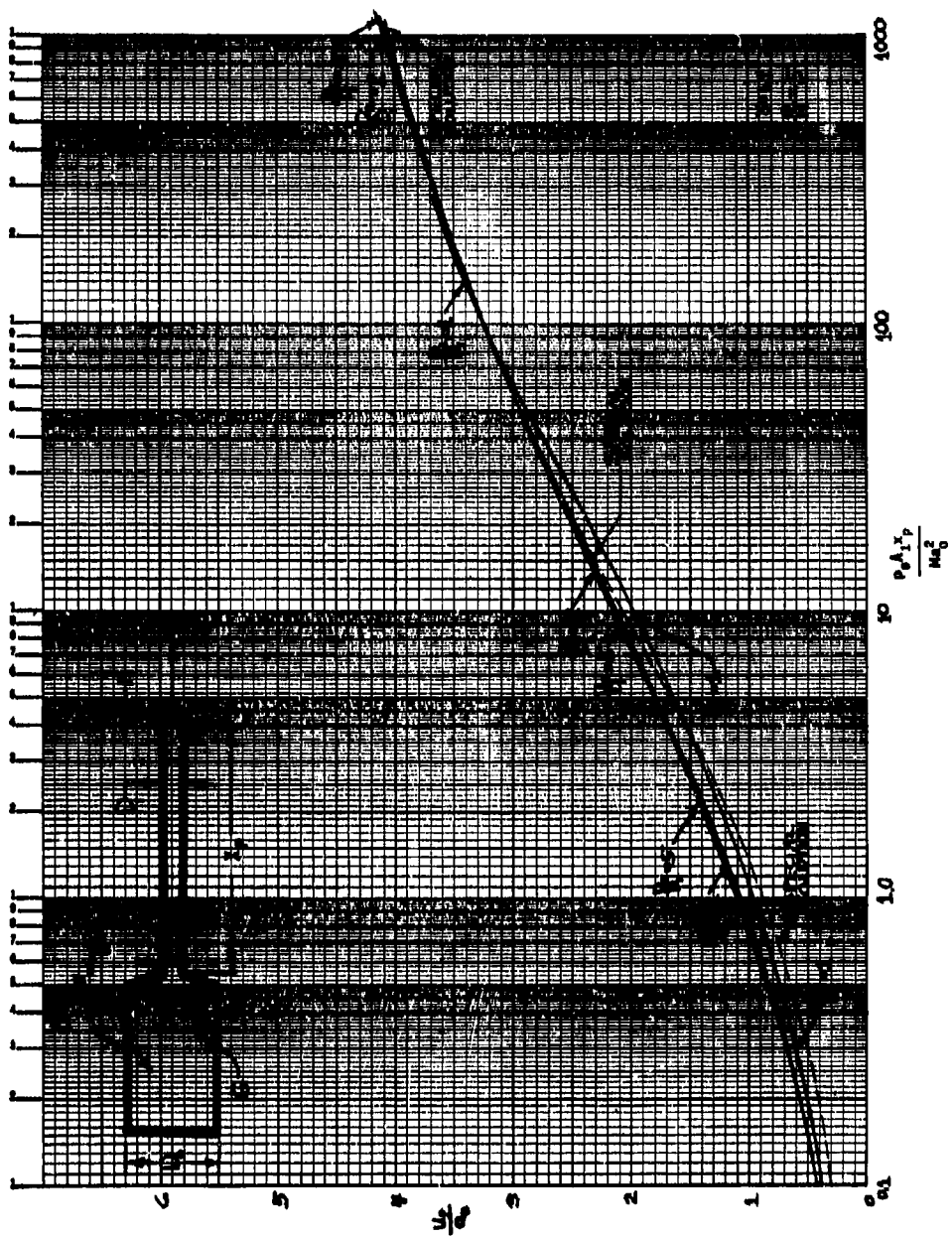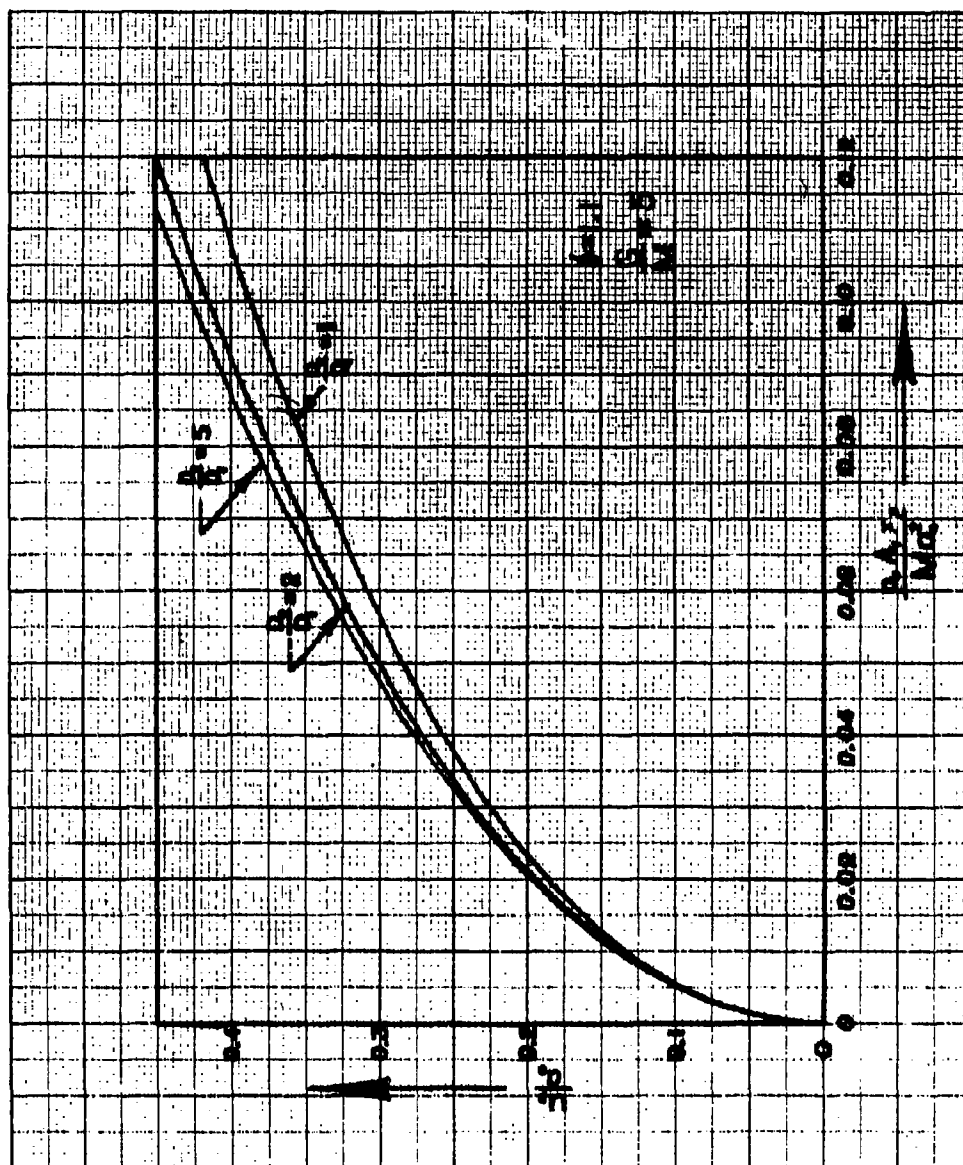
Figure 21(e1)

Figure 21(e2)
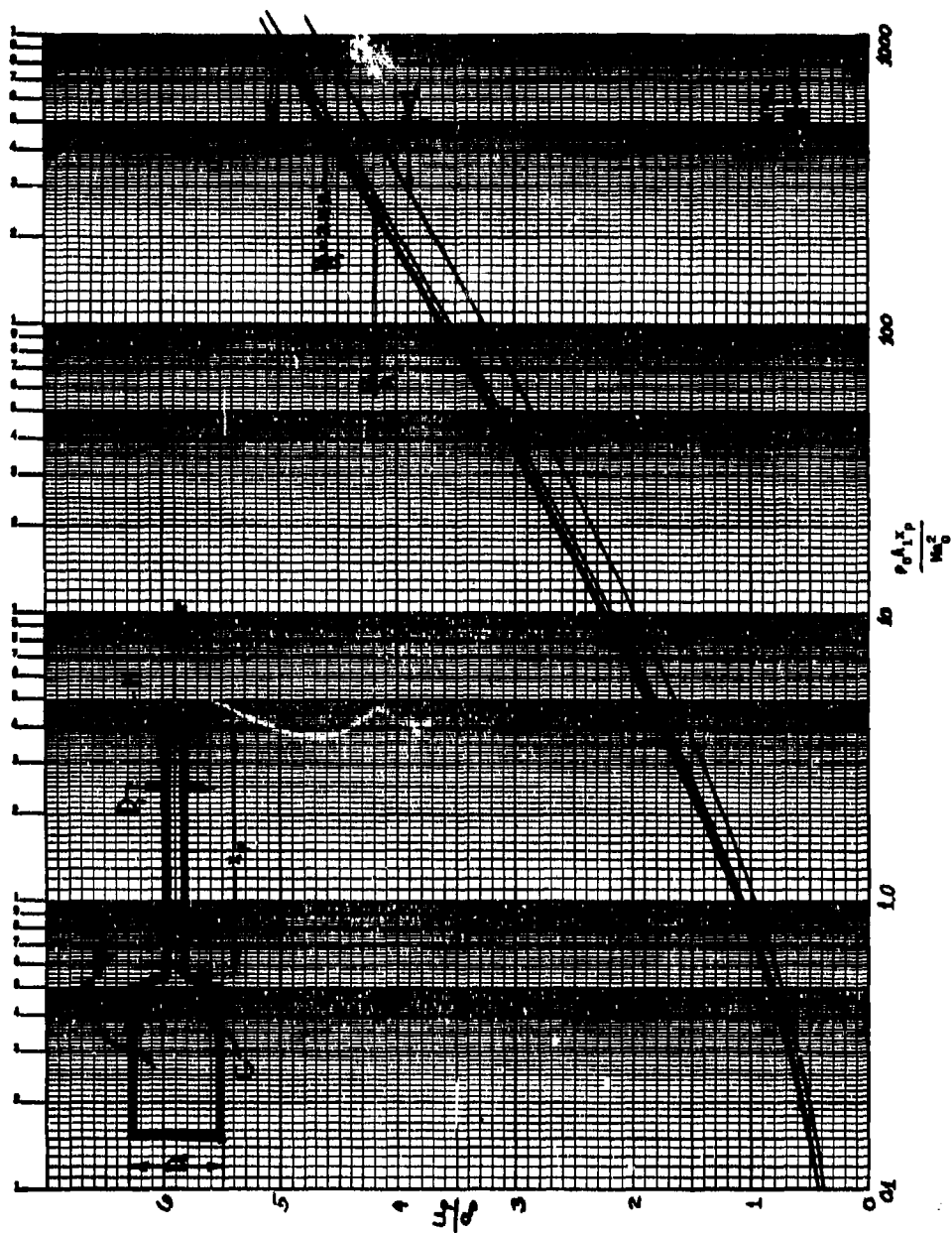
Figure 21(f1)
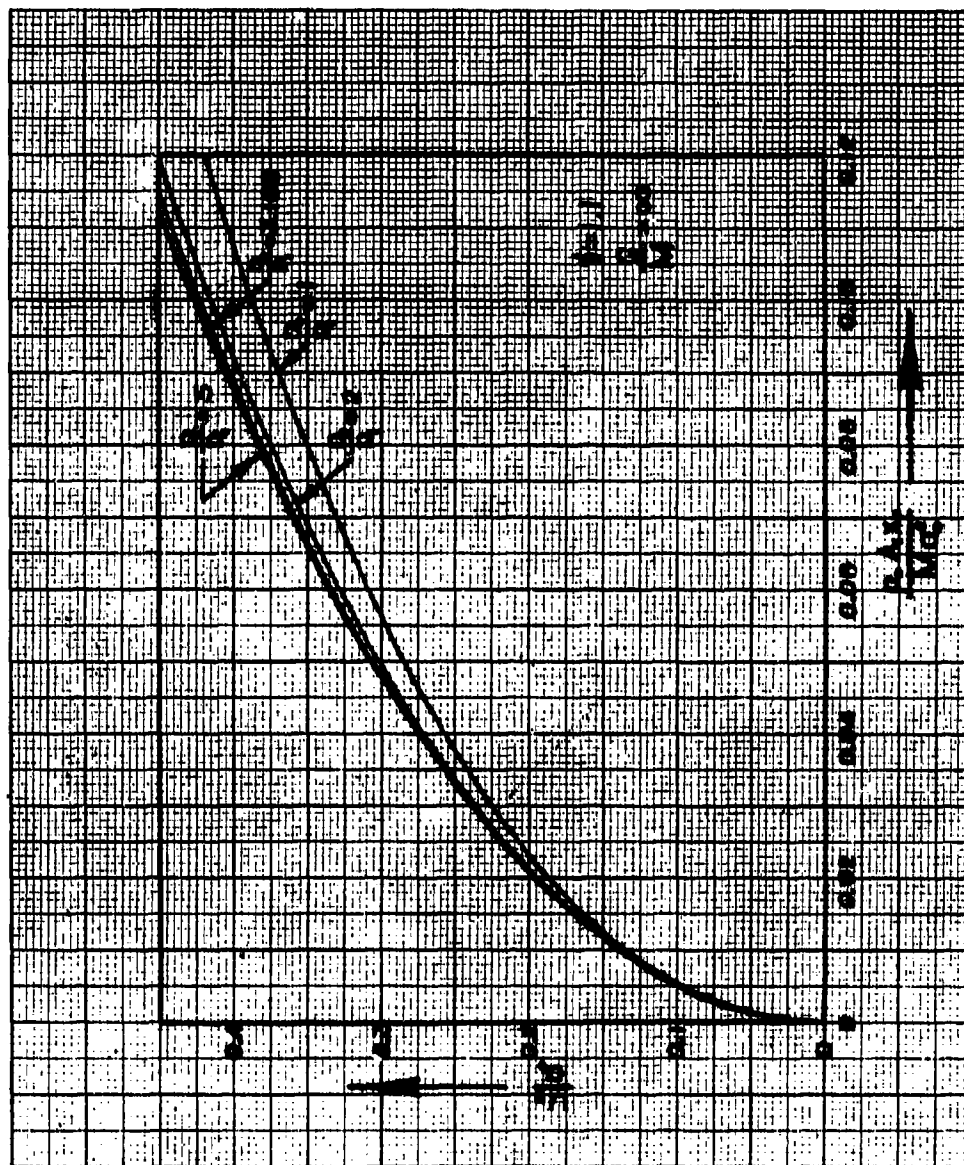
Figure 21(f2)
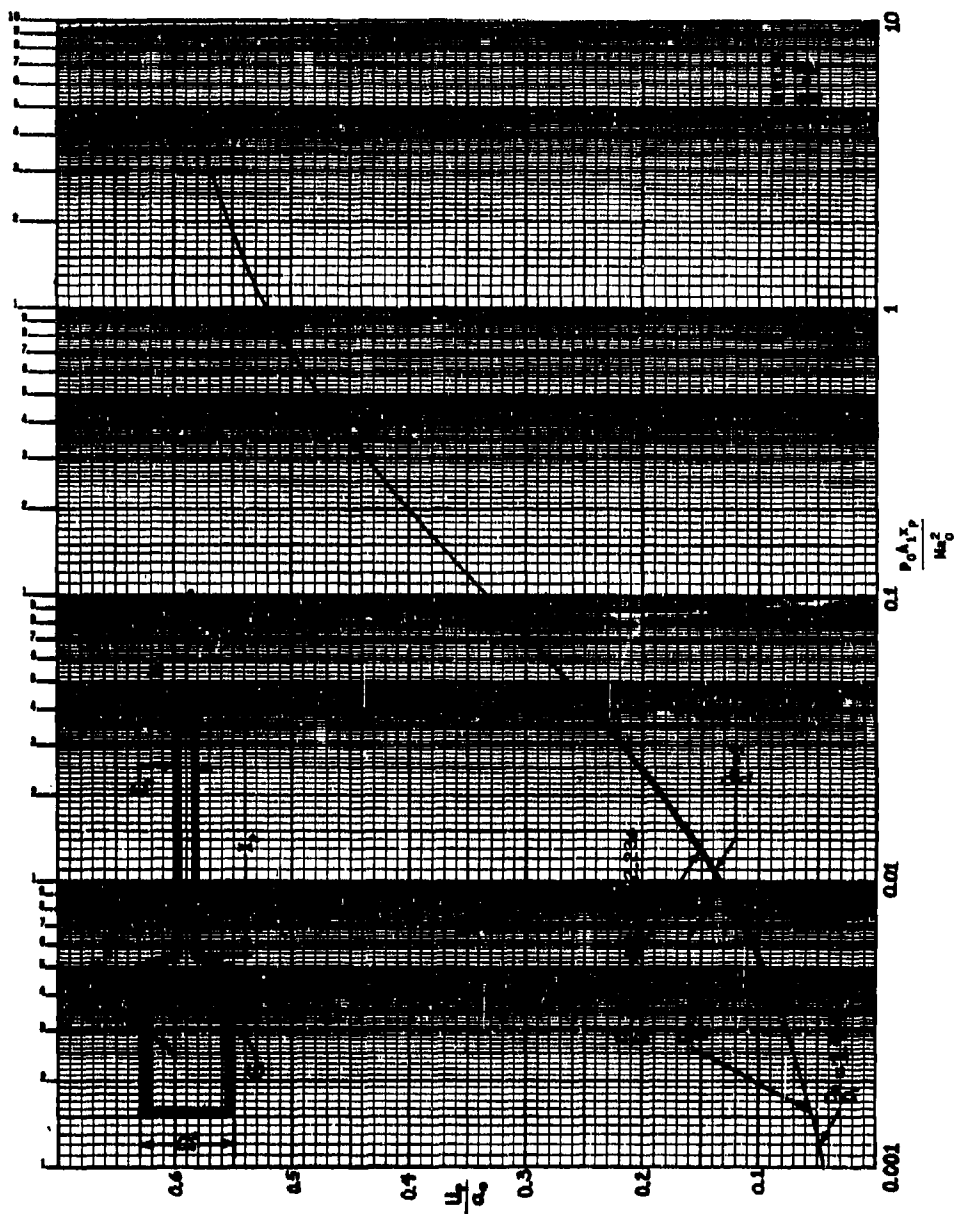
Figure 21(g1)
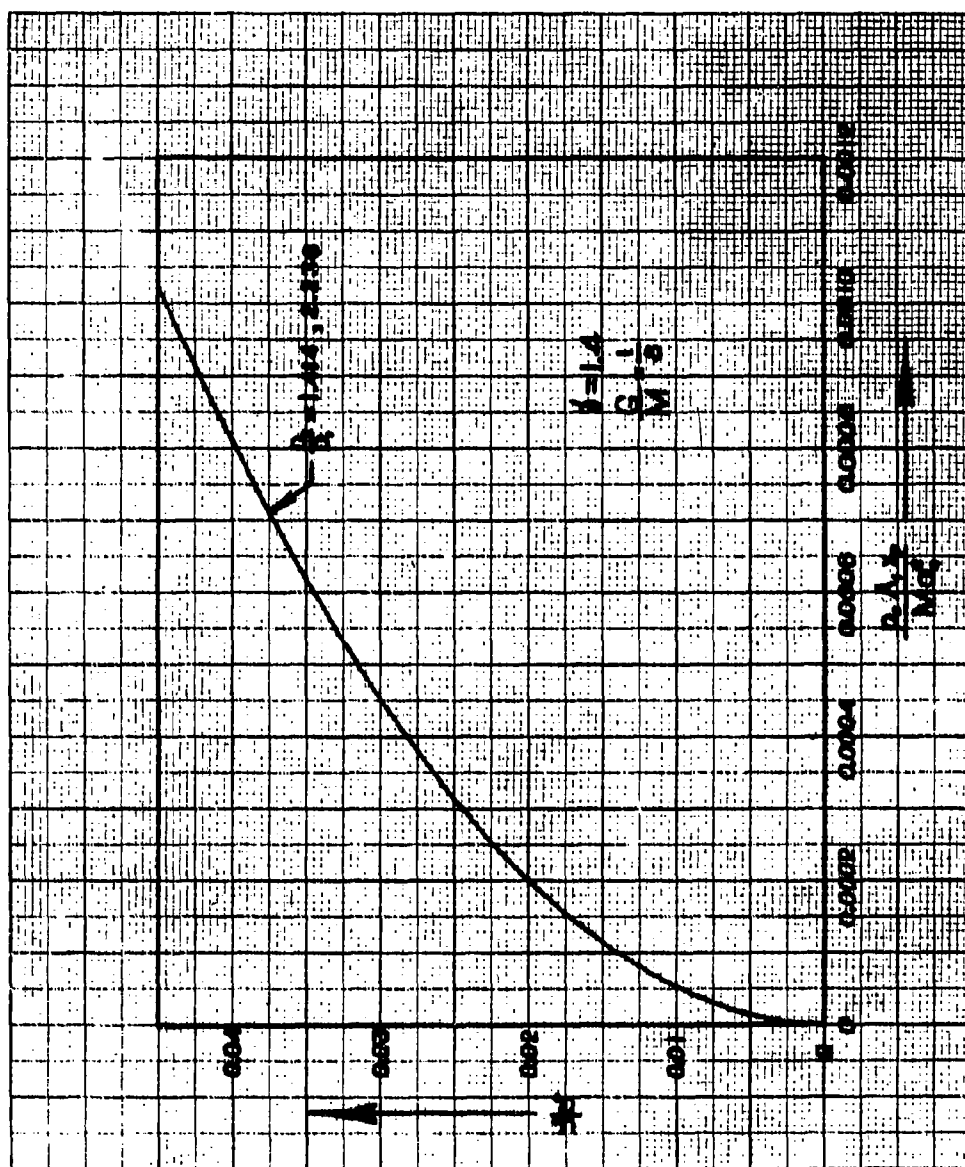
Figure 21(g2)
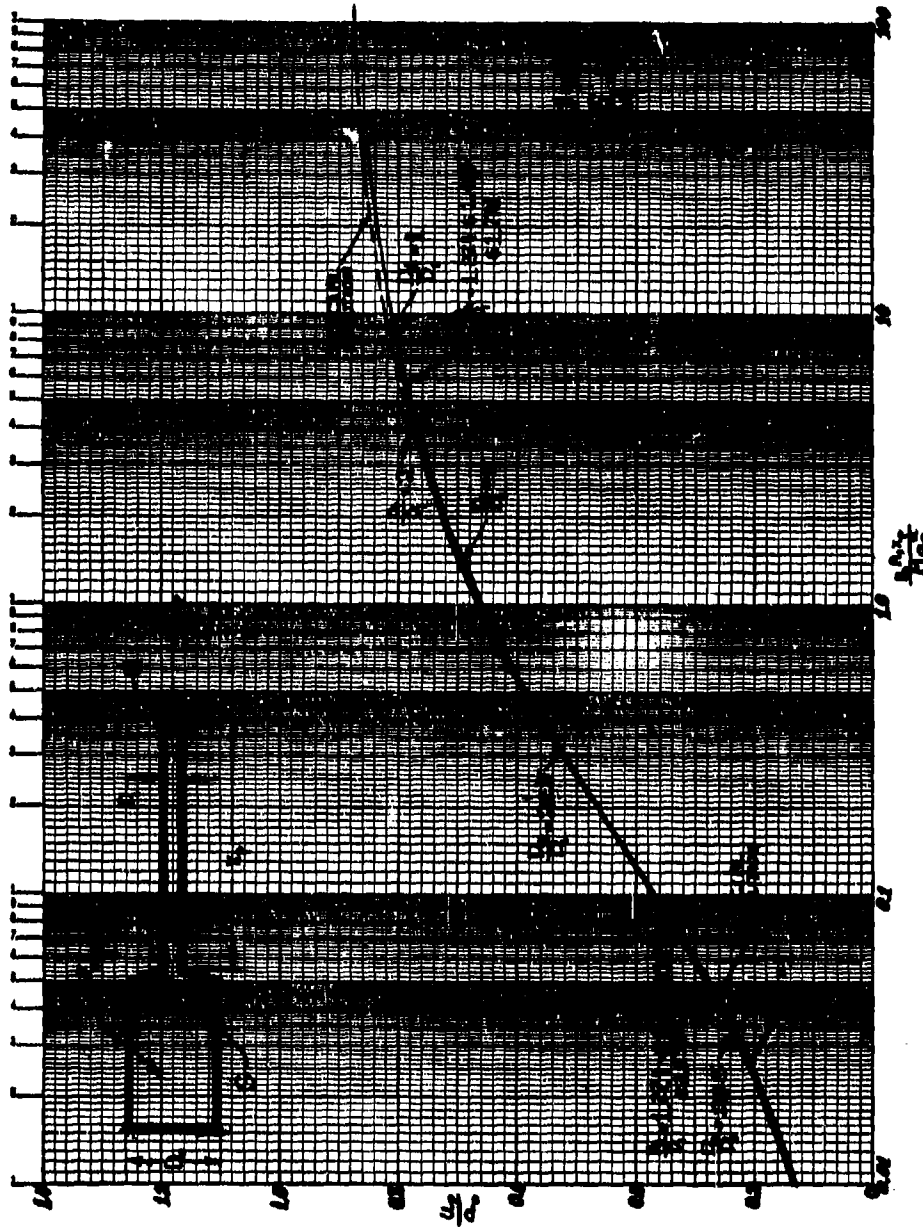
Figure 21(h1)

Figure 21(h2)

254

Figure 21(ii)

Figure 21(12)

256
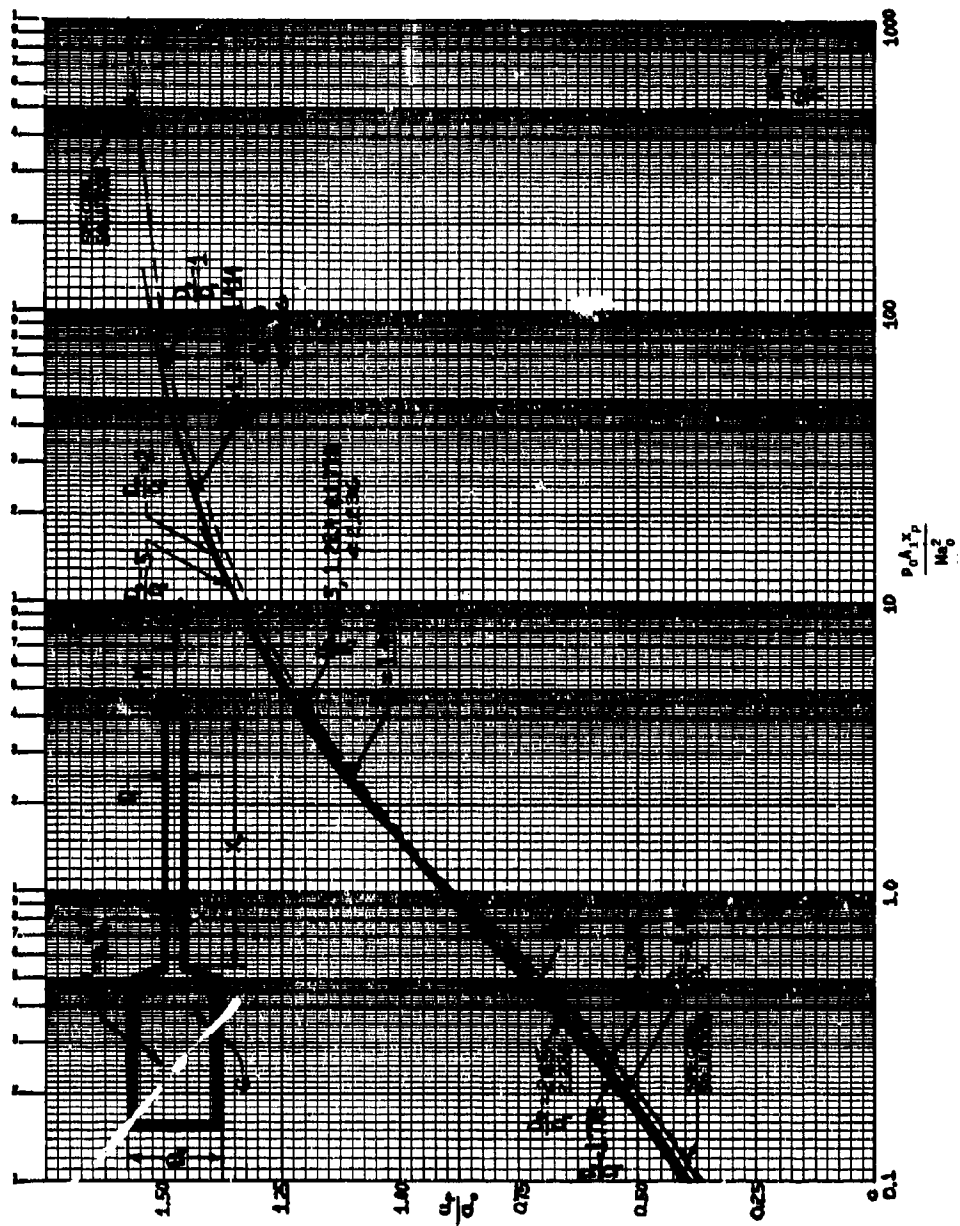
Figure 21(j1)

Figure 21(J2)

258
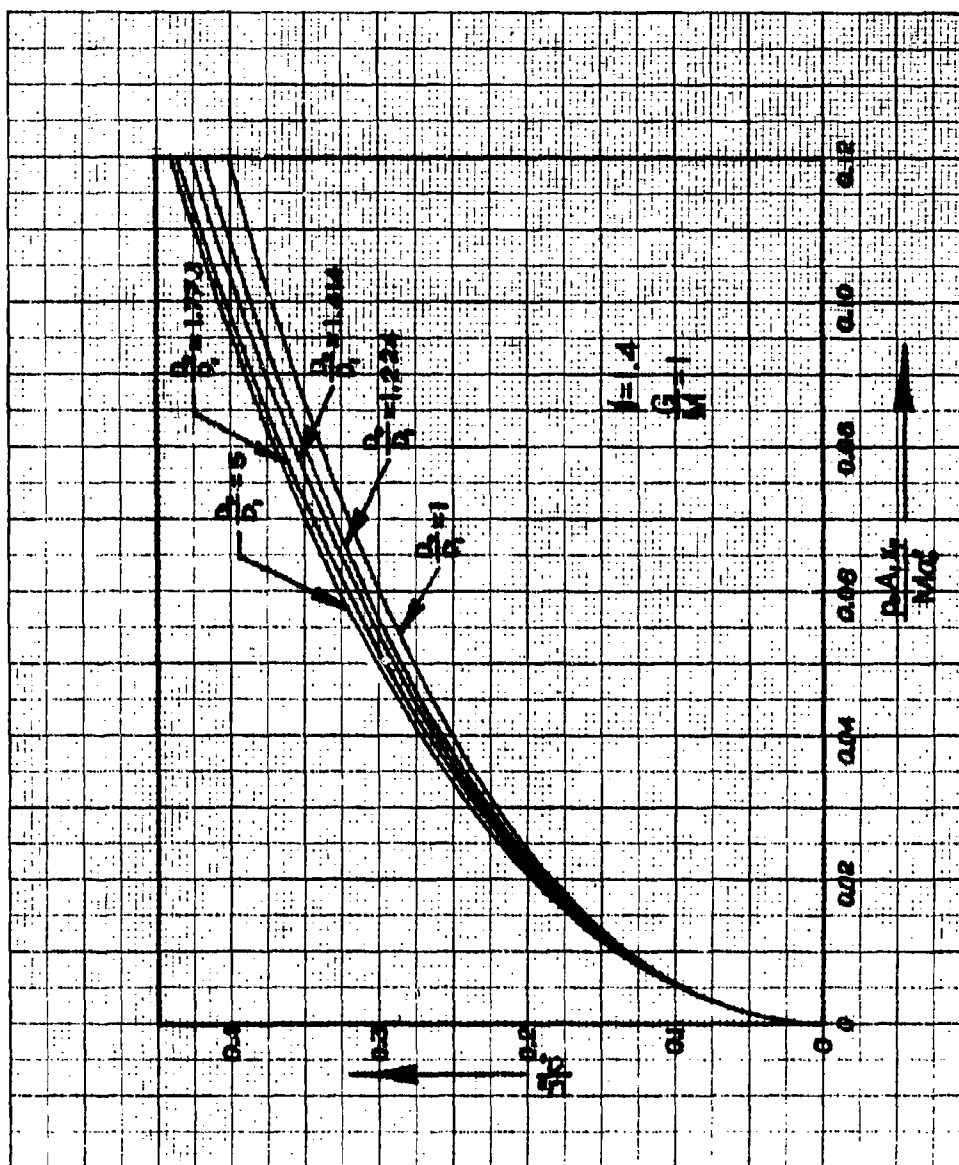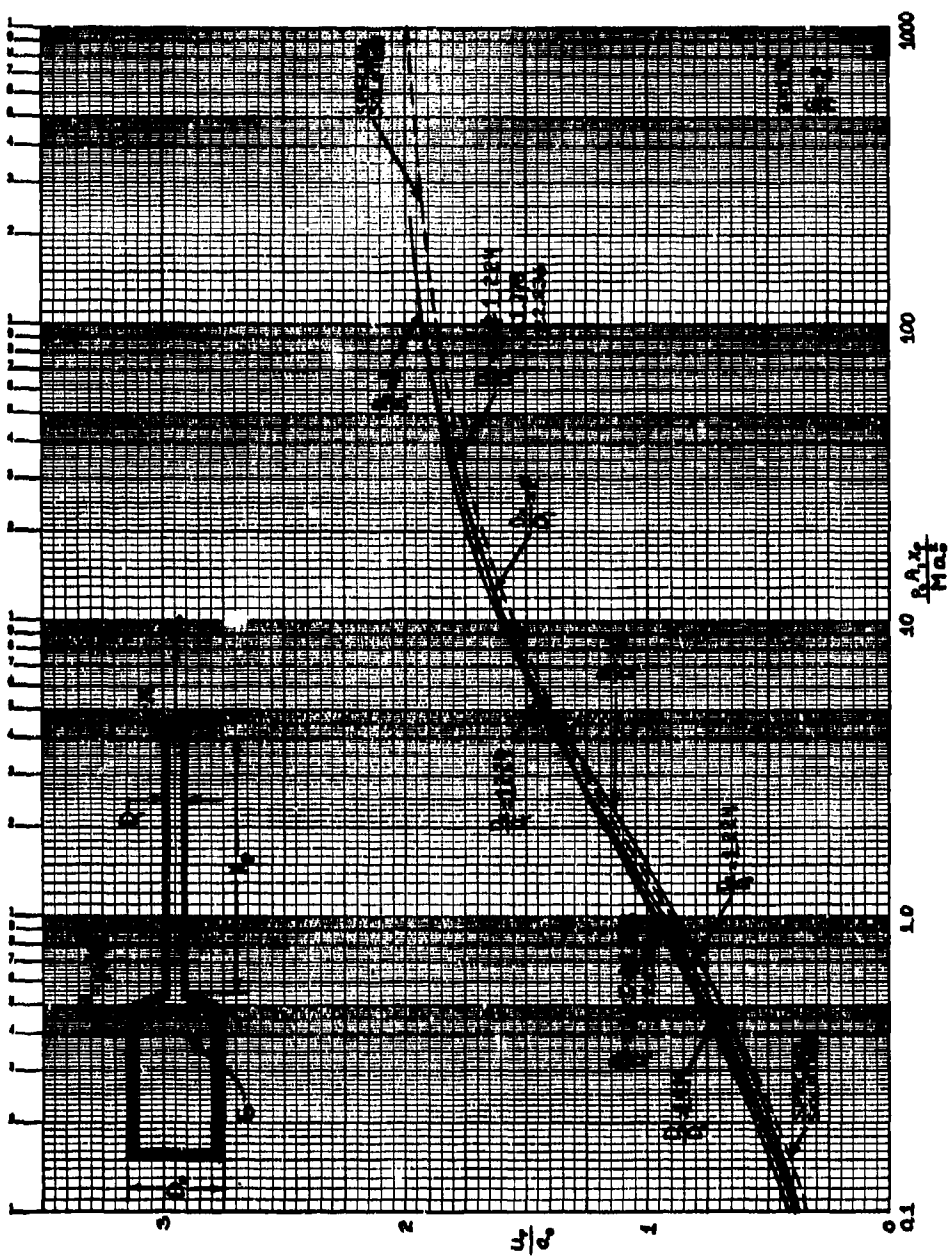
Figure 21(k1)

Figure 21(k2)
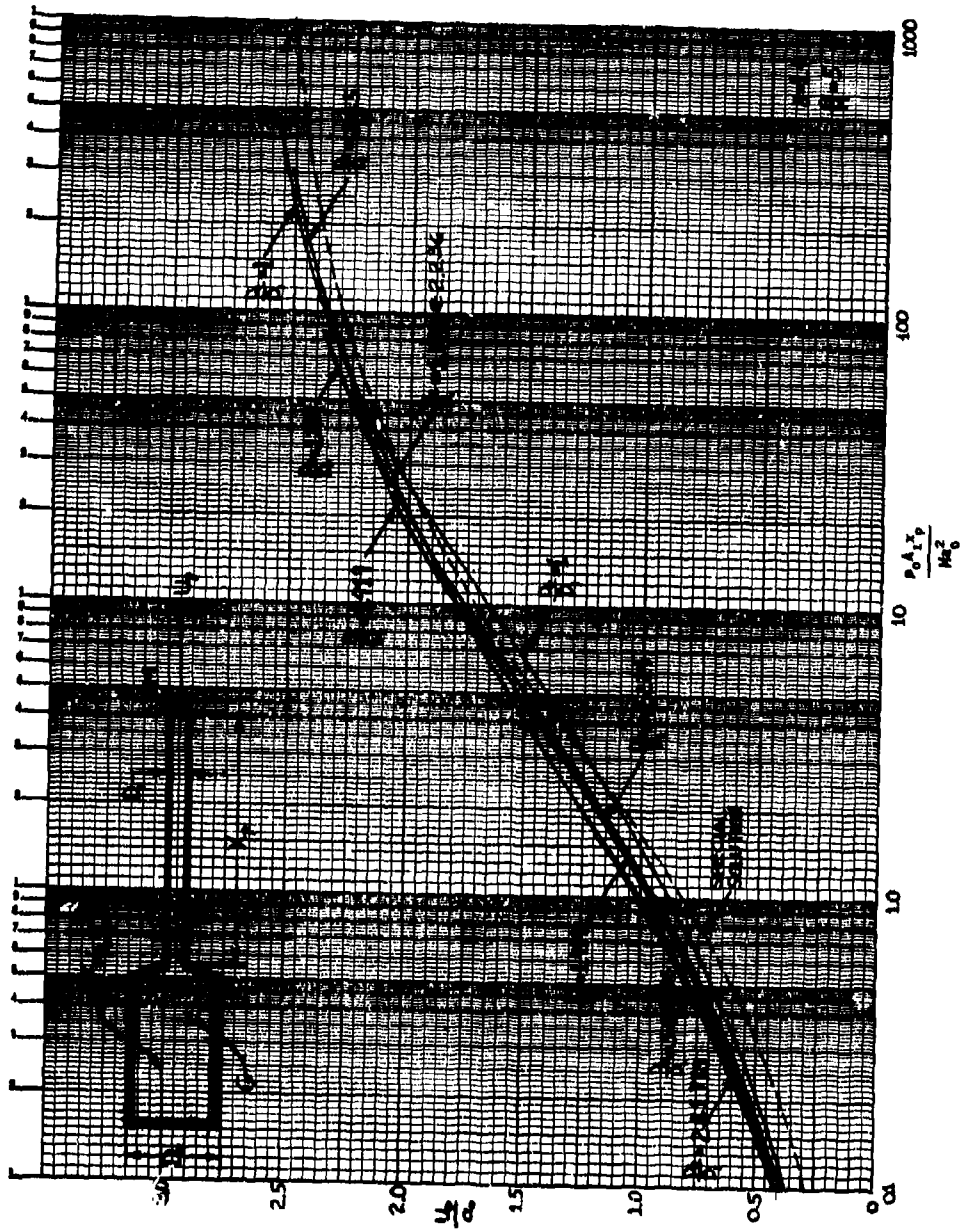
Figure 21(11)
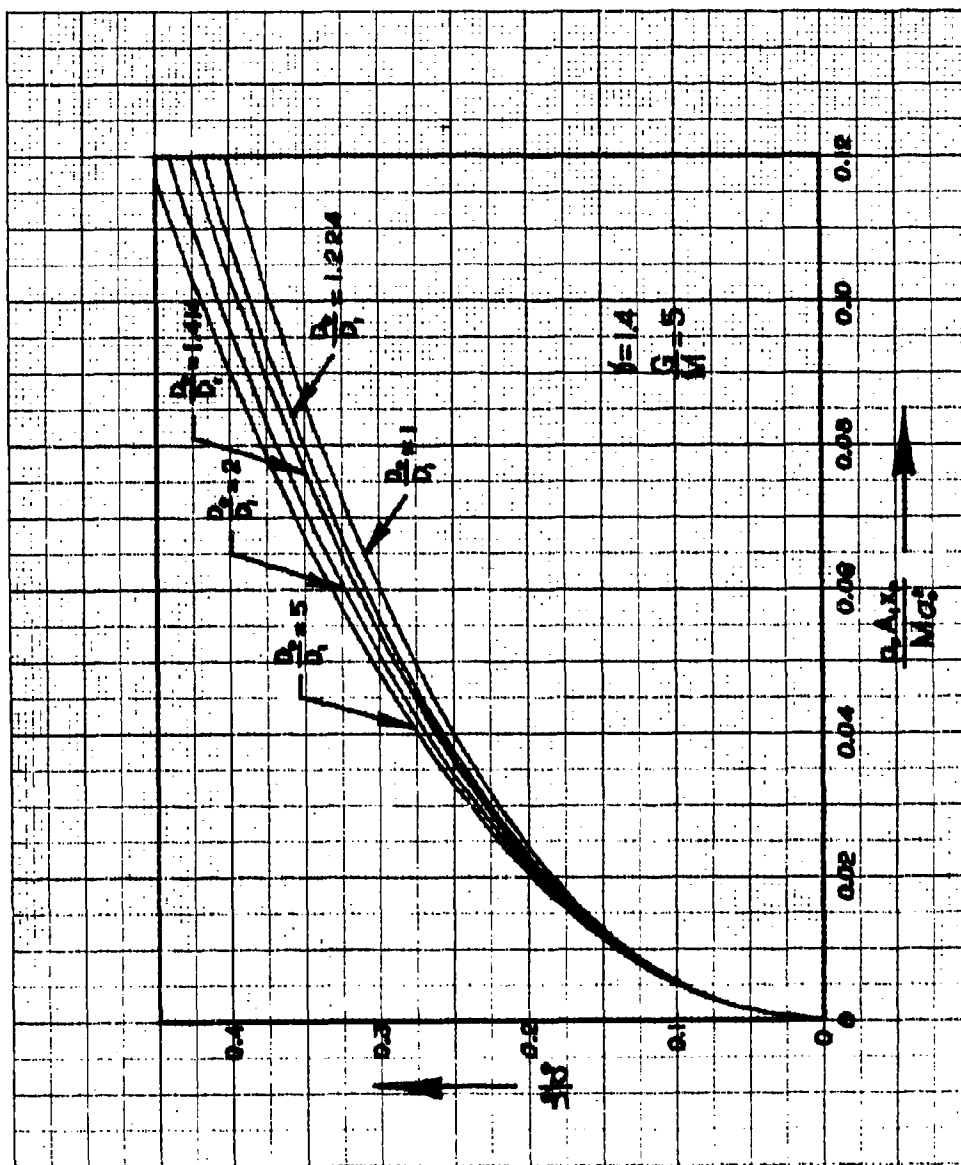
Figure 21(12)
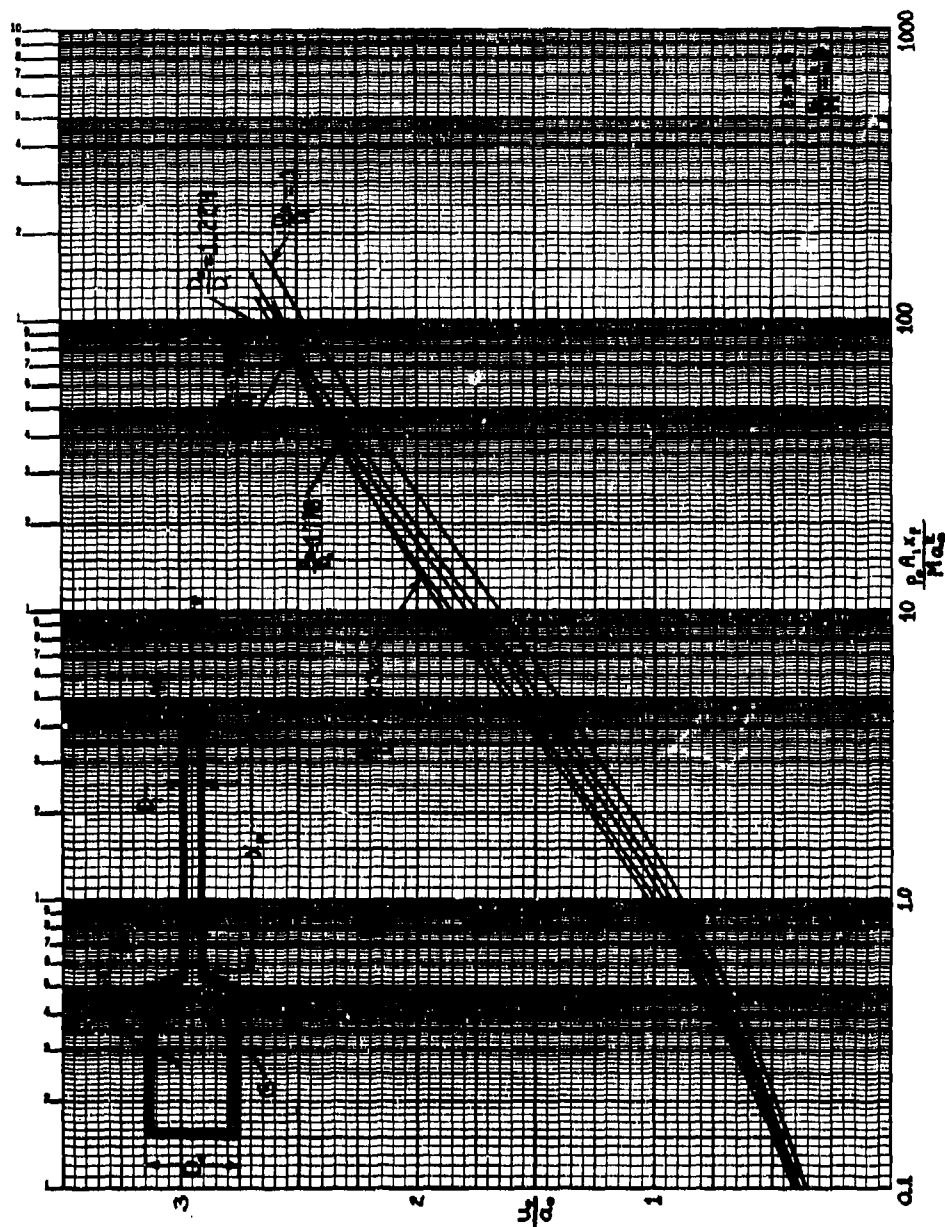
Figure 21(m1)
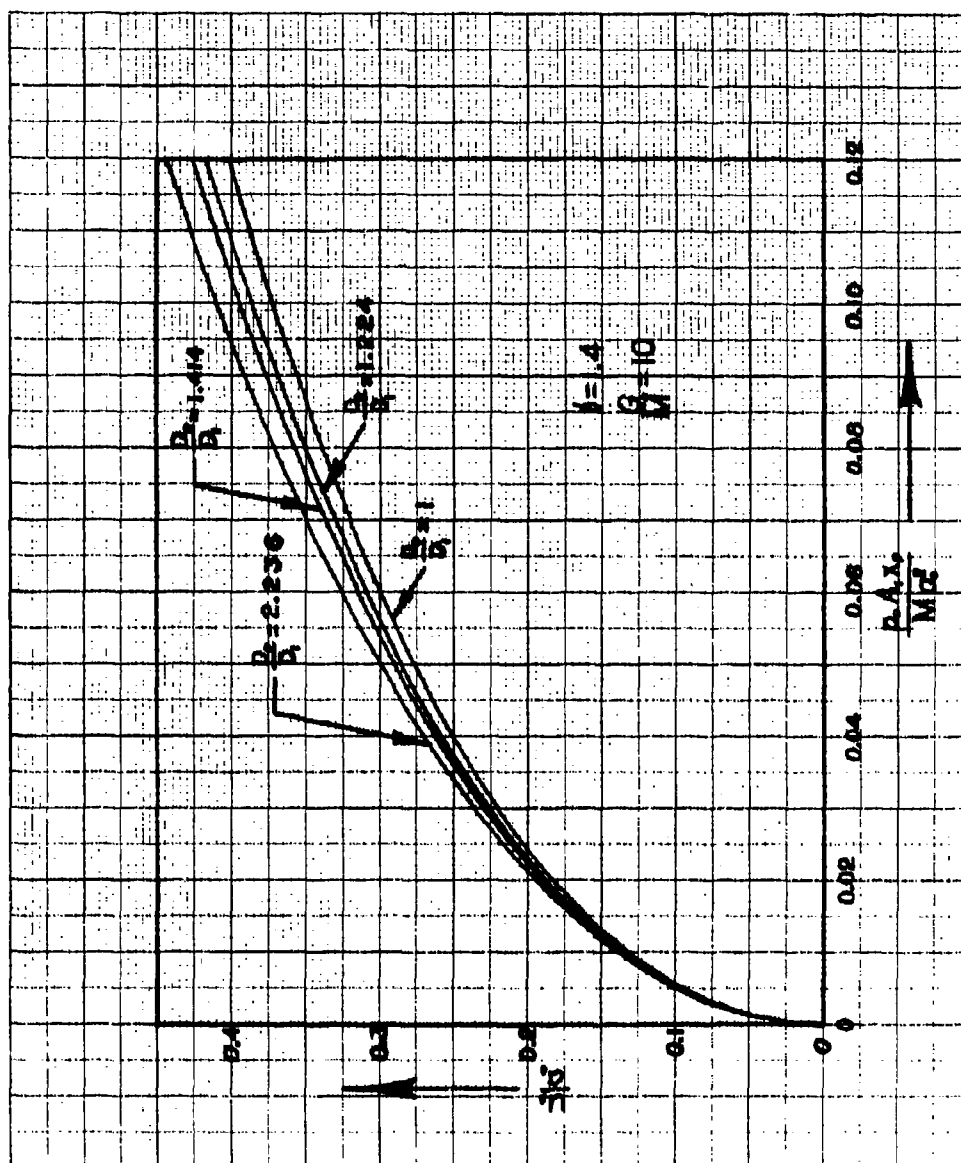
Figure 21(m2)
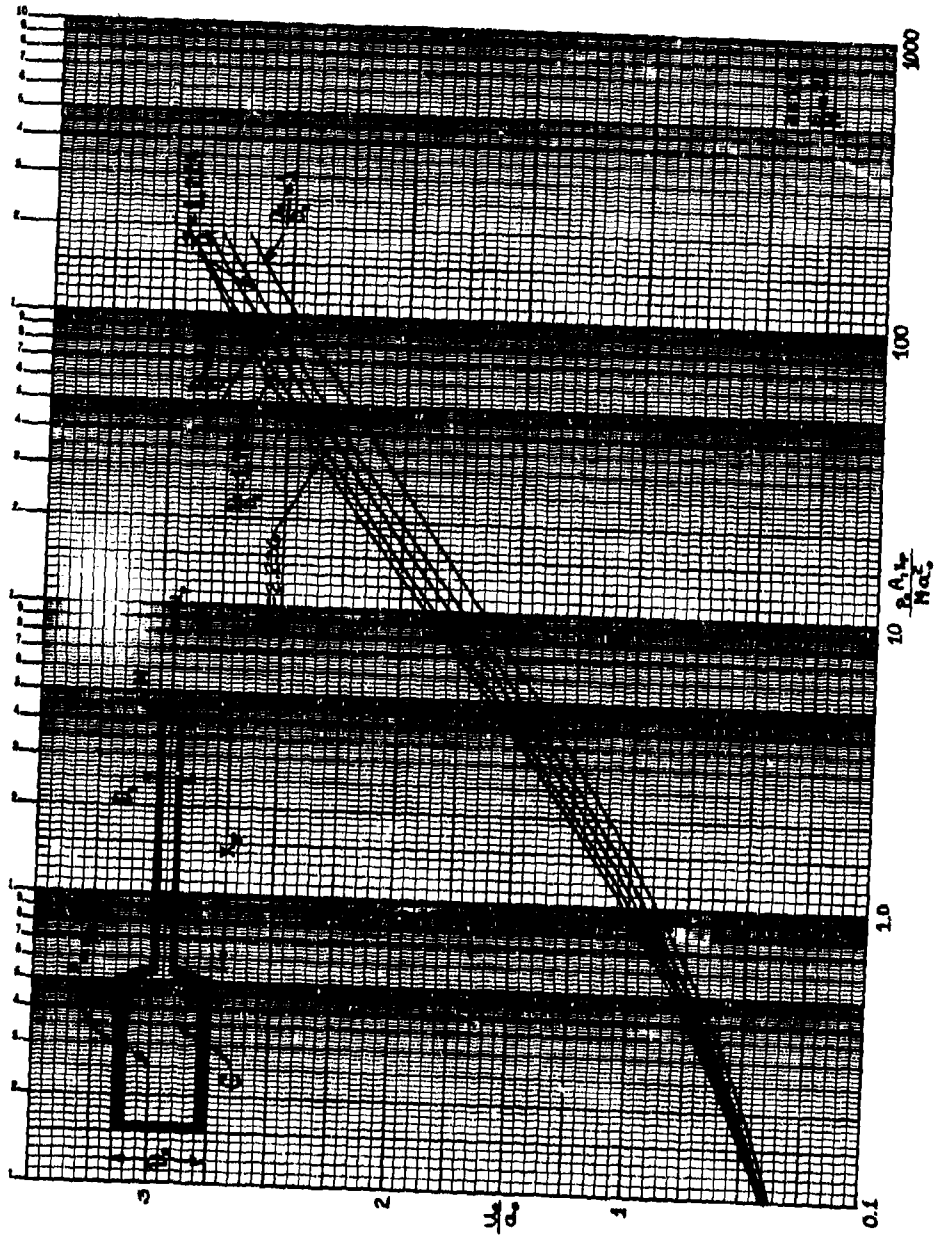
Figure 21(n1)
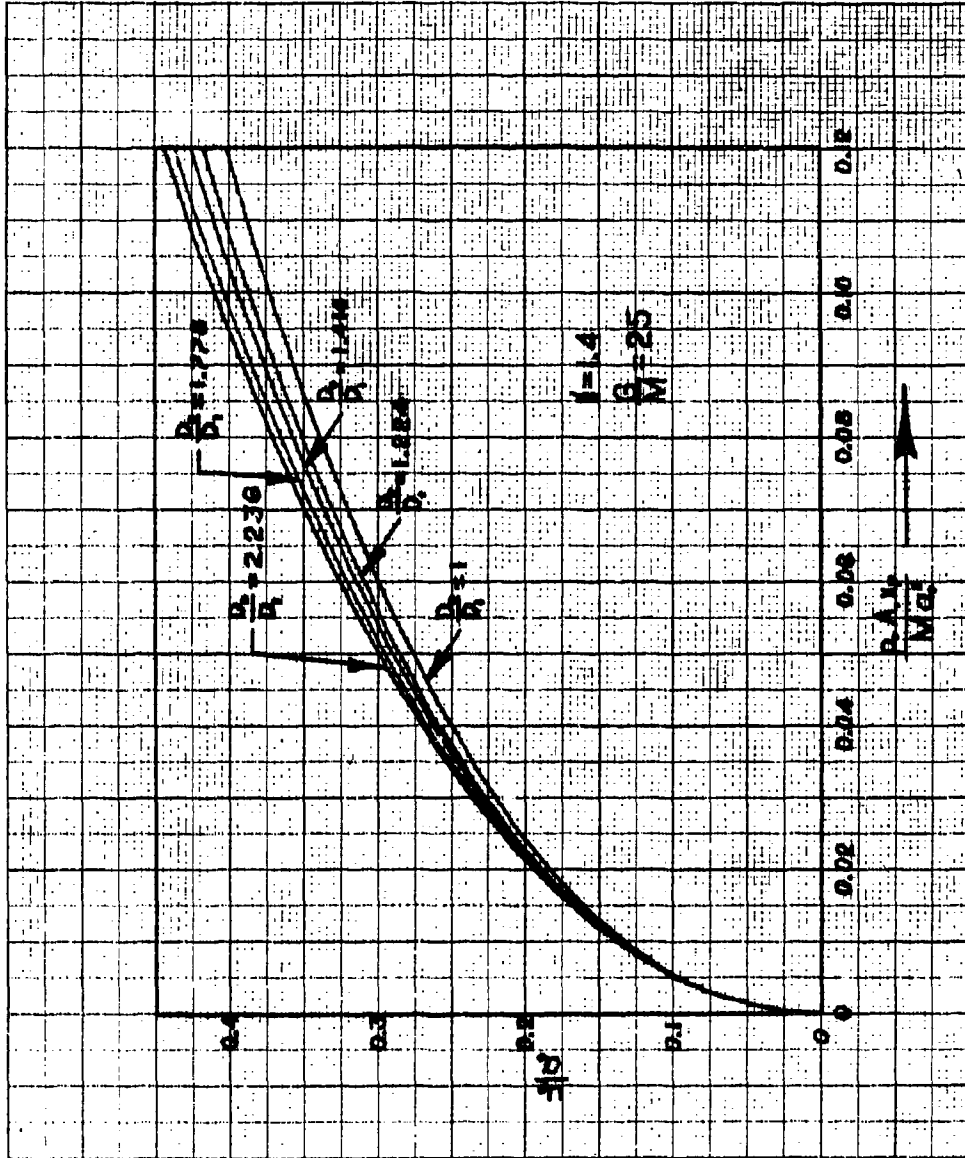
Figure 21(n2)
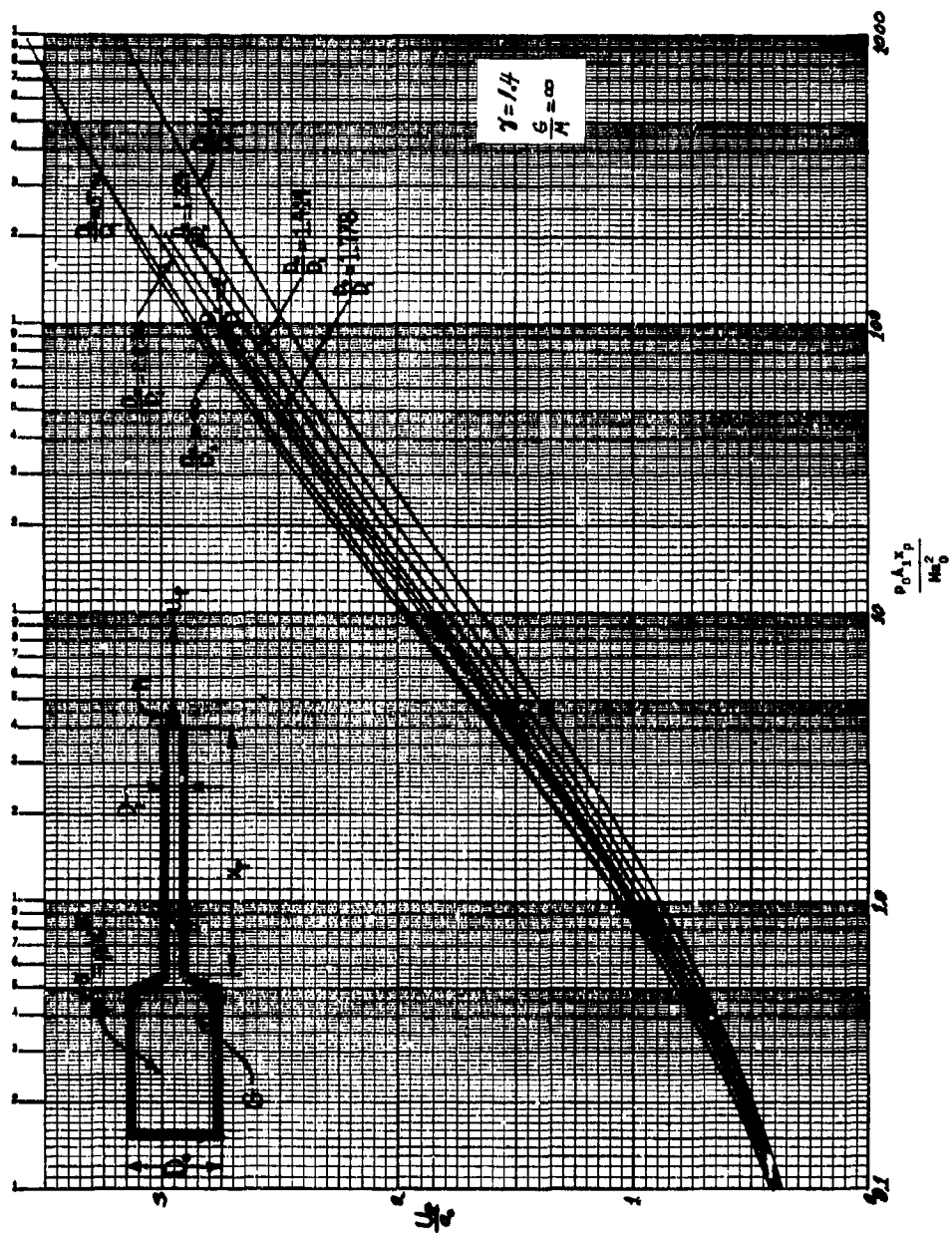
Figure 21(o1)
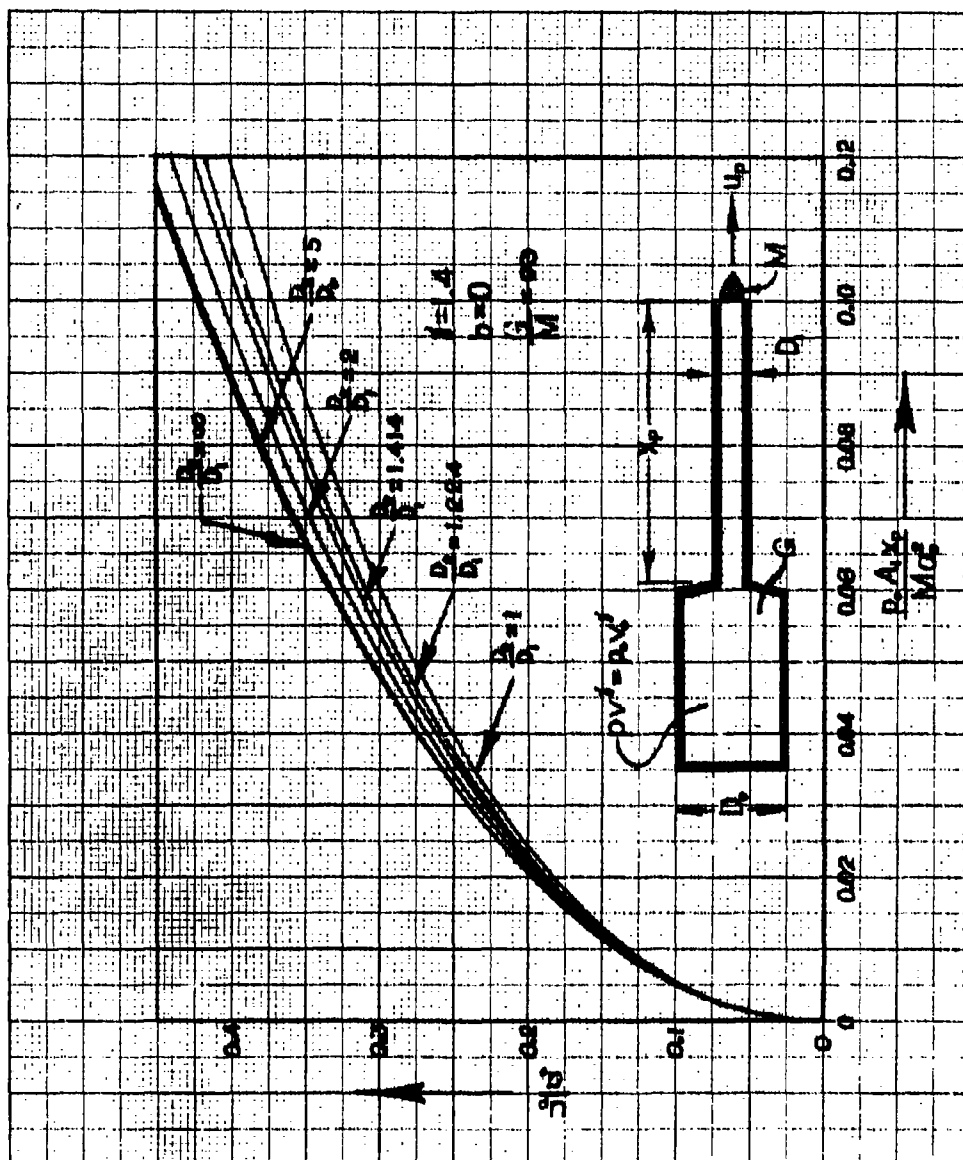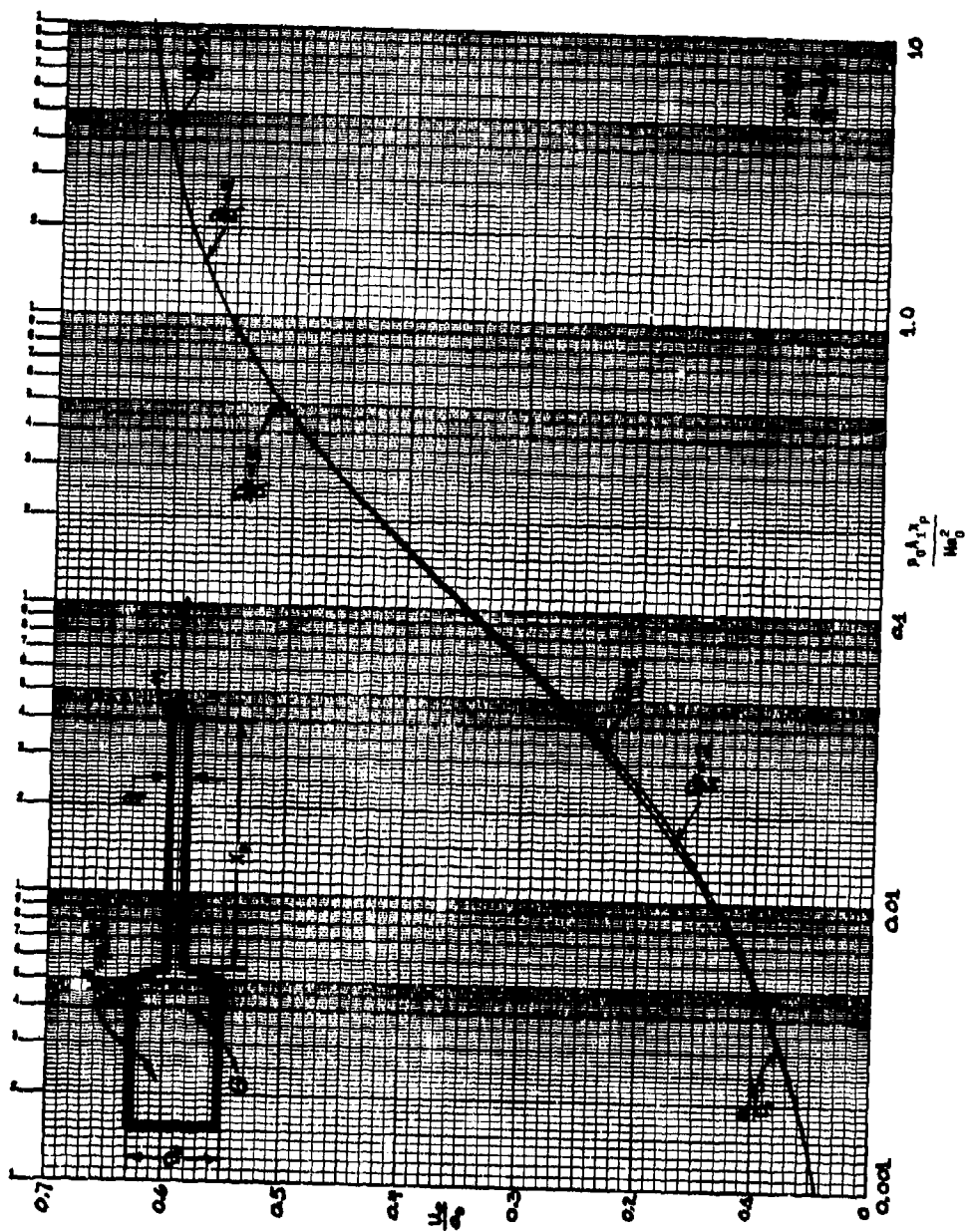
Figure 21(o2)

Figure 21(p1)

Figure 21(p2)

270

Figure 21(q1)

271
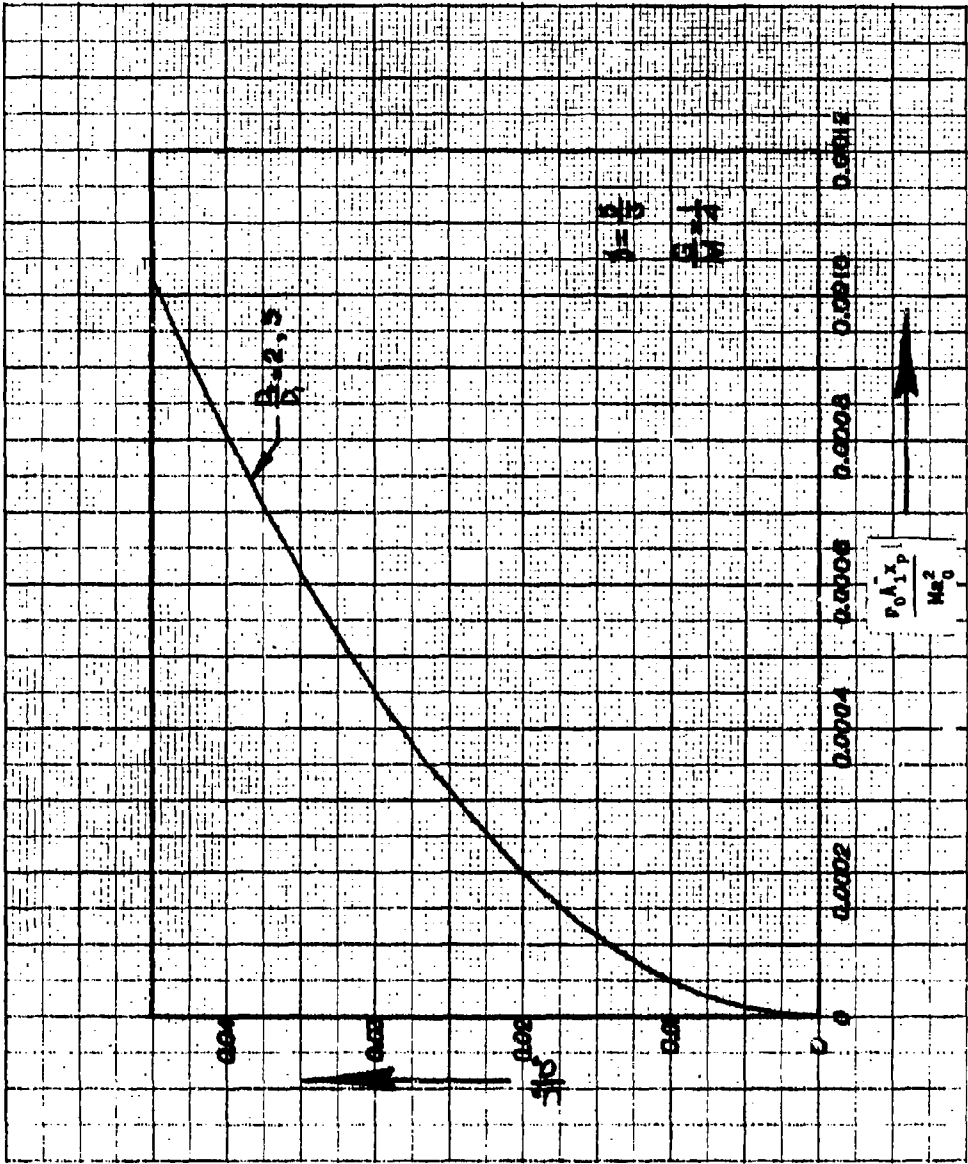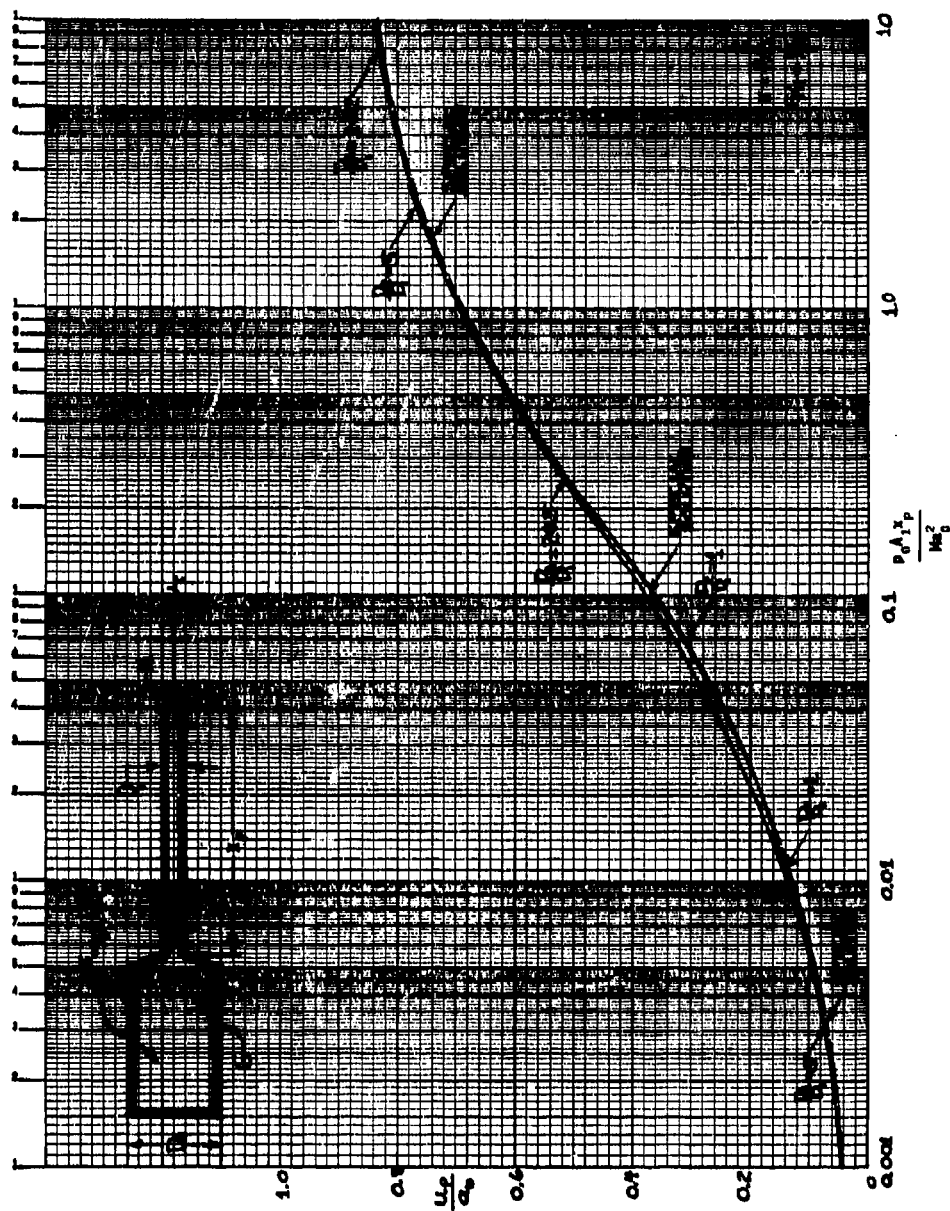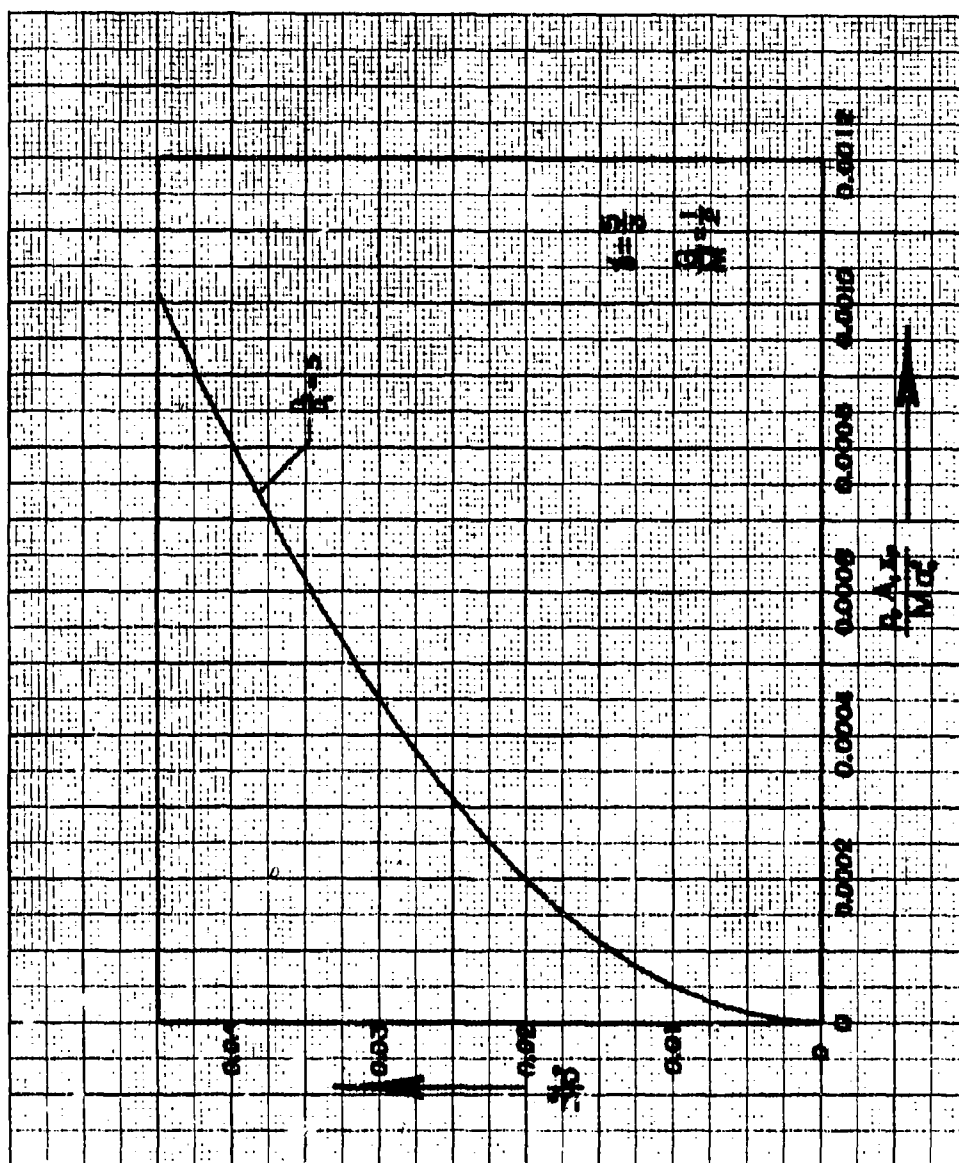
Figure 21(q2)

272
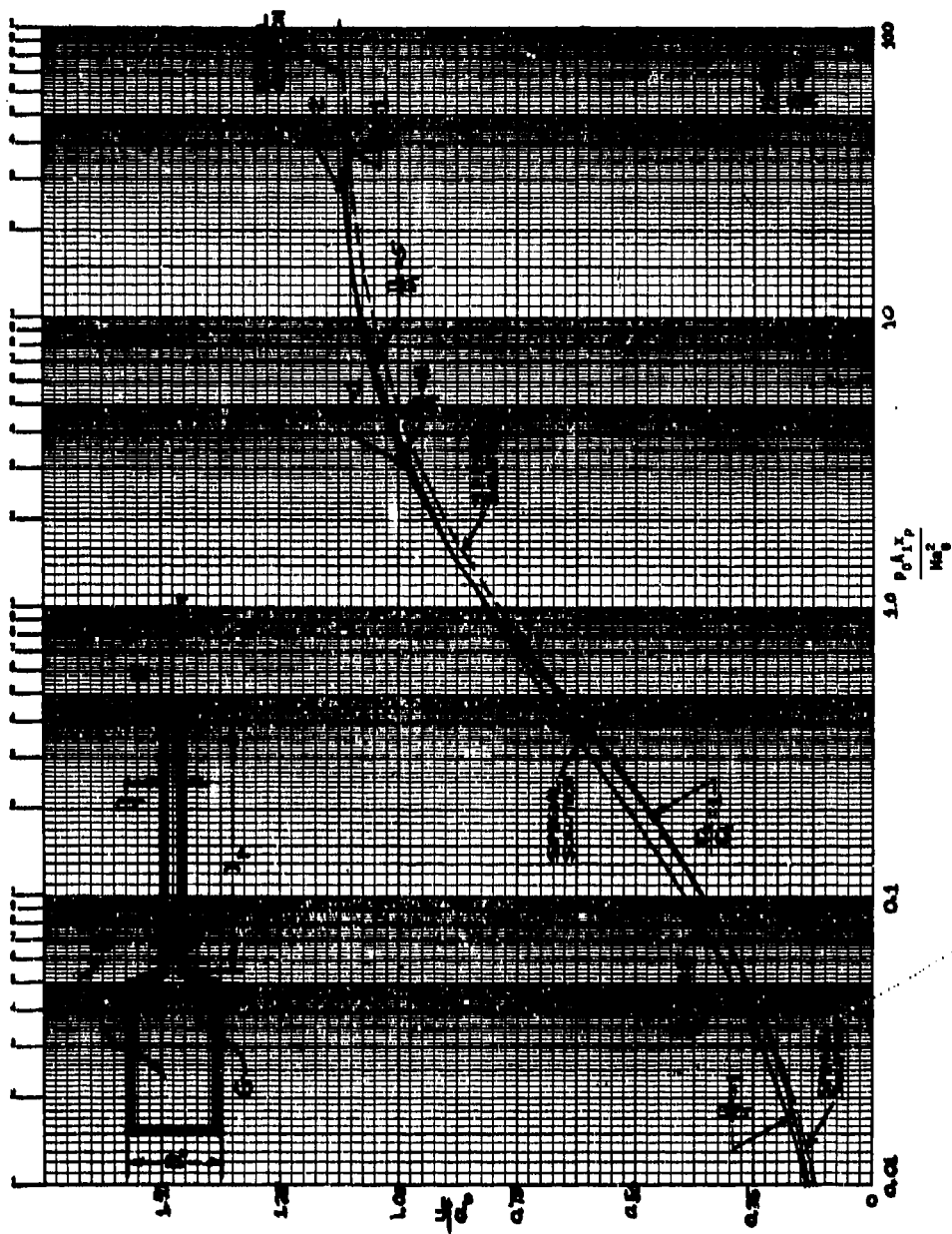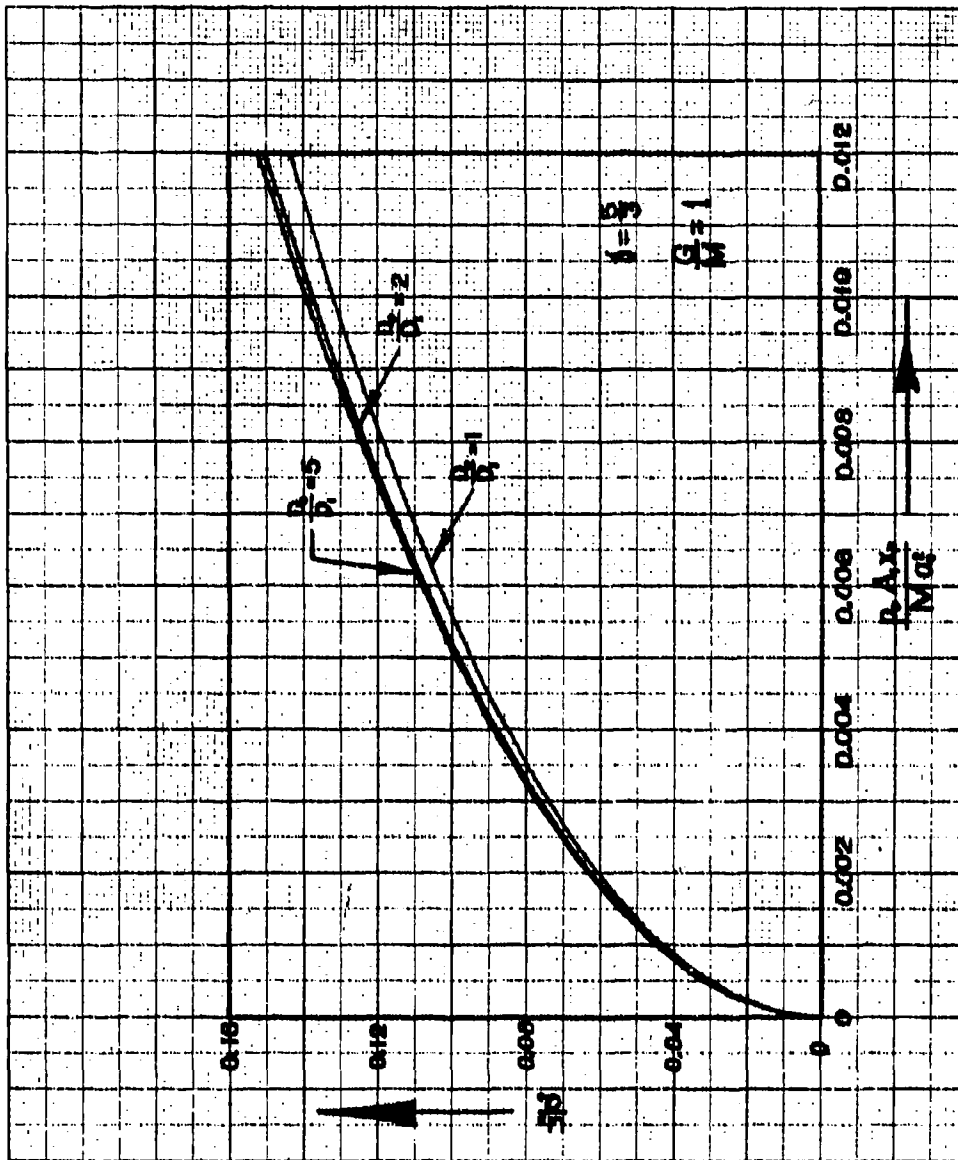
Figure 21(r1)

Figure 21(r2)
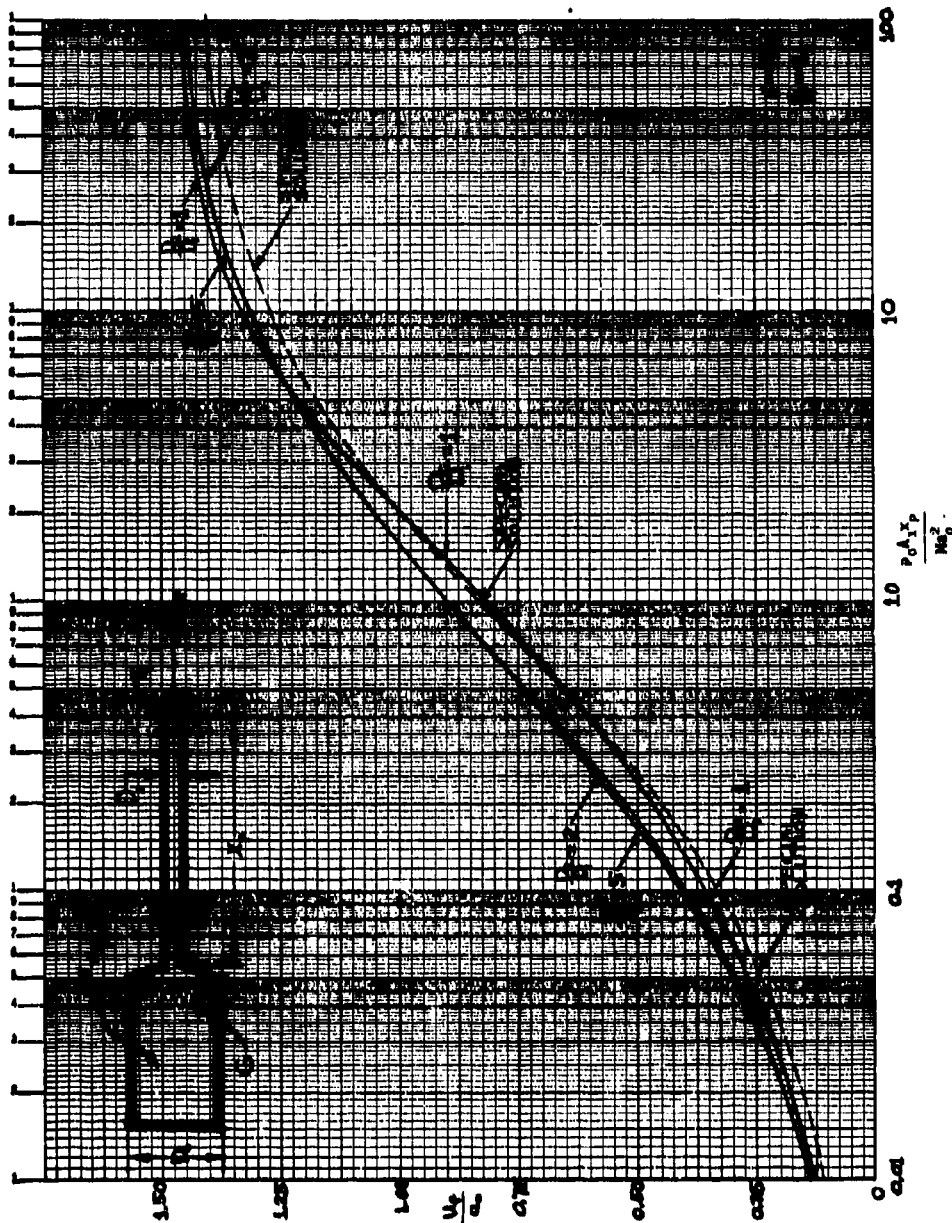
Figure 21(sl)
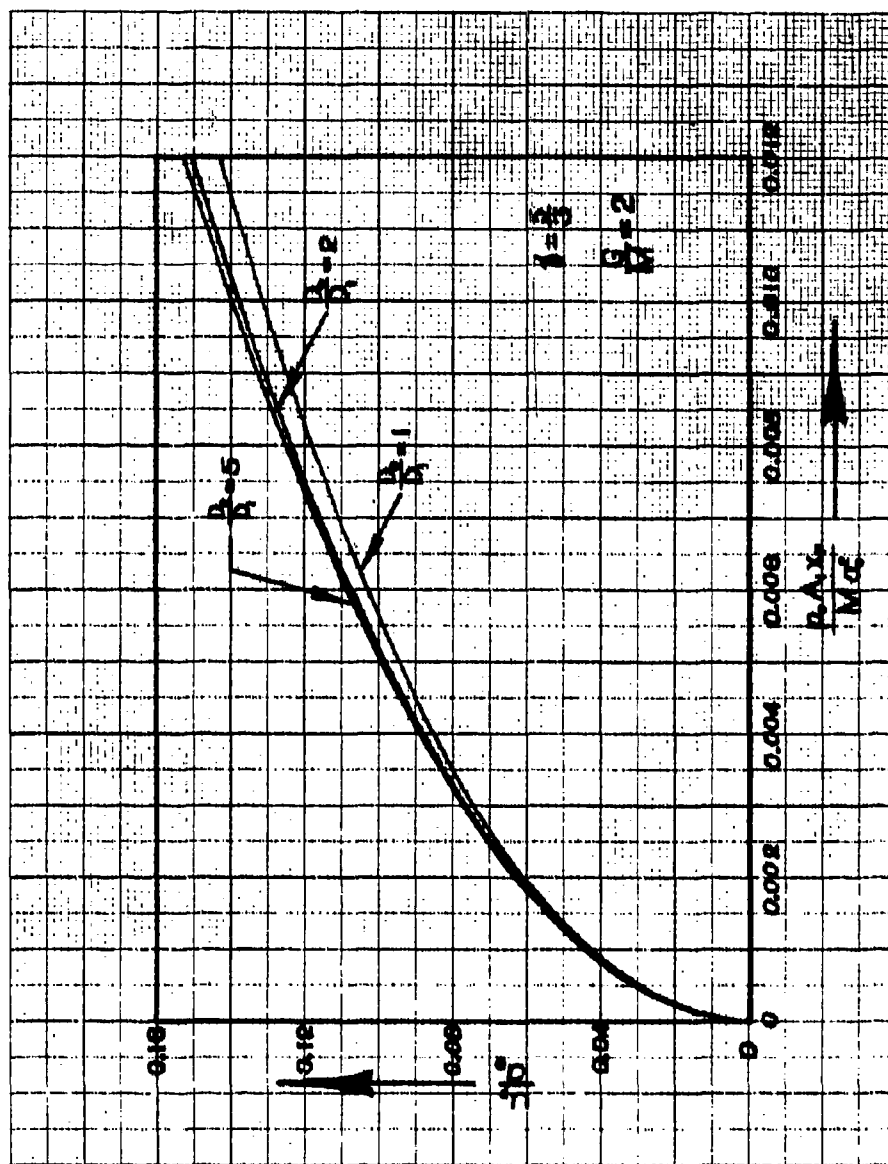
Figure 21(s2)

Figure 21(t1)

Figure 21(t2)

278

Figure 21 (ul)

Figure 21(u2)

DIMENSIONLESS PROJECTILE TRAVEL –

$$\frac{\gamma_1(\gamma_1+1)P_1 A_1 x_p}{M a_1^2} \longrightarrow$$

Figure 22

"O" RINGS

OIL OUTLET

HOLDER HOUSING

PISTON HOLDER

CHAMBER

PISTON

BARREL

SAFETY OUTLET

BRASS FILLER
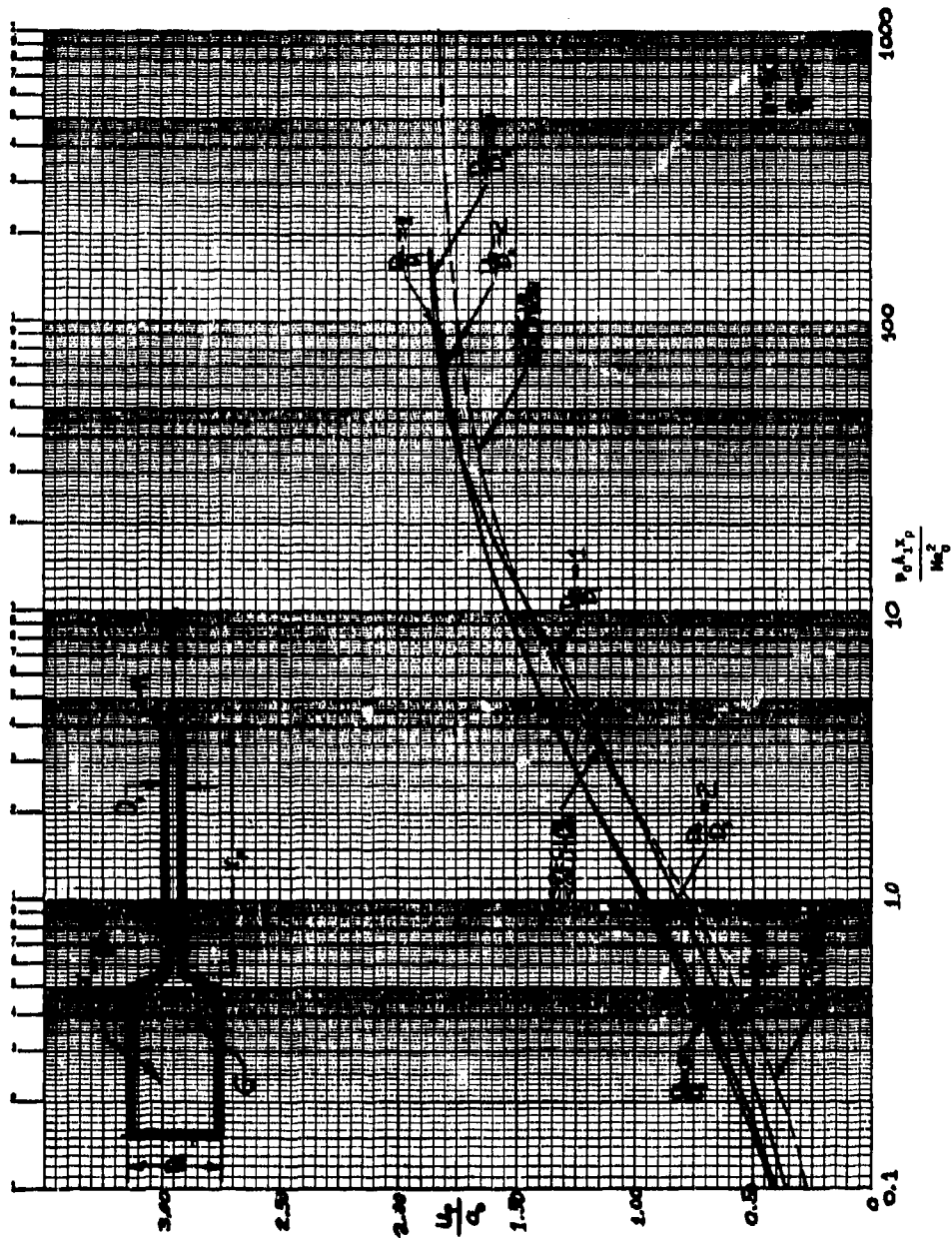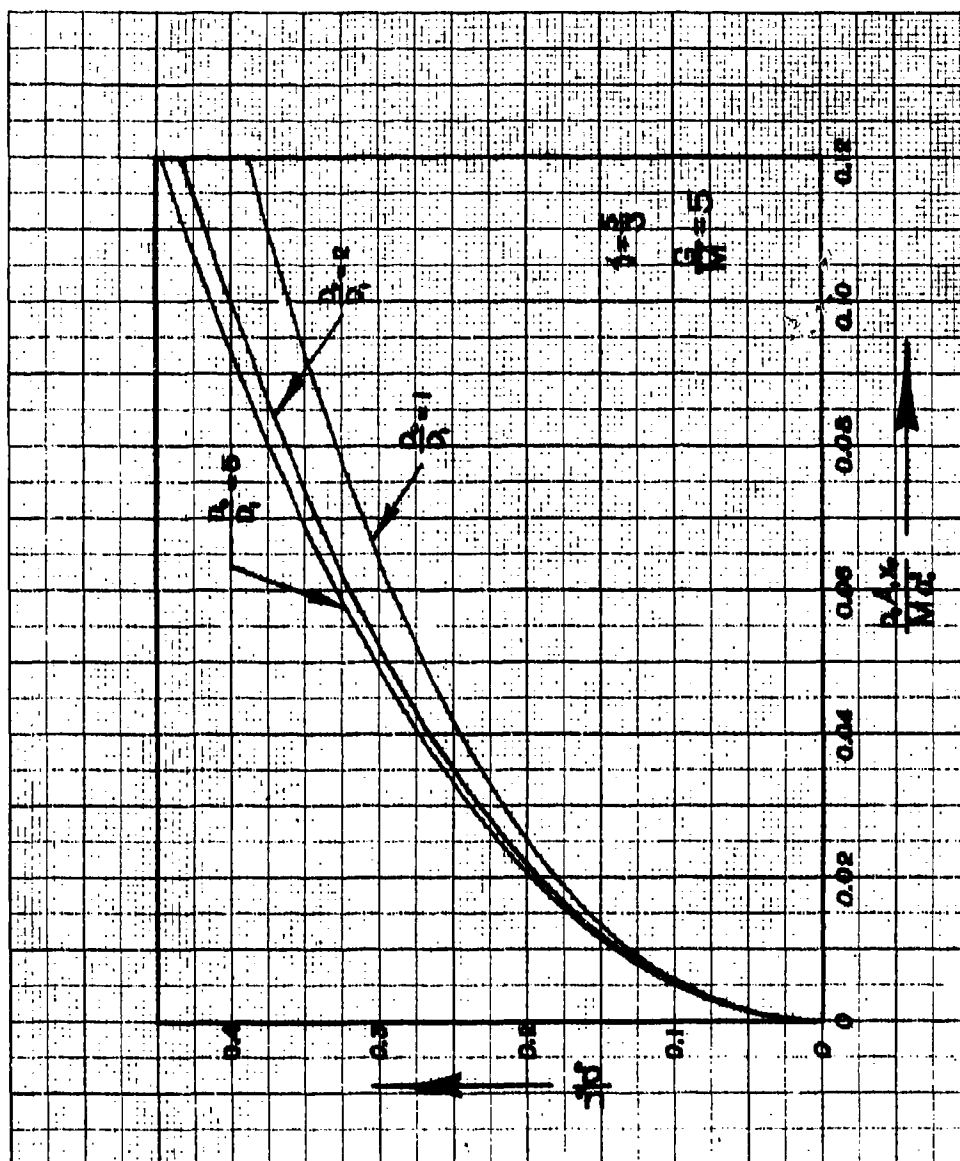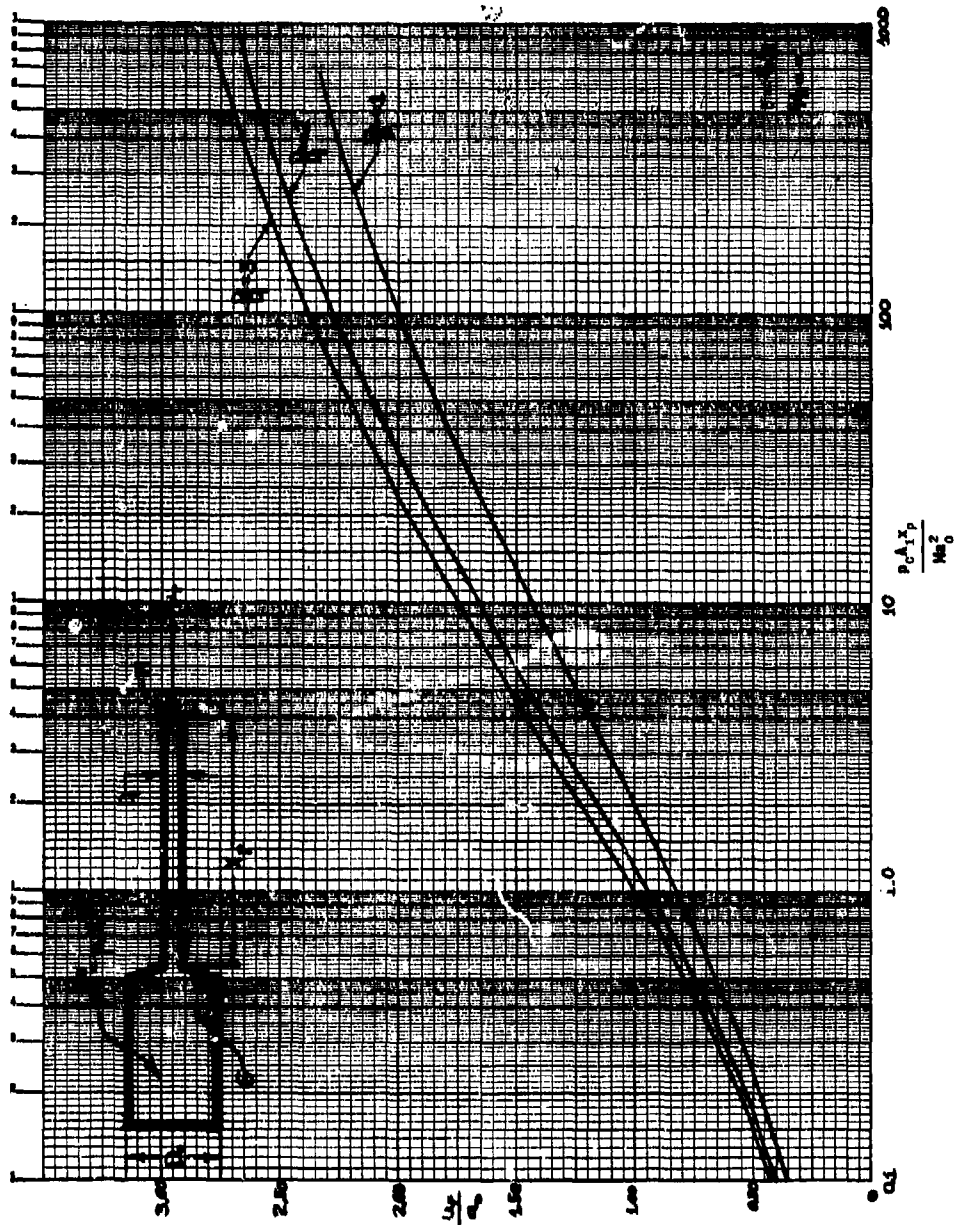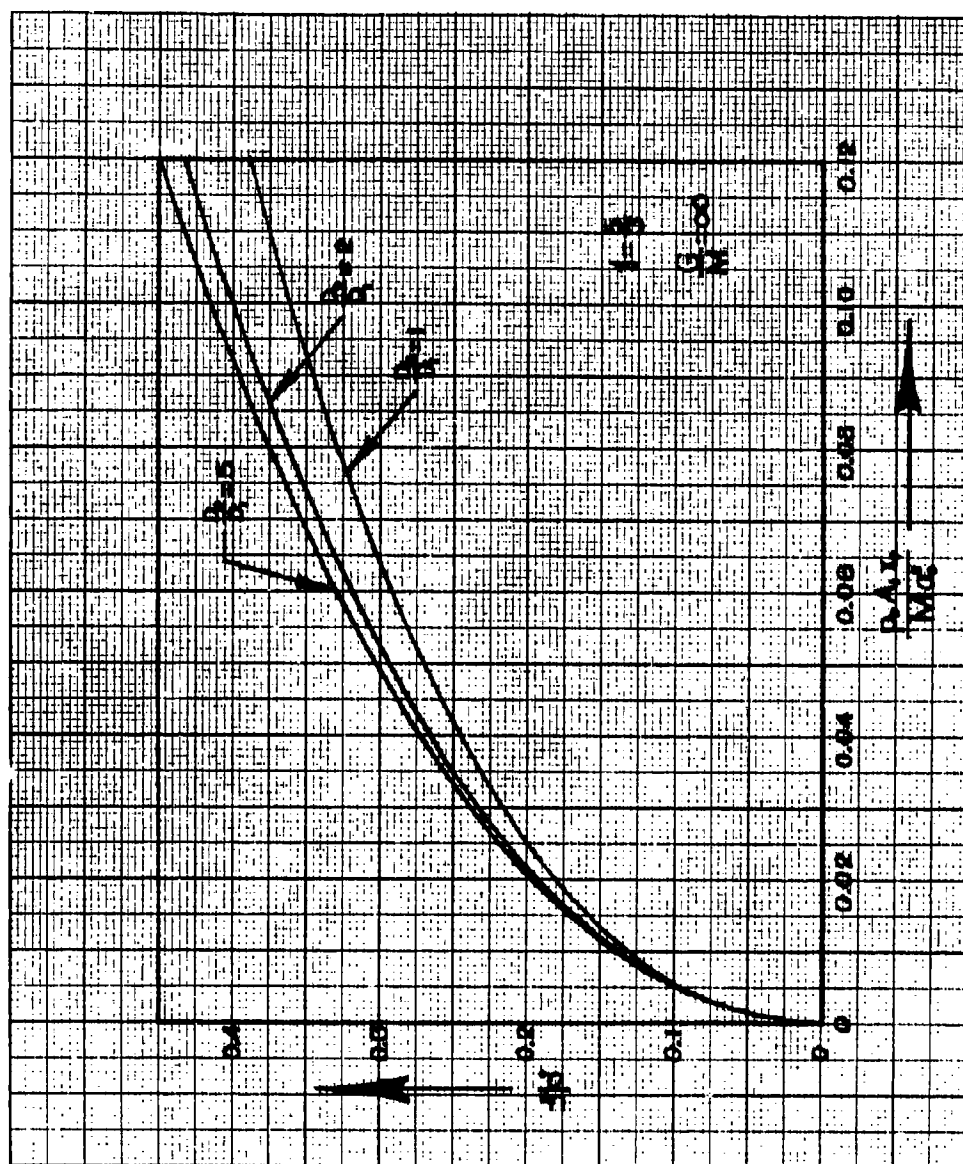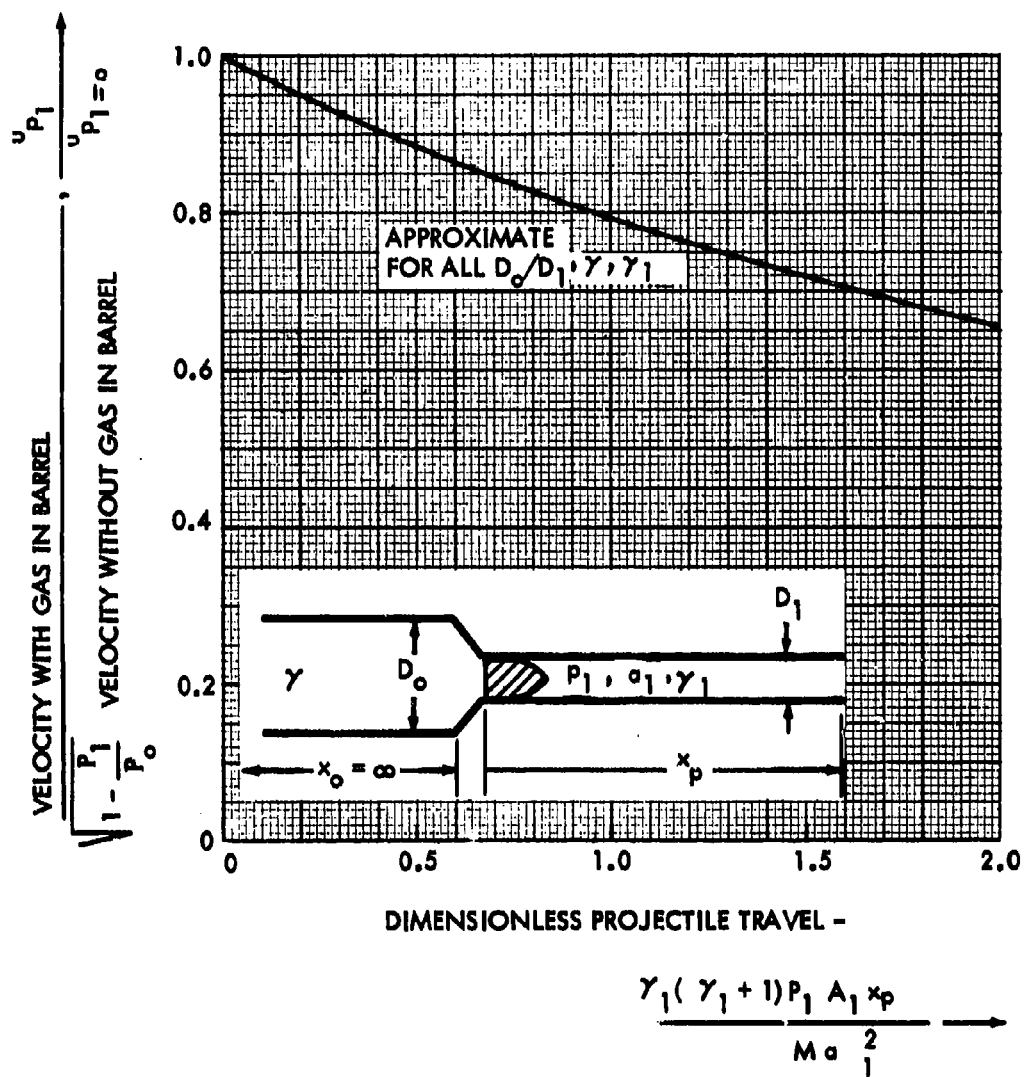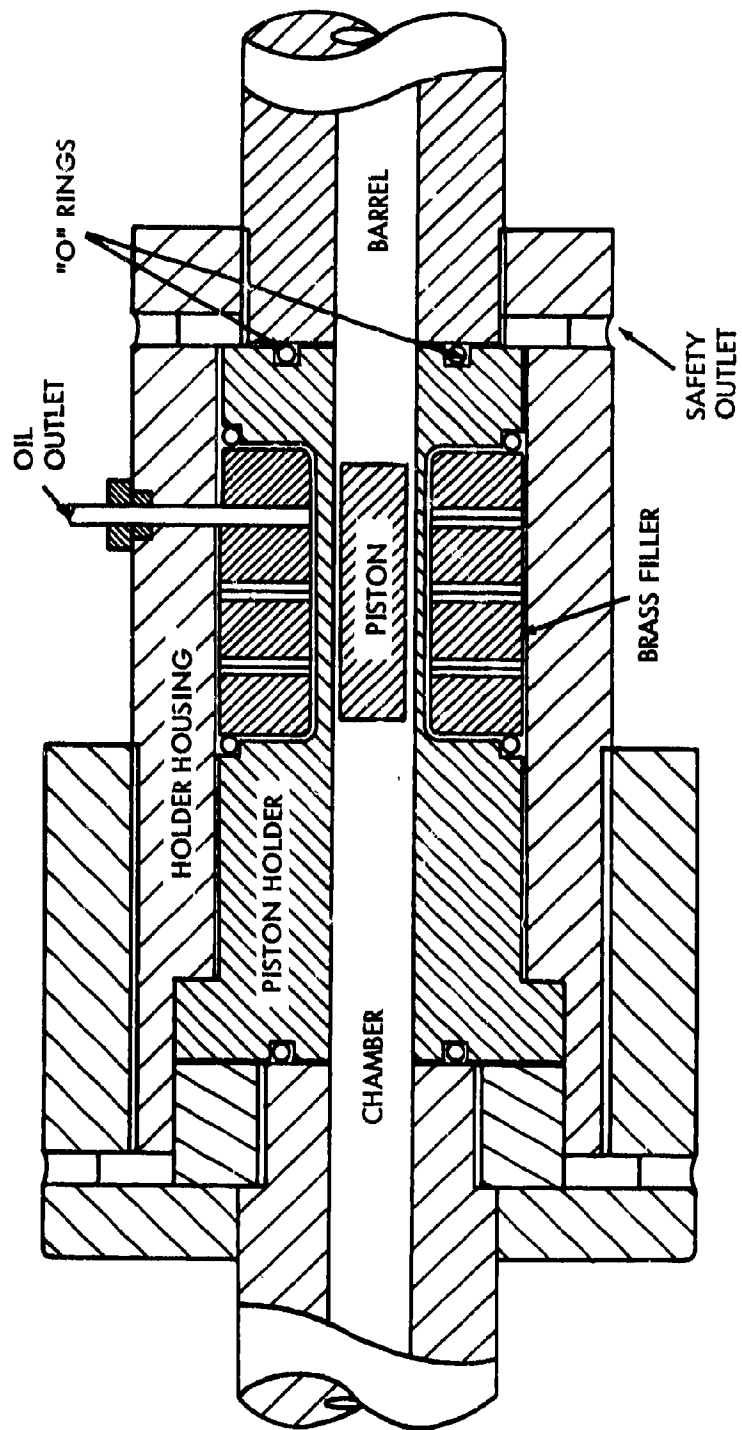
Fig. 23   Schematic diagram of piston holder

Figure 24

Figure 25

VELOCITY OF PROJECTILE, up fps

20,000

15,000

10,000

5,000

0

DISTANCE TRAVELED BY PROJECTILE Xp, ft ➔

0   10   20   30   40   50

THEORY WITHOUT BOUNDARY
LAYER EFFECTS.

THEORY WITH BOUNDARY
LAYER CORRECTIONS.

O   EXPERIMENTALLY OBTAINED
VELOCITY WITH N.O.L. TWO
STAGE GUN.

VELOCITY WITH FRICTIONAL EFFECTS / VELOCITY WITHOUT FRICTIONAL EFFECTS

$\dfrac{u_{p_f}}{u_{p_f=o}}$

1.0

0.8

0.6

0.4

0.2

0

EXTRAPOLATED

PPIG GUN

APPROXIMATE CURVE FOR
ALL γ AND FOR $x_p/D_1 = 100$ TO 250

$pv^\gamma = p_o v_o^\gamma$

D_1

u_p

$x_o = $ Long

x_p

0   1.0   2.0   3.0   4.0

$\dfrac{\gamma u_{p_f=o}}{a_o} \rightarrow$

Figure 26

Figure 27

Fig. 28(a)   Two-stage gun time distance plot (NOL gun)
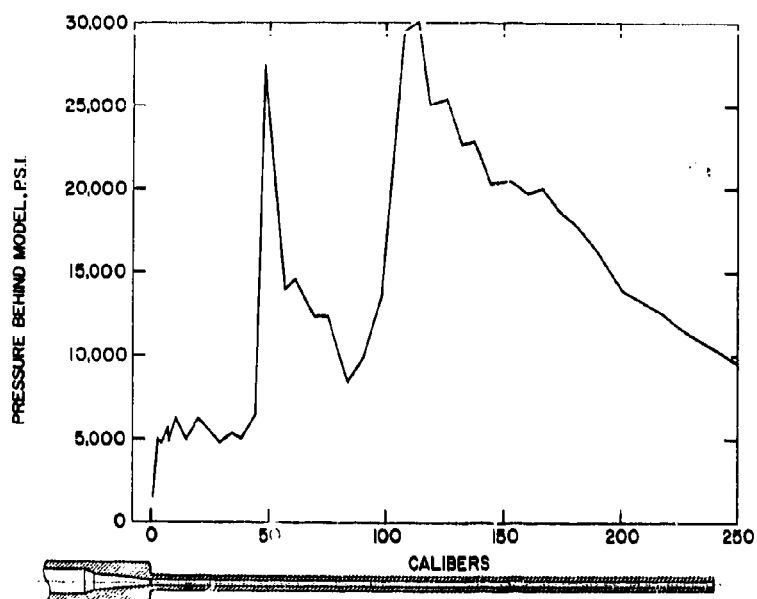
Fig. 28(b)   Pressure behind model VS bore travel in calibers
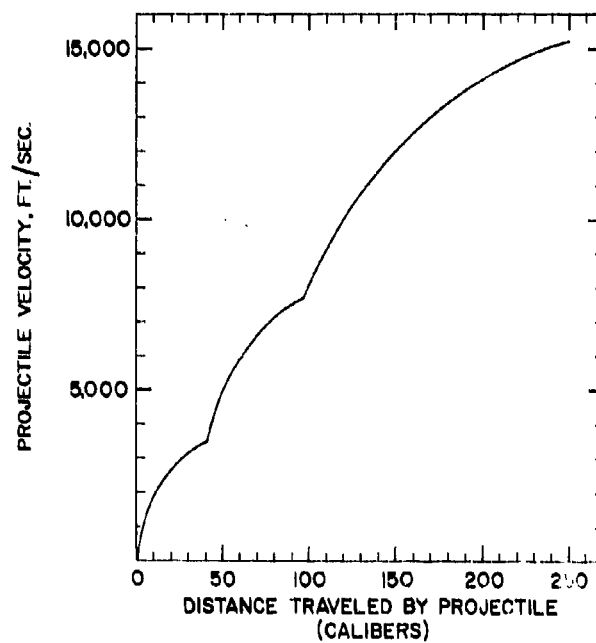
Fig. 28(c)   Projectile velocity VS bore travel in calibers (NOL gun)

PRIMARY CHAMBER 10" INSIDE DIA.

PUMP TUBE 5" INSIDE DIA.

BARREL 2" INSIDE DIA.
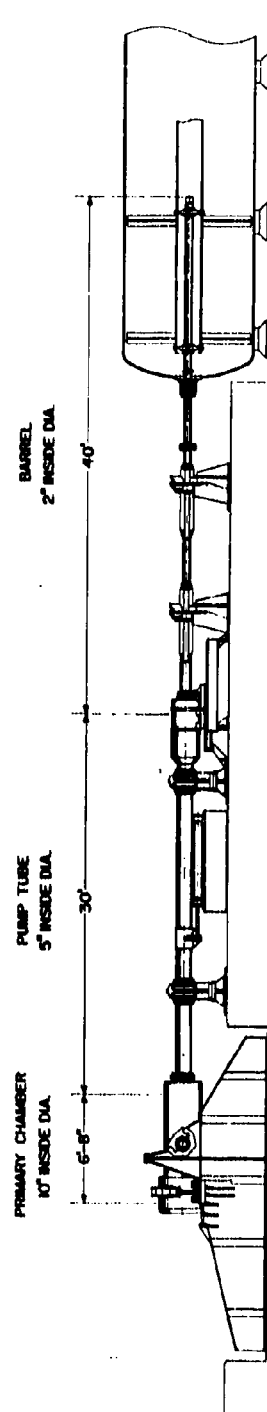
Fig. 28(d) Two-inch two-stage light gas gun (NOL)
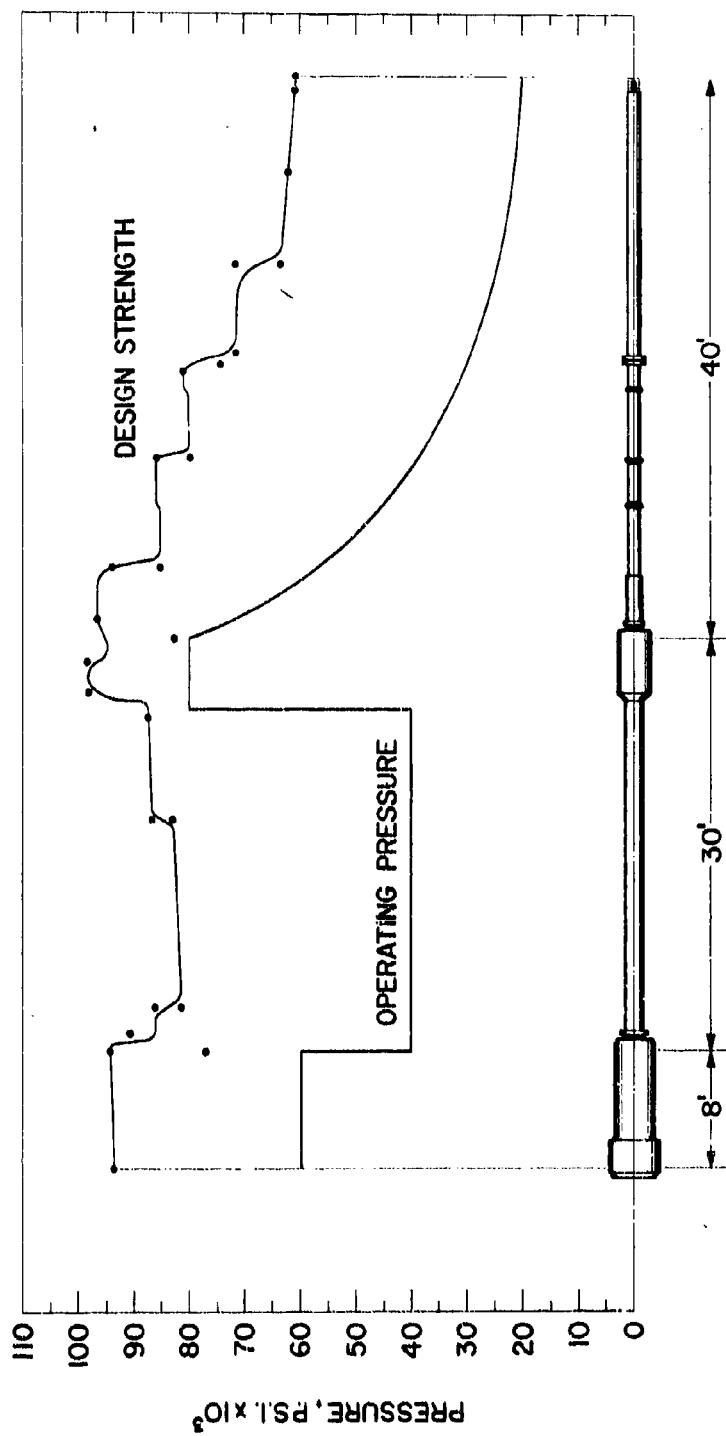
Fig. 28(e)   Two-inch two-stage light gas gun (NOL)
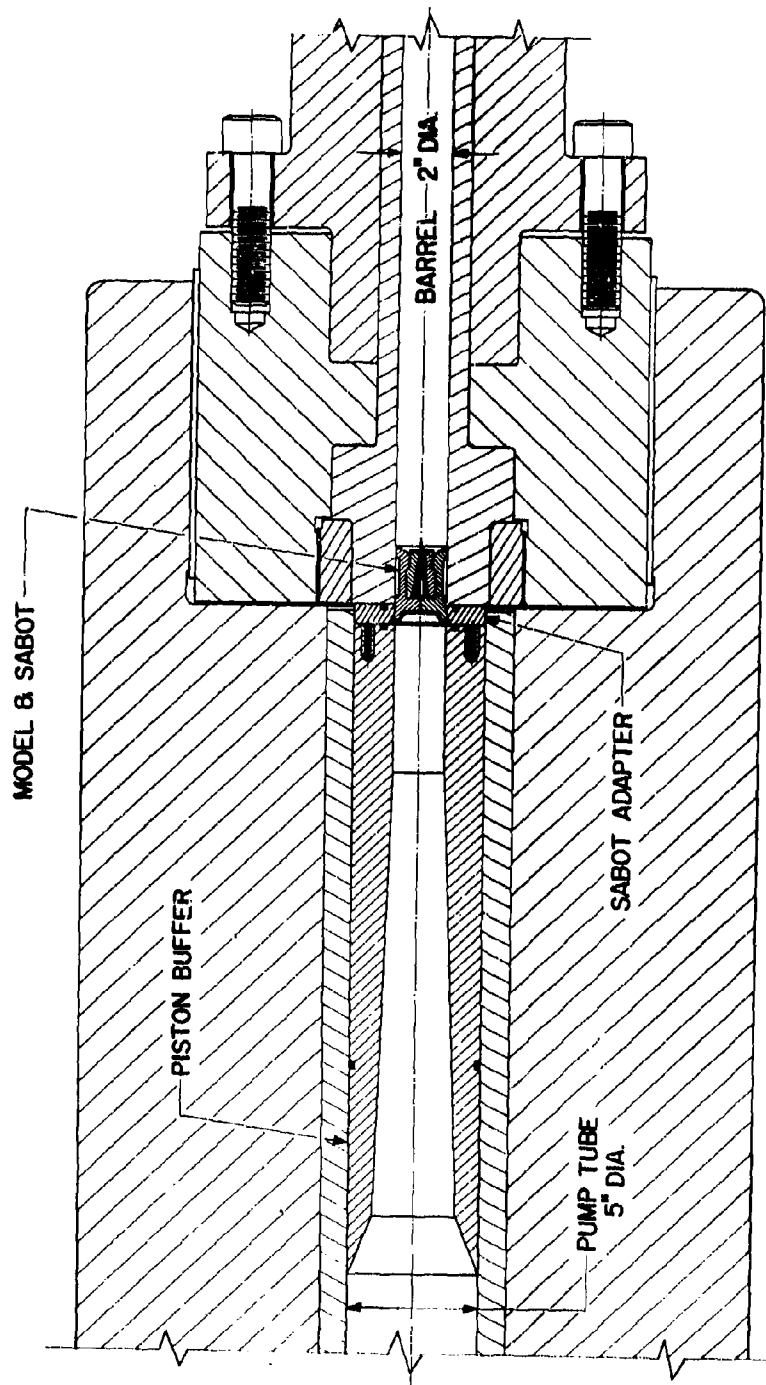
Fig. 28(f)   Pump tube – Barrel assembly
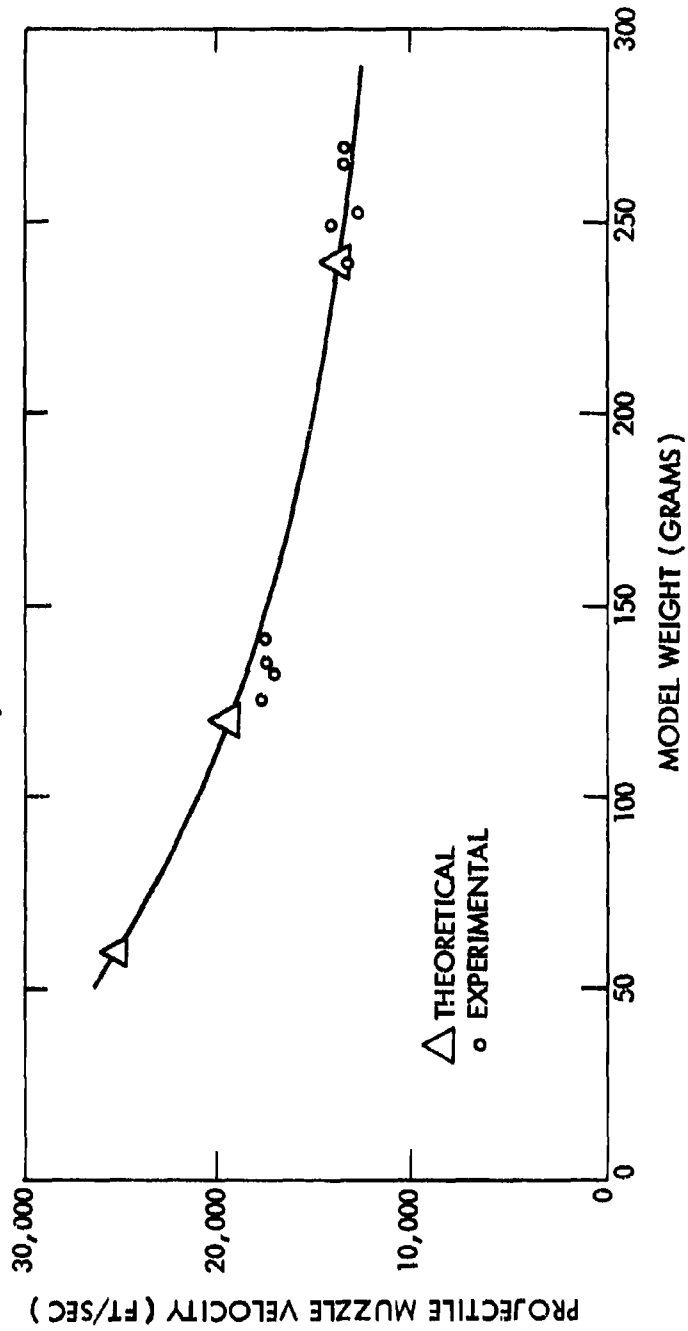
Fig. 28(g)   Comparison of theoretical calculations and experimental results for NOL two-inch-stage launcher

292
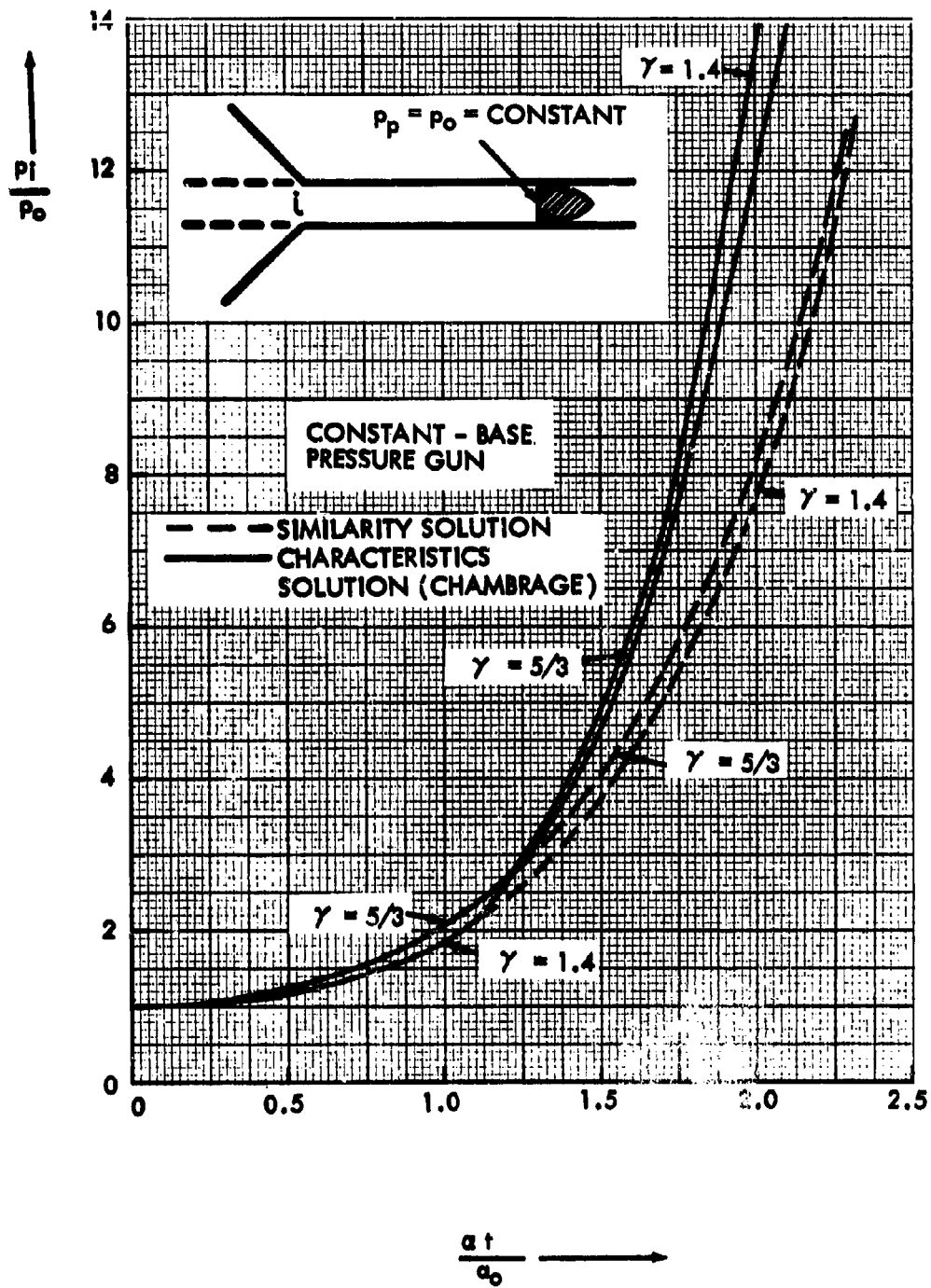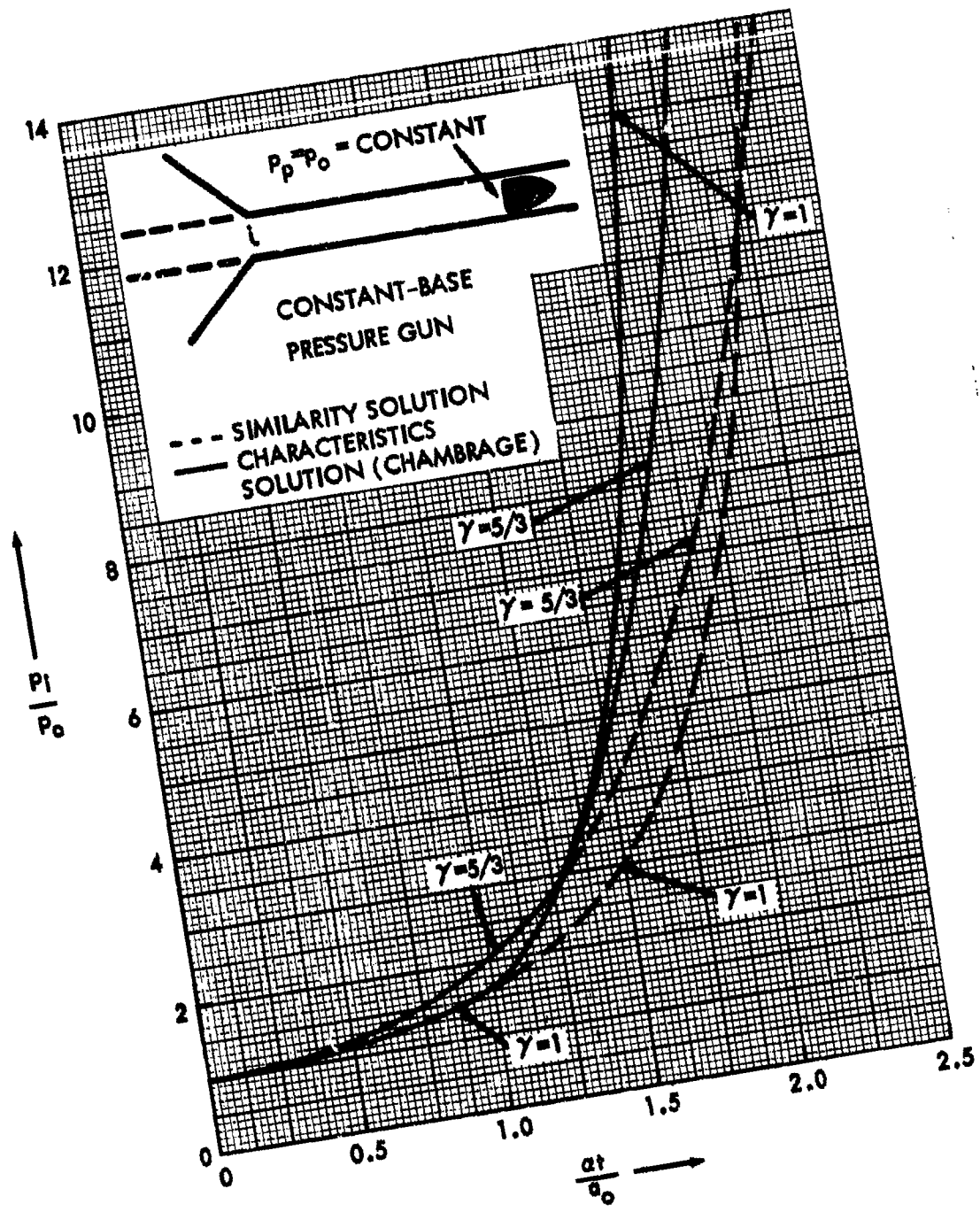
Figure 29(a)

Figure 29(b)
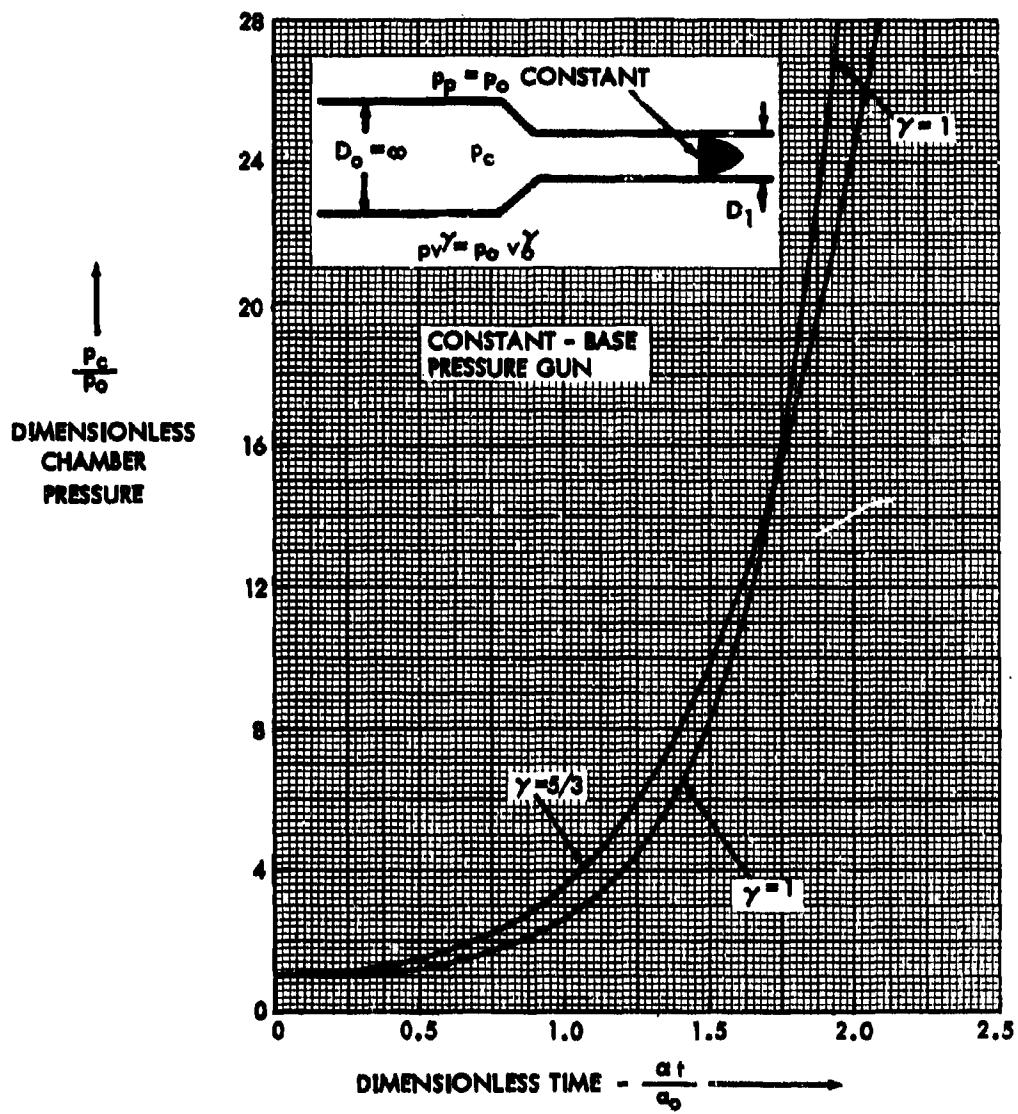
Figure 30
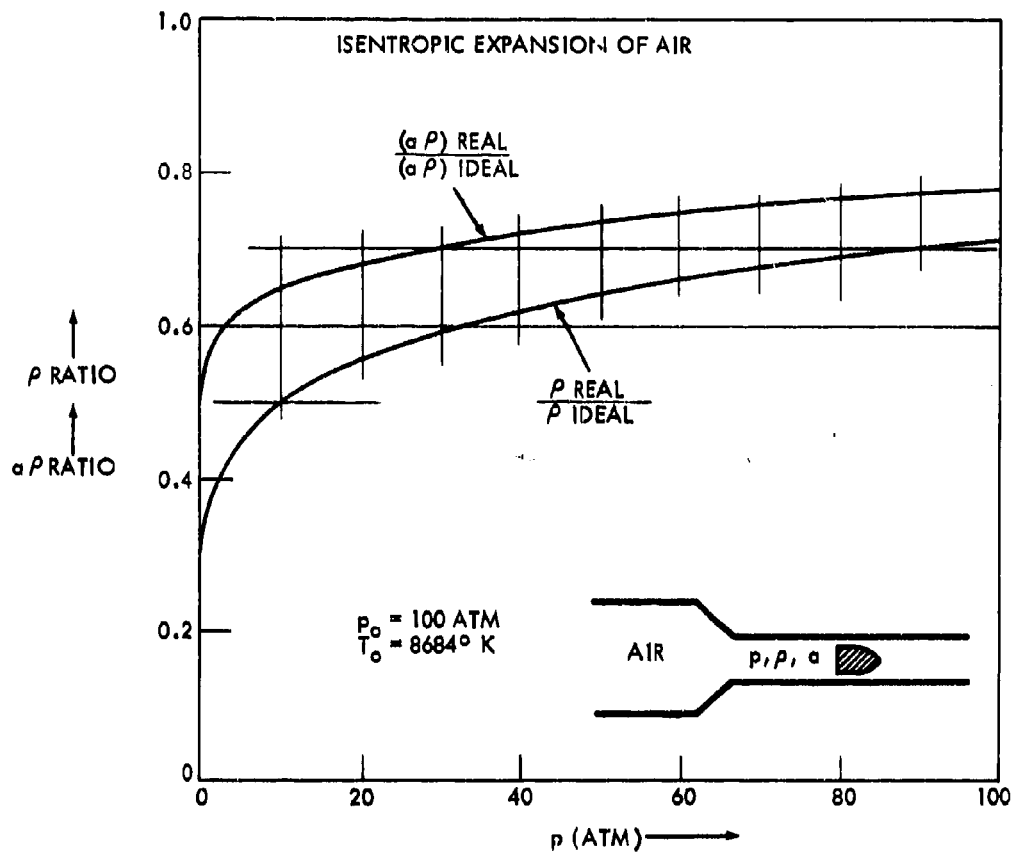
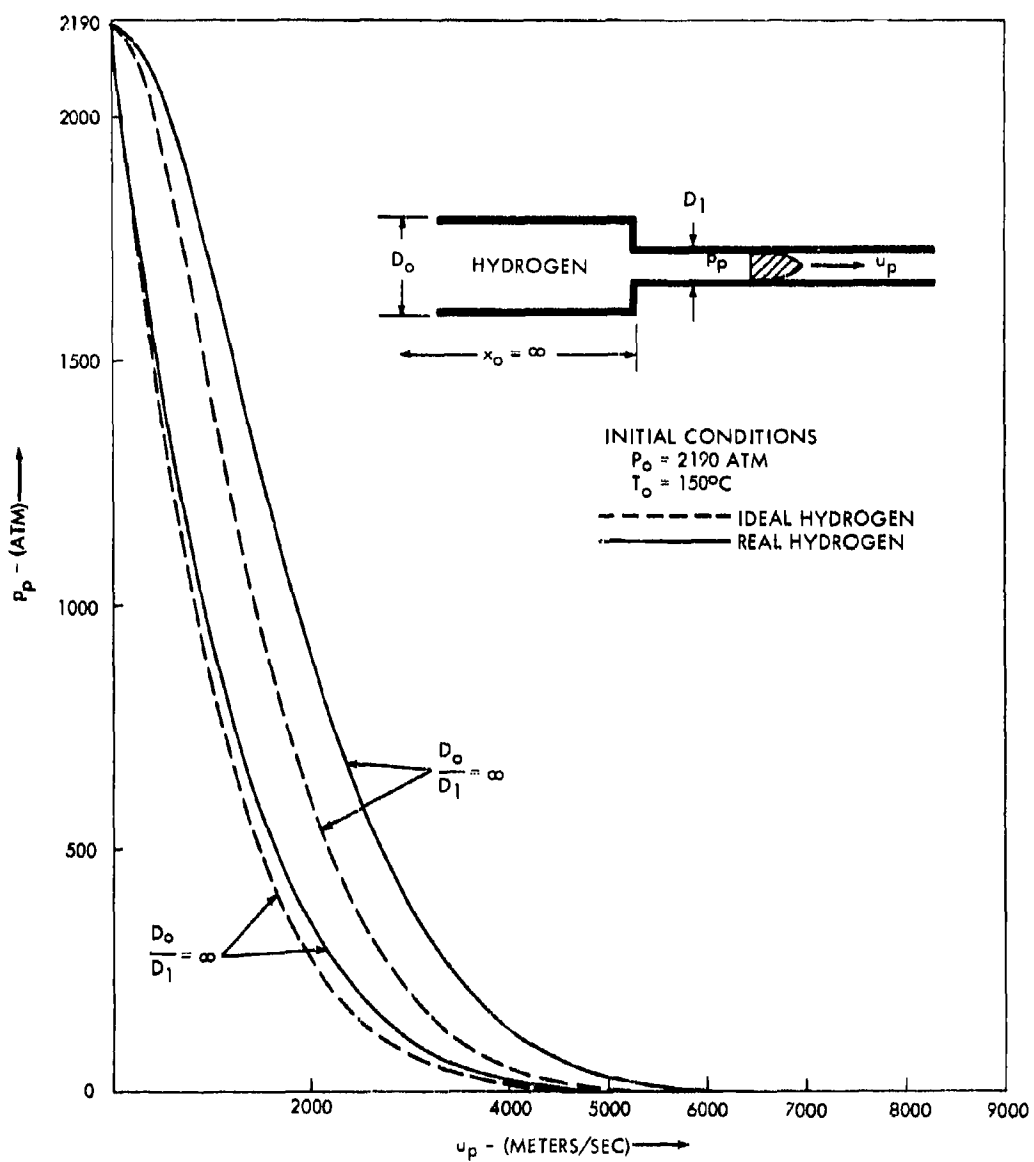Figure 31
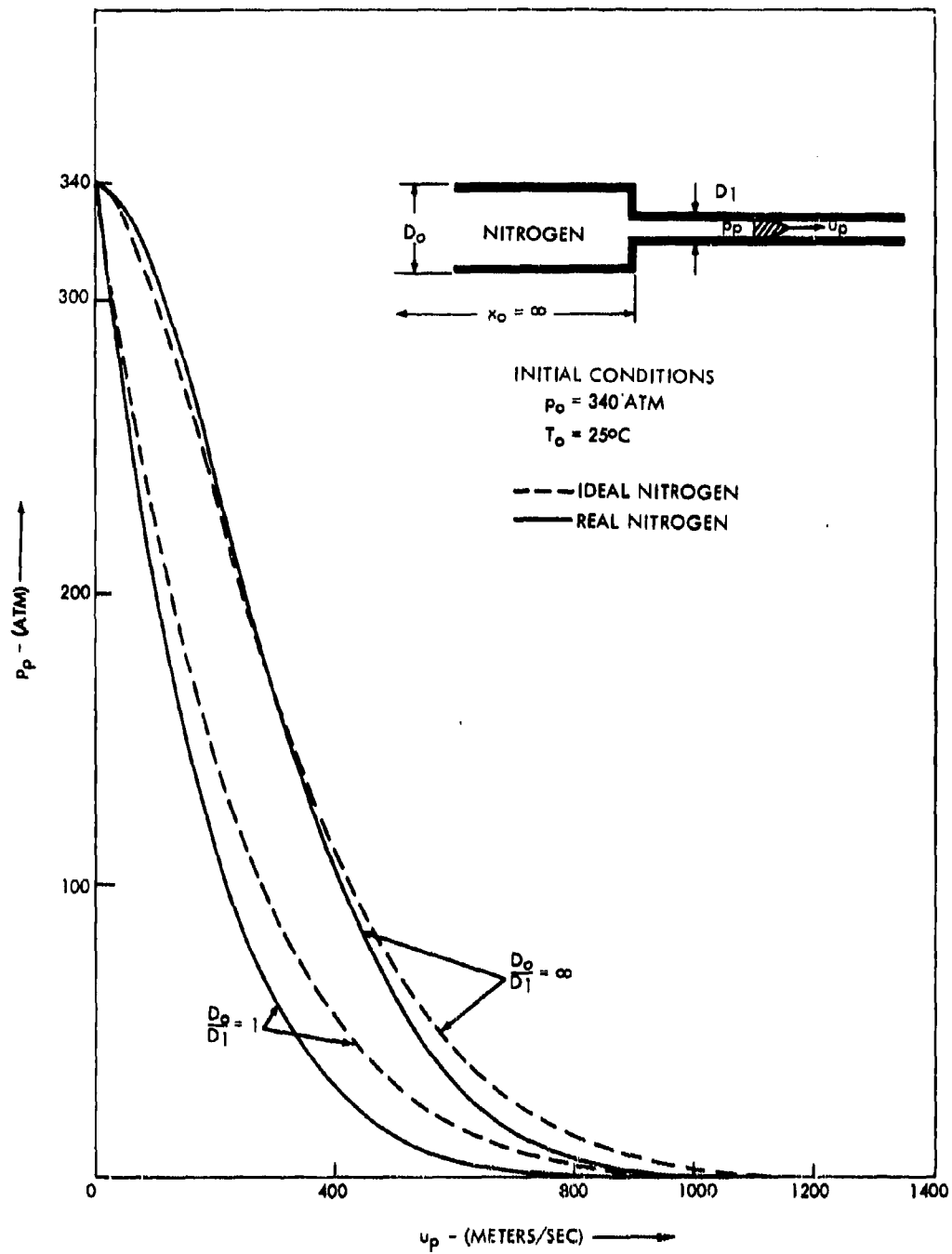
Figure 32
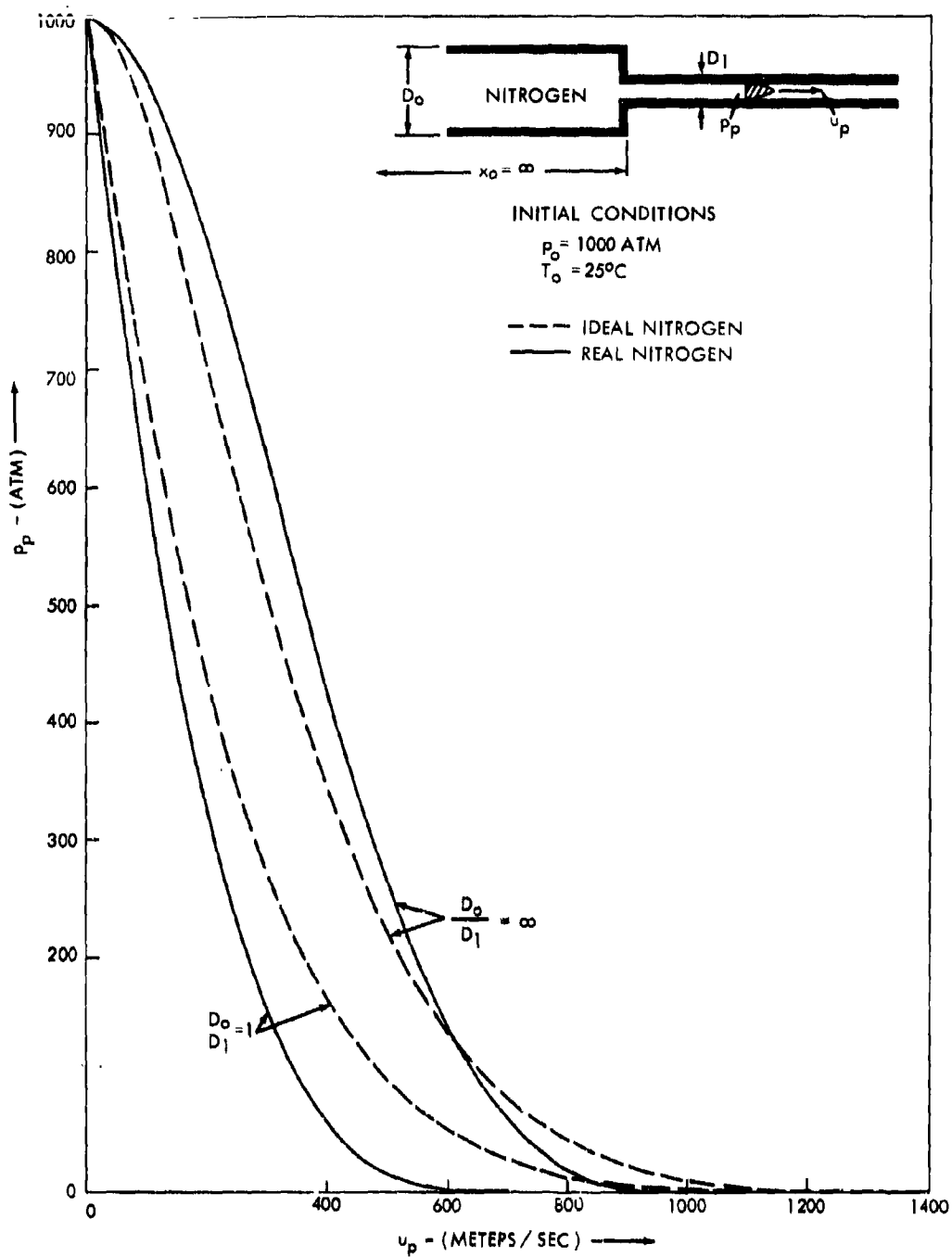
Figure 33
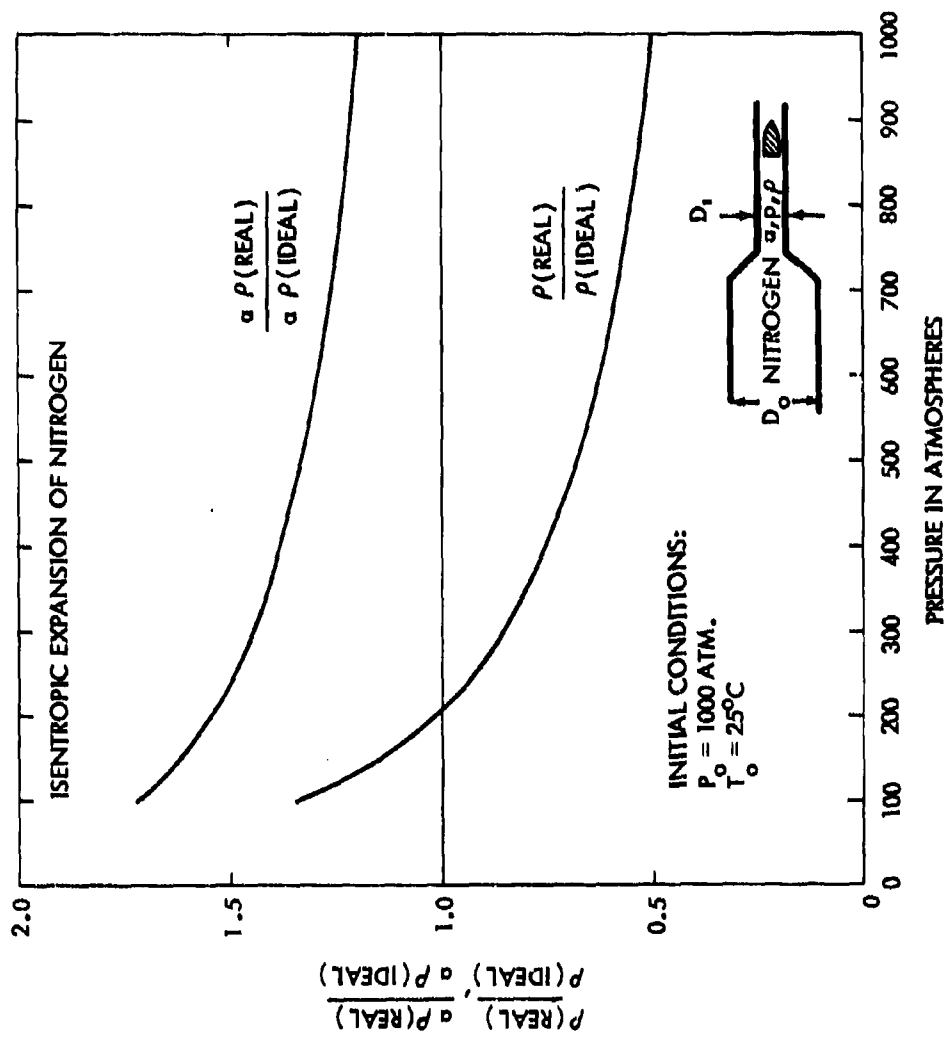
Figure 34
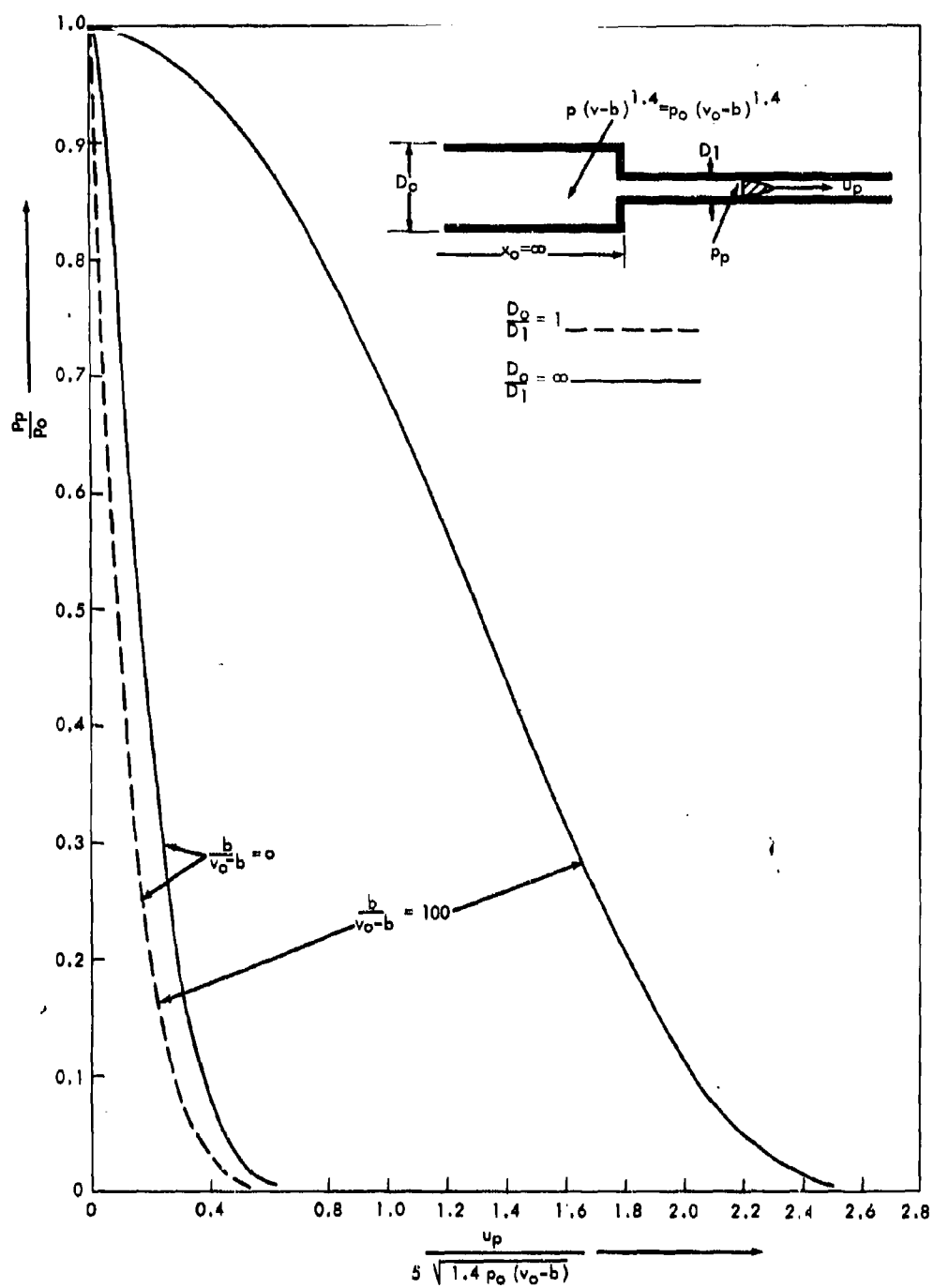
Figure 35
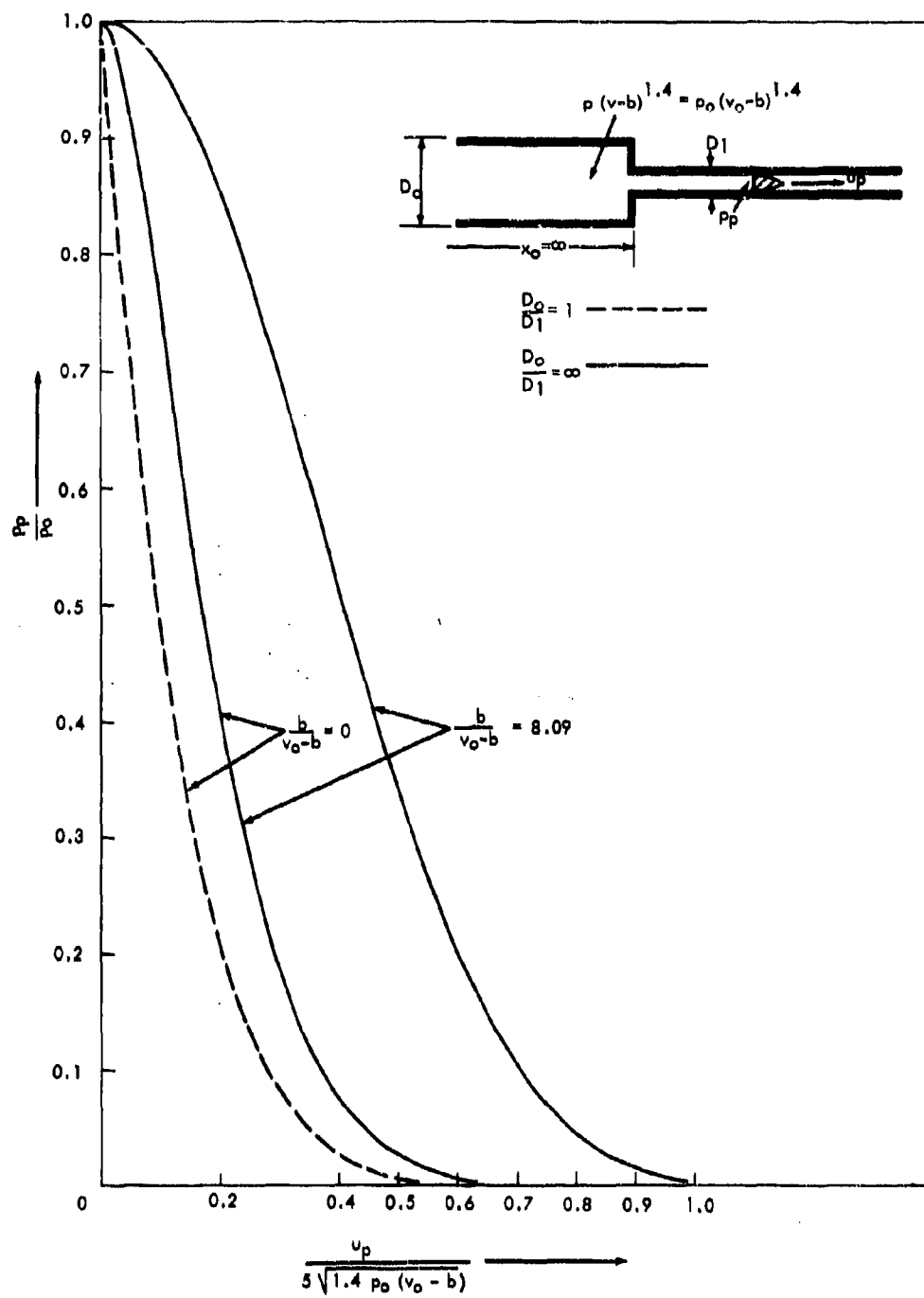
Figure 36
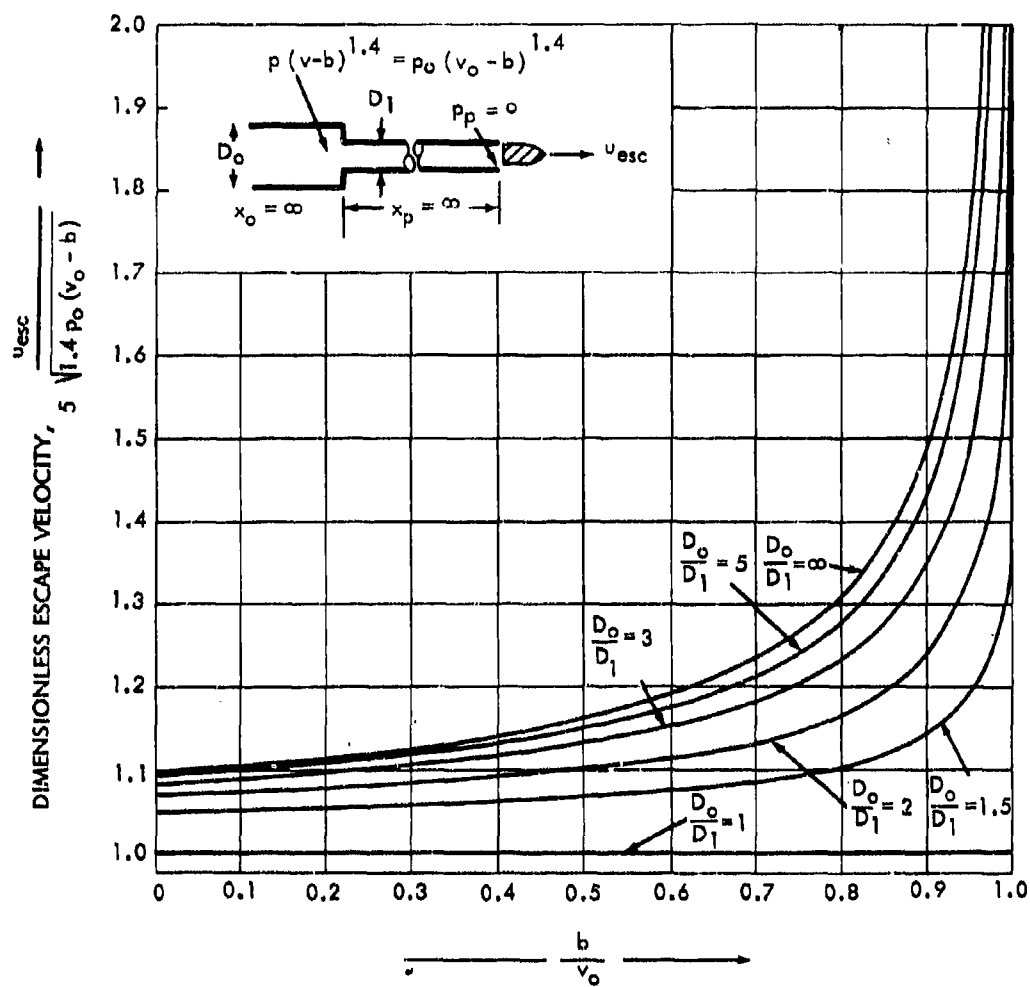
Figure 37
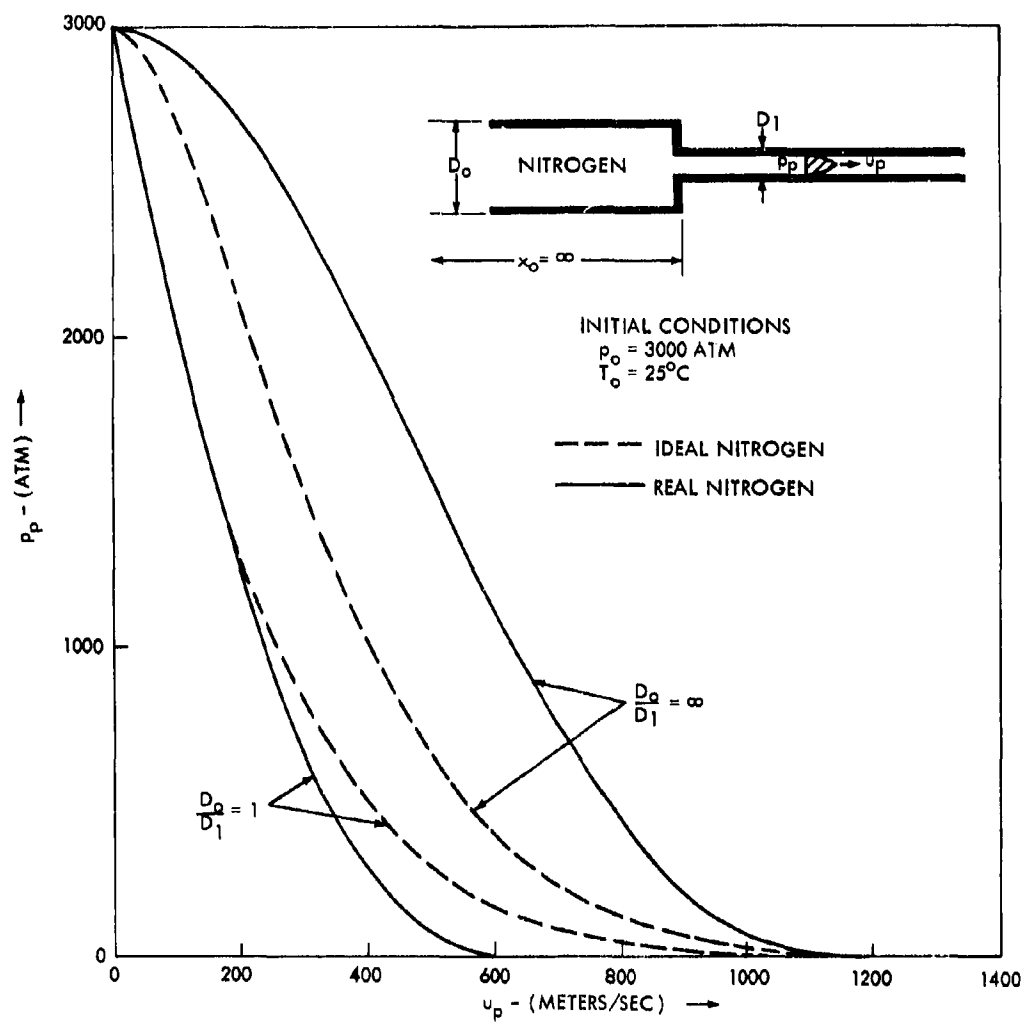
Figure 38
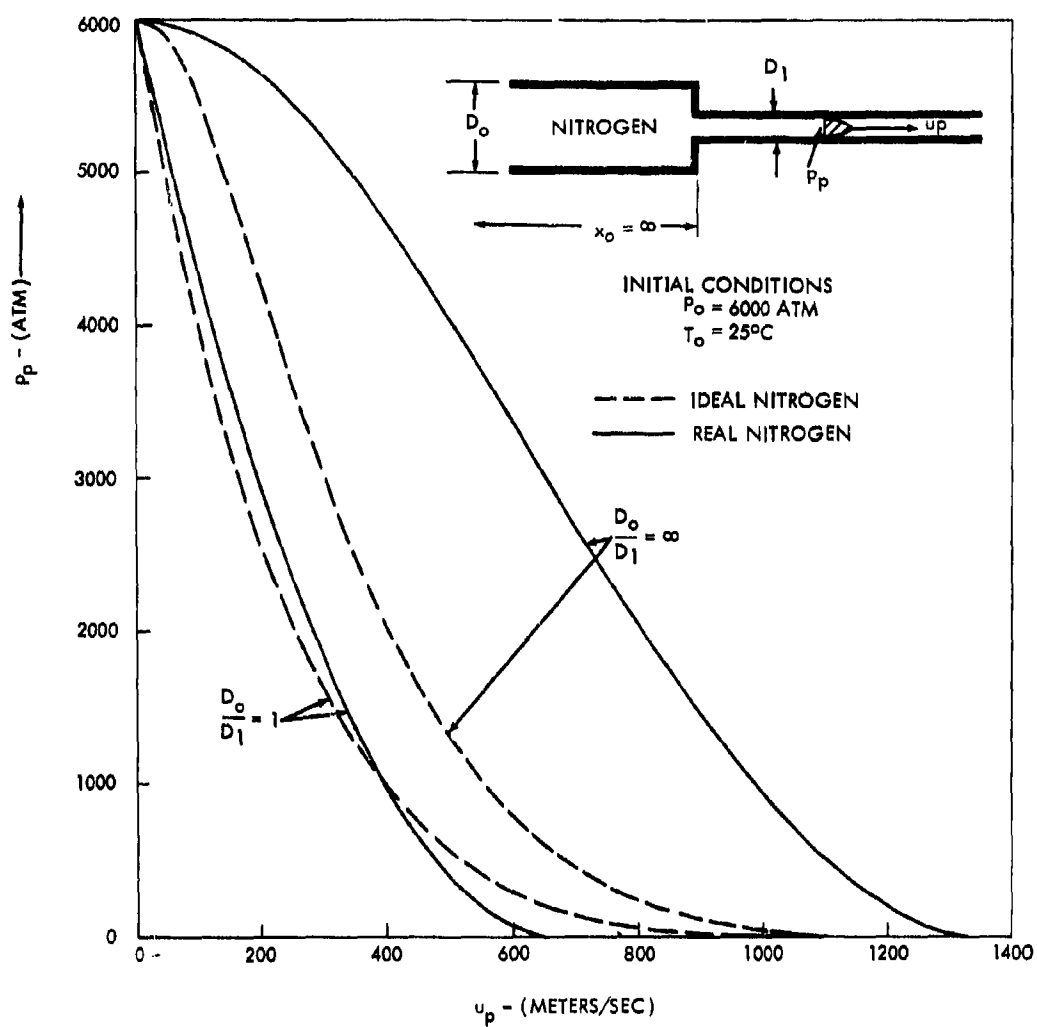
Figure 39

Figure 40
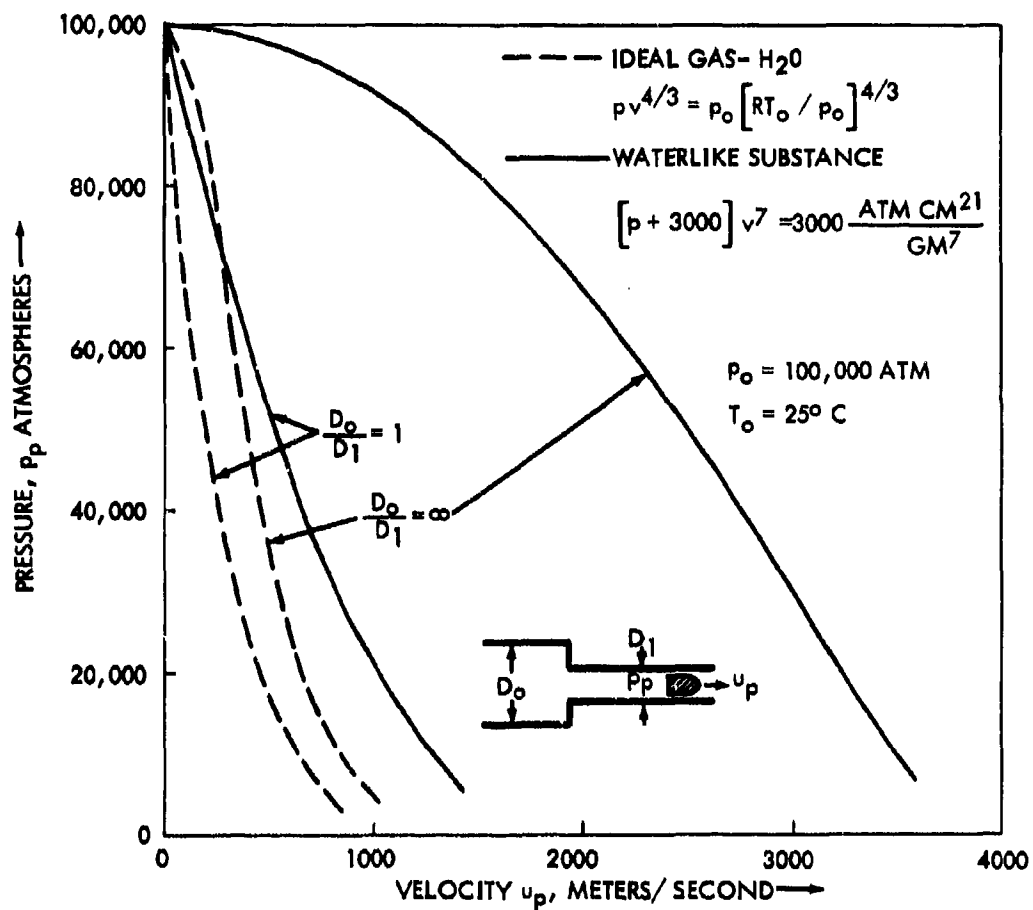
Figure 41

Figure 42

Figure 43

$$\sqrt{\frac{\overline{a}_0}{\gamma-1}}$$

OR FOR $\gamma=1$

$$\sqrt{a_0}$$

$\gamma=1$

$\gamma=1.4$

$\gamma=5/3$

PPIG GUN
SPECIAL SOLUTION

$$\frac{u_p}{a_0} = 2\sqrt{\frac{\overline{a}_0}{\gamma-1}} \sqrt{\frac{1-\left(1+\frac{\gamma \overline{x}_p}{G/M}\right)^{(1-\gamma)}}{\gamma-1}}$$

FOR $\gamma=1$

$$\frac{u_p}{a_0} = 2\sqrt{a_0} \sqrt{\ln\left(1+\frac{\overline{x}_p}{G/M}\right)}$$

$$\overline{x}_p \equiv \frac{p_0 A_1 x_p}{M a_0^2}$$

$$\frac{\gamma \overline{x}_p}{G/M} = \frac{x_p \mathcal{M}_0}{A_0/A_1}$$
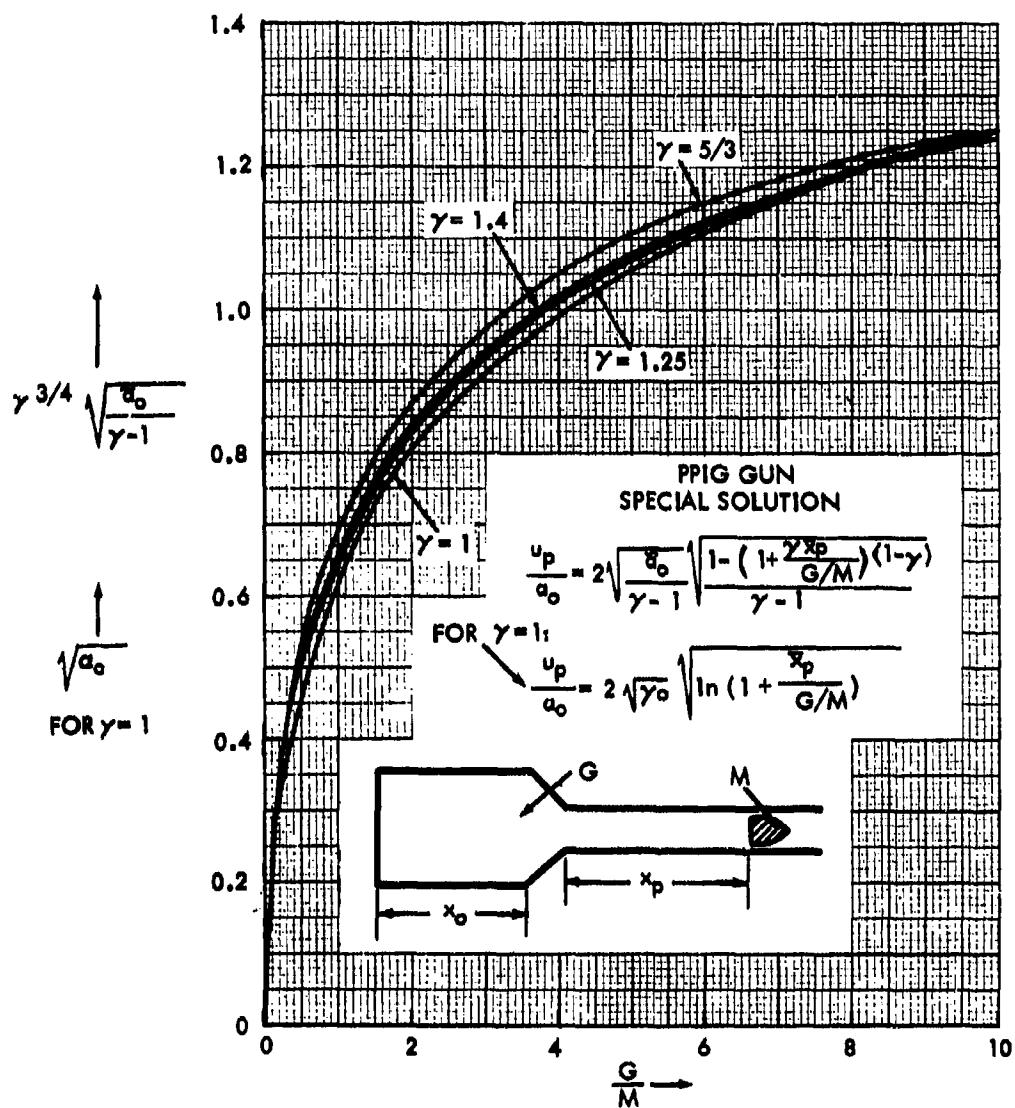
$\frac{G}{M} \longrightarrow$
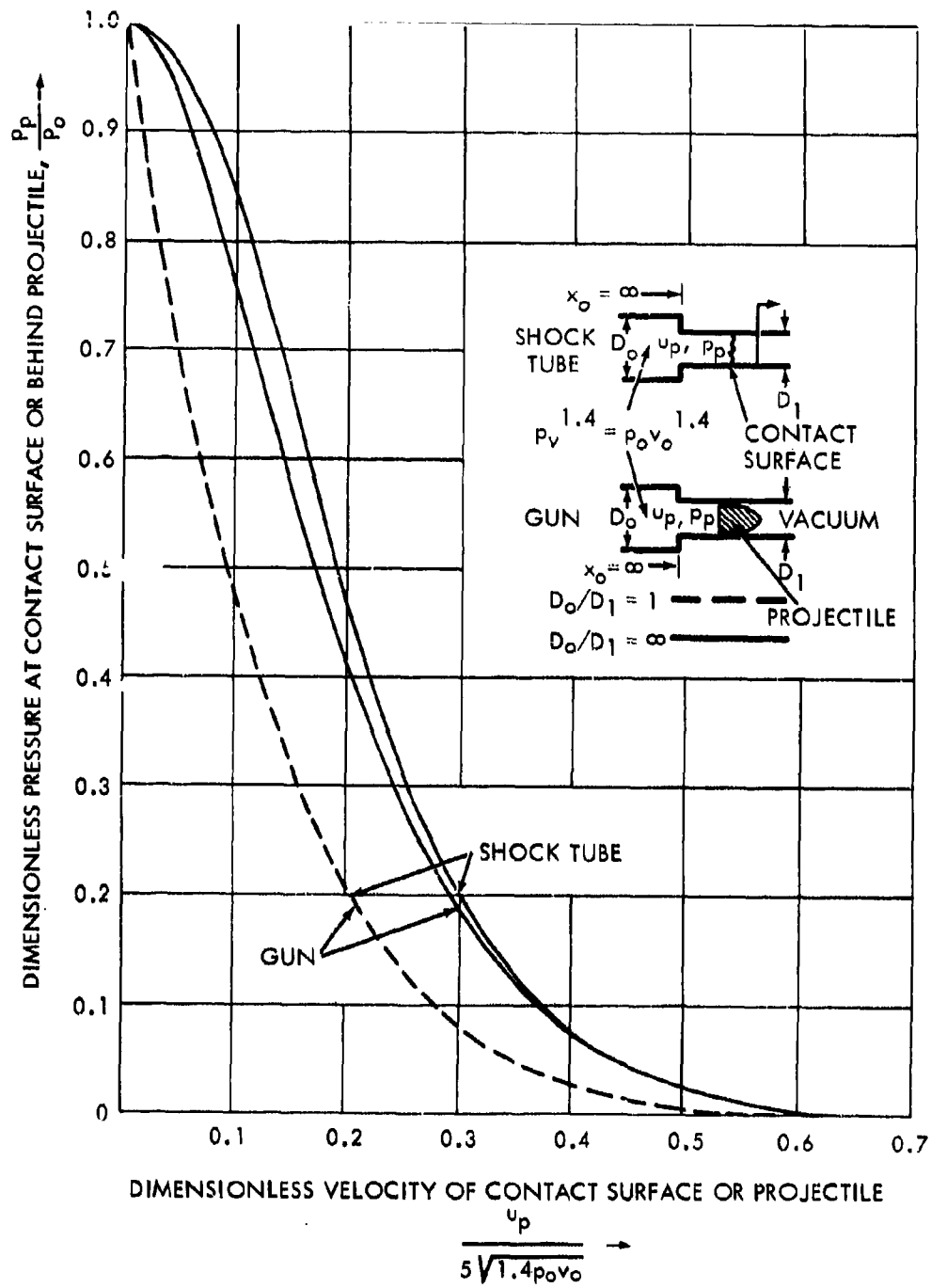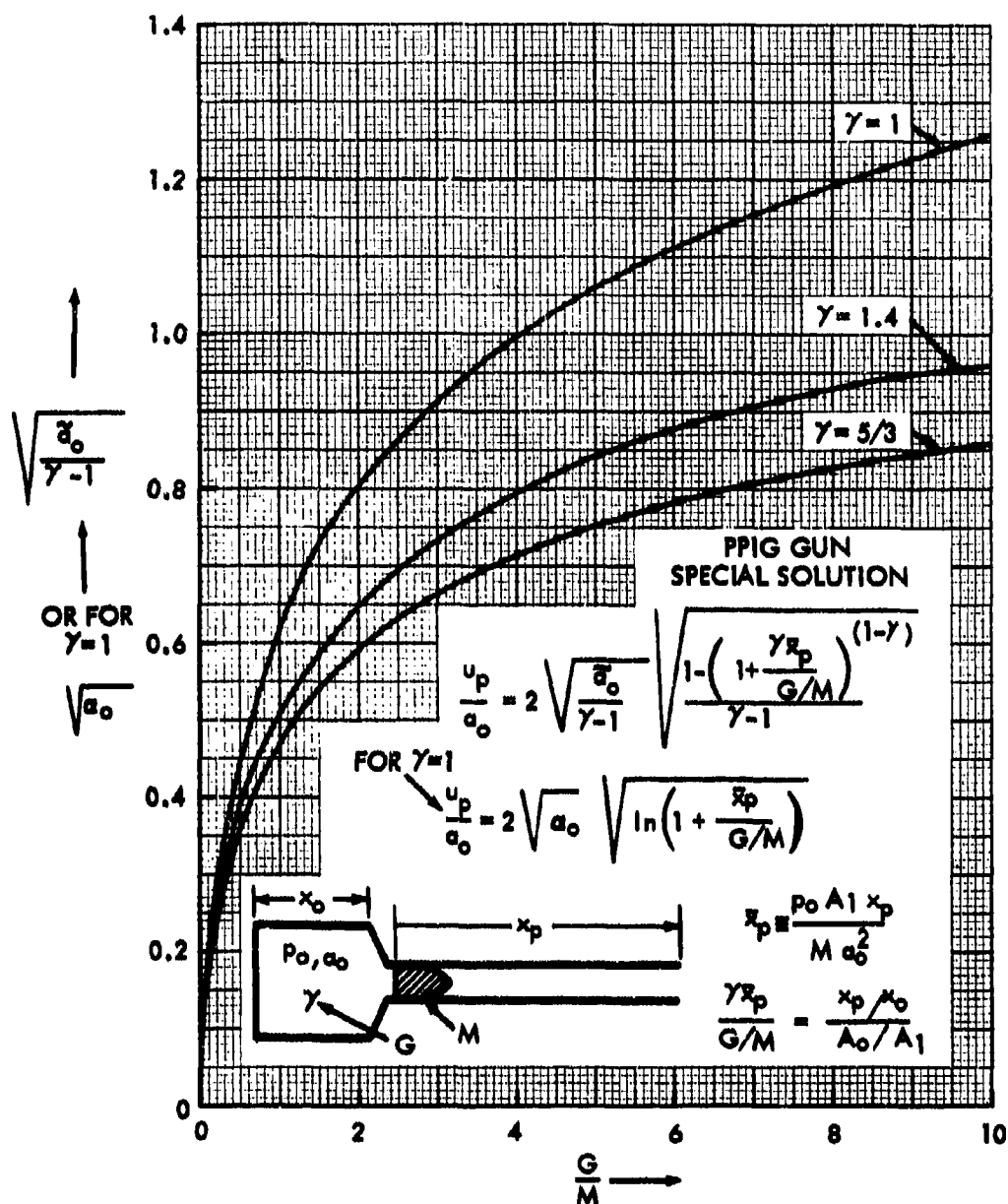
Figure 44(a)

Figure 44(b)
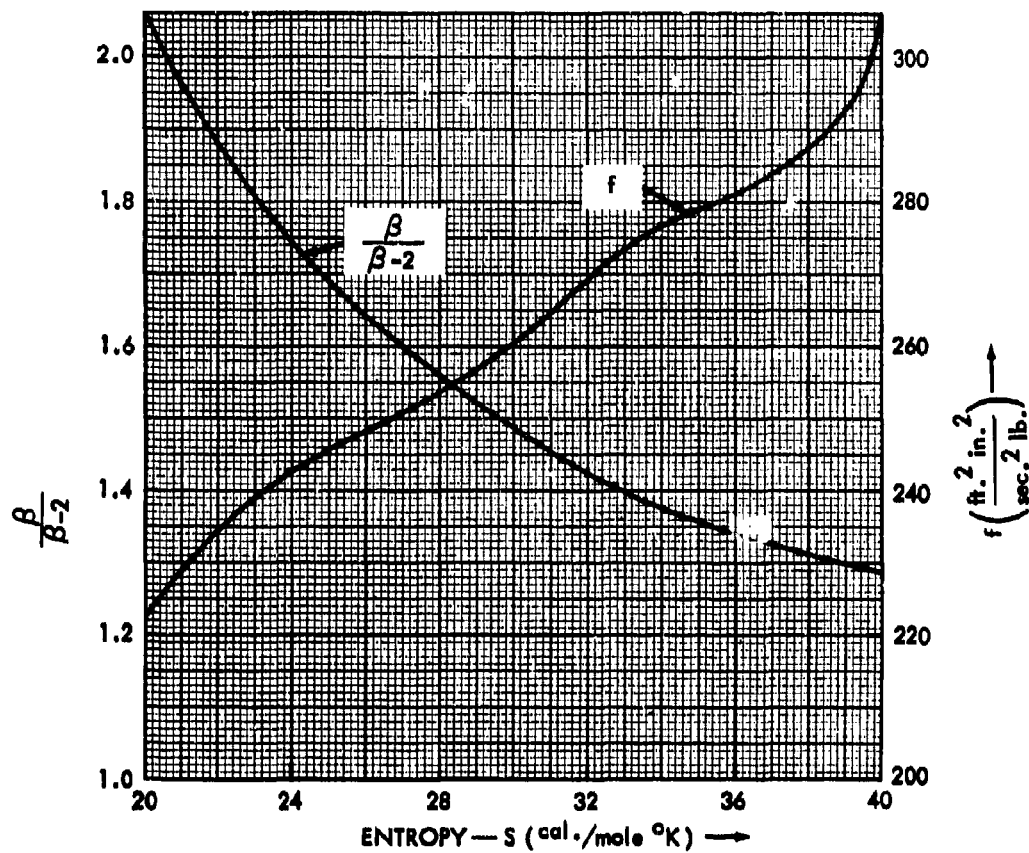
Fig.45(a) Fit of extrapolated hydrogen data to semi-empirical

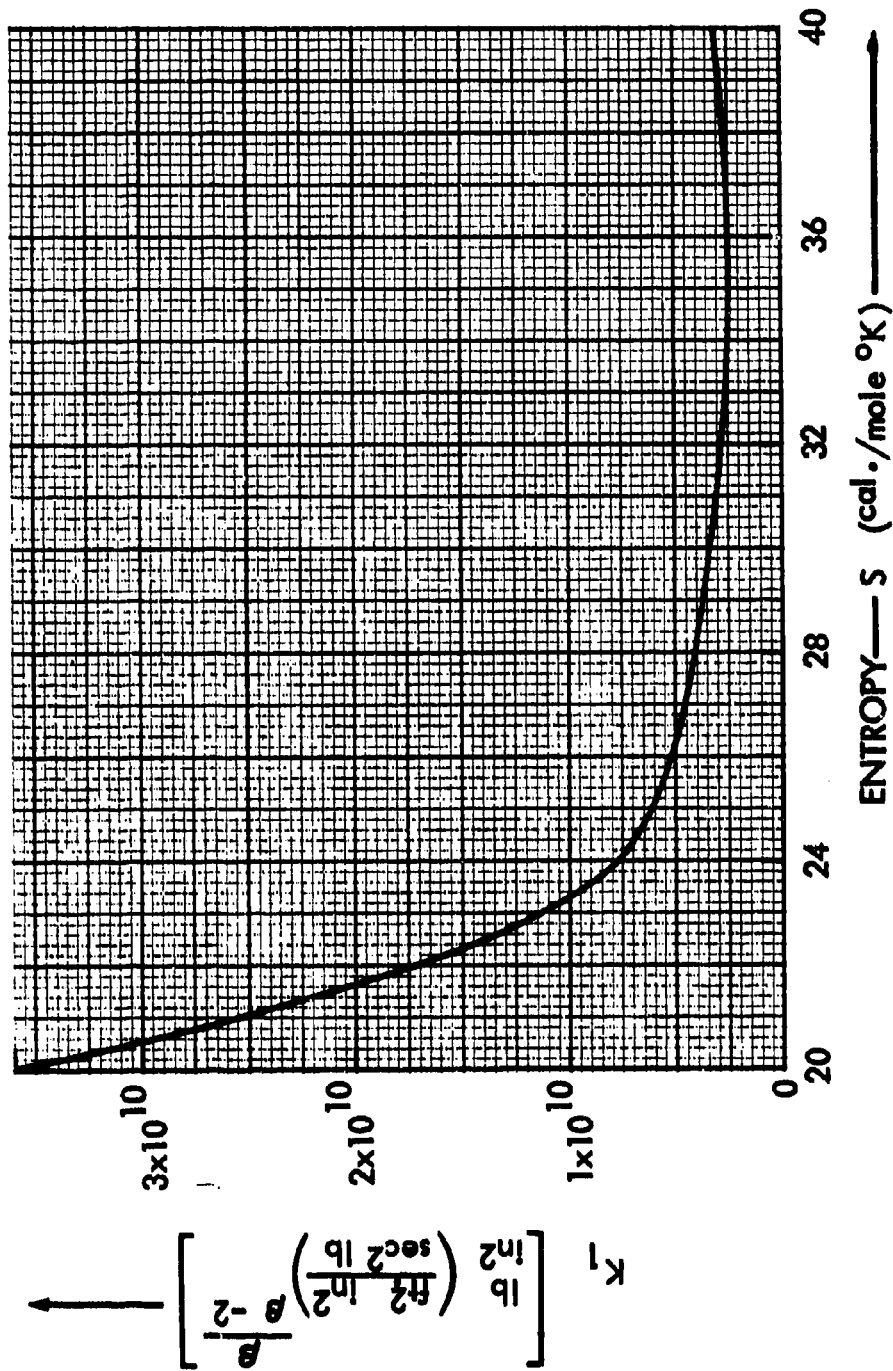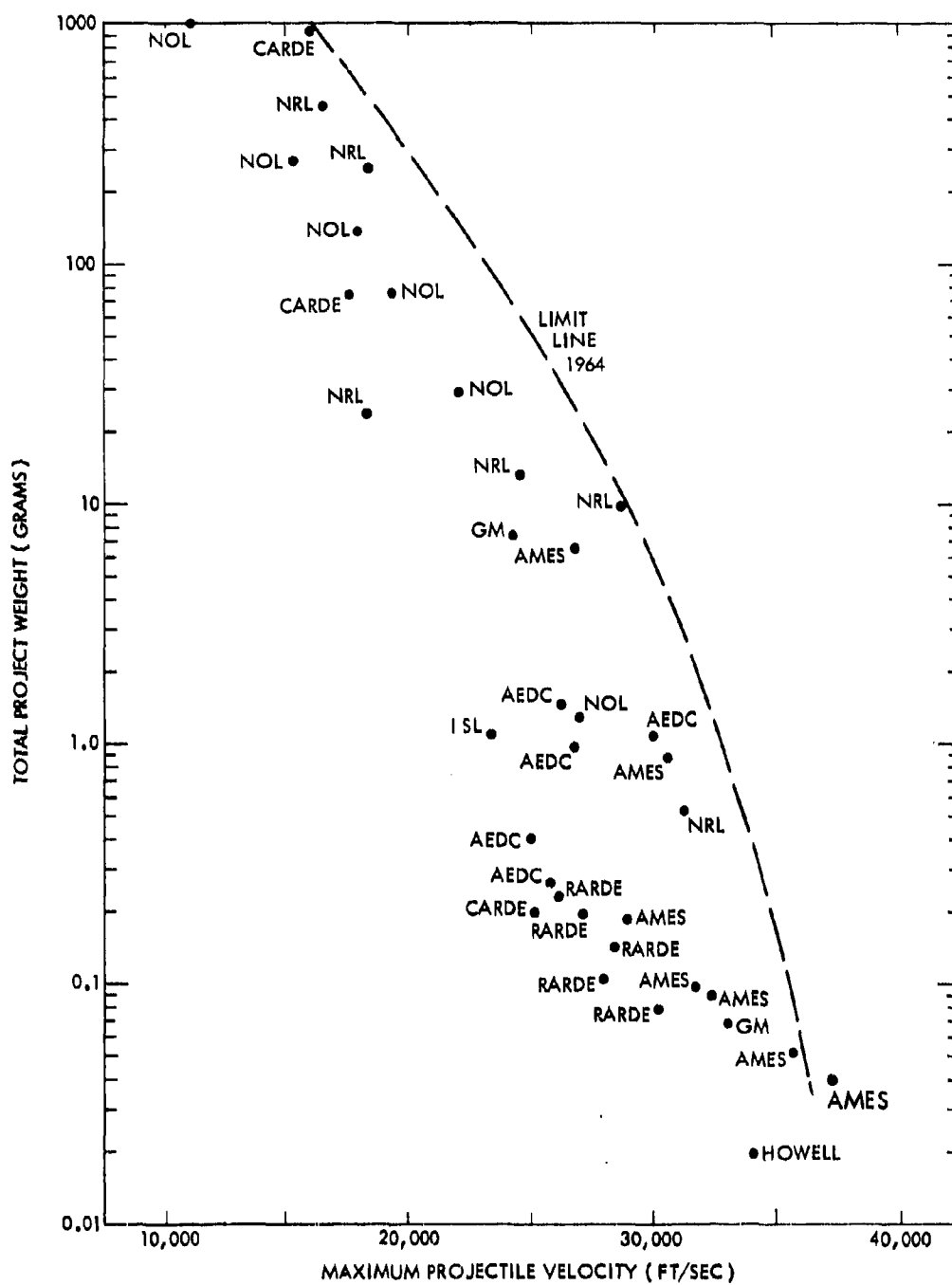isentropic equation $p(v-b)^{\frac{\beta}{\beta-2}} = K^{\frac{\beta}{\beta-2}} = K_1$
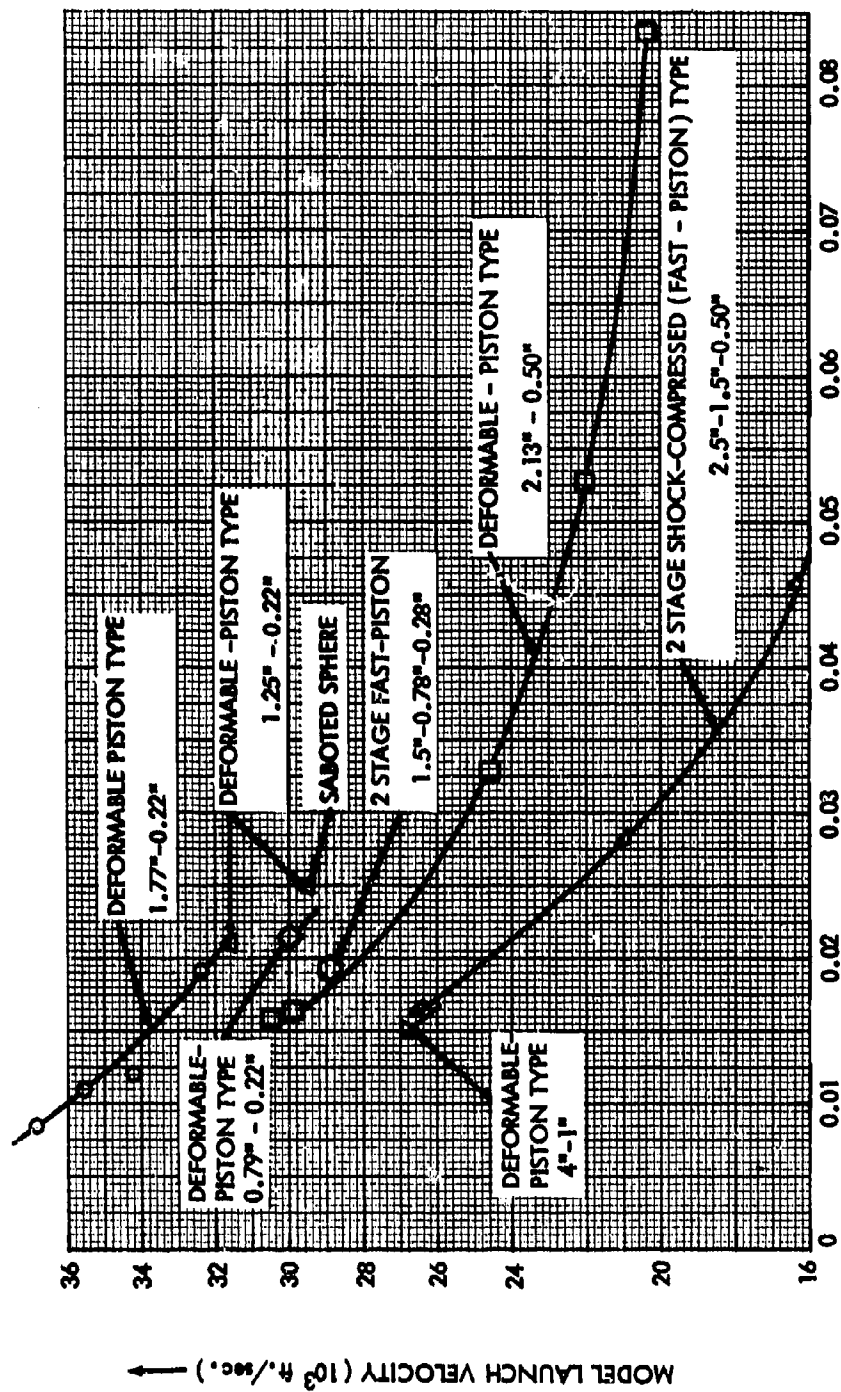
Fig. 45(b)   Fit of extrapolated hydrogen data to semi-empirical

isentropic equation $p(v-b)^{\beta-2} = K^{\beta-2} = K_1$

Figure 46

Fig. 47   Performance of light-gas guns at Ames Research Center (NASA)

AGARDograph 91 North Atlantic Treaty Organization, Advisory Group for Aerospace Research and Development THE THEORY OF HIGH SPEED GUNS Arnold E. Seigel 1965 312 p., incl. 117 refs., 10 Appendices, 47 figs. This AGARDograph summarizes the gas dynamics of high-speed guns, utilizing a gas of low molecular weight at high temperature. Theory and test results are presented. The reader is assumed to be an advanced student in engineering. The fundamental ideas and equations are fully developed. May 1965	623.428-823.1:533.6.078	AGARDograph 91 North Atlantic Treaty Organization, Advisory Group for Aerospace Research and Development THE THEORY OF HIGH SPEED GUNS Arnold E. Seigel 1965 312 p., incl. 117 refs., 10 Appendices, 47 figs. This AGARDograph summarizes the gas dynamics of high-speed guns, utilizing a gas of low molecular weight at high temperature. Theory and test results are presented. The reader is assumed to be an advanced student in engineering. The fundamental ideas and equations are fully developed. May 1965	623.428-823.1:533.6.078
AGARDograph 91 North Atlantic Treaty Organization, Advisory Group for Aerospace Research and Development THE THEORY OF HIGH SPEED GUNS Arnold E. Seigel 1965 312 p., incl. 117 refs., 10 Appendices, 47 figs. This AGARDograph summarizes the gas dynamics of high-speed guns, utilizing a gas of low molecular weight at high temperature. Theory and test results are presented. The reader is assumed to be an advanced student in engineering. The fundamental ideas and equations are fully developed. May 1965.	623.428-823.1:533.6.078	AGARDograph 91 North Atlantic Treaty Organization, Advisory Group for Aerospace Research and Development THE THEORY OF HIGH SPEED GUNS Arnold E. Seigel 1965 312 p., incl. 117 refs., 10 Appendices, 47 figs. This AGARDograph summarizes the gas dynamics of high-speed guns, utilizing a gas of low molecular weight at high temperature. Theory and test results are presented. The reader is assumed to be an advanced student in engineering. The fundamental ideas and equations are fully developed. May 1965	623.428-823.1:533.6.078